Université d'Ottawa · University of Ottawa

Université d'Ottawa · University of Ottawa

FACULTÉ DES ÉTUDES SUPÉRIEURES ET POSTDOCTORALES

FACULTY OF GRADUATE AND POSTDOCTORAL STUDIES

Erin CRERAR

AUTEUR DE LA THÈSE - AUTHOR OF THESIS

M. Sc. (Earth Sciences)

GRADE - DEGREE

Department of Earth Sciences

FACULTÉ, ÉCOLE, DÉPARTEMENT - FACULTY, SCHOOL, DEPARTMENT

TITRE DE LA THÈSE - TITLE OF THE THESIS

Sedimentology and Stratigraphic Evolution of a Tidally-influenced Marginal-marine Complex: The Lower Cretaceous McMurray Formation, Athabasca Oil Sands Deposit, Northeastern Alberta

W. Arnott

DIRECTEUR DE LA THÈSE - THESIS SUPERVISOR

CO-DIRECTEUR DE LA THÈSE - THESIS CO-SUPERVISOR

EXAMINATEURS DE LA THÈSE - THESIS EXAMINERS

A. Donaldson

A. Desrochers

J.-M. De Koninck, Ph.D.

LE DOYEN DE LA FACULTÉ DES ÉTUDES SUPÉRIEURES ET POSTDOCTORALES

SIGNATURE

DEAN OF THE FACULTY OF GRADUATE AND POSTDOCTORAL STUDIES

SEDIMENTOLOGY AND STRATIGRAPHIC EVOLUTION OF A TIDALLY-INFLUENCED MARGINAL-MARINE COMPLEX: THE LOWER CRETACEOUS McMURRAY FORMATION, ATHABASCA OIL SANDS DEPOSIT, NORTHEASTERN ALBERTA

By

Erin Elizabeth Crerar

A thesis submitted to the School of Graduate Studies and Research in partial fulfillment of the requirements for the degree of Master of Science in Earth Sciences

OTTAWA-CARLETON GEOSCIENCE CENTRE
AND
THE UNIVERSITY OF OTTAWA, CANADA

0-612-90051-7

The last thing one discovers when composing a work is what to put first

-Blaise Pascal

Abstract

Within the Lewis study area, McMurray Formation strata comprise 4 facies associations that form a depositional continuum of braided-fluvial (FA1), tidally-influenced braided- to low-accommodation meandering-fluvial and meandering-tidal channel-fills (FA2), associated overbank (FA3), and open-estuarine tidal flat deposits (FA4). The primary reservoir occurs in transgressive FA2 deposits.

Lower-FA2 channels incise older water-wet FA1 sand and consist of medium to locally-coarse, bitumen-saturated sand with rare to locally common pin-stripe laminated and/or 1-5 cm thick mud beds. Channels were initially confined by steep valley walls formed along the sub-Cretaceous unconformity. As a consequence, coeval interchannel sediment (FA3) was cannibalized by lateral channel migration and occurs only as common mud-clasts. The net result was the accumulation of a sand-rich, sheet-like deposit with locally-preserved fine-grained interchannel deposits, suggesting a high rate of lateral versus vertical accretion.

With the filling and elimination of the irregular paleotopography along the unconformity, upper-FA2 channels became unconfined and formed thick, areally extensive inclined heterolithic stratification (IHS) deposits. Similarly, coeval interchannel deposits are more widely-distributed and thickly preserved compared to underlying strata. The position of upper-FA2 channels was indirectly influenced by paleotopography along the unconformity because IHS strata are thickest and sandiest along trends that overlie earlier channel systems, suggesting that syn-depositional salt dissolution controlled channel position and infilling

history. Stratigraphically-upward there is a gradational change toward tidal-flat deposits (FA4), suggesting abandonment of the main north-south channel system and a condition of coarse-grained bedload sediment starvation.

IHS deposits of the middle McMurray Formation are interpreted to represent the lateral migration of point-bar deposits from a complex network of sinuous, meandering channels in a tide-dominated marginal marine complex. Two end-member point-bar deposits have been identified in the McMurray Formation: sand and silt-dominated inclined heterolithic stratification (IHS). Sand-dominated IHS deposits require flow conditions with either low suspended sediment concentrations, sufficient erosion of silts and mud, or simply rare and/or short lived low energy conditions for silt and mud deposition (probably either waning fluvial or tidal flow, flocculation). These conditions can occur at either the upstream end of a large point bar, upstream from the turbidity maxima or maximum tidal limit, or simply within high energy meandering systems. In contrast, silt-dominated IHS deposits require dominantly low energy conditions with high suspended sediment concentrations and frequent deposition of silt and mud via flocculation or waning fluvial or tidal flow. These conditions can occur at either the downstream end of a large point bar or within low energy, silt and mud rich environments such as in low gradient meandering systems.

Although most point-bar deposits within the Lewis study area consist of 10-30 m thick vertically-stacked successions of incomplete IHS deposits, several complete successions from channel base to overbank deposits are preserved. These deposits are between 20 and 30 m in thickness and consist of intercalated sand and mud dipping at low

(8°-12°) degrees that gradually fine-upwards into meter-thick homogenous mud representing vertical accretion deposits. The geometric similarity between meandering-fluvial channels of different scales, climatic regimes, and substrate conditions suggest that the geometry of meanders is largely governed by mechanical principles. Although the applicability of these relationships to meandering-tidal channels is equivocal, using these formulas on IHS deposits of the McMurray Formation can provide a good estimate of the channel width ($W=1.5h/\tan\beta$), depth (0.595h), meander wavelength ($\lambda=10.9w^{1.01}$), and point-bar length ($1/2\lambda$). For two examples of complete point-bar deposits, channel widths were estimated at 148 m and 336 m; channel depth 12.6 m and 18.7 m; meander wavelength 1718 m and 3930 m; and point-bar length 859 m and 1965 m.

Résumé

Dans la région d'étude près de Lewis en Alberta, la Formation de McMurray est constituée par quatre associations des faciès comprenant i) une succession fluviale anastomosée (FA1), ii) une succession fluviatile avec influence des marées (anastomosée à fluviale à méandre sous une accommodation limitée) et des chenaux de marée (FA2), iii) les sédiments d'inondation (FA3), et iv) les dépôts de plaine littorale (FA4). La plupart des ressources en bitume se retrouvent dans les dépôts transgressifs de FA2.

Les chenaux à la base de l'association de faciès (FA2) sont incisés dans les faciès plus vieux (FA1) et saturés en eau. Ces chenaux sont composés par des sables moyens à grossiers imprégnés de bitume avec localement des laminations en forme de « pin-stripe » composés de boue en couche de 1-5 cm d'épaisseur. Au début, les chenaux étaient confinés aux parois abruptes de la discordance sous-jacente. Par la suite, les sédiments inter-chenaux ont été érodés par la migration latérale des chenaux préservant de rares fragments de faciès boueux. Cette distribution suggère un taux d'accrétion latéral plus élevé que le taux d'accrétion vertical. Avec le comblement et aussi l'élimination de la topographie irrégulière de la discordance sous-Crétacé, les chenaux au sommet de FA2 représentent des dépôts latéralement étendus et épais de sable caractérisés par une stratification hétérolithique inclinée (SHI). Par conséquent, les sédiments inter-chenaux sont ici plus abondants en comparaison avec le niveau inférieur de FA2.

La position des chenaux inférieurs dans le FA2 est indirectement contrôlée par la topographie antécédente surtout celle de la discordance sous-Crétacé alors que celle des chenaux plus épais et sablonneux à SHI est probablement contrôlée par la dissolution syn-sédimentaire des dépôts salifères sous-jacents. Le passage graduel aux dépôts de plaines littorale (FA4) est suggestif de la fin d'un apport siliciclastique grossier via les chenaux estuariens orientés nord-sud du FA2.

La stratification hétérolithique inclinée (SHI) de la Formation de McMurray représente des lobes a méandres de chenaux estuariens. Il y a deux types de dépôts : i) dépôts argileux à stratification hétérolithique inclinée et, ii) dépôts sableux à stratification hétérolithique inclinée. Les dépôts sableux SHI requièrent des conditions d'écoulement avec une faible concentration de sédiment en suspension, une forte érosion de la boue et du limon, ou encore des conditions de forte énergie. Ces conditions se retrouvent en amont de grands lobes à méandres, en amont du maximum de turbidité, ou à la limite de marée maximum, ou encore dans un système à méandre énergétique. En contraste, les dépôts argileux SHI nécessitent des conditions d'énergie faible avec une forte concentration de sédiment en suspension et avec une déposition fréquente de boue. Ces conditions se retrouvent en aval des grands lobes à méandres, ou dans un environnement de faible énergie comme à la base d'un chenail à méandre.

Quoique certains lobes à méandres (10-30 m) représentent des dépôts incomplets, il existe localement des successions stratigraphiques assez complètes. Ces dépôts jusqu'à 20-30 m en épaisseur, comprennent les lits inclinés (SHI) qui sont recouverts par des sédiments plus boueux. Les équations qui expliquent les relations géométriques des chenaux à méandre modernes sont utilisées pour caractériser ceux de notre étude et comprennent : la largeur du chenail (W=1.5h/tanβ), la profondeur du chenail (0.595h), la longueur d'onde (λ=10.9w1.01), et la longueur des lobes (1/2λ). Nous avons étudié deux exemples dont les paramètres obtenus sont les suivants : i) largeur du chenail (148 m et 336 m); ii) la profondeur du chenail (12.6 m et 18.7 m); iii) la longueur d'onde (1718 m et 3930 m), et iv) la longueur des lobes (859 m et 1965 m).

ACKNOWLEDGEMENTS

If I see more clearly, it is because I stand on the shoulders of giants

Sir Issac Newton

Since my first encounter with geology as an undergraduate at the University of Alberta, my life has been filled with a wide array of student and professional geoscientists, many of whom have had either a direct or indirect influence on where I am today. Armed with their own uniqueness, these people have played a variety of roles in my life – friends, mentors, colleagues, rehabilitators, Big Rock, KLB, and Guinness companions, stress-relievers, dictators, teachers, supervisors, editors, comedians, and inspirations....To the friends I have made throughout my graduate and undergraduate studies (even with those without geological bones in their body), I thank you for making my experiences truly enjoyable. Academically, I would like to thank Dr. Ben Rostron for challenging and encouraging me with my first 'big' project. Also thanks to Dr. George Pemberton, who presented me with far more value and insight with his laws of stratigraphy and historical 'asides' than can possibly be learned from any sedimentological manual.

Funding for this thesis project, as well as access to core and well log data-sets, petrographical samples, and core photographs, was provided generously by Petro-Canada Oil and Gas. I would like to extend a special 'thank you' to everyone on the Oil Sands team who contributed to the success of this project, in particular Blair Mattison, Mark Savage, and Warren Walsh. Sedimentological discussions with Dr. Richard Evoy were also extremely helpful. I would also like to thank Dr. Arthur Sweet (GSC, Calgary) for his palynomorph interpretations and for various discussions throughout the duration of this project.

To Bill Arnott, there are very few ways to express the positive impact that he has had as a supervisor, teacher, meticulous editor and sedimentologist. Bill has always encouraged me to learn more about what life as a sediment particle might be like by sending me into the field, recommending papers to read and seminars to attend, and most importantly by giving me the freedom to think, work, and act independently. I am truly grateful for his enthusiasm towards sedimentology (an understatement if there ever was one), and for the challenges and opportunities that he has presented me with throughout the duration of this thesis. Many of the ideas and concepts presented in this thesis have benefited greatly from discussions with several individuals, in particular: Don Cummings (and his gargantuan library o' sedimentology), Murray Gingras, Francis Hein, Jason Lavigne, Suzanne Leclair, Grant Mossop, Michel Robin, and Derald Smith. Thank you also to the members of my committee – Drs. Al Donaldson and André Desrochers – whose comments and suggestions helped to improve the final product (et merci André pour m'avoir aidé avec la traduction de mon résumé). And to Sonia Préfontaine, for her cheerful drafting and organizational talents (now where did I put that log again?).

Finally, to my family, for their endless love, support and encouragement, even if they were never really sure what I saw in them rocks of mine. And of course to 'the girls' – Lori J. Meyer, Paula Piilonen, and Natalie Sirman – without whom, I most certainly would have developed a 'pea-brain' somewhere along the way....

TABLE OF CONTENTS

List of Figures

List of Tables

CHAPTER 1:

INTRODUCTION

The Western Canada Sedimentary Basin is host to substantial volumes of natural gas, conventional and heavy oil. Of these deposits, the oil sands of northeastern Alberta represent most of this resource that in the next decade is projected to represent approximately three quarters of Alberta's total oil supply (Alberta Energy and Utilities Board 2001). The Athabasca Oil Sands is the most areally extensive of the three main oil sand deposits (Peace River, Athabasca and Cold Lake) (Fig. 1.1) and hosts nearly 207 billion cubic meters (10^9 m^3) of in-place bitumen (Alberta Energy and Utilities Board, 2001), the majority of which occurs within the Lower Cretaceous McMurray Formation. Less than 10% of the Athabasca Oil Sands deposit, however, can be recovered using conventional surface mining techniques. Additional exploitation of the tar sands requires expensive steam injection methods to facilitate subsurface production of viscous heavy oil. Subsurface mapping in the McMurray Formation has been persistently challenging because of its lithological and ichnological heterogeneous nature, the lack of regional correlatable markers and the common lateral facies changes that occur over scales of only a few hundred meters. As a consequence, a detailed understanding of the physical and chemical conditions that control mud/sand ratios, bioturbation type and abundance and grain size, to mention only a few variables, is needed to predict reservoir sand distribution and sedimentological heterogeneities in order to maximize production and minimize capital expenditure.

Figure 1.1: Location of the 3 major oil sands deposits in Alberta (Athabasca, Cold Lake, and Peace River) and 2 minor deposits (Wabasca and Lloydminister). Bitumen reserves from Alberta Energy and Utilities Board (2001). All bitumen-bearing formations are Lower Cretaceous except where indicated.

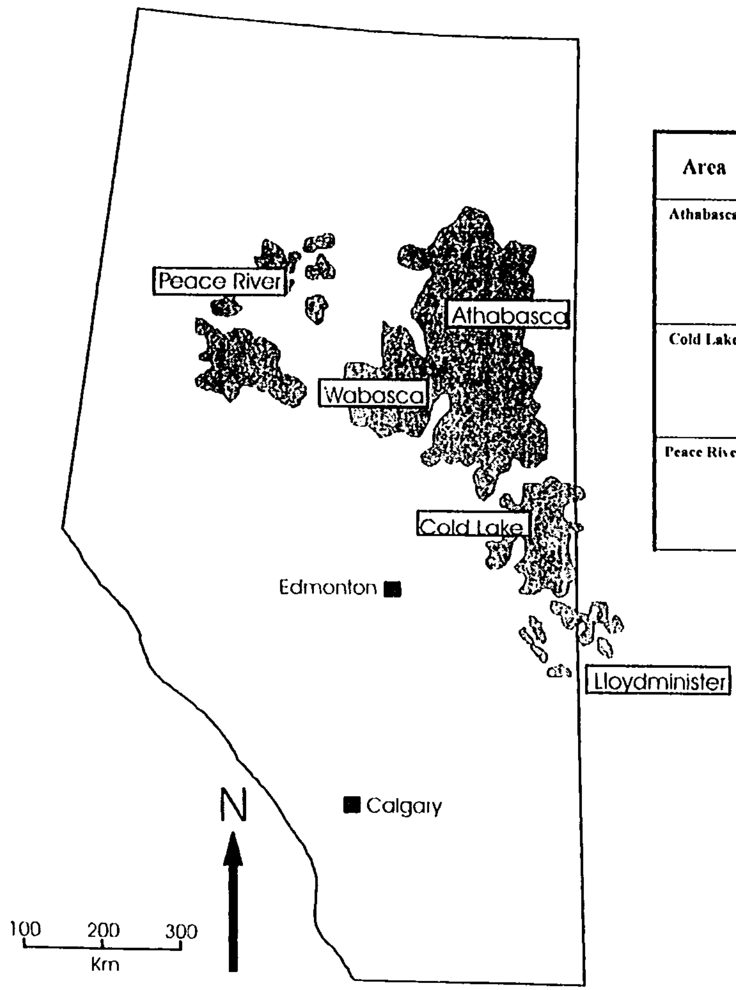

Area	Deposit	Areal Extent (10^3 Ha)	Average pay thickness (m)	Bitumen in place (10^6 m^3)
Athabasca	Grand Rapids	689	7.2	8678
	Wabiskaw-McMurray (mineable)	286	30.5	17998
	Wabiskaw-McMurray (in situ)	4329	19	119234
	Nisku/Grosmont (Devonian)	4666	9.2	60830
				206 740
Cold Lake	Grand Rapids	1709	5.8	17304
	Clearwater	589	15	11051
	Wabiskaw-McMurray	658	5.8	3592
				31947
Peace River	Bluesky-Gething	1254	8.7	9926
	Belloy (Permian)	26	8.0	282
	Debolt/Shunda (Mississippian)	471	18.3	10310
				20518

1.1

REGIONAL GEOLOGY

Western Canada Sedimentary Basin

Beginning in the mid-Jurassic, allochthonous terranes collided along the western margin of North America, marking a transformation from a stable passive margin system to an actively subsiding foreland basin. Oblique collision and eastward thrusting of supracrustal rocks continued through to the Late Cretaceous/Early Tertiary, and substantially thickened the western continental margin. Subsequent lithospheric loading caused the area adjacent to the fold and thrust belt to subside, forming the asymmetric-shaped Western Canadian Foreland Basin. Strata of the basin form a northeastward-tapering wedge of terrigenous clastic sediments derived from both the advancing orogenic belt and the Canadian Shield in the east (Fig. 1.2) (Price 1973; Monger and Price 1979; Cant and Stockmal 1989; Stockmal *et al.* 1992).

Lower Mannville Group deposition

Sedimentary rocks of the Western Canadian Foreland Basin have been informally subdivided into several discrete clastic wedges (Cant and Stockmal 1989; Leckie and Smith 1992) (Fig. 1.3). Individual wedges are bounded above and below either by unconformities or major lithological changes that have been interpreted to correlate with tectonic events and/or changes in relative sea level (Stockmal *et al.* 1992). The McMurray Formation is the basal unit of the Lower Cretaceous (mid Barremian to mid Albian) Mannville Group and represents the second major clastic wedge in the Alberta Foreland Basin (Cant and Stockmal

Figure 1.2: Schematic cross-section of the Western Canada Sedimentary Basin. Sedimentary wedge tapers to the northeast onto the Canadian Shield (modified from Molgat 2000 and Masters 1984).

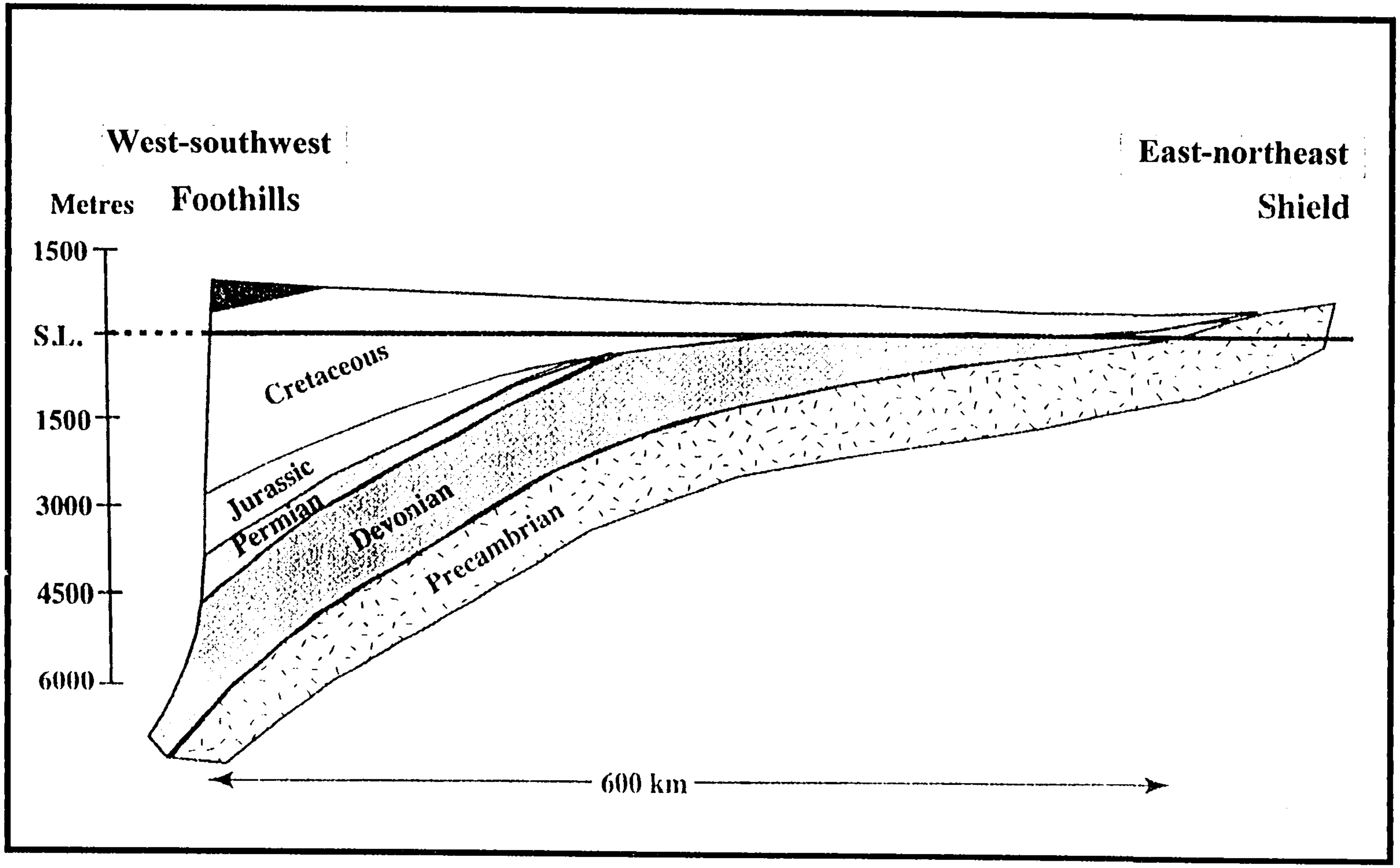
West-southwest
Foothills
East-northeast
Shield
Metres
1500
S.L.
1500
3000
4500
6000
Cretaceous
Jurassic
Permian
Devonian
Precambrian
600 km

1.2

Figure 1.3: Clastic wedges of the Western Canada Foreland Basin in relation to timing of accreted terranes and global sea level. Mannville Group deposition is interpreted to follow accretion of the Bridge River Terrane (Br). The depositional hiatus from the Valganian (V) to the mid-Barremian (B) represents the sub-Cretaceous unconformity (from Cant and Stockmal 1989).

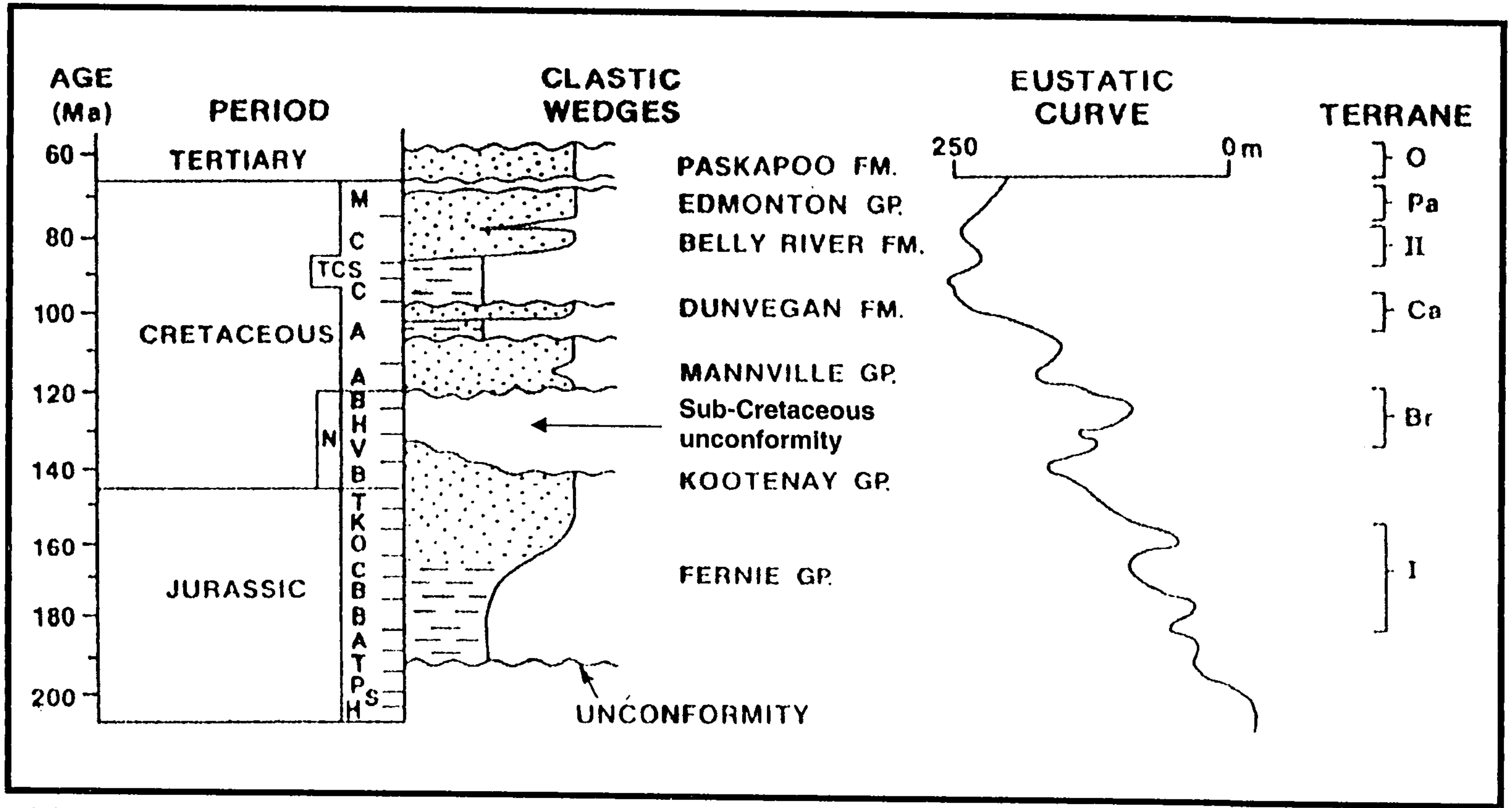
AGE (Ma)
PERIOD
CLASTIC WEDGES
EUSTATIC CURVE
TERRANE
60
80
100
120
140
160
180
200
TERTIARY
CRETACEOUS
JURASSIC
M
C
TCS
C
A
A
B
H
N
V
B
T
K
O
C
B
B
A
T
P
S
H
PASKAPOO FM.
EDMONTON GP.
BELLY RIVER FM.
DUNVEGAN FM.
MANNVILLE GP.
Sub-Cretaceous unconformity
KOOTENAY GP.
FERNIE GP.
UNCONFORMITY
250
0 m
O
Pa
II
Ca
Br
I
1.3

1989). Sediment of the Mannville Group was deposited above a basin-wide unconformity (sub-Cretaceous unconformity) that developed over tilted Jurassic to Lower Paleozoic strata in response to a fall of relative sea level. Deposition of Mannville sediment, which coincided with the early stages of relative sea level rise and southward transgression of the Northern Boreal sea, has been correlated with accretion of the Bridge River Terrane (Cant and Stockmal 1989) during the Columbian Orogeny (Stott 1984). In most places, the Mannville Group is overlain by marine shale of the Colorado Group, although locally this marine flooding surface is separated from underlying Mannville strata by the mid-Albian unconformity (Stelck and Kramers 1980).

Strata of the Mannville Group have been informally subdivided into a lower transgressive and upper highstand unit (Cant and Abrahamson 1996) (Fig. 1.4). Stratigraphic relationships between laterally equivalent Mannville strata are complex because basin-scale contacts are generally diachronous. As summarized in Figure 1.5, the Lower Mannville Group corresponds to nonmarine to marginal marine strata (Gething, McMurray, Dina, Ellerslie, Sunburst, and Cutbank) and progradational shoreface sands (Bluesky, Wabasca and Cummings). Upper Mannville strata comprise marine and non-marine strata of the Glauconite, Lloydminster, Clearwater and Spirit River formations. The contact between the Lower and the Upper Mannville is a marine flooding surface that marks the base of the Clearwater Shale in the Athabasca region, the Wilrich Shale of the Spirit River Formation in the Peace River area, and the marginal marine Ostracode member in southern Alberta (Fig. 1.4). In sequence stratigraphic terms the Lower Mannville Group represents a transgressive systems tract (TST), the Upper Mannville Group represents a highstand systems tract (HST),

Figure 1.4: Schematic illustration of large-scale sequence stratigraphic subdivisions of the Mannville Group; TST (transgressive systems tract); MFS (marine flooding surface); HST (highstand systems tract) (modified from Cant 1998).

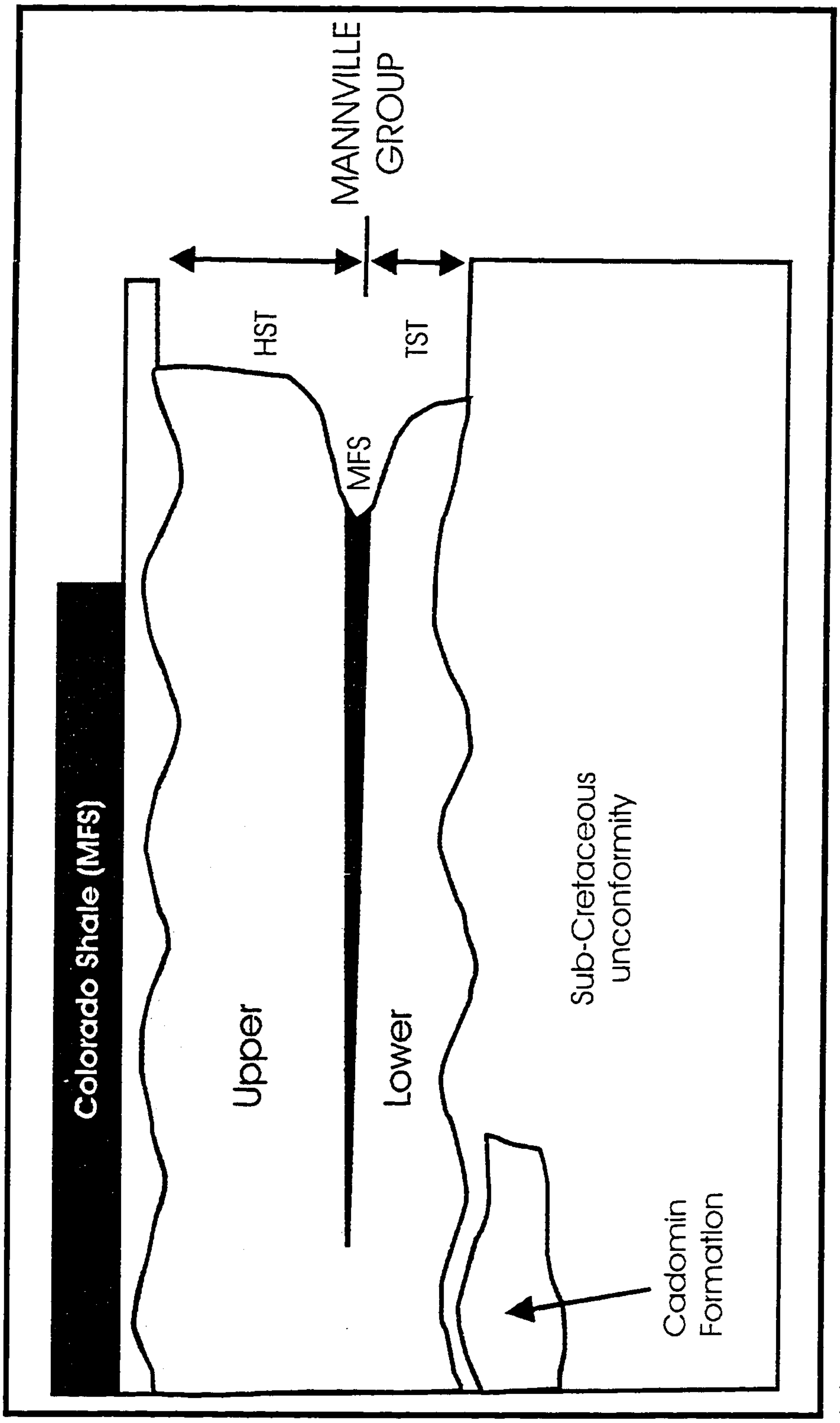
MANNVILLE
GROUP
HST
TST
MFS
Colorado Shale (MFS)
Upper
Lower
Sub-Cretaceous
unconformity
Cadomin
Formation

1.4

Figure 1.5: Stratigraphic nomenclature of Lower Mannville Group strata in the Western Canada Sedimentary Basin (from Hubbard *et al.* 1999).

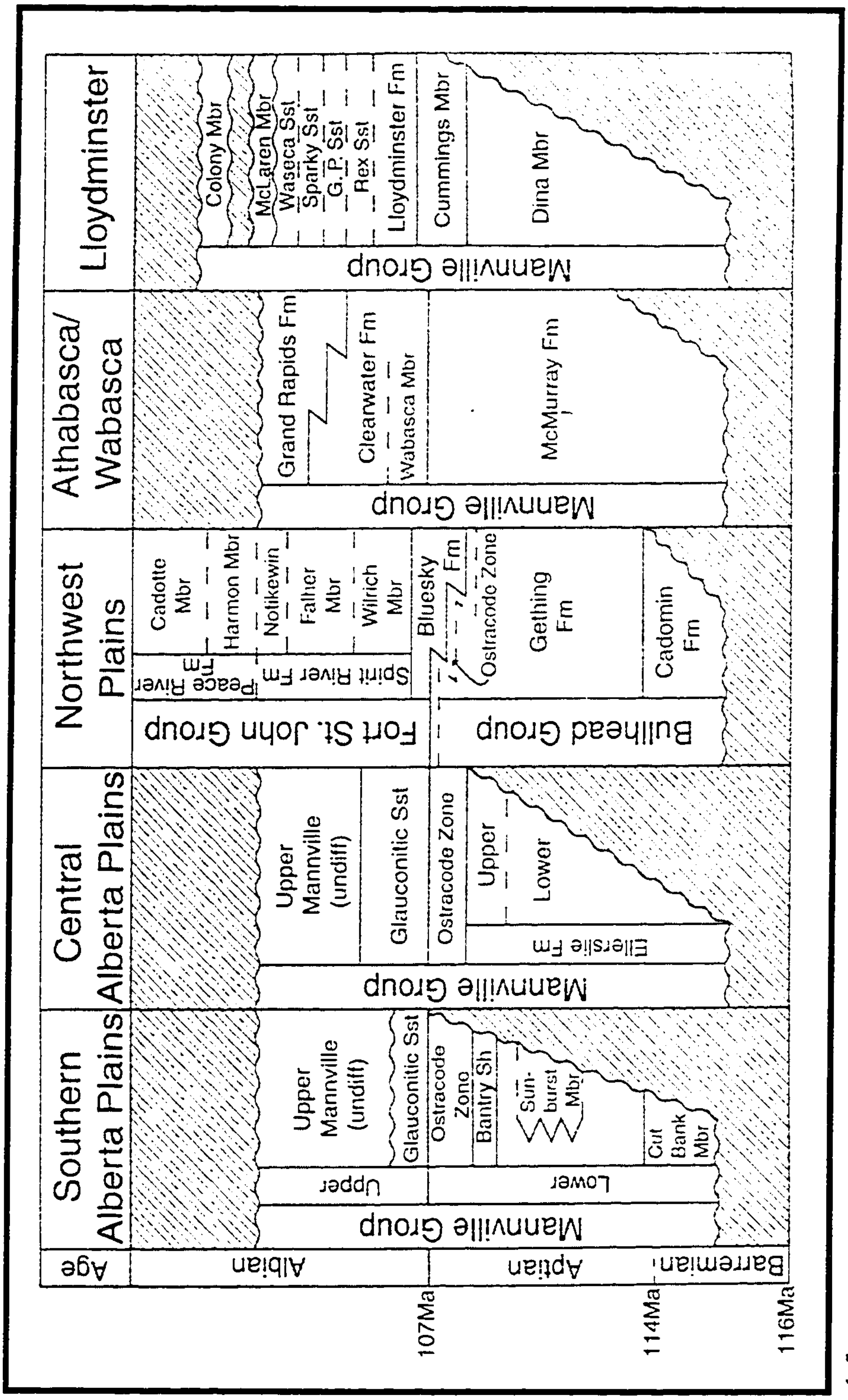
Age
Albian
Aptian
Barremian
107Ma
114Ma
116Ma
Southern Alberta Plains
Mannville Group
Upper
Lower
Upper Mannville (undiff)
Glauconitic Sst
Ostracode Zone
Bantry Sh
Sun-burst Mbr
Cut Bank Mbr
Central Alberta Plains
Mannville Group
Upper Mannville (undiff)
Glauconitic Sst
Ostracode Zone
Upper
Lower
Ellerslie Fm
Northwest Plains
Fort St. John Group
Bullhead Group
Peace River Fm
Spirit River Fm
Cadotte Mbr
Harmon Mbr
Notikewin
Falher Mbr
Wilrich Mbr
Bluesky Fm
Ostracode Zone
Gething Fm
Cadomin Fm
Athabasca/ Wabasca
Mannville Group
Grand Rapids Fm
Clearwater Fm
Wabasca Mbr
McMurray Fm
Lloydminster
Mannville Group
Colony Mbr
McLaren Mbr
Waseca Sst
Sparky Sst
G.P. Sst
Rex Sst
Lloydminster Fm
Cummings Mbr
Dina Mbr

1.5

and a maximum marine flooding surface (MMFS) separates the two units (Cant and Abrahamson 1996).

Basin paleogeography and tectonic elements during Lower Mannville Group deposition

Several regional and local paleotopographical features formed important physiographic controls on sediment distribution in the Lower Mannville Group. Most important was the basin-wide sub-Cretaceous unconformity, an irregular surface directly underlying Lower Mannville Group strata that represents a depositional hiatus of up to 27 million years (Stewart 1963; Leckie and Smith 1992; Cant and Abrahamson 1996). The sub-Cretaceous unconformity consists of a number of regional northwest-southeast trending ridges and valleys developed on westward dipping Paleozoic to early Mesozoic strata. By the early Albian, coinciding with the base of the Upper Mannville Group, the unconformity was covered as rising relative sea level blanketed the basin with marine shale (MMFS). Many factors, several of which are interrelated, were responsible for enhancing and maintaining the paleotopographical relief on the sub-Cretaceous unconformity, including reactivation of deep-seated crustal structures, differential erosion, the overall morphology of the foreland basin, and salt dissolution (Figs. 1.6-1.8).

Regional deep-seated crustal features include the Peace River Arch (PRA), which was tectonically quiescent during Lower Mannville time, and the Sweetgrass Arch (SGA), which was active during Mannville deposition and strongly affected sedimentation in southeastern Alberta (Fig. 1.6). Differential erosion of underlying Paleozoic carbonates was key in creating a regional drainage system comprising northwest-southeast trending ridges and

Figure 1.6: Major tectonic elements of the Alberta Basin during Mannville Group deposition (mid Barremian to mid Albian) relative to the oil sand deposits. PRA = Peace River Arch (Stelck 1975); SGA = Sweetgrass Arch (modified from Leckie and Smith (1992) (salt dissolution zone), Hayes *et al.* (1994) (PRA, SGA, and foredeep), and Smith (1994) (tar sands deposits)).

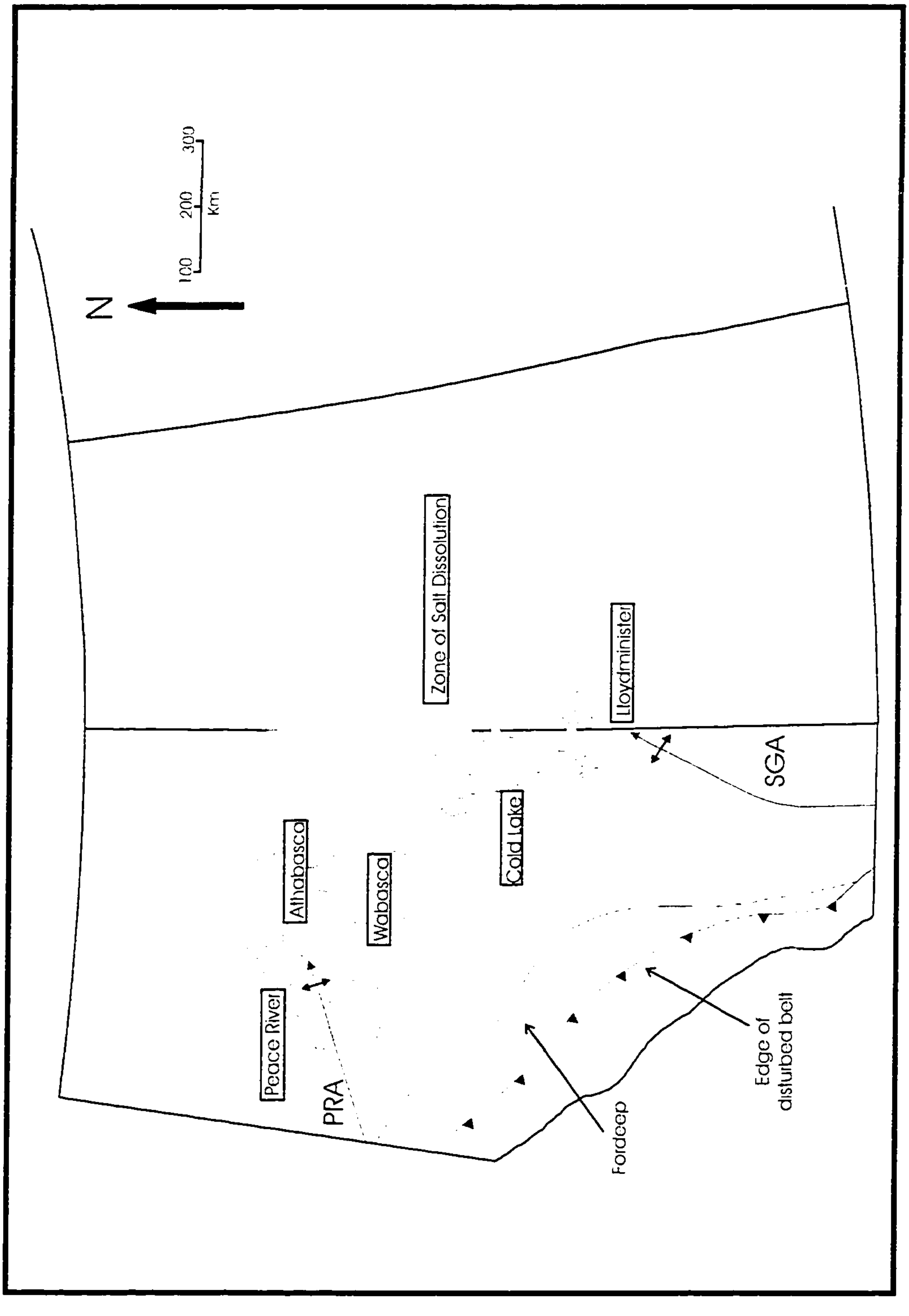

N
100
200
300
Km
Zone of Salt Dissolution
Lloydminister
Athabasca
Wabasca
Cold Lake
Peace River
SGA
PRA
Fordeep
Edge of
disturbed belt

1.6

Figure 1.7: Paleogeography of the Western Canada Sedimentary Basin during Early Mannville time. See text for explanation of major elements. Modified from Smith (1994) and Leckie and Smith (1992).

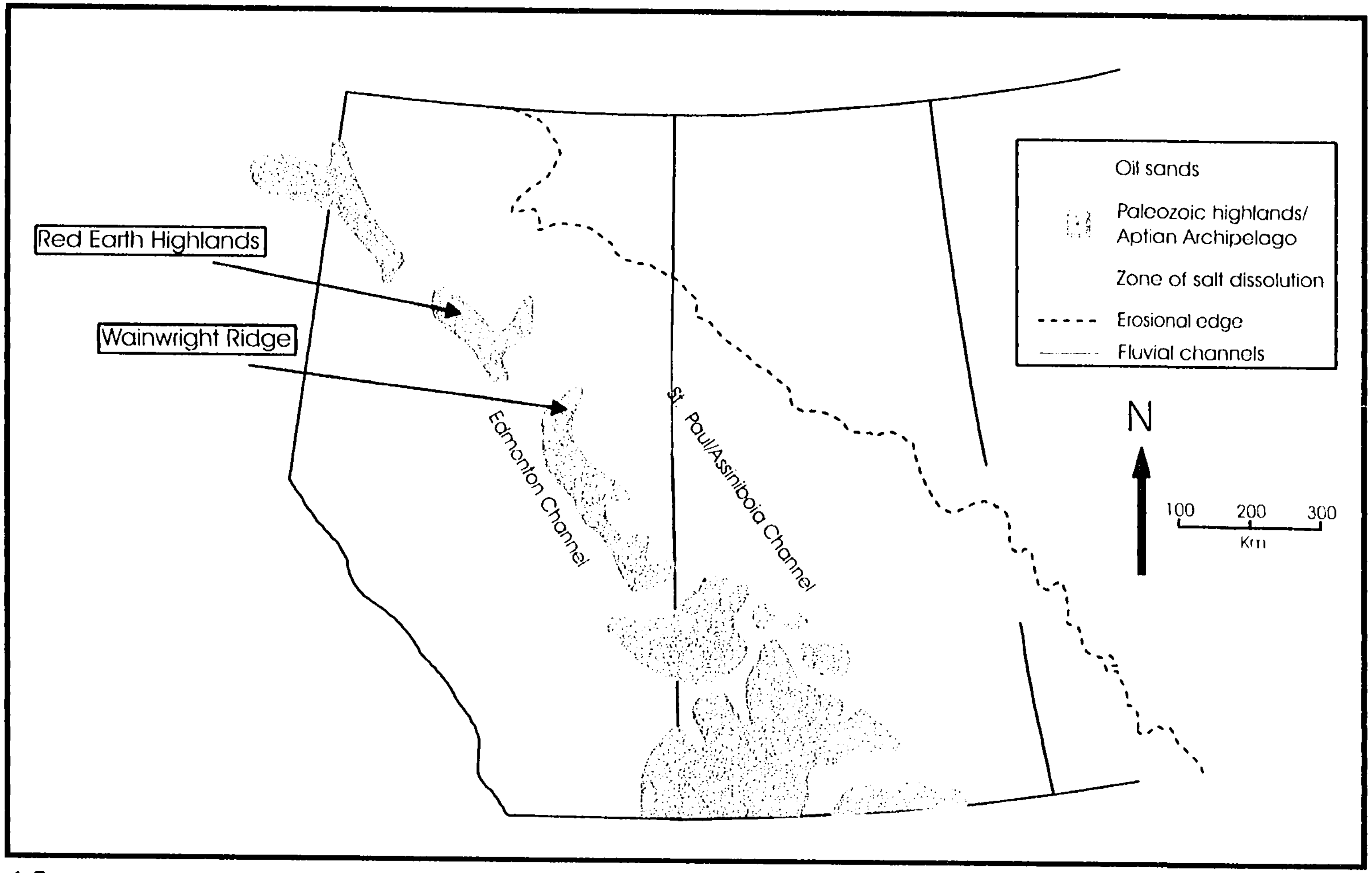

Red Earth Highlands
Wainwright Ridge
Edmonton Channel
St. Paul/Assiniboia Channel
Oil sands
Paleozoic highlands/
Aptian Archipelago
Zone of salt dissolution
Erosional edge
Fluvial channels
N
100
200
300
Km

1.7

Figure 1.8: Regional controls on accommodation space in the Western Canada Sedimentary Basin: (1) tectonic subsidence in the west; (2) erosional paleovalleys in the central region; and, (3) salt dissolution in the east (modified from Cant and Abrahamson 1996).

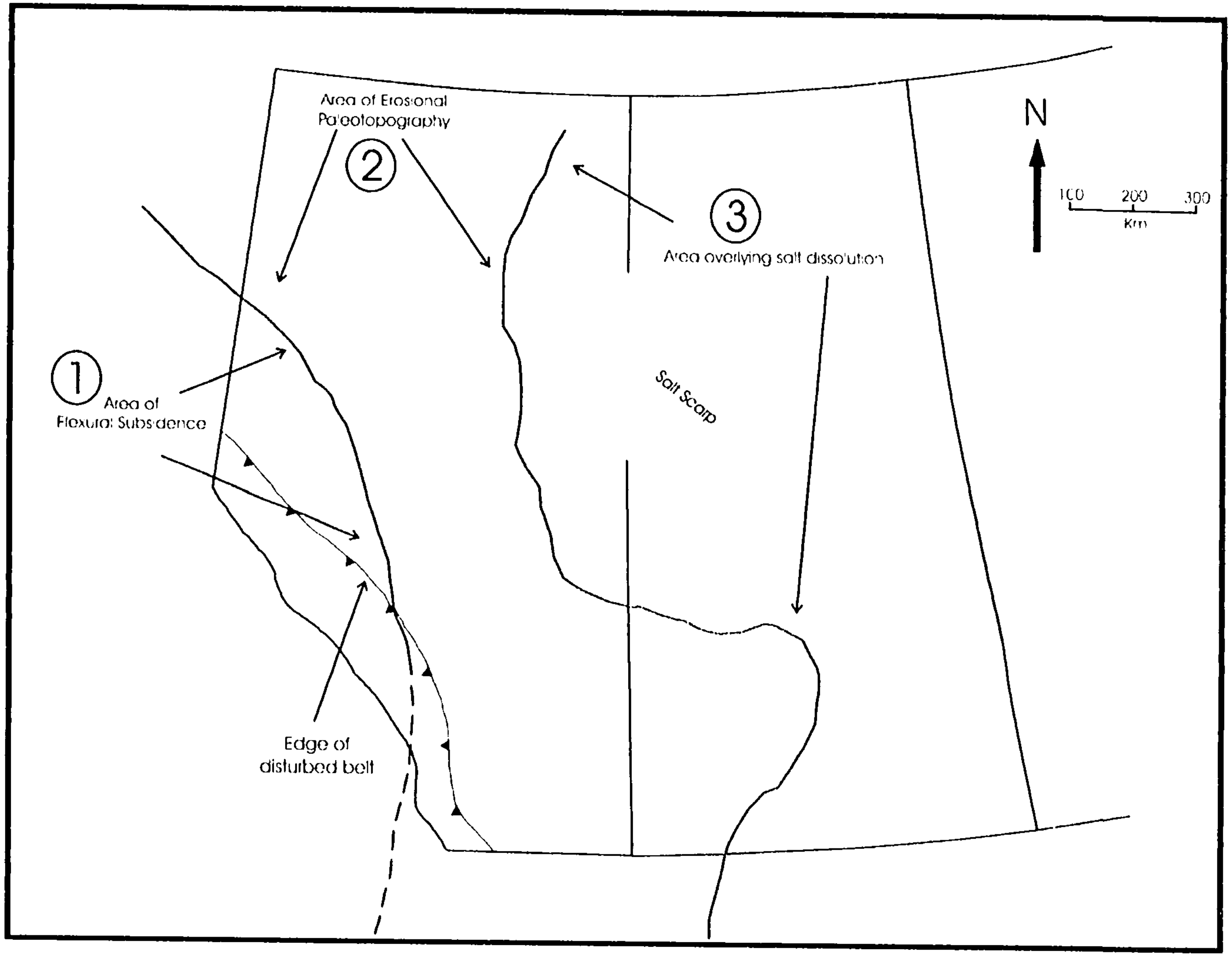
N
100 200 300
Km
Area of Erosional Paleotopography
2
3
Area overlying salt dissolution
1
Area of Flexural Subsidence
Salt Scarp
Edge of disturbed belt

1.8

valleys (Fig. 1.7). Most prominent is a chain of highlands informally termed the Aptian Archipelago (Rudkin 1964) that extended from British Columbia to Saskatchewan during the Barremian through to the early Albian (Christopher 1974). In addition to forming a regional east-west drainage divide that separated the western Edmonton Channel from the eastern St.Paul Channel (Williams 1963) or Assiniboia Valley (Leckie and Smith 1992), these highlands also created sub-basins within the Lower Mannville Group. The Red Earth Highlands isolated the Peace River from the Athabasca Oil Sands deposit (Fig. 1.7), and Grosmont High, an extension of the Wainright Ridge, separates the Wabasca from the Athabasca deposit (Fig. 1.9).

Regional northwest-southeast trending topographical lows on the sub-Cretaceous unconformity surface have been attributed to large-scale variations of accommodation space in the Western Canada Sedimentary Basin (WCSB) (Cant and Abrahamson 1996) (Fig. 1.8). In the west, topographical lows are attributed to tectonic subsidence, particularly in the foredeep and in the vicinity of the PRA. In the central part of the WCSB, accommodation space was created by large erosional drainage networks. In contrast, dissolution in the underlying middle Devonian Prairie Evaporite Formation created space for deposition of the McMurray Formation in the easternmost extent of the WCSB.

Figure 1.9: Structural elements of the Athabasca region in relation to the Lewis study area. The Grosmont High is a splay from the Wainright Ridge (Fig. 1.7) and separates the Wabasca from the Athabasca Oil Sands deposit. The Wabasca subbasin was previously termed the Central sub-basin (Wightman *et al.* 1995) but has been subsequently re-named by Ranger and Pemberton (1997) to reflect the thicker accumulation of Wabasca Member (Clearwater Formation) sand in this area. Diagram modified from Wightman *et al.* (1995).

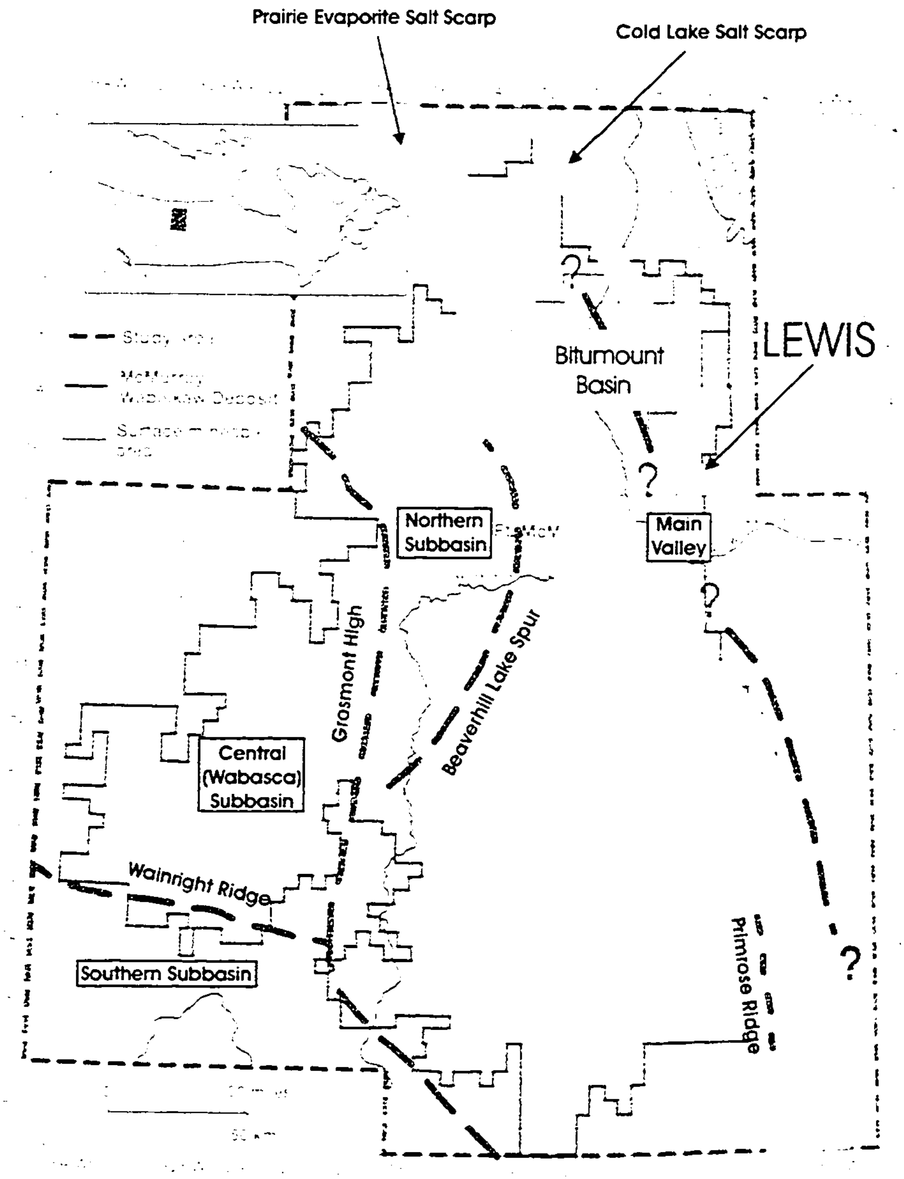
Prairie Evaporite Salt Scarp
Cold Lake Salt Scarp
LEWIS
Bitumount Basin
Main Valley
Northern Subbasin
Grosmont High
Beaverhill Lake Spur
Central (Wabasca) Subbasin
Wainright Ridge
Southern Subbasin
Primrose Ridge

1.9

DEPOSITIONAL AND STRUCTURAL ELEMENTS OF THE ATHABASCA REGION

Stratigraphy of the Athabasca region

The Athabasca Oil Sands of northeastern Alberta encompasses townships 67-104, ranges 2W4-5W5 (Fig. 1.9). In this area the Mannville Group comprises the McMurray, Clearwater and Grand Rapids formations. The McMurray Formation was deposited within topographical lows on the sub-Cretaceous unconformity during an overall transgression and consists of strata suggesting a northward change from fluvial through to brackish-water sedimentation. Although deposition never occurred under fully marine conditions, evidence of marine-influenced sedimentation in the McMurray Formation becomes increasingly apparent stratigraphically upward and geographically northward (Jeletzky 1971; Ranger and Pemberton 1997). Deposition of the McMurray Formation was terminated by a fall of relative sea level. The ensuing southward transgression of the Boreal sea deposited shoreface sand of the Wabasca Member of the Clearwater Formation above the unconformity. Continued transgression deposited the regionally extensive Clearwater Shale in the Athabasca region, the base of which represents a maximum marine flooding surface (MMFS). The Clearwater Formation is then overlain by the Grand Rapids Formation which consists of a lower progradational deltaic sand unit and an upper transgressive shallow marine sand unit (Minken 1974). A fall of relative sea level, followed by transgression of both the Boreal and (southern) Gulfian seas and related deposition of the Colorado Shale, marks the top of the Grand Rapids Formation and end of Mannville Group deposition (Jackson 1984).

From a reservoir perspective, the McMurray-Wabasca interval is collectively considered to be a single entity, due largely to hydraulic connectivity formed by common sand-on-sand contacts (Wightman *et al.* 1995). Stratigraphically, however, the McMurray-Wabasca contact is a regional unconformity marked by an abrupt change to fully marine conditions and also a significant petrographical change from Canadian Shield-derived quartzose sand of the McMurray Formation to feldspar-rich sand of the Wabasca Member derived from the western cordillera (Wightman *et al.* 1995). Overall, the McMurray/Wabasca interval represents a transgressive systems tract (TST), bounded below by a type 1 unconformity (sub-Cretaceous unconformity) and above by a maximum marine flooding surface marked by the base of the Clearwater Shale (McPhee 1994; Wightman *et al.* 1995; Cant and Abrahamson 1996). Highstand deposits (HST) are represented by the Upper Mannville Grand Rapids Formation.

In the Athabasca region, the majority of the bitumen reserves occur in the McMurray/Wabasca interval, although most of these reserves occur within the thicker McMurray Formation (Wightman *et al.* 1995). The Wabasca Member contains significant reserves in the western Athabasca region, which Ranger and Pemberton (1997) consider to be part of the Wabasca sub-basin (Fig. 1.9). The Grand Rapids Formation, where present, is typically thin and does not contain significant reserves in the Athabasca region (Wightman *et al.* 1995).

Depositional controls and sediment distribution within the Athabasca region

Within the Athabasca region, several prominent structural highs and lows along the sub-Cretaceous unconformity affected sediment distribution of the McMurray-Wabasca interval (Stewart 1963) (Fig. 1.9). Most prominent are paleotopographical lows created by pre-, syn- and post-depositional salt dissolution of the underlying middle Devonian Prairie Evaporate Formation, which was originally up to 180 m in thickness and is presently several hundred meters below the base of the McMurray Formation (Christopher 1974; Edmunds 1980; Cant and Abrahamson 1996; Drees 1994). Paleotopographical highs include the Wainright Ridge, the Grosmont High and the Beaver Hill Lake Spur, which effectively created sub-basins for deposition of the Athabasca Oil Sands (Figure 1.9).

The thickest area of sediment accumulation is in the Main Valley, a northwesterly-trending low interpreted to have formed as a consequence of dissolution of the underlying middle Devonian Prairie Evaporite Formation (McPhee and Wightman 1991). Paleovalley-fills range between 60 and 100 m in thickness, although they more commonly are >90 m thick and filled mostly with strata of the McMurray Formation (Wightman *et al.* 1995). North of Township 90 deposits remain thick despite Pleistocene erosion and fan out laterally to form the informally termed "bitumount basin". This funnel-shaped low coincides with the region marked by dissolution of both the (Devonian) Prairie Evaporite and Cold Lake formations (see Fig. 1.9) (Wightman *et al.* 1991); the funnel-shaped geometry has led to speculations that it represents the position of a paleo-estuarine mouth (e.g. Wightman and Pemberton 1993). West of the salt low, sand thins to <50 m, except in local northeasterly-trending tributaries extending from the Grosmont High where sediment is up to 60 m thick.

The Wainright Ridge and associated spurs (Grosmont High, Beaver Hill Lake Spur) effectively confined most of McMurray deposition to the Main Valley. As a consequence, the western Athabasca region (Wabasca sub-basin) became virtually starved of sediment during much of McMurray time. Sediment thinned to <10 m thick over the Wainright Ridge and associated spurs, although locally may be up to 30 m thick. West of these ridges, in the Wabasca sub-basin, strata are dominated by 40-45 m thick accumulations of Wabasca Member sand. Where the McMurray Formation is preserved, successions are commonly mud-dominated, although locally 20-25 m thick sand successions occur and pinch out to the north.

THE McMURRAY FORMATION

Previous work

Since the late 1800s numerous geological publications have been produced on the Athabasca Oil Sands deposit (see Hein 2000 for a comprehensive review). Bell (1884) and McConnell (1891, 1893) produced the first geological descriptions of the Athabasca Oil Sands, identified this deposit as Lower Cretaceous in age and proposed a Devonian source for the bitumen. The name McMurray Formation was first proposed by McLearn (1917) to describe oil-impregnated sands overlying limestone deposits along the Athabasca River. Subsequent descriptions of the oil sands were almost exclusively conducted by Canadian governmental surveys along major rivers in the Athabasca Oil Sands region through to the mid 1900s (cf. Ells 1926). The most detailed and comprehensive of the early sedimentological studies in the McMurray Formation and Wabasca member of the

Clearwater Formation were conducted by Carrigy (1959, 1963a, b 1966, 1971, 1973) and Carrigy and Kramers (1973). Carrigy subdivided the McMurray Formation into lower, middle and upper units. This informal subdivision has persisted to the present, and many subsequent studies have adopted this three-fold subdivision.

In the 1970s and 1980s, there was a concerted effort to understand both the paleoenvironmental significance of McMurray Formation strata and the sedimentology of reservoir sand units. Early work by Carrigy (1971, 1973) and Nelson and Glaister (1978) interpreted strata of the McMurray Formation to be deltaic in origin. Subsequent individual and collaborative research by Flach and Mossop (cf. Mossop 1980a, b, Mossop and Flach 1983; Flach 1984; Flach and Mossop 1985) have also applied a deltaic model to detailed outcrop- and subsurface-based sedimentological studies. The seminal work by Flach and Mossop significantly advanced our understanding of the architectural elements of the McMurray Formation, with detailed subsurface mapping and correlations, estimations of paleochannel dimensions, and the incorporation of sedimentological, palaeontological, and ichnological data sets to assist with paleoenvironmental interpretations. Furthermore, their focus on sedimentological variability within reservoir sand units has had invaluable economic consequences.

Many of these studies sparked considerable debate over the extent of marine influence during McMurray Formation deposition – a debate that continued into the 1990s. In part, much of the confusion stemmed from the fact that McMurray Formation strata are essentially devoid of macrofossils. Furthermore, the few studies that have incorporated micropalaeontology into depositional models suggest non-marine to brackish-water conditions (Singh 1964; James 1977; Burden 1984; Flach and Mossop 1985; Sweet 2002). However, recent advances in ichnological research have more significantly improved our understanding of the palaeoenvironmental conditions during deposition (Pemberton *et al.* 1982). Ichnological assemblages within McMurray Formation strata comprise a low diversity, high abundance assemblage of diminutive and simple marine forms, suggesting stressed-ecological environmental conditions. Evidence of marine influence is apparent throughout McMurray deposition, especially within the upper member of the formation, suggesting that the overall interpretation is one of a fluvial system undergoing transgression (Flach and Mossop 1985). A brackish water interpretation has since been applied to several localized and regional studies of the McMurray Formation (cf. Mattison and Pemberton 1988; Bechtel *et al.* 1994; Yuill *et al.* 1994, Ranger and Pemberton 1997).

With the exception of work by Stewart and MacCallum (1978), many studies in the 1970s and 1980s disregarded the term "estuarine" to describe the McMurray palaeoenvironment. In part, this was because it was believed that true "estuarine" deposits must exhibit paleocurrent reversals and show evidence of a funnel-shaped physiography (cf. Flach and Mossop 1985). Although many researchers preferred to describe McMurray Formation strata as "deltaic", this interpretation was also acknowledged to be problematic because the general stratigraphy did not conform to the classic deltaic model whereby marine mud is gradationally overlain by delta-front sand (Flach and Mossop 1985). Rather, McMurray Formation strata exhibit an upward-fining succession, with an increase in marine influence stratigraphically upwards (Pemberton *et al.* 1982; Flach and Mossop 1985). With recent advances in both the estuarine facies model (Dalrymple *et al.* 1992) and in tidally-influenced sedimentation (cf. Smith 1988; Nio and Yang 1991), more recent researchers have interpreted McMurray Formation strata to have been deposited within an estuarine system (Mattison and Pemberton 1988; Ranger and Pemberton 1997; Wightman and Pemberton 1997).

In the 1990s considerable attention was focussed on creating a regional stratigraphic and palaeoenvironmental framework for the Athabasca Oil Sands deposit (Wightman *et al.* 1995; Ranger and Pemberton 1997; Wightman and Pemberton 1997; Wightman *et al.* 1997). With a better understanding of the regional geology of this deposit, along with improved reservoir stimulation technologies for subsurface production, a growing number of commercial *in-situ* pilot projects are being approved. As such, many recent studies have concentrated on innovative ways of mapping, modeling, and predicting the sedimentolgical variability within specific reservoir sand units of the McMurray Formation (cf. Langenberg *et al.* 2002; Blakney and Gingras 2002).

Stratigraphy and stratigraphic sub-divisions

Depositional age of the Mannville Group is constrained by palynomorphs, most of which suggest that sediment of the McMurray Formation was deposited from the Barremian to the end of the Aptian (see Burden 1984 for detailed discussion; also McLearn 1945; Singh 1964). Although one study suggests a much older age date for basal Mannville Group strata in the Athabasca Region (Late Valanginian or Hauterivian) (Burden 1984), this date has not been replicated by subsequent palynological analyses (F. Hein, personal communication, 2002). In other parts of the Western Canada Sedimentary Basin (WCSB), coeval strata include the Dina/Cummings members in Saskatchewan, the Cadomin and Gething formations and Ostracode member of the Bullhead Group in the northwest Alberta plains, the Ellerslie Formation and Ostracode member in the central Alberta plains, and the Cutbank and Sunburst members, the Bantry Shale and Ostracode member of the Lower Mannville Group of the southern Alberta plains (Fig. 1.5).

Historically, the McMurray Formation has been subdivided into three informal units: a lower fluvial-dominated, a middle estuarine point bar, and an upper coastal plain succession (Carrigy 1959; Stewart and MacCallum 1978). More recently, it has been suggested that the middle and upper members simply represent autocyclic changes within co-existing sub-environments, and therefore regionally correlatable chronostratigraphic surfaces separating these two members are not readily identifiable (Flach 1984; Flach and Mossop 1985; Wightman and Pemberton 1997; Hein *et al.* 2000; Hein and Dolby 2001; Lagenberg *et al.* 2002). Accordingly, Hein *et al.* (2000) suggested that a two-fold subdivision consisting of a lower fluvial and an upper estuarine/coastal plain succession be applied to regional McMurray stratigraphy. However, some lease-specific studies, like this one, have illustrated that significant lithological differences exist between middle and upper McMurray members to warrant the use of a tripartite subdivision (cf. Cody *et al.* 2001; see Chapter II).

The lower member of the McMurray Formation is characterized by massive to high-angle cross-stratified fine to coarse pebbly sand with common coal and rooted zones. Additionally, palynomorph assemblages and a general lack of bioturbation suggest that the lower member was deposited in a dominantly non-marine environment. Based on these observations, many researchers have interpreted the lower member to have been deposited in shallow (5-10 m) braided- to meandering-fluvial channels (Carrigy 1973; Flach and Mossop 1985) that were consistently restricted to paleotopographical lows on the sub-Cretaceous unconformity. The middle member of the McMurray Formation is dominated by shallow-dipping (10°-12°) interstratified fine sand and mud. Although originally interpreted to be fluvial lateral accretion deposits (Mossop and Flach 1983), more recent studies suggest that middle McMurray Formation strata were deposited within marine-influenced estuarine channels (e.g. Wightman and Pemberton 1997). These channels were created in response to a base level fall and incised older coastal bay, lagoon and shoreface sand (Pemberton *et al.* 1982; Ranger and Pemberton 1997). Middle McMurray estuarine deposits form the primary reservoir unit in the Athabasca Oil Sands and as a consequence considerable attention has been recently devoted to understanding the stratigraphic architecture of these strata (e.g. Cody *et al.* 2001). The upper member of the McMurray Formation consists of tidally-influenced deposits and/or marine bar sand (Flach and Mossop 1985). Commonly gas charged, the upper McMurray is thickest to the north in the vicinity of the bitumount basin (see Fig. 1.9).

STUDY AREA AND METHODOLOGY

The study area encompasses the Lewis property, an *in situ* oil sands lease currently owned and operated by Petro-Canada Oil and Gas. Lewis is situated approximately 40 km northeast of the city of Fort McMurray and encompasses Townships 91-92, and Ranges 6-8W4. In a paleogeographical context, Lewis is positioned just east of the main McMurray paleovalley and south of the bitumount basin (see Fig. 1.9). A database consisting of 161 geophysical well logs and 140 cored wells were available for study (Fig. 1.10). Each of these wells was used to

Figure 1.10: Location of logged cores, petrographical and palynological samples for this study.

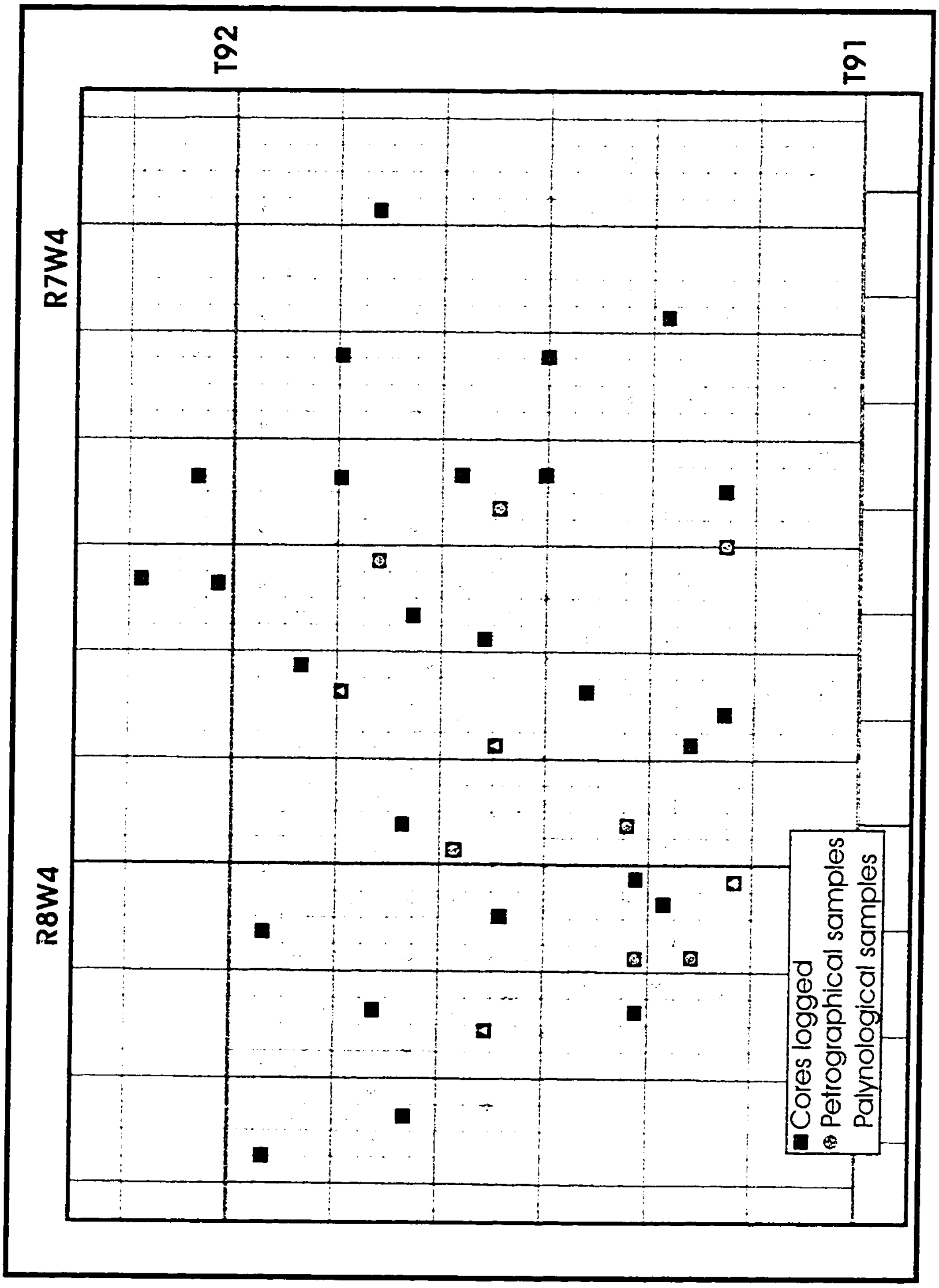
R7W4
R8W4
T92
T91
Cores logged
Petrographical samples
Palynological samples

1.10

determine regional stratigraphic horizons that assisted in lateral facies correlations and the creation of isopach and structural maps for the area (see Chapter II and Appendices 2 and 3). Over half of the available wells were used to determine cut-off values for gross sand and net pay maps (Appendix 2). Of the cored wells, 37 cores totalling more than 2800 m in length were selected for detailed study based on geographical position, well-concentration, and lithological variability based on geophysical well log attributes (Appendix 1). Additional cores and core photographs (provided by Petro-Canada Oil and Gas) were studied to help refine stratigraphic correlations. 21 petrographical samples were analyzed to determine mineralogy, textural attributes, and variability in bitumen staining (Appendix 5). Finally, 15 samples from 4 well locations were processed and analyzed for palynomorphs by Dr. A.R. Sweet of the Geological Survey of Canada (Sweet 2002 and Appendix 4).

OBJECTIVES

The primary objective of this study was to decipher the distribution of facies and the stratigraphic architecture of the McMurray Formation within the Lewis study area. These findings were then used to develop a detailed sedimentological model used to reconstruct the paleoenvironment of deposition. Because of the economic importance of the Athabasca Oil Sands deposit, emphasis was placed on identifying and understanding the distribution of both the main reservoir sand units and other sedimentolgical features that may form potential baffles and/or barriers to fluid flow within the reservoir. In order to better understand one of these reservoir units, a secondary focus of this thesis was to outline in some detail the depositional variables that control point-bar development. In particular, emphasis was placed on understanding the controls on sand- versus mud-dominated point-bars and the mechanisms responsible for mud deposition on marine-influenced point-bars.

STATEMENT OF CONTRIBUTION

This study builds on the well-established regional geology of the McMurray Formation by illustrating that changes in grain size, sediment flux, and accommodation space (lateral and vertical) significantly influenced the evolution of channel systems in the study area. The resultant stratigraphic changes ultimately control the quality and distribution of reservoir sand units, as well as the proportion of muddy interchannel (non-reservoir) deposits. Furthermore, this study has elaborated on previous methods used to estimate middle McMurray paleochannel dimensions by outlining sedimentological controls on tidal point-bar deposition, and using this information to distinguish between single- and amalgamated point-bar deposits. By doing so, this study has also revealed the necessity to conduct further research on modern tidal channels in order to improve our understanding of the geometric relationships of meandering-tidal channels and the tidal-point-bar facies model.

CHAPTER 2:

FACIES DISTRIBUTION AND STRATIGRAPHIC ARCHITECTURE OF THE LOWER CRETACEOUS McMURRAY AND CLEARWATER FORMATIONS, LEWIS PROPERTY, NORTHEASTERN ALBERTA

INTRODUCTION

The Western Canada Sedimentary Basin is host to significant volumes of natural gas, conventional, and heavy oil deposits. Of these deposits, the oil sands of northeastern Alberta represent most of this resource and it is estimated that within the next decade tar sand production will represent approximately three quarters of Alberta's total oil supply (Alberta Energy and Utilities Board 2001). The Athabasca Oil Sands is the most areally extensive of the 3 main deposits (Peace River, Athabasca and Cold Lake) (Fig. 2.1) and hosts nearly 207 billion cubic meters (10^9 m^3) of in-place bitumen (Alberta Energy and Utilities Board 2001), the majority of which occurs within the Lower Cretaceous McMurray Formation. Less than 10% of the Athabasca Oil Sands deposit, however, can be recovered using conventional surface mining techniques. Additional exploitation requires expensive reservoir stimulation methods, generally by steam injection, to facilitate subsurface production of viscous heavy oil. These stimulation methods require detailed subsurface mapping to understand stratal architecture and sand/mud ratios in order to maximize steam penetration into the reservoir sand. Subsurface mapping, however, has been persistently challenging due to the lithological and ichnological variability of McMurray Formation strata, the lack of regional correlatable

Figure 2.1: Location of the 3 major oil sands deposits in Alberta (Athabasca, Cold Lake, and Peace River) and 2 minor deposits (Wabasca and Lloydminister). Bitumen reserves from Alberta Energy and Utilities Board (2001). All bitumen-bearing formations are Lower Cretaceous except where indicated.

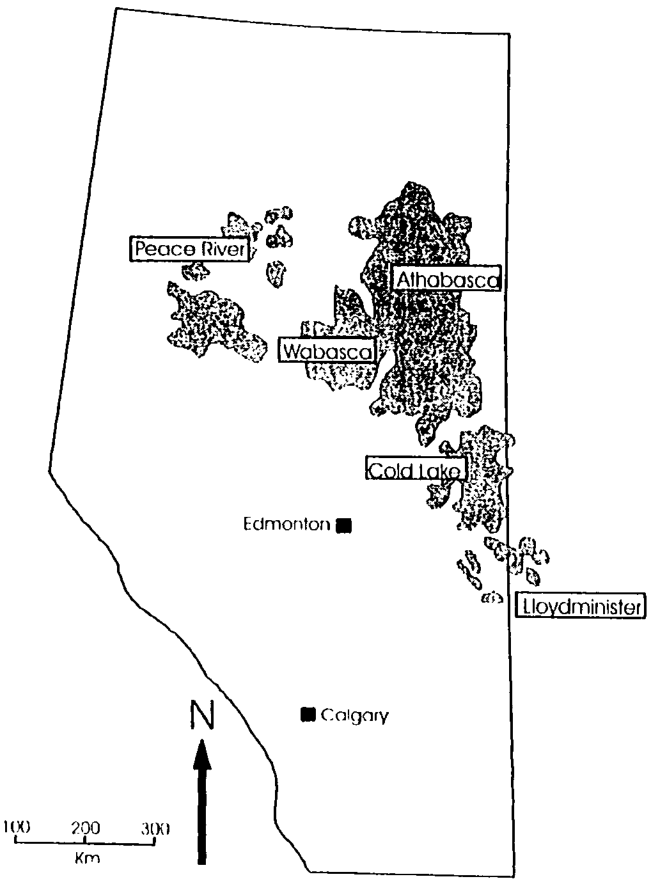

Area	Deposit	Areal Extent (10^3 Ha)	Average pay thickness (m)	Bitumen in place (10^6 m^3)
Athabasca	Grand Rapids	689	7.2	8678
	Wabiskaw-McMurray (mineable)	286	30.5	17998
	Wabiskaw-McMurray (in situ)	4329	19	119234
	Nisku Grosmont (Devonian)	4666	9.2	60830
				206 740
Cold Lake	Grand Rapids	1709	5.8	17304
	Clearwater	589	15	11051
	Wabiskaw-McMurray	658	5.8	3592
				31947
Peace River	Bluesky-Gething	1254	8.7	9926
	Belloy (Permian)	26	8.0	282
	Debolt Shunda (Mississippian)	471	18.3	10310
				20518

2.1

surfaces and recurrent lateral facies changes over only a few hundred meters. In recent years, high concentration drilling programs have been conducted in many oil sands production areas (cf. Mattison *et al.* 2001), which has permitted high resolution sedimentological and stratigraphic models to be developed that better delineate the allo- and auto-cyclical controls that influenced the distribution of facies and geometrical stacking patterns of strata in the McMurray Formation. Ultimately, the goal of these studies is to better delineate the distribution of reservoir sand and understand the depositional controls on sedimentological heterogeneities in order to maximize production and minimize capital expenditure.

Regional Stratigraphy and Depositional Setting

In the Athabasca Oil Sands region, strata of the Lower Cretaceous Mannville Group comprise the McMurray, Clearwater and Grand Rapids formations (Fig. 2.2). The McMurray Formation was deposited within topographical lows along the sub-Cretaceous unconformity during a longer-term transgression and consists of strata suggesting a change from fluvial through to brackish-water sedimentation. Although deposition never occurred under fully marine conditions, evidence of marine influenced sedimentation in the McMurray Formation becomes increasingly apparent stratigraphically upward and geographically northward (Jeletzky 1971; Ranger and Pemberton 1997). Deposition of the McMurray Formation was terminated by a fall of relative sea level (Strobl *et al.* 1993). The ensuing southward transgression of the Boreal Sea deposited shoreface sand of the Wabasca Member of the Clearwater Formation unconformably above the McMurray Formation. Continued transgression deposited the Clearwater Shale through the Athabasca region, the base of

Figure 2.2: Stratigraphy of the Athabasca Oil Sands deposit (from Wightman *et al.* 1995).

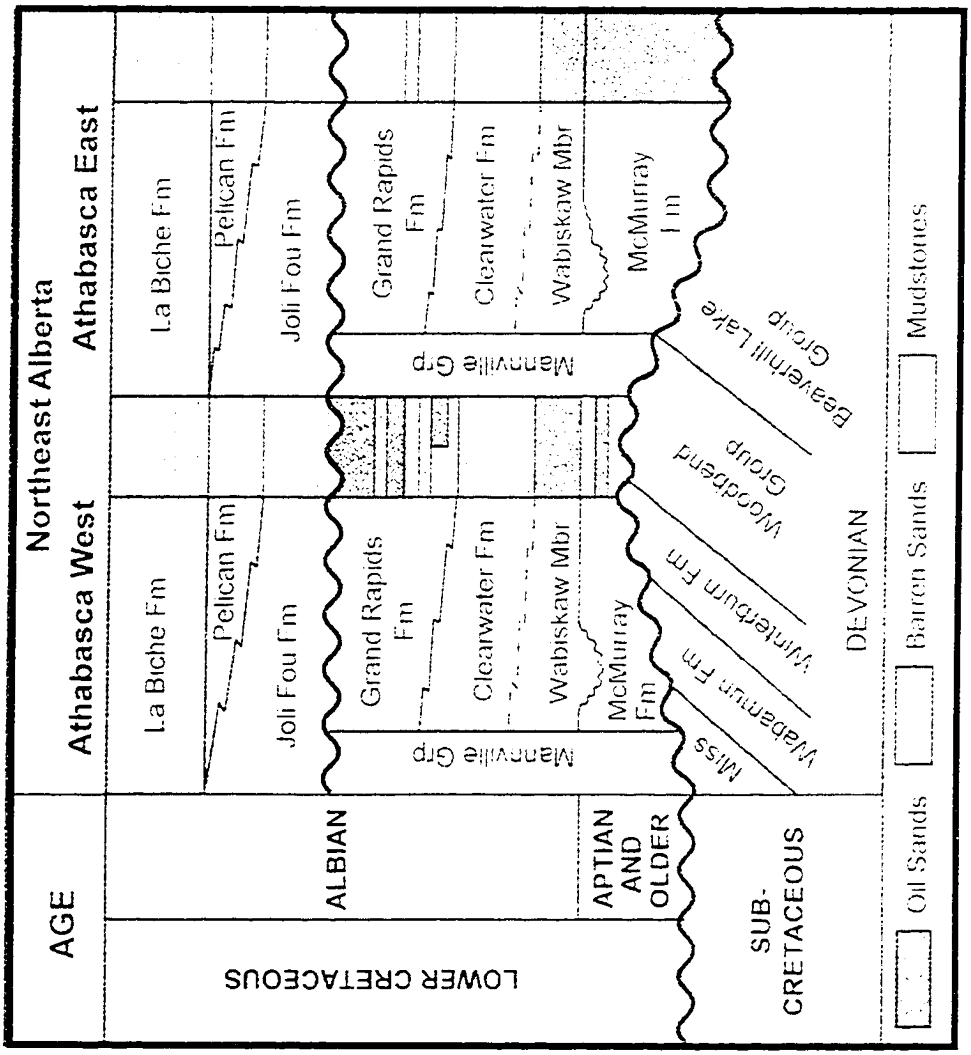

AGE
Northeast Alberta
Athabasca West
Athabasca East
LOWER CRETACEOUS
ALBIAN
APTIAN AND OLDER
SUB-CRETACEOUS
La Biche Fm
Pelican Fm
Joli Fou Fm
Grand Rapids Fm
Clearwater Fm
Wabiskaw Mbr
McMurray Fm
Mannville Grp
Miss
Wabamun Fm
Winterburn Fm
Woodbend Group
Beaverhill Lake Group
DEVONIAN
Oil Sands
Barren Sands
Mudstones

2.2

which represents a maximum marine flooding surface (MMFS). The Clearwater Formation is overlain by the Grand Rapids Formation which consists of a lower progradational deltaic sand unit and an upper transgressive shallow marine sand unit (Minken 1974). A fall of relative sea level, followed by transgression of both the northern Boreal and southern Gulfian seas and subsequent deposition of the Colorado Shale, marks the top of the Grand Rapids Formation and end of Mannville Group deposition (Jackson 1984).

The sub-Cretaceous unconformity, which significantly affected McMurray sedimentation, comprises a northwest-southeast trending ridge and valley system. In the Athabasca Oil Sands region, the paleotopography of the unconformity was significantly enhanced by dissolution in the underlying middle Devonian Prairie Evaporite Formation (Christopher 1974), which influenced McMurray sedimentation pre-, syn- and post-depositionally (McPhee and Wightman 1991; Wightman *et al.* 1991). Regionally, salt dissolution created a northwest-trending trough informally termed the main valley (Keith *et al.* 1990; McGillivray *et al.* 1992) where thick (60 m – 100 m) accumulations of McMurray Formation strata occur. North of Township 90 thick deposits fan out laterally to form the informally termed "bitumount basin", a funnel-shaped low coinciding with the region bounded to the east and west by the Prairie Evaporite and Cold Lake salt scarps (Fig. 2.3) (Wightman *et al.* 1991). The funnel-shaped geometry has led some authors to suggest that it represents the position of a paleo-estuarine mouth (cf. Wightman and Pemberton 1993).

Although the contact between the McMurray Formation and the Wabasca Member is a regional unconformity, the McMurray-Wabasca interval is considered to be a single reservoir unit, due largely to hydraulic connectivity formed by common sand-on-sand

Figure 2.3: Structural elements of the Athabasca region in relation to the Lewis study area. Central subbasin (Wightman *et al.* 1995) named Wabasca Subbasin by Ranger and Pemberton (1997), reflecting a thicker accumulation of Wabasca Member sands in this region. Diagram modified from Wightman *et al.* (1995).

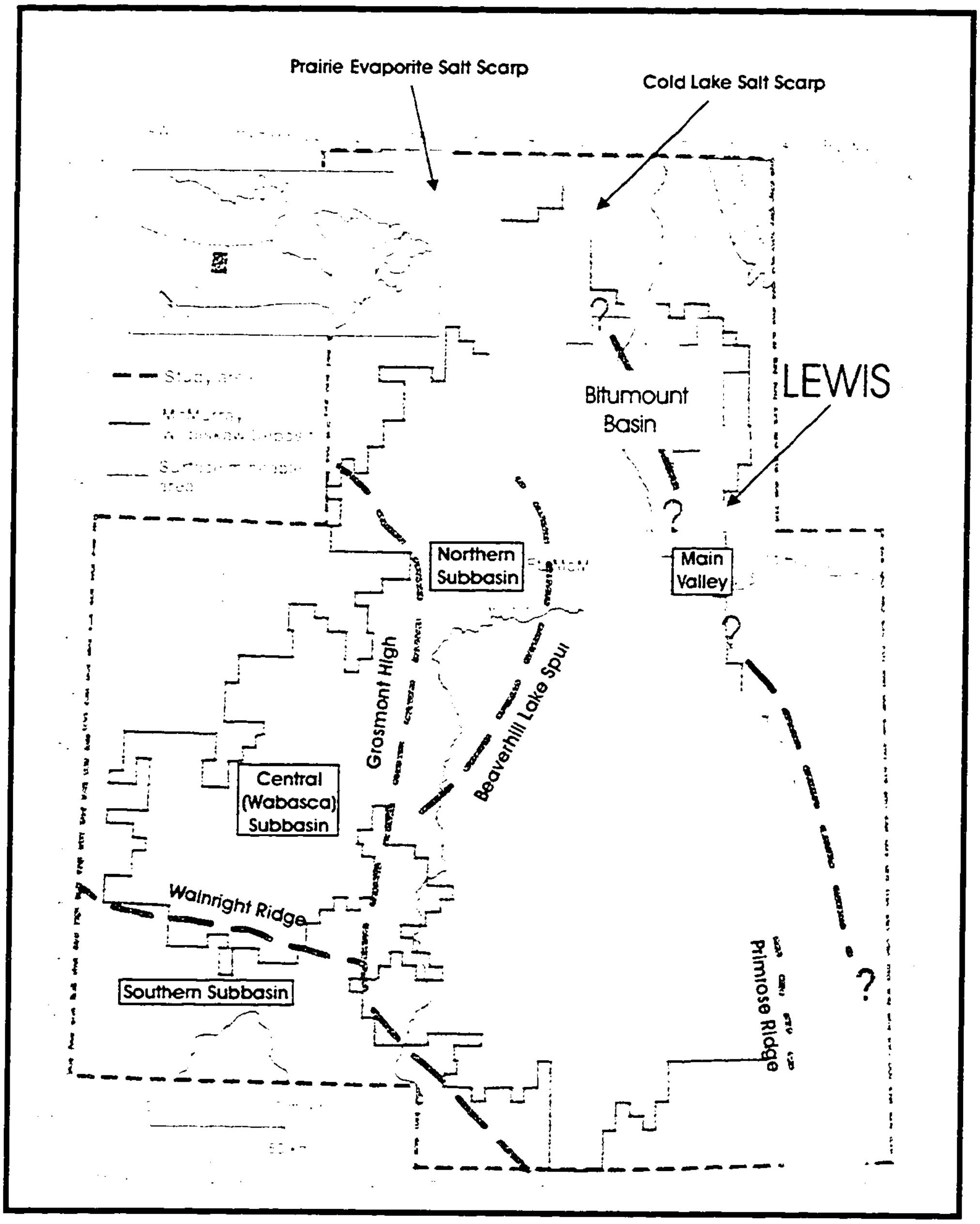
Prairie Evaporite Salt Scarp
Cold Lake Salt Scarp
LEWIS
Bitumount Basin
Northern Subbasin
Main Valley
Grosmont High
Beaverhill Lake Spur
Central (Wabasca) Subbasin
Wainright Ridge
Southern Subbasin
Primrose Ridge

2.3

contacts (Wightman *et al.* 1995). The majority of the bitumen reserves in the Athabasca Oil Sands deposit occur in the McMurray/Wabasca interval, although most of the reserve occurs within the thicker McMurray Formation (Wightman *et al.* 1995). In the western Athabasca region, also termed the Wabasca sub-basin by Ranger and Pemberton (1997), the Wabasca Member forms the primary reserve (Fig. 2.3). The Grand Rapids Formation, if present, is typically thin and does not contain significant reserves in the Athabasca region (Wightman *et al.* 1995). Within the Lewis study area, the majority of the bitumen occurs within the McMurray Formation.

Historically, the McMurray Formation has been subdivided into 3 informal units: a lower fluvial-dominated, a middle estuarine point-bar, and an upper coastal plain succession (Carrigy 1959). In recent years, it has been suggested that the middle and upper members simply represent autocyclic changes within co-existing sub-environments, and therefore regionally correlatable chronostratigraphic surfaces separating these two members are not readily identifiable (Flach 1984; Flach and Mossop 1985; Wightman and Pemberton 1997; Hein *et al.* 2000; Hein and Dolby 2001; Lagenberg *et al.* 2002). Accordingly, Hein *et al.* (2000) suggested that a two-fold subdivision consisting of a lower fluvial and an upper estuarine/coastal plain succession be applied to regional McMurray stratigraphy. However, some lease-specific studies, like this one, have demonstrated that sufficient lithological differences exist between middle and upper McMurray members to warrant the use of a tripartite subdivision (cf. Cody *et al.* 2001).

The lower member of the McMurray Formation is characterized by massive to high-angle cross-stratified fine to coarse pebbly sand with common coal and rooted zones.

Additionally, palynomorph assemblages and a general lack of bioturbation suggest that the lower member was deposited in a dominantly non-marine environment. Based on these observations, many researchers have interpreted the lower member to have been deposited within shallow (5-10 m) braided- to meandering-fluvial channels (Carrigy 1973; Flach and Mossop 1985) that were restricted to paleotopographical lows along the sub-Cretaceous unconformity. The middle member of the McMurray Formation is dominated by shallow-dipping (10°-12°) intercalations of fine sand and mud. Although originally interpreted to be laterally-accreting fluvial deposits (Mossop and Flach 1983), more recent studies suggest that middle McMurray Formation strata were deposited within marine-influenced estuarine channels (Smith 1987; Wightman and Pemberton 1997). Middle McMurray estuarine deposits form the primary reservoir unit within the Athabasca Oil Sands and in recent years considerable attention has been given to the origin of these strata and their areal distribution (Cody *et al.* 2001). The upper member of the McMurray Formation consists of tidally-influenced deposits and/or marine bar sands (Flach and Mossop 1985). Commonly gas charged, these strata are thickest to the north in the vicinity of the bitumount basin.

Database and Methodology

The study area encompasses the Lewis property, an *in situ* oil sands lease currently owned and operated by Petro-Canada Oil and Gas. The Lewis property is situated approximately 40 km northeast of the city of Fort McMurray, Alberta and encompasses Townships 91-92, and Ranges 6-8W4. In a paleogeographical context, Lewis occurs just east of the main McMurray paleovalley and south of the bitumount sub-basin (Fig. 2.3). A database consisting of 161 geophysical well logs and 140 cored wells were available for study (Fig. 2.4). Each of these wells was used to determine regional stratigraphic horizons that assisted in lateral facies correlations and formulation of a variety of maps based on these correlations (Appendices 2 and 3). Over half of the available wells were used to determine cut-off values for gross sand and net pay maps (Appendix 2). Of the cored wells, 37 cores totalling more than 2800 m in length were selected for detailed study according to geographical position, well-concentration, and lithological variability based on geophysical well log attributes (Appendix 1). Additional cores and core photographs (provided by Petro-Canada Oil and Gas) were studied in order to refine stratigraphic correlations. 21 petrographical samples were analyzed to determine mineralogy, textural attributes, and variability in bitumen staining (Appendix 5). Finally, 15 samples from 4 well locations were processed and analyzed for palynomorphs by Dr. A.R. Sweet of the Geological Survey of Canada (Sweet 2002 and Appendix 4).

DEPOSITIONAL FACIES AND FACIES ASSOCIATIONS

Based on grain size, sand/mud ratios, physical sedimentary structures and ichnology, the McMurray and Clearwater formations have been subdivided into 8 distinct facies that are described and interpreted in Table 2.1. Facies, in turn, are organized into 5 facies associations (FA) (Table 2.2) based on geometric stacking patterns and genetic relationships. The distribution of facies and facies associations are strongly affected by the paleotopography along the sub-Cretaceous unconformity (Fig. 2.5). FA1 consists of

Figure 2.4: Location of measured cores, petrographical and palynological samples for this study. Location of stratigraphic cross-sections (Figs. 2.6-2.7 (bold) and Appendix 2) are also shown. Note also that the location of the modern Lower Steepbank River roughly coincides with the position of the main Cretaceous-aged paleovalley where the thickest accumulation of McMurray Formation sand occurs (see Figs. 2.39-2.40).

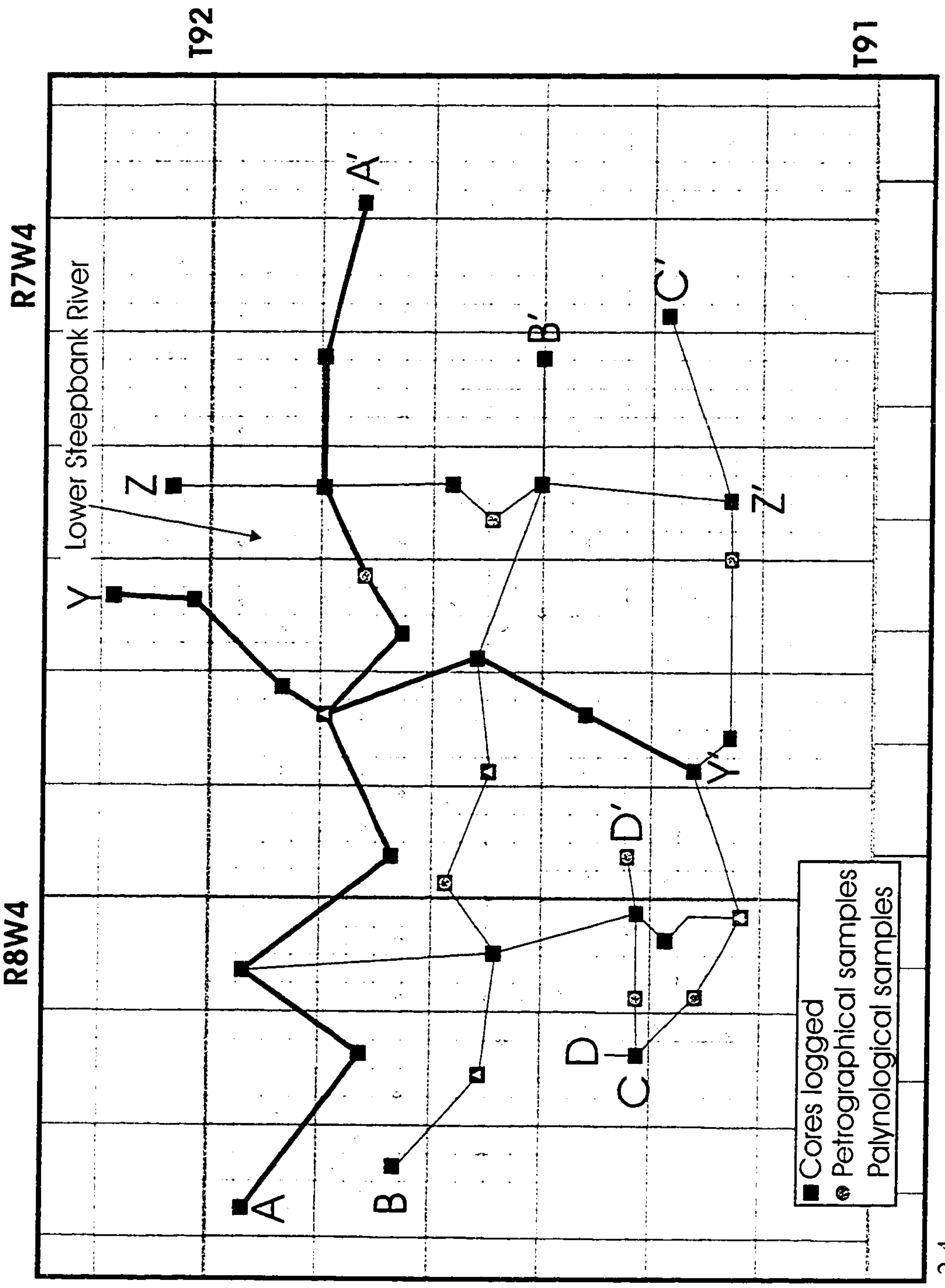

R8W4
R7W4
T92
T91
Lower Steepbank River
A
A'
B
B'
C
C'
D
D'
Y
Y'
Z
Z'
Cores logged
Petrographical samples
Palynological samples
2.4

Table 2.1: Summary of description and interpretations of the 8 facies identified in the Lewis study area.

Facies		Grain Size & Sorting	Physical Sedimentary Structures		Ichnology/Palaeontology		Thickness
F1 Moderately well sorted cross-stratified sand with mud	**F1a** Cross-stratified sand	fL to mU +/- qz pebbles; Abrupt cm- to m-scale gs changes; moderately well sorted	Med- to small-scale cross-stratification		absent to rare *Planolites*, *Cylindrichnus*, *Ophiomorpha* in clasts	Absent or rare *Cylindrichnus*, *Rosselia*	<5-30 m
	F1b Cross-stratified sand with mud			Mud layers: Lenticular, wavy, +/- pin-stripe lamination		Uncommon *Planolites*; rare *Skolithos*, *Ophiomorpha*, and *Cylindrichnus* in mud	
F2 Poorly-sorted pebbly sand		Silt to pebble Poorly sorted	Massive bedding Medium-scale cross-stratification		absent		<5-10's of meters; 10-12 m avg.
F3 Glauconitic silty-sand		Silt to mL sand; moderate to well sorted	Obliterated by bioturbation		Common to abundant; dm-length *Skolithos*; *Teichichnus* and *Rosselia*		Typically <1 m; up to 7 m
F4 Mottled clay		Clay to silt; pebbles	Fissile to massive; convoluted bedding locally		Absent		<1-5 m
F5 Unbioturbated mudstone		Clay to silt; local vfU to mU sand beds	Fissile to massive mud; massive sand		Abundant terrestrial gymnosperm pollen and fern spores; rare to abundant dinoflagellates; brackish-water algae and pollen; bioturbation absent in mud; variable trace fossil assemblages in sand (absent/rare or abundant and cryptic); dominant burrows: *Gyrolithes*, *Rosselia*, *Cylindrichnus*, *Palaeophycus*, *Planolites*		2-30 m; 12 m avg.
F6 *Chondrites* burrowed mudstone		Clay to silt; rare glauconitic sand	Fissile to massive		Abundant *Chondrites*; *Skolithos*, *Planolites*		10's of m
F7 Inclined heterolithic stratification (IHS) /epsilon cross stratification	**F7a** Epsilon cross-stratified or sand-dominated IHS	Well to v. well sorted fL to fU sand interstratified at low angle inclined with silt and/or mud layers	Small-, med-scale cross stratification or massive bedding in sand; mud layers variable: cm-dm thick mud beds; cm-dm thick laminated sand/silt beds (wavy, lenticular, or pinstripe)		Uncommon *Cylindrichnus* in sand; mud beds variable: unbioturbated; rare *Planolites* and/or *Ophiomorpha*; common-abundant low diversity diminutive traces including any of (*Cylindrichnus*, *Planolites*, *Ophiomorpha*, *Rosselia*, *Gyrolithes*, *Asterosoma*, *Teichichnus*, *Skolithos*, *Thalassinoides*, escape traces)		10-30 m; 20-25 m avg.
	F7b Mud-dominated IHS						<5-25 m; 15-20 m avg.
F8 Horizontally stratified sand/mud		v.Well sorted; vf to f sand and mud	Asymmetrical ripples in sand; starved ripples common; structures commonly obliterated by bioturbation		Variable; rare *Planolites*, *Skolithos* to diverse, mottled bioturbate texture including any of *Planolites*, *Skolithos*, *Teichichnus*, *Rosselia*, *Arenicolites*, *Cylindrichnus*, escape traces; sharp bioturbated contacts common		<1-23 m

Physical Sedimentary Structures		Ichnology/Palaeontology		Thickness	Other Characteristics	Interpretation	Occurrence
led- to all-scale cross- tification	Mud layers: Lenticular, wavy, +/- pin-stripe lamination	absent to rare *Planolites*, *Cylindrichnus*, *Ophiomorpha* in clasts	Absent or rare *Cylindrichnus*, *Rosselia* Uncommon *Planolites*; rare *Skolithos*, *Ophiomorpha*, and *Cylindrichnus* in mud	<5-30 m	Mud, coal, and wood clasts common	Fluvial to tidally-influenced channel-fill; fluctuating low to moderate energy; bedload transport; unidirectional flow; mud = waning flow (fluvial or tidal where rhythmic); clasts = bank collapse; biot.= temporal changes in ecological conditions possibly related to periodic salt-water intrusion	Mostly at base of Facies Association 2; F1a also occurs in upper part of Facies Association 1
Massive bedding Medium-scale cross-stratification		absent		<5-10's of meters; 10-12 m avg.	Rare mud clasts, roots; common coal clasts, organic debris	Braided-fluvial system; high energy unidirectional flow (dunes), episodes of rapid deposition, or local bank collapse (massive)	Facies Association 1; locally in Facies Association 2
literated by bioturbation		Common to abundant; dm-length *Skolithos*; *Teichichnus* and *Rosselia*		Typically <1 m; up to 7 m	glauconite	Marine shoreface; glauconite indicates slow sedimentation rates	Facies Association 5
ile to massive; convoluted bedding locally		Absent		<1-5 m	Mottled; waxy; granular to crumbly	Soil	Facies Association 1, 3
issile to massive mud; massive sand		Abundant terrestrial gymnosperm pollen and fern spores; rare to abundant dinoflagellates; brackish-water algae and pollen; bioturbation absent in mud; variable trace fossil assemblages in sand (absent/rare or abundant and cryptic); dominant burrows: *Gyrolithes*, *Rosselia*, *Cylindrichnus*, *Palaeophycus*, *Planolites*		2-30 m; 12 m avg.	Local mottles; rare coalified roots, coal clasts; common organic debris; carbonate cemented beds	Terrestrial floodbasin/ swamp; ichnology and palynology suggest definitive marine influence and fluctuating salinity; low energy, suspension settling; sand possibly from adjacent channels (flood episodes)	Facies Association 3
Fissile to massive		Abundant *Chondrites*; *Skolithos*, *Planolites*		10's of m	Calcite cemented bands; rare pyrite	Low energy, offshore	Facies Association 5
mall-, med-scale cross ratification or massive ding in sand; mud layers able: cm-dm thick mud ; cm-dm thick laminated sand/silt beds (wavy, nticular, or pinstripe)		Uncommon *Cylindrichnus* in sand; mud beds variable: unbioturbated; rare *Planolites* and/or *Ophiomorpha*; common-abundant low diversity diminutive traces including any of (*Cylindrichnus*, *Planolites*, *Ophiomorpha*, *Rosselia*, *Gyrolithes*, *Asterosoma*, *Teichichnus*, *Skolithos*, *Thalassinoides*, escape traces)		10-30 m; 20-25 m avg. <5-25 m; 15-20 m avg.	Mud clasts locally; rare coal	Lateral accretion deposits produced by tidal point bar migration; sand-dominated = higher energy; silt-dominated = lower energy; biot. indicative of brackish water conditions	Facies Association 2
nmetrical ripples in sand; rved ripples common; structures commonly iterated by bioturbation		Variable; rare *Planolites*, *Skolithos* to diverse, mottled bioturbate texture including any of *Planolites*, *Skolithos*, *Teichichnus*, *Rosselia*, *Arenicolites*, *Cylindrichnus*, escape traces; sharp bioturbated contacts common		<1-23 m	Synaeresis cracks; coal and organic debris; soft sediment deformation, microfaulting common	Tidal flat; tidal rhythmicity	Facies Association 4; minor component of Facies Association 3

Table 2.2: Description, interpretation, and sequence stratigraphic nomenclature of facies associations in the Lewis study area. Lower, middle, and upper refer to informal members of the McMurray Formation and are labelled according to the dominant facies association within them, although there is some overlap. CW = Clearwater Formation. LST = lowstand systems tract; TST = transgressive systems tract; HST = highstand systems tract.

Stratigraphic unit	Facies Association		Facies	Interpretation	Systems Tract
Lower	FA1	Fluvial channel association	F1, F2	Braided-fluvial system	LST
Middle	FA2	Tidally-influenced channel deposits	F1, F7	Tidally-influenced fluvial deposits and IHS	TST
	FA3	Abandoned channel/interdistributary deposits	F4, F5, F8	Soils, mixed tidal flats and swamps	
Upper	FA4	Tidal flat association	F1, F8	Mixed tidal flats, tidal bars and channels	
CW	FA5	Shoreface to offshore association	F3, F6	Shoreface sand and offshore mud	HST

Figure 2.5: Structure and isopach maps illustrating the influence of the sub-Cretaceous unconformity on sediment distribution in the Lewis study area.

Figure 2.5 (a): Structure map of the top of the sub-Cretaceous unconformity. Structural lows are interpreted to be due to local salt dissolution in the middle Devonian Prairie Evaporite Formation.

Figure 2.5 (b): Isopach map of the McMurray/Wabasca interval (top of the Devonian to the base of the Clearwater Shale). Because the base of the Clearwater Shale is a regional flooding surface and therefore approximately horizontal (see Chapter I) this map represents the paleotopography of the sub-Cretaceous unconformity. Note that the thickest areas of sediment accumulation coincide with structural lows on the sub-Cretaceous unconformity (Fig. 2.5(a)).

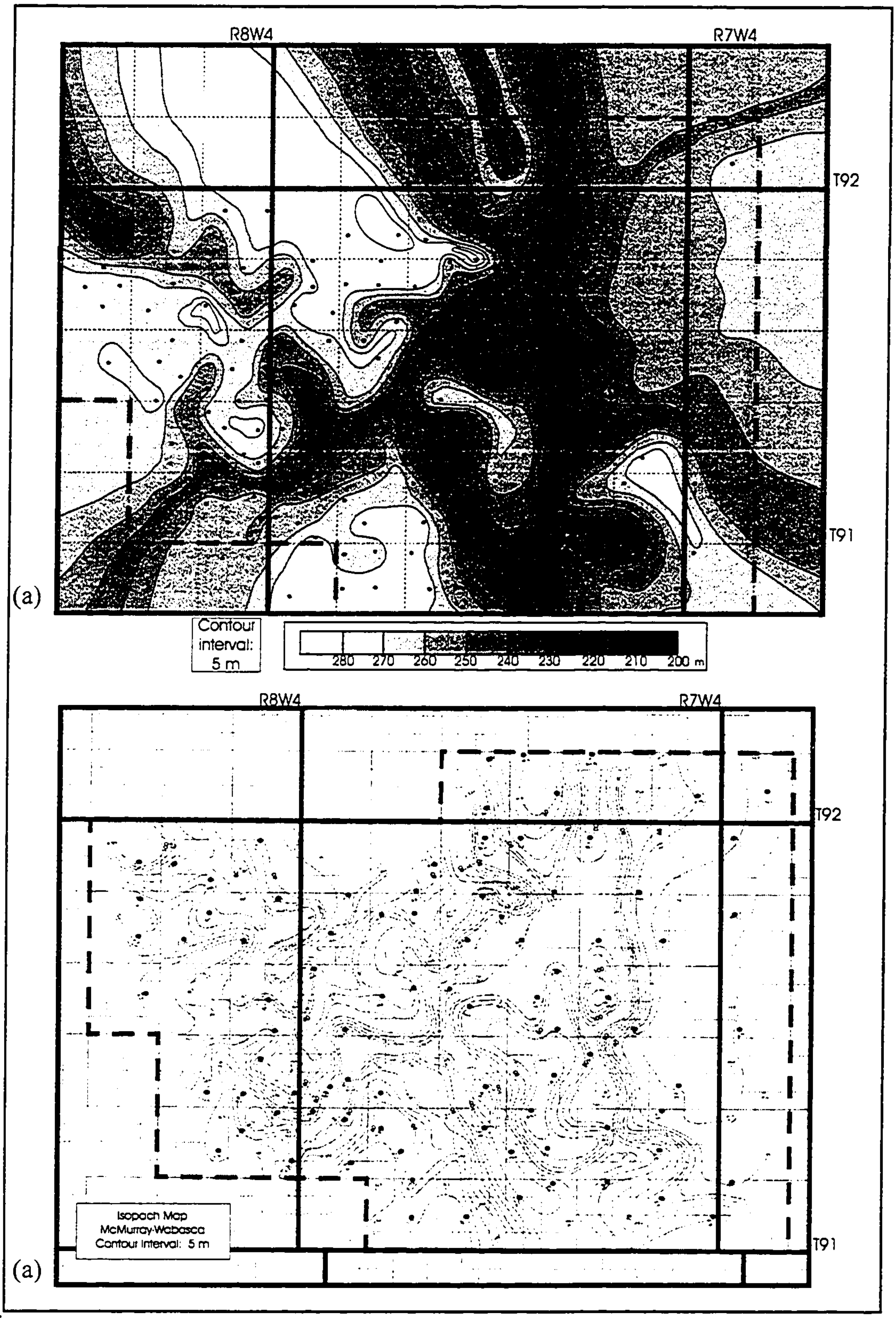
R8W4
R7W4
T92
T91
(a)
Contour interval: 5 m
280 270 260 250 240 230 220 210 200 m
R8W4
R7W4
T92
T91
Isopach Map
McMurray-Wabasca
Contour Interval: 5 m
(a)

2.5

lowstand fluvial deposits of the lower McMurray Formation and are preserved only within paleo-lows along the sub-Cretaceous unconformity. These are overlain abruptly by transgressive deposits of the middle McMurray Formation which comprise tidally-influenced channel fills (FA2) and associated tidal flat and interchannel deposits (FA3). Continued transgression resulted in deposition of upper McMurray open estuarine deposits of FA4. FA5 represents transgressive shoreface and offshore deposits of the Clearwater Formation. Two stratigraphic cross-sections (Figs. 2.6-2.7) and a series of facies slice maps (Fig. 2.8) measured at 10 m increments beneath the base of the Clearwater Shale are included to show relationships between key facies and facies associations

Facies Descriptions and Interpretations

<u>Facies 1: Moderately well sorted medium cross-stratified sand with mud</u>

Subfacies 1a: Cross-stratified sand

Facies 1a is composed of moderately well sorted lower fine to upper medium-grained sand with uncommon sub-rounded to angular quartz pebbles commonly oriented parallel to cross-stratification. Abrupt fining- and coarsening-upward successions commonly occur within this facies, although meter-scale gradational contacts are present locally (Fig. 2.9). Mineralogy is dominated by sub-angular to sub-rounded quartz, which is mostly monocrystalline and undulatory. Chert is common but makes up no more than 5% of the

Figure 2.6: West to east stratigraphic cross-section through the Lewis study area illustrating the lateral relationships between major facies. Correlations, facies, and facies associations interpretations are based on observations in core. Cored interval is indicated by the blue bar. Datum is the base of the Clearwater Shale, a regional flooding surface.

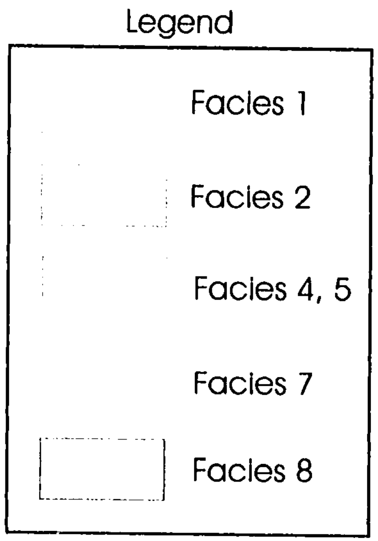

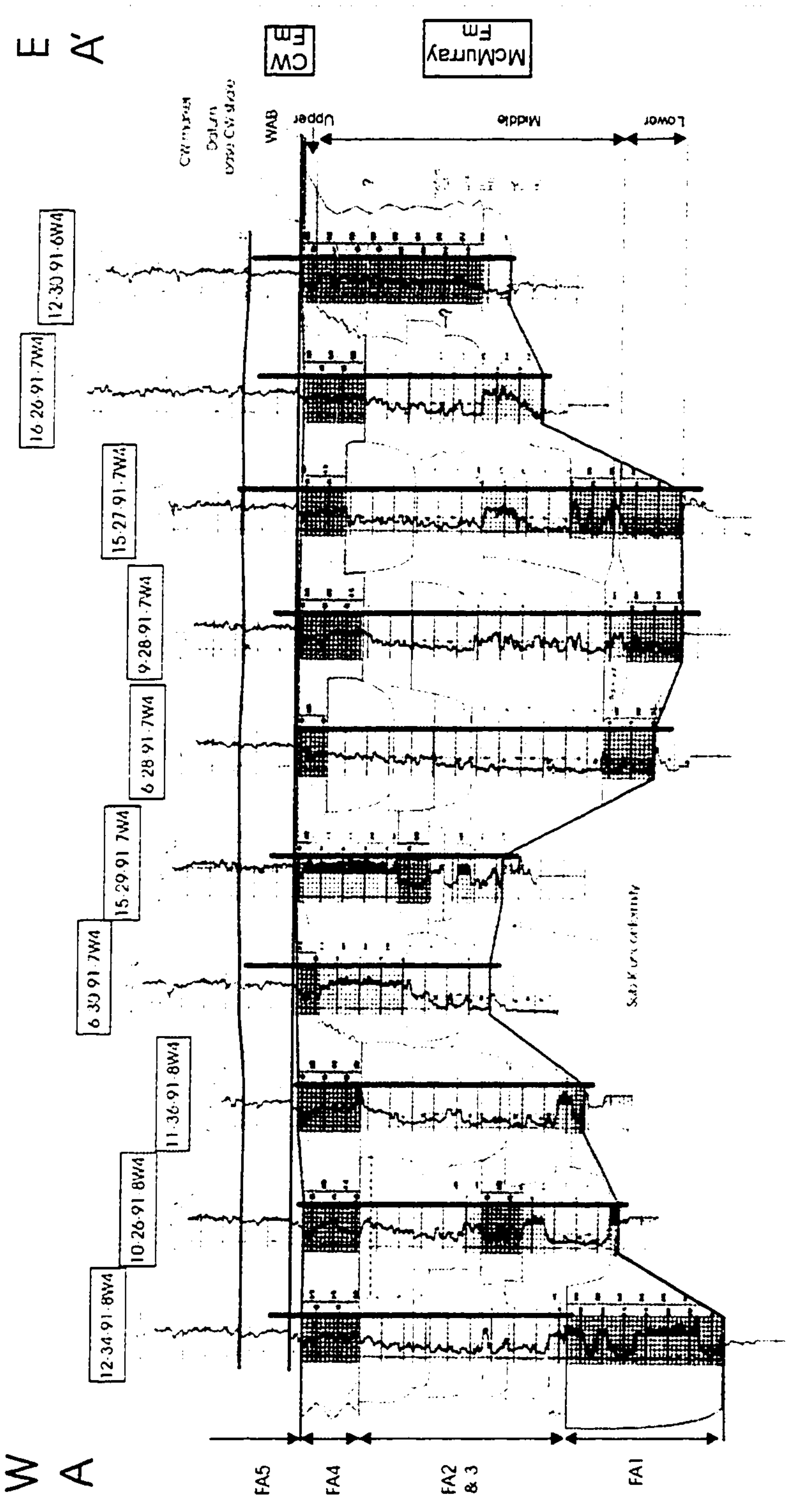
W
A
E
A'
12-30-91-6W4
16-26-91-7W4
15-27-91-7W4
9-28-91-7W4
6-28-91-7W4
15-29-91-7W4
6-30-91-7W4
11-36-91-8W4
10-26-91-8W4
12-34-91-8W4
CW Fm
McMurray Fm
WAB
Upper
Middle
Lower
FA5
FA4
FA2 & 3
FA1

2.6

Figure 2.7: North to south stratigraphic cross-section through the Lewis study area illustrating the lateral relationships between major facies. Correlations, facies, and facies associations interpretations are based on observations in core. Cored interval indicated by the blue bar. Datum is the base of the Clearwater Shale, a regional flooding surface. See Figure 2.6 for legend.

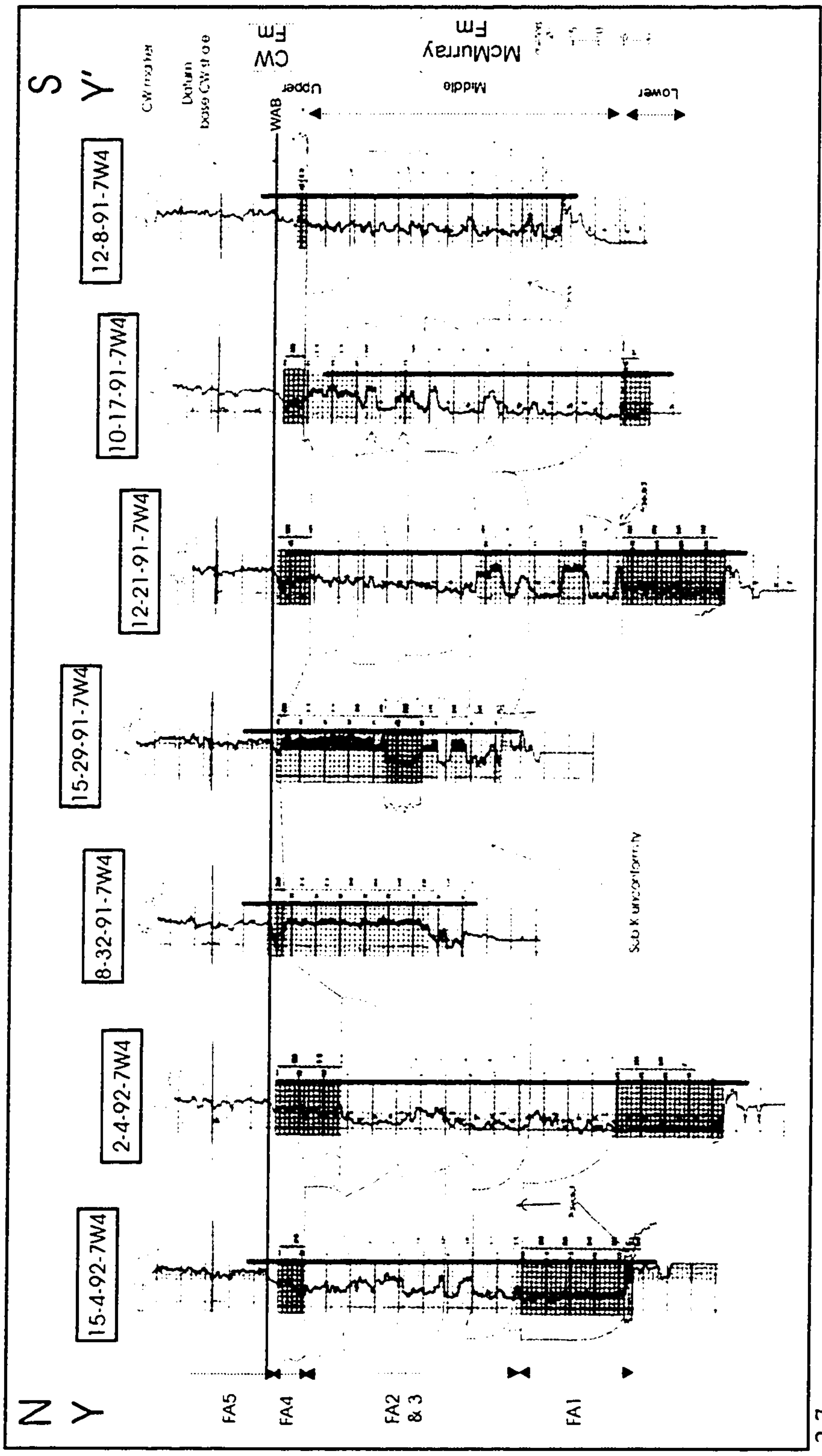

N
Y
S
Y'
15-4-92-7W4
2-4-92-7W4
8-32-91-7W4
15-29-91-7W4
12-21-91-7W4
10-17-91-7W4
12-8-91-7W4
WAB
Upper
Middle
Lower
CW Fm
McMurray Fm
FA5
FA4
FA2 & 3
FA1

2.7

Figure 2.8: Facies slice maps measured at 10 m increments beneath the base of the Clearwater Shale.

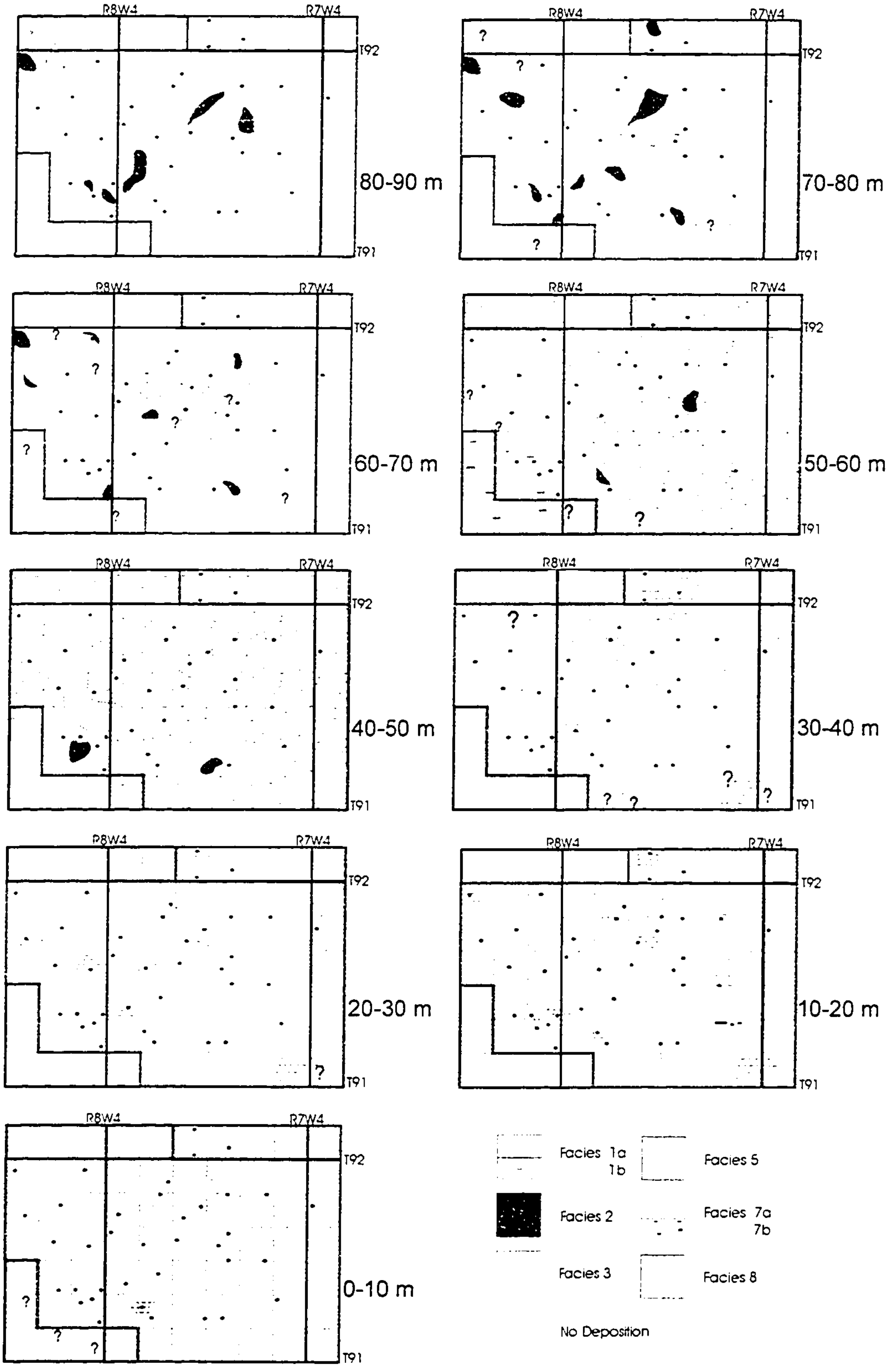

R8W4
R7W4
T92
T91
80-90 m
70-80 m
60-70 m
50-60 m
40-50 m
30-40 m
20-30 m
10-20 m
0-10 m
Facies 1a
1b
Facies 2
Facies 3
Facies 5
Facies 7a
7b
Facies 8
No Deposition

2.8

Figure 2.9: Facies 1: Abrupt upward-fining and -coarsening beds. Photo from well 12-34-91-8W4, Core 25 2 of 2, 180.5 m depth. Penny is 19 mm diameter.

Figure 2.10: Cross stratified medium-grained sand of Facies 1

Figure 2.10 (a): Medium- and small-scale cross-stratification is made evident by changes in grain size and associated lean bitumen staining. Photo from well 2-22-91-7W4, Core 31 1 of 2 and Core 30 2 of 2, ~208 m -211 m depth. Core boxes are 75 cm long.

Figure 2.10 (b): Medium-scale cross-stratified sand cropping out along the Christina River. Stripe pattern is the result of alternating bitumen stained (black) upper fine sand and water-bearing (white) lower- to upper-medium sand. Backpack for scale.

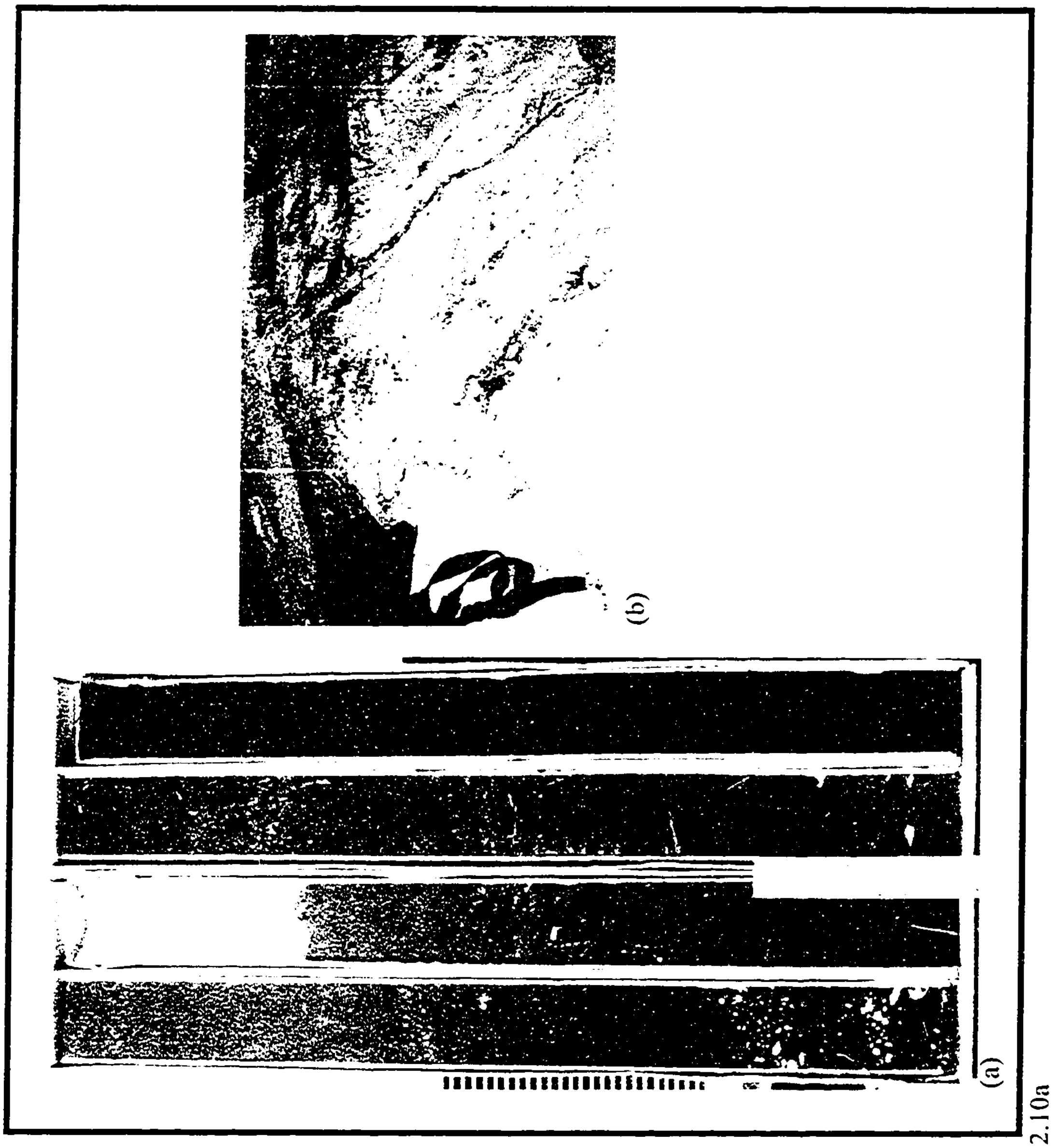

2.10a

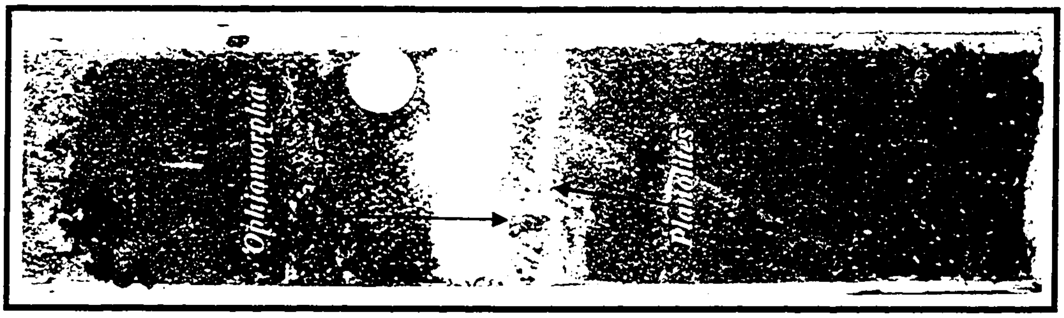

2.9

framework grains, feldspars no more than 4% and muscovite and zircon occur as accessory minerals.

Sand in this facies is typically bitumen saturated, making the identification of physical sedimentary structures in core commonly problematic. Best discerned by fractures in core and/or alternating light/dark bitumen staining, physical sedimentary structures of F1 are dominated by medium-scale, planar-tabular or trough cross-stratification (Fig. 2.10). Small-scale cross-stratification is typically only resolvable where bitumen staining is not as pervasive. Carbonaceous material, mainly in the form of coal fragments, wood clasts and >5 cm thick horizons of organic debris, is common; decimeter- to meter-thick low grade coal layers are also observed (Fig. 2.11). Bioturbation is generally absent in this sub-facies, although rare *Cylindrichnus* and *Rosselia* are observed.

Mud clasts are common and range from plate to angular equant shapes; platy clasts are typically imbricated parallel to cross-stratification. Some clasts are internally inter-laminated with bitumen-saturated very fine sand and mud, and may also be burrowed with rare, diminutive *Planolites* or *Cylindrichnus* and/or large *Ophiomorpha* (Fig. 2.12). Clast size is variable, ranging from 0.5 cm to greater than 1 meter in thickness (thick clasts are differentiated from beds by the occurrence of internal soft sediment deformation and very high angle (>>30°) irregular clast/sand bed contacts (Fig. 2.13)). Although generally dispersed in a sand matrix, clasts commonly occur in highly concentrated horizons that range from a few centimeters to several meters thick. Uncommonly, clasts are pyritized or sideritized.

Figure 2.11: Facies 1. Very fine-grained sand bed interlaminated with carbonaceous debris. Photo from well 1-12-91-8W4, Core 21 1 of 2, ~176 m depth. Scale is 25 mm diameter.

Figure 2.12: Facies 1. Abundant mud clasts in F1 sand. Note silt interlaminae (pin-stripe lamination) and rare *Planolites* burrows in some clasts. Photo from well 9-28-91-7W4, 204.6 m – 206.2 m depth. Core boxes 75 cm long.

Figure 2.13: Facies 1. Deformed large mud clasts. Photo from well 15-4-92-7W4, 186.7 m – 188.2 m depth. Core boxes 75 cm long.

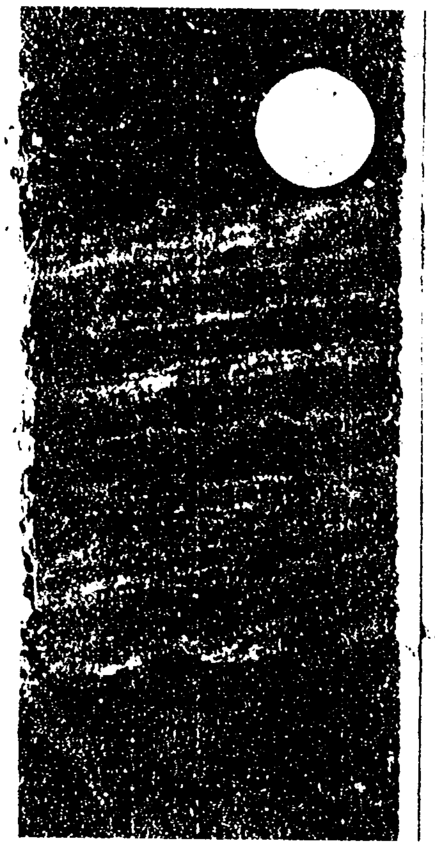

2.11


Pin-stripe lamination
Planolites

2.12


Large, deformed breccia clasts

2.13

Subfacies 1b: Cross-stratified sand with silt

In places, sand (F1a) is interstratified with laterally discontinuous, irregularly-spaced silt beds and/or successions of interlaminated silt and sand layers (Fig. 2.14). Silt beds are commonly less than 5 cm thick, whereas interlaminated layers may reach thicknesses of up to 10-15 cm. Pin-stripe lamination is observed locally, but more commonly interlaminated layers display lenticular and wavy bedding (Fig. 2.15). Silt beds and pin-stripe laminated sand and silt layers are generally unbioturbated, whereas uncommon *Planolites*, and rare *Skolithos*, *Ophiomorpha* and *Cylindrichnus* burrows are observed in lenticular and wavy bedded sand and silt.

Interpretation:

F1 was deposited under moderate to high energy unidirectional flow conditions producing medium- (dunes) and rare small- (current ripples) scale bedforms. Fluctuations in current energy and flow depth are made evident by the pervasiveness of abruptly graded beds and dispersed quartz pebbles. Alternatively, bedding-parallel quartz pebble layers may represent erosional lags. Waning flow and low energy conditions are manifested in F1 by normally graded beds, *in situ* coal beds and (in F1b) silt layers. The frequent but irregular changes in flow velocity and depth that produced F1 strata are commonly observed in modern fluvial systems where fluctuations in discharge is generally a seasonally-related phenomenon (e.g. Gastaldo *et al.* 1995). Furthermore, the abundance of organic material, in particular *in situ* coal beds, suggests a dominantly non-marine sediment source. Angular mud clasts suggest limited transport and are interpreted to have been eroded from fine-

Figure 2.14: Facies 1. Uncommon silt/mud layers in F1 sand. Photo from well 2-4-92-7W4, 197.7 m – 201.5 m depth. Core box 75 cm long.

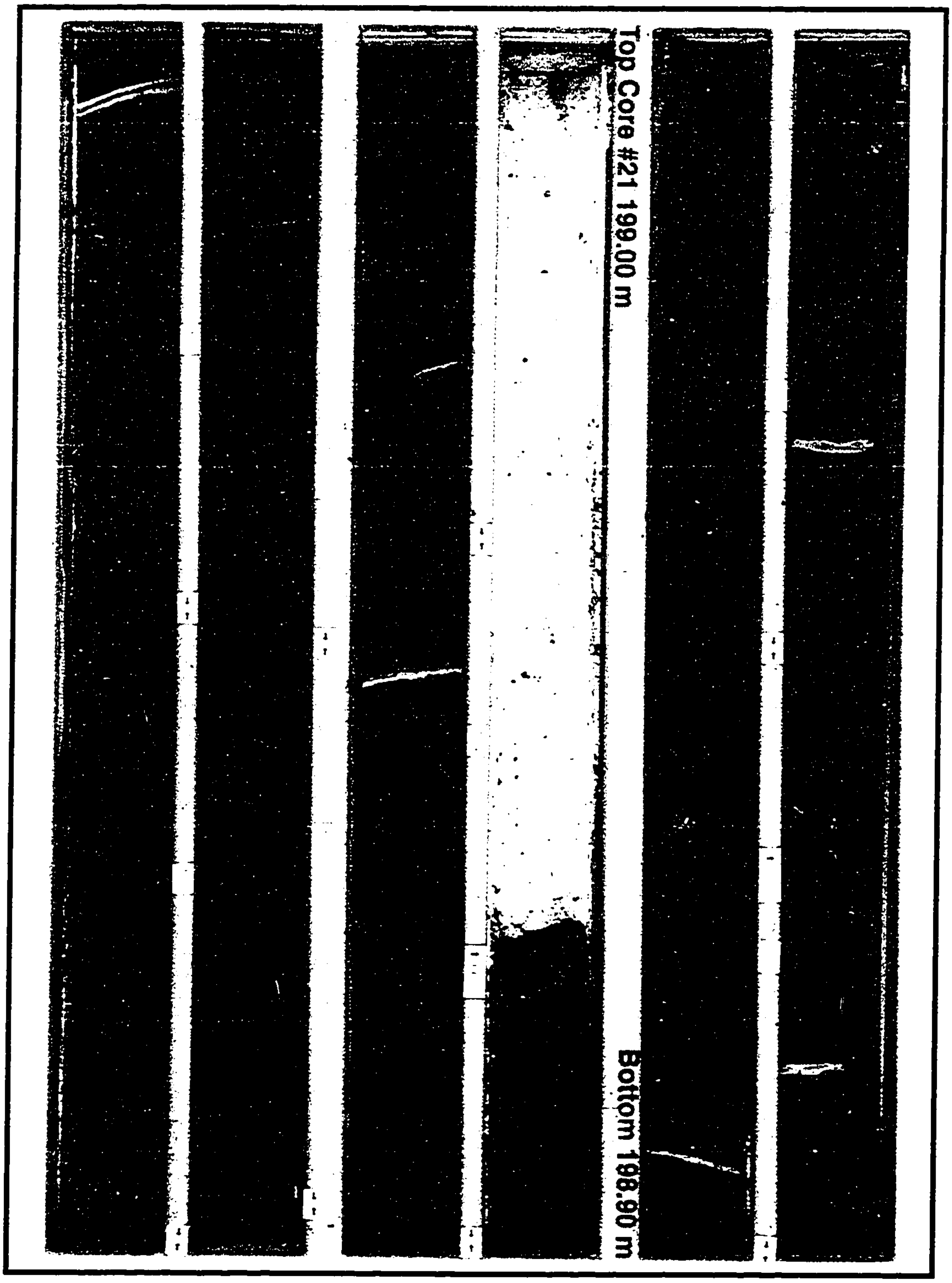

2.14

Figure 2.15: Facies 1. Pin-stripe laminated and bioturbated beds within F1 sand. Photo from well 15-4-92-7W4, 197.3 m – 201.6 m depth. Core boxes 75cm long

Top Core #21 198.90 m
Bottom 198.65 m
Cylindrichnus
Planolites
Pin-stripe lamination

2.15

grained semi-consolidated interchannel substrates. Clasts may have been incorporated into F1 sands as a result of bank collapse, likely during low water levels after material was able to dewater and desiccate or alternatively, may have been undercut by channel erosion.

Despite the fact that there is clear physical sedimentological evidence to suggest that this facies was deposited in a fluvial-dominated system, the cyclic nature of many of the mud layers (F1b) is characteristic of tidal processes. Although not exclusively diagnostic of tidally-influenced sedimentation, lenticular bedding and pin-stripe lamination are common in tidal environments whereby fine grained layers represent deposition during the regular slack-water stage (Nio and Yang 1991). Tidal influence has been interpreted to have propogated 10s to 100s of kilometers upstream from the coeval shoreline, forming tidal sedimentary features within fluvially-dominated systems (Allen 1991; Shanley *et al.* 1992; Lavigne 1999). Intuitively, the interpretation of tidally-influenced sedimentation should be supported by a preserved ichnocoenese reminiscent of ecologically stressed conditions – a condition generally ascribed to the mixing of fresh and saline water. Where mud layers and clasts contain low diversity assemblages of impoverished marine forms as well as examples of somewhat complex burrow morphologies including *Cylindrichnus* and *Ophiomorpha*, one may surmise that depositional conditions were ecologically stressed. The majority of layers, however, contain a marked paucity of trace fossils or are burrowed by small, simple forms including *Planolites* and *Skolithos*. This observation may indicate ecologically stressed conditions in a marine-influenced setting that precluded colonization by organisms (e.g. paucity of oxygen; high turbidity; unsuitable substrate, and high sedimentation rates), or simply non-marine conditions (cf. Nadon 1994). Because the physical influence of tides can extend 10s of kilometers upstream from the salinity limit, physical sedimentary structures may indicate tidally-influenced sedimentation, whereas the biogenic assemblage may not (Allen 1991; Shanley *et al.* 1992; Lavigne 1999).

In summary, F1a is interpreted to have been deposited in a fluvial to tidally-influenced channel complex. Mud layers in F1b suggest that waning- or low-energy flow conditions were more common during deposition (relative to F1a) or, alternatively, are simply better preserved because of a lower frequency of high-energy, erosive events. Trace fossil assemblages generally comprise simple and impoverished marine forms, but also include more complex morphologies such as *Cylindrichnus* and *Ophiomorpha*. These forms suggest that at least episodically the area became more favorable, albeit still ecologically stressed, and supported a more diverse and abundant tracemaking assemblage.

Facies 2: Poorly-sorted pebbly sand

Strata of Facies 2 are poorly-sorted and consist of grains ranging from silt to pebble size; coarser particles (sand or coarser) are angular- to sub-rounded (Fig. 2.16). Mineralogy consist predominantly (~90%) of mono- and less commonly polycrystalline quartz. Although constituting typically no more than 3% of the overall mineralogy, feldspar grains tend to be large, commonly disaggregated and altered to clay minerals locally. Chert, rare lithic fragments, biotite and muscovite grains are present in varying abundance and typically comprise <5% of the framework grains. Authigenic pyrite crystals in a clay matrix occur at irregular stratigraphic intervals (Fig. 2.17).

Figure 2.16: Sharp-based, poorly-sorted pebbly sand of Facies 2. Photo from well 10-17-91-7W4, 212.9 m - 215.3 m depth. Core box 75 cm long.

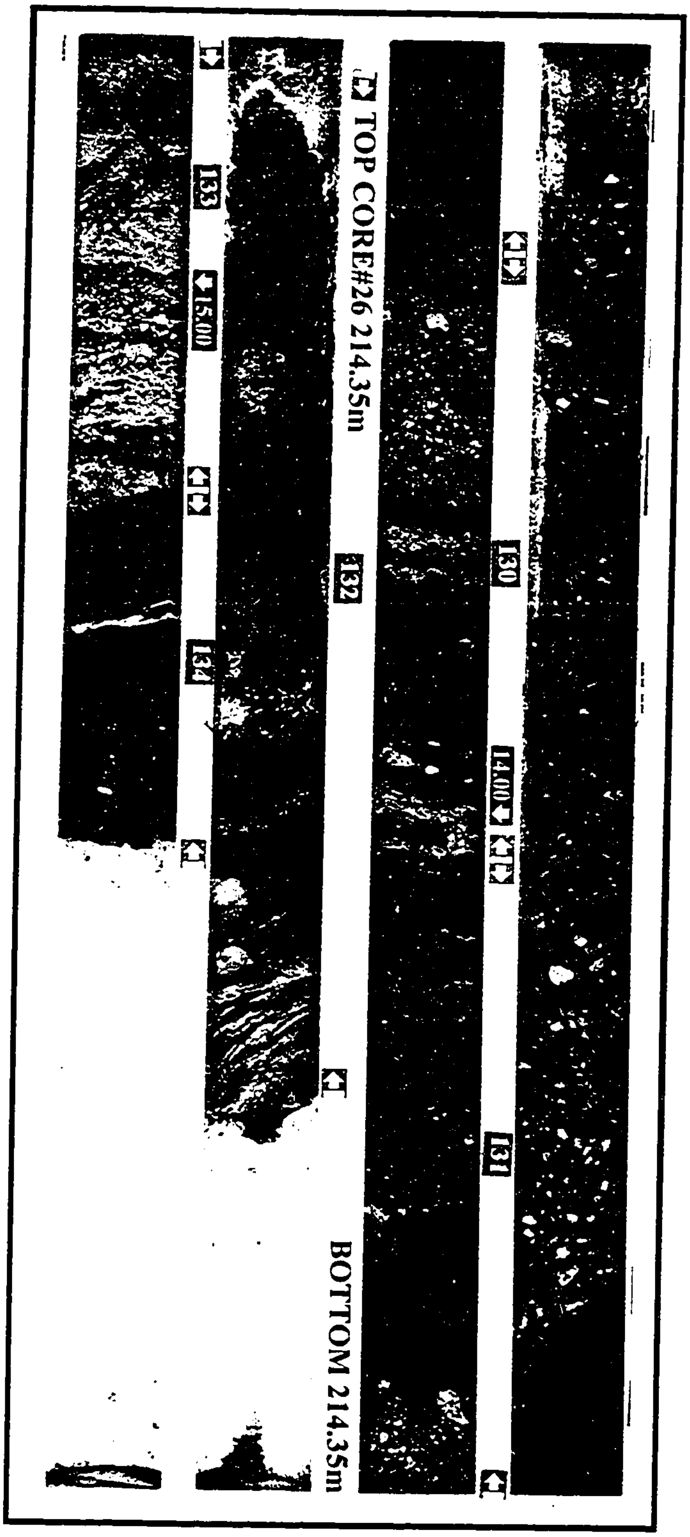
TOP CORE#26 214.35m
BOTTOM 214.35m
130
131
132
133
134
14.00
15.00

2.16

Figure 2.17: Photomicrograph of Facies 2. Subangular to subrounded mono- and polycrystalline quartz grains of F2. Note intergranular carbonate (white) and associated authigenic pyrite (black). Photo from well 5-10-91-7W4, 206.1 m depth. 35X mag.

Figure 2.17(a): plane-polarized light

Figure 2.17(b): cross-polarized light

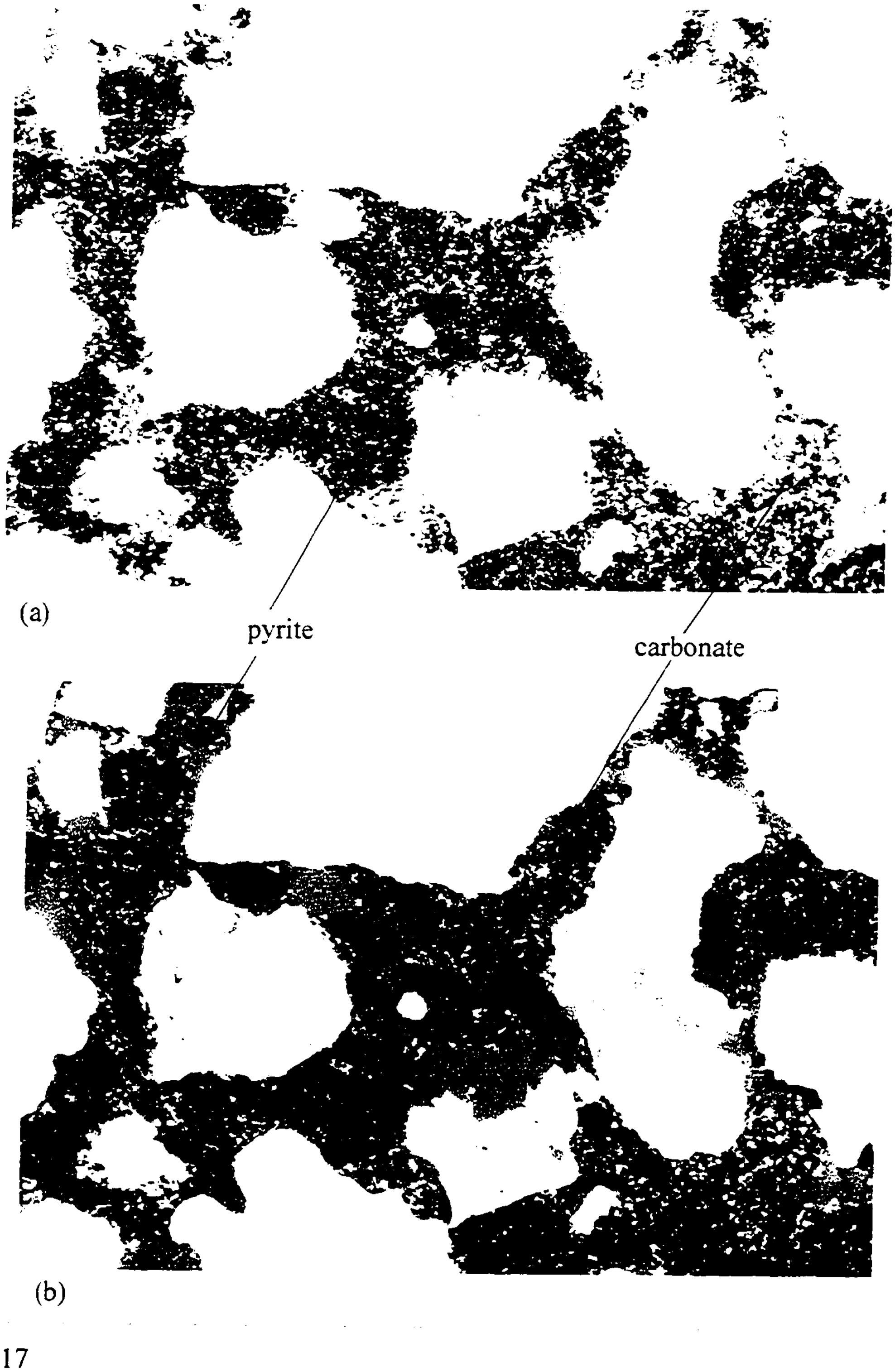

2.17

In most cases, F2 sand appears massive, but locally planar, high angle fractures demarcating medium-scale cross-stratification can be observed. Abrupt fining- and coarsening-upward successions are common locally. Mud clasts are rare and where present are commonly small (<1 cm), irregularly shaped, unlaminated and unbioturbated. Coal clasts, organic debris, and pyritized and sideritized clasts occur in varying abundance in this facies. Locally, long (dm-scale) root structures are also present (Fig. 2.18). Although pervasive bitumen staining is observed, it is more commonly absent or patchy and generally does not parallel cross-stratification (as observed in F1) (Fig. 2.19). However, intergranular bitumen is observed in petrographical samples that in hand sample appear to be non-saturated (Fig. 2.20).

Interpretation:

The textural and mineralogical immaturity of F2 sand suggests that transport from the source area was minimal and/or sediment reworking was negligible. Medium-scale cross-stratification is interpreted to be the result of migration of two-dimensional subaqueous dunes. Conversely, interbeds of massive sand suggest deposition from rapidly waning flow or alternatively, bank collapse related to local sediment liquefaction (Rust and Jones 1986). Abrupt grain size changes are suggestive of fluctuating energy conditions. The presence of large root structures suggests that in places, F2 sand was vegetated, signifying subaerial and relatively stable substrates. Additionally, common coal and organic material, combined with the lack of trace fossils, suggests that deposition occurred within a dominantly non-marine environment.

Figure 2.18: Large mud-filled rootlet in strata of Facies 2. Photo from well 1-12-91-8W4, Core 28 2 of 2. ~190.5 m depth. Scale is 2.5 cm in diameter.

Figure 2.19: Patchy bitumen-stained massive sand of Facies 2. Photo from well 1-12-91-8W4, Core 30 2 of 2, 194.5 m – 196.0 m depth. Scale is 2.5 cm in diameter.

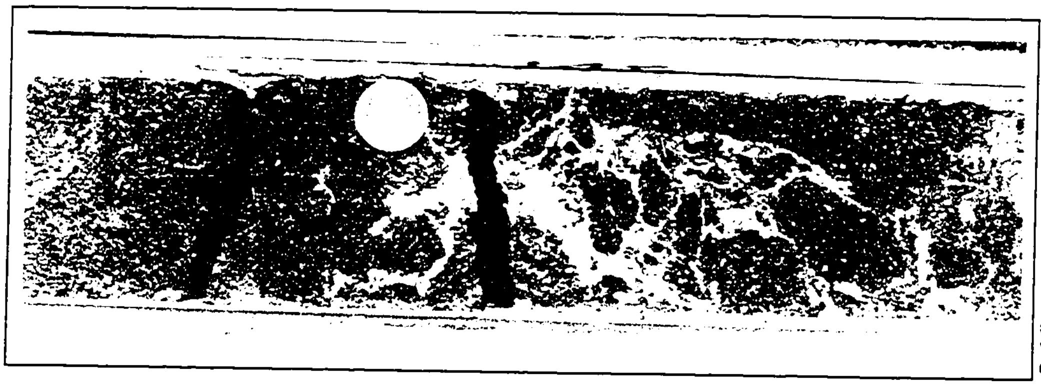

2.18

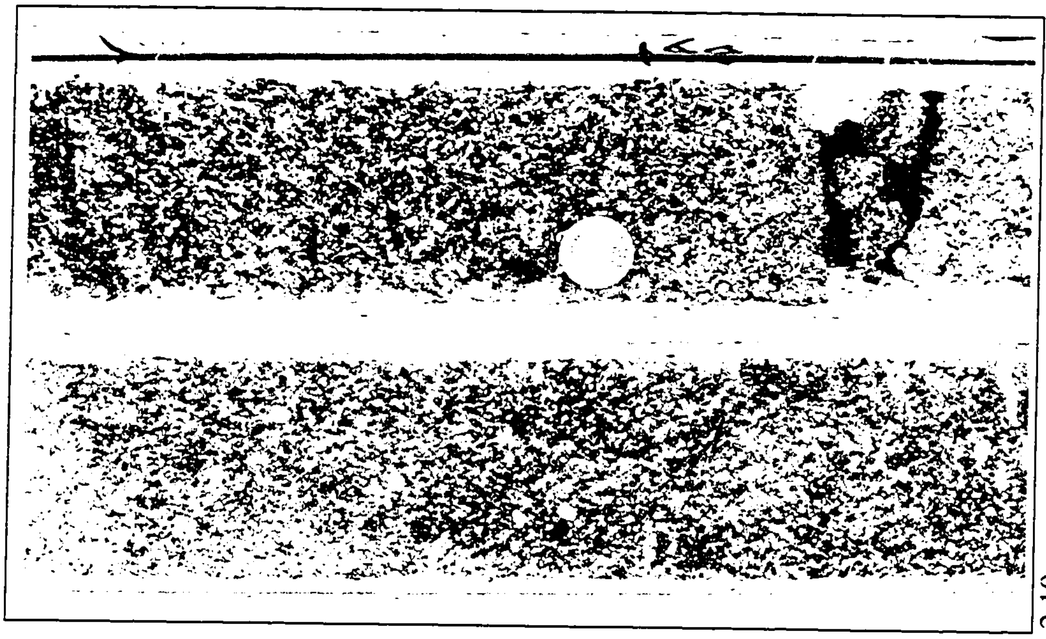

2.19

Figure 2.20: Core, well-log, and photomicrograph of Facies 2. Photomicrograph illustrates intergranular bitumen (black) around feldspar grain in Facies 2. Strata appears unsaturated in core. Location of photomicrograph indicated by green dots. Photo from well 3-18-91-7W4, 219.5 m depth. Core boxes 75 cm long.

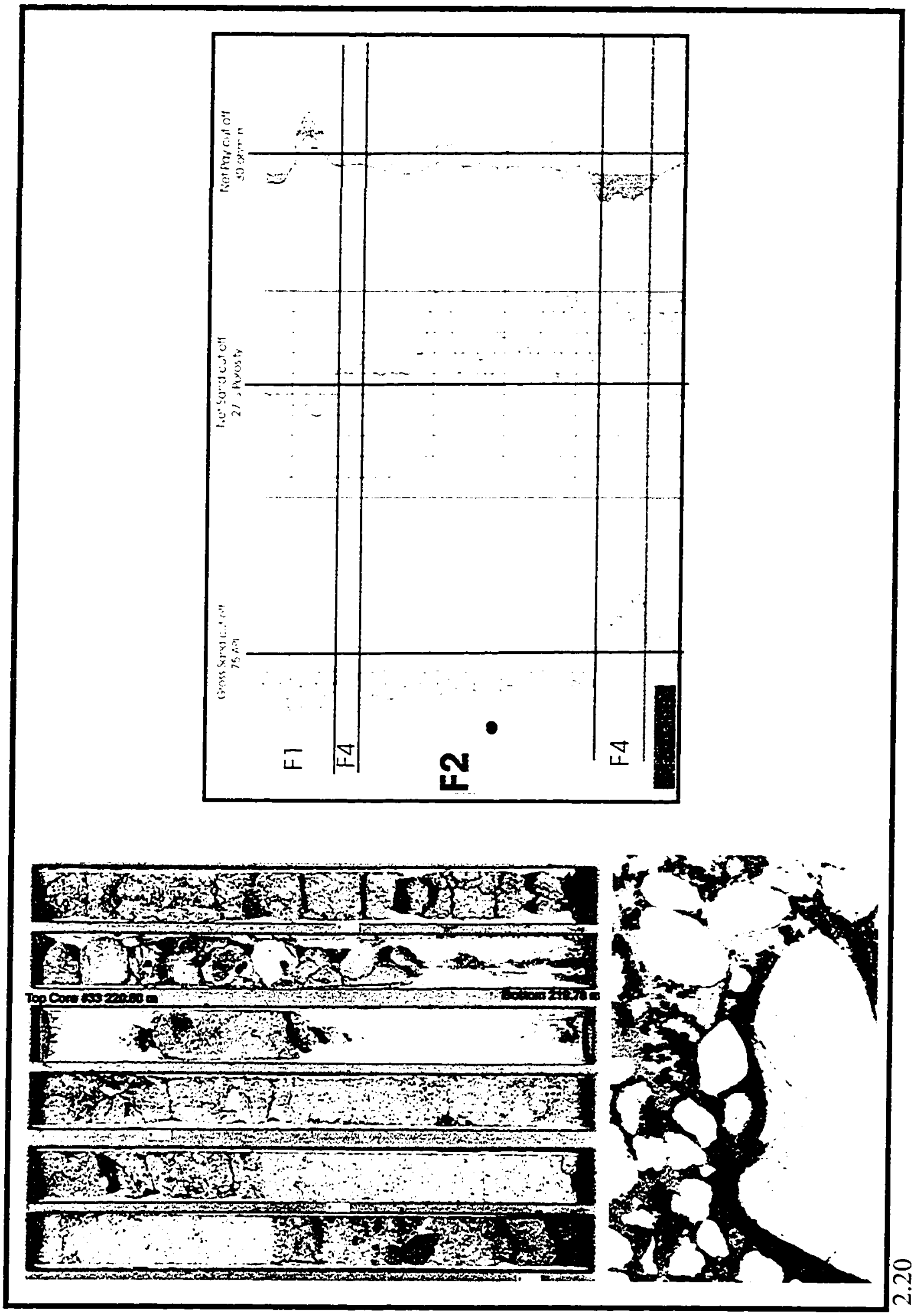

2.20

Facies 3: Glauconitic silty-sand

Although F3 can be up to 7 m thick, it is typically <1 m thick. The base of F3 is marked by the abrupt appearance of very dark grey silt with upper fine to lower medium non-bitumen-saturated sand and glauconitic sand. However, where the underlying strata consist of dark grey silt the base of F3 can be difficult to recognize in core. Characteristically strata of F3 consists of glauconitic sand grains burrowed with large (dm-long) *Skolithos. Teichichnus, Rosselia*, and other unidentifiable glauconite-filled burrows are also common (Fig. 2.21).

Interpretation:

Glauconite is an authigenic mineral formed via the alteration of organic matter (i.e. fecal pellets, coprolites, or skeletal debris) and/or micas (muscovite/illite) when they react with iron cations (Carozzi 1993). This reaction commonly occurs on sediment-starved open-marine seafloors where porous substrates are in direct contact with iron-rich seawater (Carozzi 1993). The abundance of glauconite in F3, coupled with the suite of large vertical feeding and dwelling burrows of the *Skolithos* (and *Cruziana*) ichnofacies indicates that deposition occurred in a dominantly open-marine environment. Sedimentologically, this facies was dominated by high-energy conditions (sand), most likely associated with storms, with intervening periods of low energy (mud).

Figure 2.21: Facies 3. Long *Skolithos* burrow in glauconitic sand. Photo from well 12-34-91-8W4, Core 6 1 of 2, ~136 m depth. Penny is 19 mm in diameter.

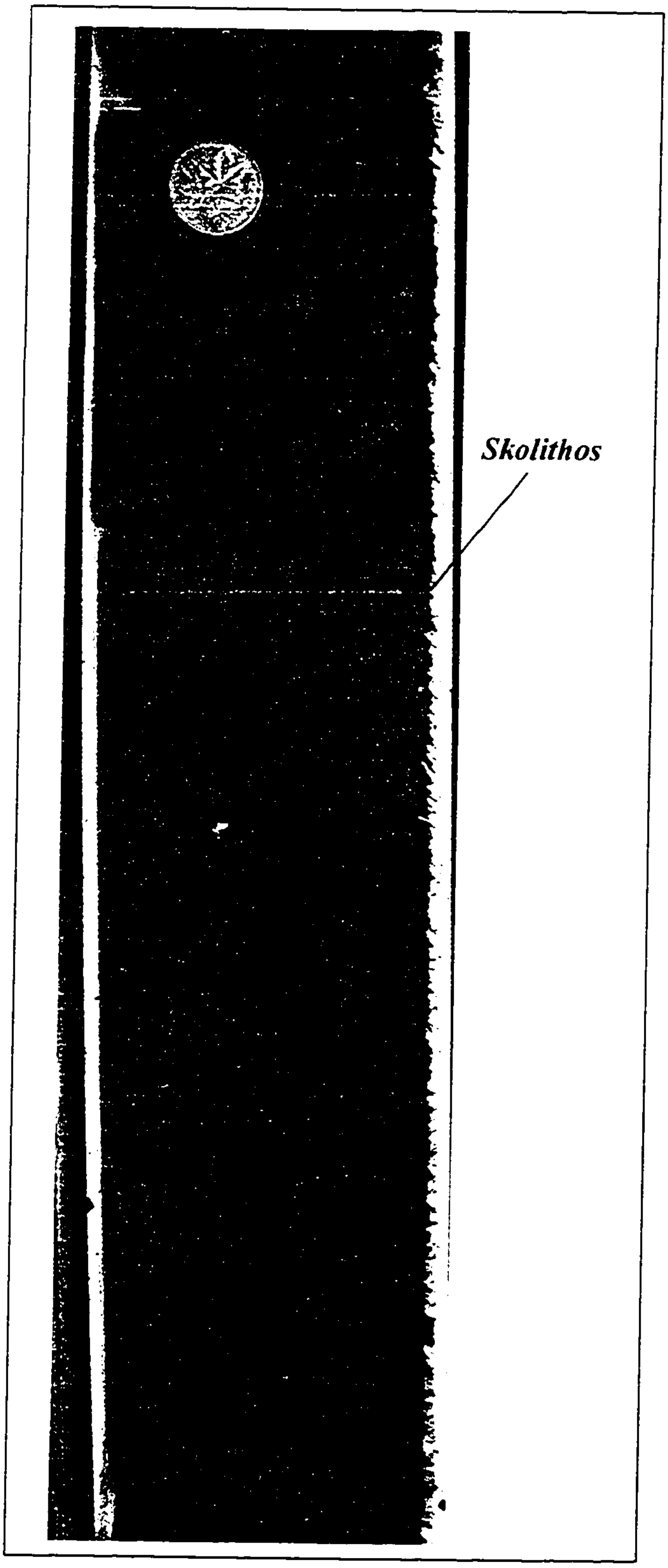

2.21

Facies 4: Mottled clay

Facies 4 is characterized by a black/light grey and/or green mottled texture and decimeter-thick vertical changes in colour that grade between light and dark grey, pale green, and yellow (Fig. 2.22). Although well consolidated, strata are commonly fractured and locally display a fissile texture. F4 strata are typically thin, ranging from <1 m to a maximum of 5 m, averaging 3 m in thickness. High density, sideritized beds occur locally. Abrupt centimeter-scale changes from calcareous to non-calcareous beds are common. Additionally, F4 exhibits both waxy and non-waxy appearance.

Large (1-2 cm diameter) irregular shaped clasts such as limestone rock fragments, pyritized mud-clasts, quartz pebbles, and coal are common and randomly dispersed throughout this facies. Disseminated organic matter and medium to coarse grained bitumen or non-bitumen stained sand also occur, commonly defining convolute bedding (Fig. 2.22). Shell fragments occur locally and only where F4 defines the base of the McMurray Formation. The lower contact of F4, where cored, is sharp or gradational, whereas the upper contact is sharp and commonly at very high angles (>>30 degrees). Additionally, debris from the overlying strata is occasionally incorporated within fractures of F4 (Fig. 2.23).

Interpretation:

The combination of mottles, colour variations, waxy lustre, fractures and calcareous horizons suggest that F4 was created by soil-forming processes (Retallack 1988). Mottles commonly form in waterlogged soils that locally become temporarily depleted in oxygen by soil bacteria, causing local reducing conditions. The lack of root structures is also suggestive

Figure 2.22: Mottled green and light grey coloured clay of Facies 4 strata. Note also deformed bedding in middle two core boxes. Photo from well 15-29-91-7W4, Core 24 1 and 2 of 2, 198.7 m - 195.8 m. Core boxes are 75 cm long.

Figure 2.23: Facies 4. Pyritized clasts in strata of Facies 4. Photo from well 2-4-92-7W4, Core 39 2 of 2, ~242.5 m depth.


py

2.23

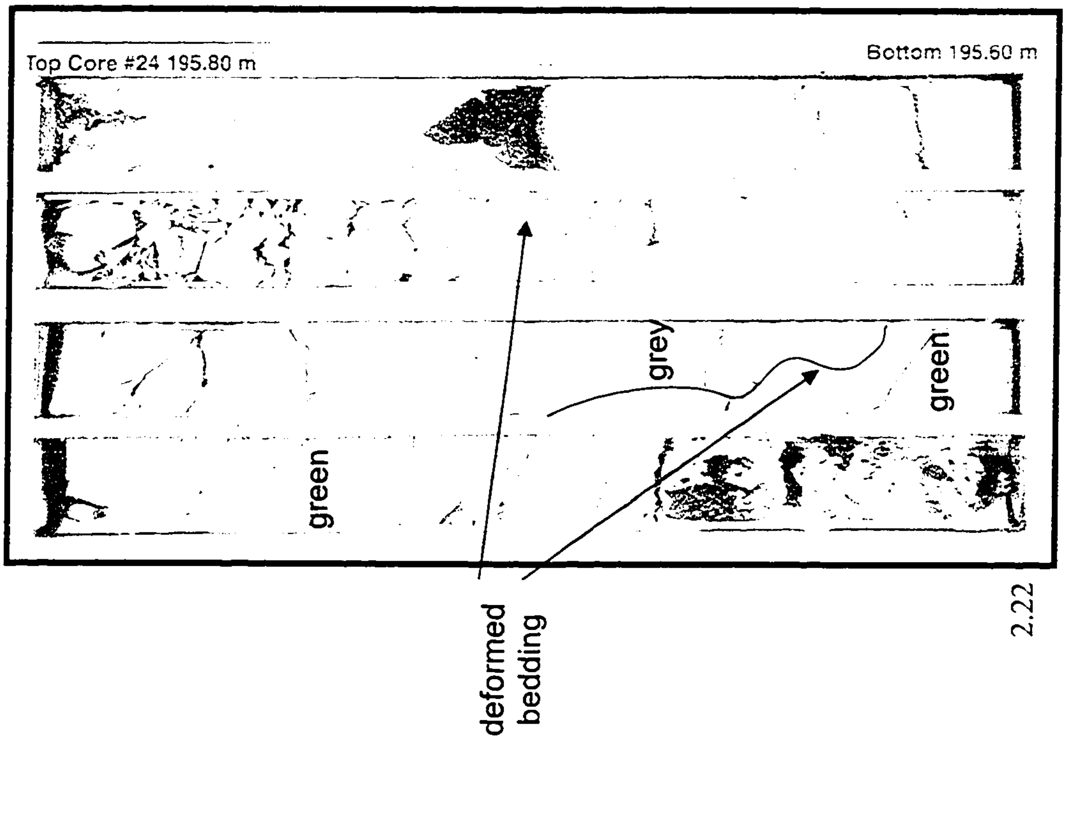
Top Core #24 195.80 m
Bottom 195.60 m
green
grey
green
deformed
bedding

2.22

of waterlogged soil conditions. Green colouration has also been attributed to anaerobic microbial decay of organic matter in soil shortly after burial below the water table. The presence of pyrite and sideritized layers also supports a reducing chemical environment. Waxy luster is the result of repeated wetting and drying (causing swelling and shrinking of soil) and abrasion during burial. Fractures are similar to granular or crumbly soil peds observed in soil A or B horizons. Moreover, gradational colour contacts are commonly observed in soil horizons.

Clasts (particularly carbonate) and sand incorporated into F4 are likely related to erosion and slumping from surrounding topographic highs on the irregular Devonian surface, which varies by 10s of meters even over short horizontal distances. Some non-calcareous clasts may also reflect channel scour bases.

Facies 5: Unbioturbated silty-mudstone

Facies 5 ranges from 2-30 m, but averages about 12 m in thickness. Basal and upper contacts are typically sharp and planar, although gradational contacts over 0.25 m to 2 m occur locally and only where the facies succession is more than 10 m thick. Strata of F5 vary from light grey mudstone to silty-mudstone, although medium to dark grey strata are locally observed (Fig. 2.24). Decimeter-thick black-grey mottles occur locally. Horizontal to very low-angle lamination made evident by fractures and/or by alternating dark grey-/light grey-coloured silt layers is typical of this facies. In addition, massive or contorted bedding is also common (Fig. 2.25). Coalified roots and large (cm-scale) coal clasts are rare, whereas discontinuous coal/organic laminae are more common (Fig. 2.26). Carbonate-cemented

Figure 2.24: Facies 5 – Unbioturbated Silty-Mudstone

Figure 2.24 (a): Light-grey silty-mudstone of Facies 5. Note also fissile nature and yellow-coloured (siderite(?) cemented) band in upper left corner. Photo from well 15-29-91-7W4, Core 11 1 of 2 & Core 10 2 of 2, 165.8 m - 163.5 m depth. Core boxes are 75 cm long.

Figure 2.24 (b): Dark grey mudstone of Facies 5. Note also rare and irregularly-spaced black (bitumen-stained) sand layers (rare to unbioturbated (Sr)). Photo from well 3-18-91-7W4, 146.0 m - 148.2 m depth. Core boxes are 75 cm long.

Figure 2.25: Contorted bedding/slump feature in Facies 5. Note also mud clast in left core box. (nb. light grey mud appears green because of photographic reproduction). Photo from well 5-10-91-7W4, 169.8 m – 172.0 m depth. Core box is 75 cm long.

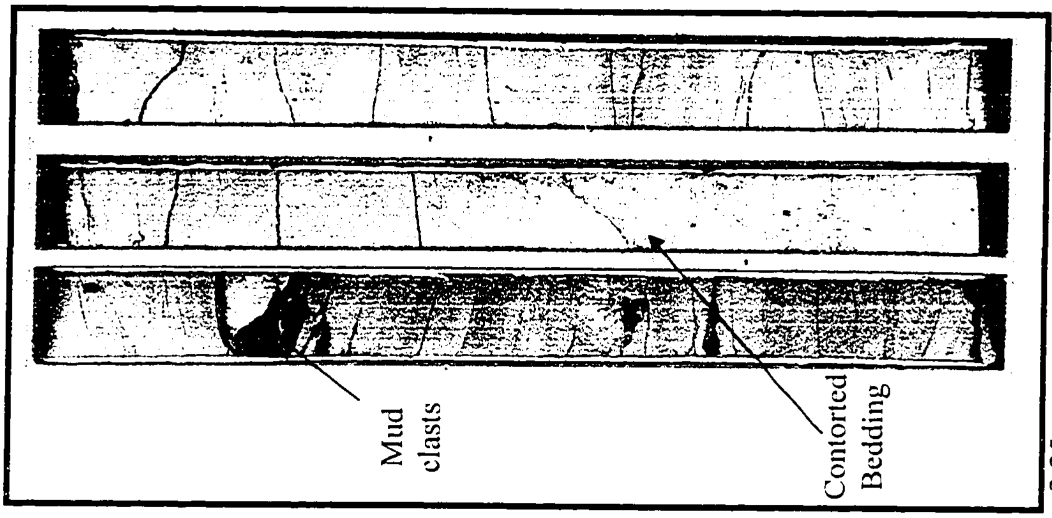

Mud clasts
Contorted Bedding

2.25

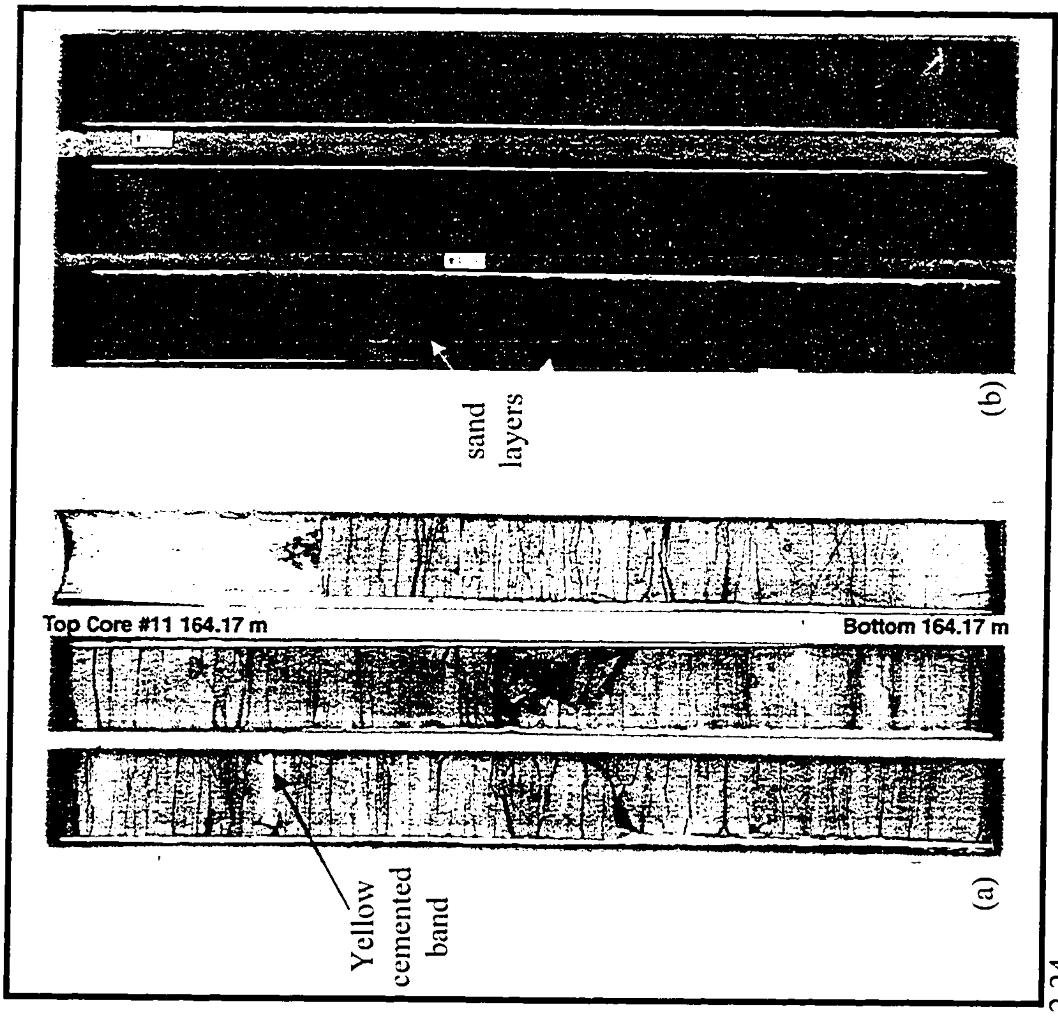

Top Core #11 164.17 m
Bottom 164.17 m
sand layers
(b)
Yellow cemented band
(a)

2.24

Figure 2.26: Facies 5. Coalified rootlet. Photo from well 15-29-91-7W4, ~153.5 m depth. Lens cap 30 mm diameter.

Figure 2.27: Rare to unbioturbated sand layers (Sr) in strata of Facies 5.

Figure 2.27 (a): Thin, irregular-spaced sand layers. Photo from Core 6-8-91-7W4, ~148.0 m – 146.5 m depth. Core box 75 cm long.

Figure 2.27 (b): Thinly interstratified (pin-stripe laminated) silt and fine-grained sand. Bioturbation is absent. Photo from well 9-12-91-8W4, ~157 m depth. Core box is 19 mm wide.

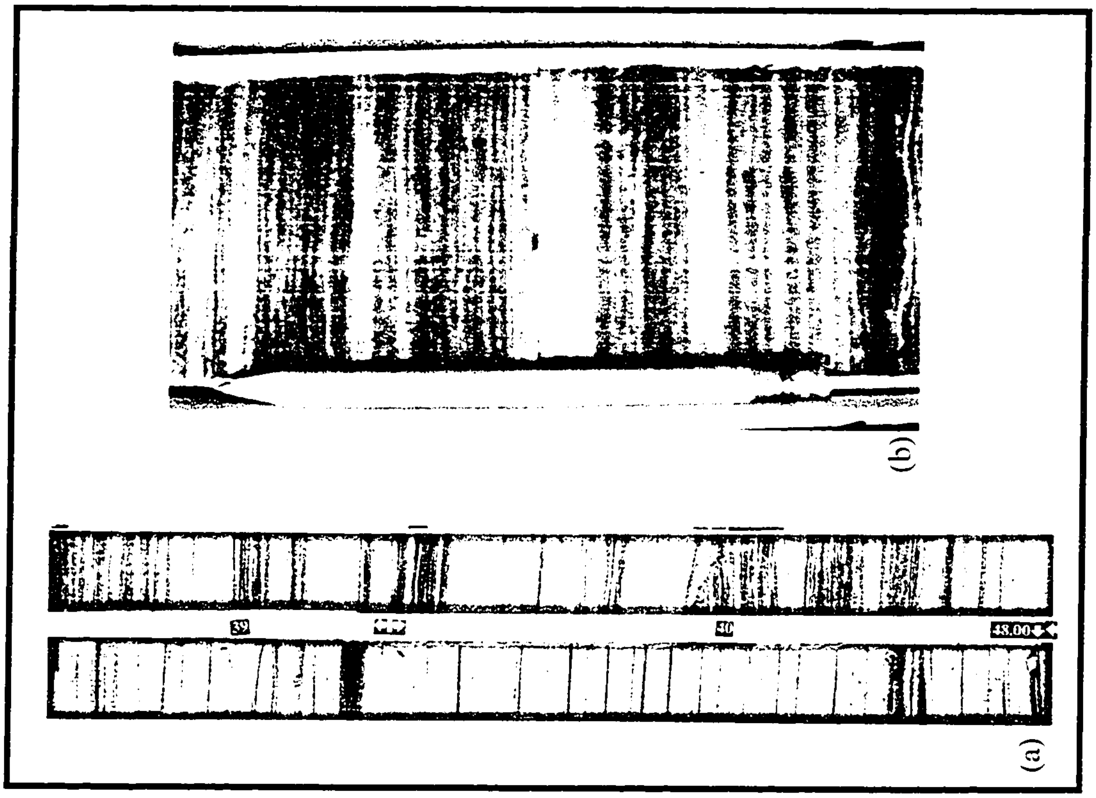

2.27

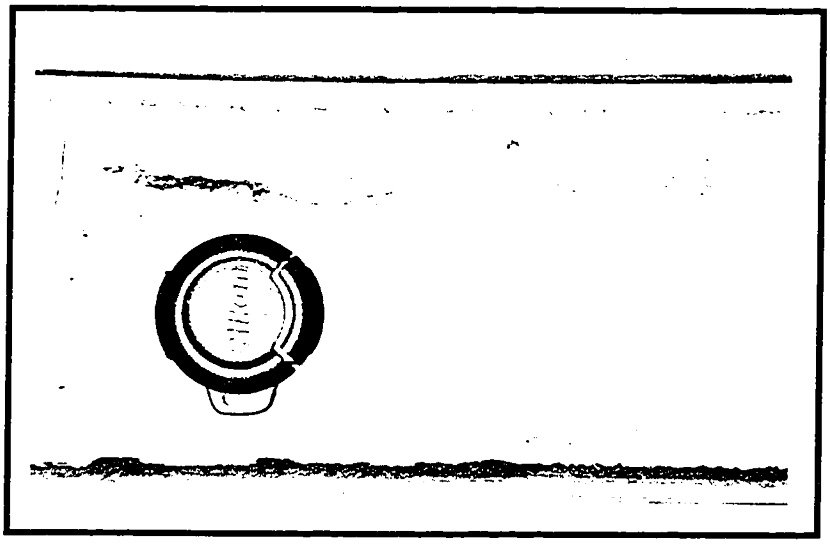

2.26

beds, 1 to 5 cm thick occur locally and at irregular stratigraphic intervals (Fig. 2.24 (a)). White, irregular-spaced lower to upper very fine sand laminae burrowed with rare diminutive (2-3 mm diameter) *Planolites* are common. In many places horizontal layers of bioturbated upper very fine to upper fine bitumen-stained sand layers ranging from laminae to 15 cm thick beds are horizontally interstratified with F5 strata. Three distinct burrowing styles occur within these sand layers: (a) unbioturbated to rare *Planolites* or *Ophiomorpha* burrows (Sr) (Fig. 2.27); (b) a monospecific *Gyrolithes* assemblage or large feeding and dwelling burrows (Sg, Sl) (Fig. 2.28); and (c) intensely bioturbated with diminutive burrows (Sd) (Fig. 2.29). Unbioturbated or rarely-bioturbated sand layers (Sr) are generally thin (<2 cm) and uncommon. In contrast, thicker (>5 cm) and more common sand layers typically exhibit a high-density, monospecific assemblage of *Gyrolithes* (Sg), or robust (~1 cm wide), well developed, and commonly re-burrowed *Cylindrichnus*, *Rosselia*, *Planolites* and *Palaeophycus* (Sl). Where bioturbation is even more intense the sand exhibits a bioturbate texture (Sd) wherein remnant planar stratification is only observed locally. Although ichnofossils are difficult to identify, *Planolites* burrows dominate and *Cylindrichnus* and *Terebellina*(?) are also present.

Palynomorphs of F5 are dominated by a high diversity and low abundance assemblage of wind-distributed gymnosperm pollen such as those from the Taxodiaceae, Cupressacea, and Taxaceae families (Sweet 2002; see Appendix 4). Lycopod, fern and bryophyte spores are present; the most abundant is *Gleicheniidites senonicus*. Freshwater algae also occur, albeit rarely. Dinoflagellates and other marine algae such as *Exesipollenites tumulus*, which has been previously identified in the McMurray Formation (Burden 1984),

Figure 2.28: Decimeter-thick robust (Sr) or *Gyrolithes* burrowed (Sg) sand layers in strata of Facies 5.

Figure 2.28 (a): Large, well developed *Gyrolithes* burrows in bitumen-saturated sand layers. Burrows are filled with mud. Photo from well 15-22-91-7W4, 201.4 m - 201.7 m depth. Core boxes 7.5 cm wide.

Figure 2.28 (b): Small *Gyrolithes* burrows in sand layers. Note that sand layers are thinner compared to Figure 2.20 (a). Photo from well 1-12-91-8W4; Core 16 2 of 2, ~158 m – 159 m depth. Coin is 25 mm in diameter.

Figure 2.28 (c): *Rosselia* (*Ros*) and *Cylindrichnus* (*Cy*) burrows. *Rosselia* has been re-burrowed by *Planolites*. Photo from well 1-12-91-8W4; Core 15, 2 of 2, ~154.5 m depth. Coin is 25 mm in diameter.

Figure 2.28(d): Robust *Cylindrichnus* (*Cy*) burrows. *Planolites* (*Pl*) and *Rosselia* (*Ros*) burrows also present. Photo from well 1-12-91-8W4; Core 15 1 of 2, ~153.5 m depth. Coin is 25 mm in diameter.

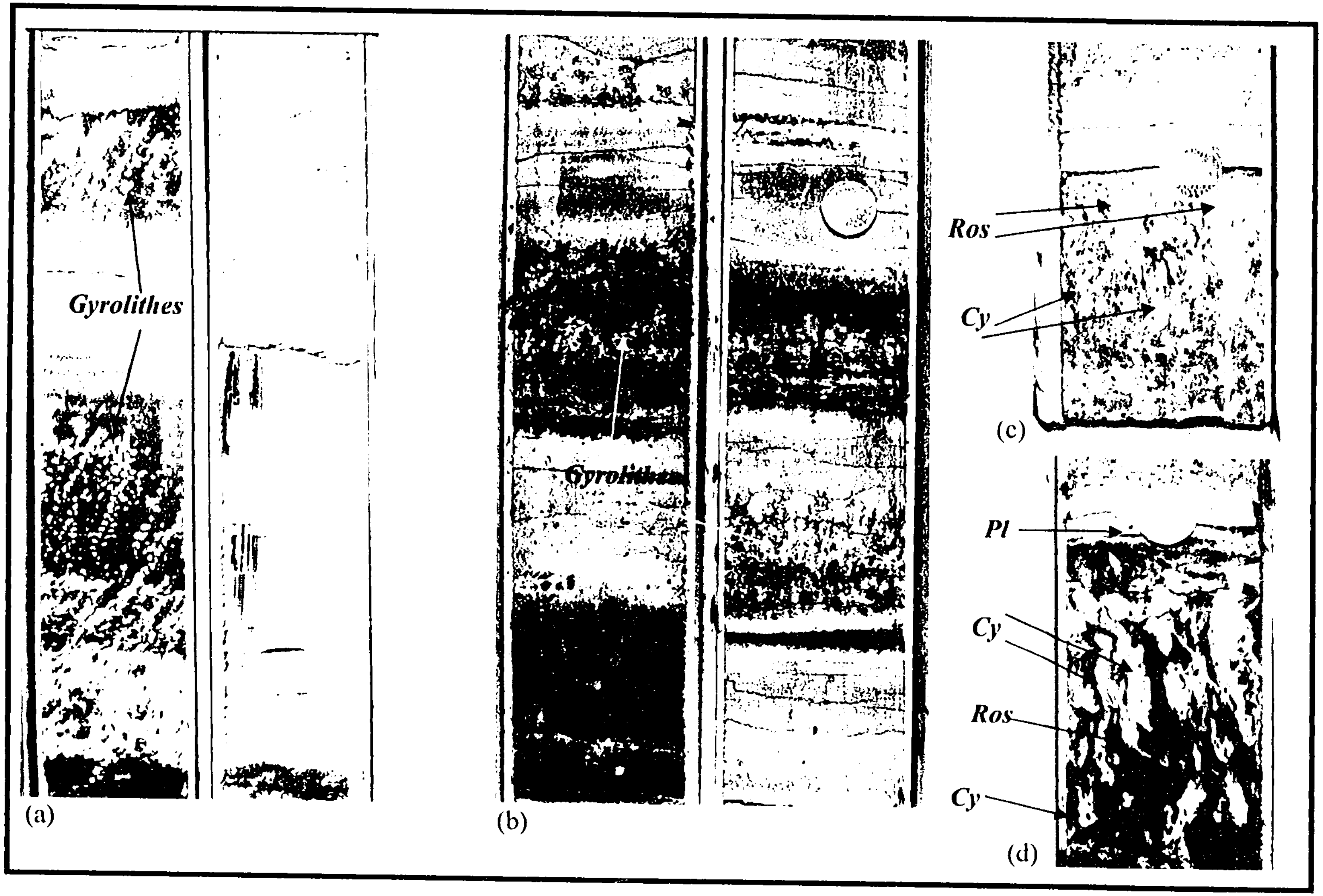

2.28

Figure 2.29: Facies 5. Diminutive and abundant bioturbation in sand layers (Sd).

Figure 2.29 (a): Abundant and diminutive bioturbation within sand layers. Photo from well 16-26-91-7W4, ~217 m – 220 m depth. Core boxes 75 cm long.

Figure 2.29 (b): Diminutive *Planolites* burrows in sandy-mud. Photo from well 5-20-91-7W4, Core 10 2 of 2, ~180.1 m – 180.5 m depth. Lens cap 30 mm in diameter.

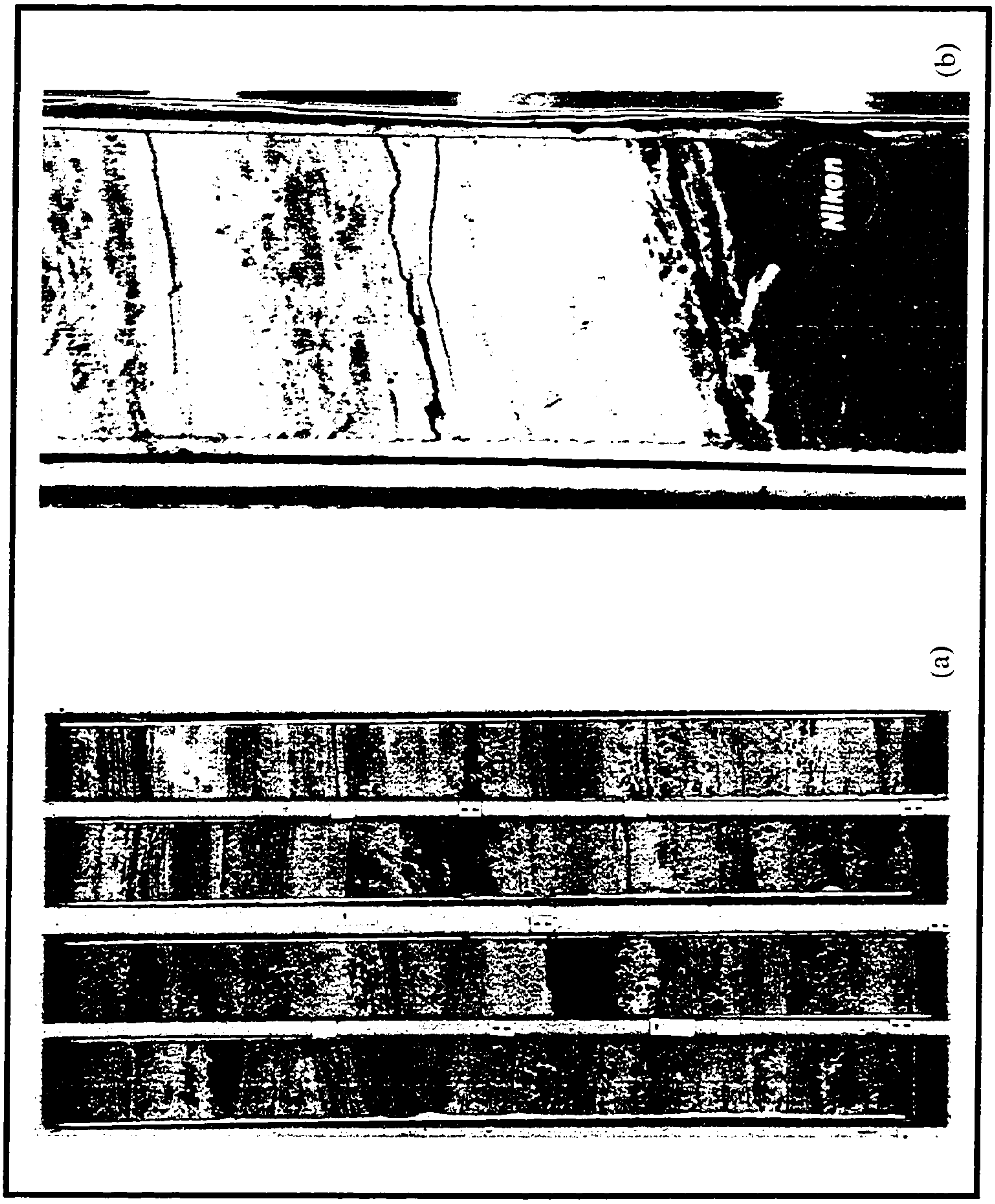

2.29

are present, but tend to be slightly more abundant where sand interlayers are absent. Moreover, where sand layers are common, lower total numbers of palynomorphs were observed.

Interpretation:

The predominance of thick successions of mudstone and silty-mudstone suggests that deposition occurred under low-energy conditions dominated by suspension settling. The dark-colour of the mud horizons coupled with common disseminated organic matter suggests that suspended organic material was abundant in the water column. Localized mottles are similar to features described in soil A horizons and probably represent diffuse mineral aggregates incorporated into soils (Retallack 1988; Molgat 2000). Although the presence of mottles alone is not diagnostic of soils or peds, the combined presence of *in situ* coalified rootlets suggests that F5 was intermittently subaerially exposed.

Sediment influx was variable, possibly seasonally, as evident by the frequency of laminated muds. Also, the paucity of trace fossils, the good preservational state of palynomorphs and the commonality of massive and convoluted bedding throughout the muddy successions suggests that sedimentation rates were most probably generally high. High concentrations of clay-sized particles fall rapidly from suspension where fresh and saline waters mix through the process of flocculation (cf. Allen 1991). As a consequence, dispersed clay particles agglomerate to form larger particles termed flocs; because of their increased weight clay flocs are able to deposit in moderately-high energy zones. Clay flocculation commonly occurs in expansive areas that coincide with the turbidity maximum zone in marginal-marine estuaries (Hughes *et al.* 1998).

White upper very fine sand laminae in F5 may have been wind-blown, but coarser, bitumen-saturated layers require a more competent mode of transport. Lacking visible physical sedimentary structures, these very well sorted sand layers likely represent periodic and rapid influx of sand into an area otherwise dominated by subaqueous suspension settling of organic and mud particles. This may be possible during storm surges or breaching of swamp margins by fluvial systems.

The ichnological assemblages within F5 are curiously varied, and nearly always mutually exclusive. Several ecological conditions influence burrowing assemblages, including the nature of the substrate (composition and firmness) and environmental stresses (turbidity, oxygen content, or nutrient availability, sedimentation rate, salinity fluctuations, etc.) (cf. Howard and Frey 1973; Gingras *et al.* 1999). Many of these parameters are interdependent and it is generally difficult to assess which (if any) is of greater importance when interpreting ancient deposits. High sedimentation rates, coupled with a sand-starved substrate may have precluded trace makers in thin sand layers (Sr). In other places, however, sand beds are of a consistent thickness whereas the preserved ichnocoenese are highly variable. The fact that such discrete ichnological variations exist in a facies that is generally sedimentologically uniform throughout suggests that water chemistry may have had an important effect on tracemaker behaviour. Numerous studies have documented how low salinity and salinity fluctuations affect the distribution of organisms within modern coastal environments (cf. Howard and Frey 1973; Gingras *et al.* 1999). More recently, these findings have been applied to ancient successions where the preserved ichnocoenese has been used as a proxy for paleo-salinity (Pemberton *et al.* 1982; Lavigne 1999; Hubbard *et al.* 1999).

Diminutive and simple burrow morphologies (Sd) have traditionally been correlated with ecologically-stressed conditions that suppress the growth and development of organisms (cf. Spaargaren 1995; Gingras 1999). In contrast, robust feeding/dwelling burrows (*Rosselia, Cylindrichnus, and Palaeophycus*) (Sl) are more suggestive of nutrient-rich environments where salinity approaches that of normal seawater, allowing sufficient time for organisms to grow and adapt. In the McMurray Formation, *Cylindrichnus* burrows have commonly been interpreted to inhabit areas of marginally higher salinities than other tracemakers (M. Gingras, personal communication, 2002). Curiously, monospecific *Gyrolithes* assemblages (Sg), commonly linked with lower energy environments and low salinities in the Cretaceous of western Canada (cf. Hubbard *et al.* 1999), periodically alternate with beds of robust burrows (Sl). This suggests that salinity commonly fluctuated during deposition. Evidence for a marine (saline) influence is also supported by palynomorph assemblages in muddy successions. The presence of dinoflagellates, in particular, is indicative of a marine influence. However, the relatively low numbers of marine taxa in these strata, suggests lower than normal marine salinities during deposition. The relative abundance of accessory algae and pollen taxa generally associated with brackish, near-shore, and/or marine conditions (e.g. *Classopollis*, *Lecaniella foveata*, *Exesipollenites tumulus*, *Canningia*, and *Gleicheniidites*) in F5 strata further supports a low salinity environment.

Despite the fact that palynomorphs associated with marine and brackish water environments occur in F5, gymnosperm pollen and fern spores associated with continental environments overwhelmingly dominate the palynomorph assemblage. This implies that F5 was deposited in a predominantly continental environment, near or in a forested swamp-margin area (Sweet 2002, Appendix 4). The low proportion of marine-associated taxa relative to terrestrial counterparts causes one to question the origin of marine forms: are they *in situ* or are they detrital elements? If palynomorphs are detrital, what are the implications for estimating proximity to the shoreline at the site of deposition? Core intervals greater than 10 m long that contain abundant dinoflagellates (e.g. 15-29-91-7W4) suggest *in situ* preservation. Arguably, in wells containing fewer marine forms (e.g. 11-23-91-8W4), dinoflagellates may have been supplied by a variety of transport mechanisms (e.g. storm surges, wind, birds, etc.) (A. Sweet, personal communication 2002). Alternatively, low abundance may represent poor preservation, for example in instances where sand is more abundant and total palynomorph counts are comparatively low (e.g. 5-20-91-7W4). Nonetheless, the persistence of dinoflagellates in all of the sampled wells suggests deposition in a marine-influenced environment.

In summary, based on palynomorph assemblages, soil features, and carbonaceous material, F5 was deposited in a predominantly continental environment, in or adjacent to a forested swamp or swamp-margin habitat. Furthermore, the ichnological and palynological record suggests that the environment had a definitive marine influence which most probably produced brackish water conditions characterized by frequent salinity changes.

Facies 6: *Chondrites* burrowed mudstone

F6 is decameters thick and consists of fissile mudstone to well consolidated and mottled medium grey silty mudstone. The basal contact of F6 is sharp to gradational over several centimeters. Calcite-cemented zones, 1 to 8 cm thick, are common and irregularly spaced. Rare pyrite nodules are also present. Strata are typically burrowed by *Chondrites,* although glauconite-filled vertical and horizontal *Planolites* burrows do occur (Fig. 2.30). Glauconite, though rare, is present in centimeter-thick, irregular-spaced layers.

Interpretation:

The dominance of fissile mudstone, the presence of glauconite, and the high concentration of the feeding trace *Chondrites* indicate slow deposition in a low-energy, offshore environment. Pyrite nodules are interpreted to have formed during early diagenesis and indicate local reducing conditions in the shallow subsurface. Calcite layers, which follow distinct bedding horizons, may represent condensed sections (Loutit *et al.* 1988). A condensed section forms during periods of very low sedimentation rates, a condition of sediment starvation, and overlies transgressive systems tract (TST) deposits and, in turn, is overlain by highstand systems tract (HST) deposits (Baum and Vail 1988). If TST deposits are porous, marine cements, like calcite, can precipitate in pores. Although it is possible that condensed sections are represented by calcite horizons within Facies 6, other indicators of condensed sections like glauconite or high concentrations of planktonic organisms were not observed in these layers.

Figure 2.30: Fissile mud of Facies 6. Note white, mm-diameter *Chondrites* burrows in middle core box. Photo from well 15-29-91-7W4, Core 2 1 of 2 and Core 1 2 of 2, ~145.5 m - 143.4 m depth. Core boxes 75 cm long

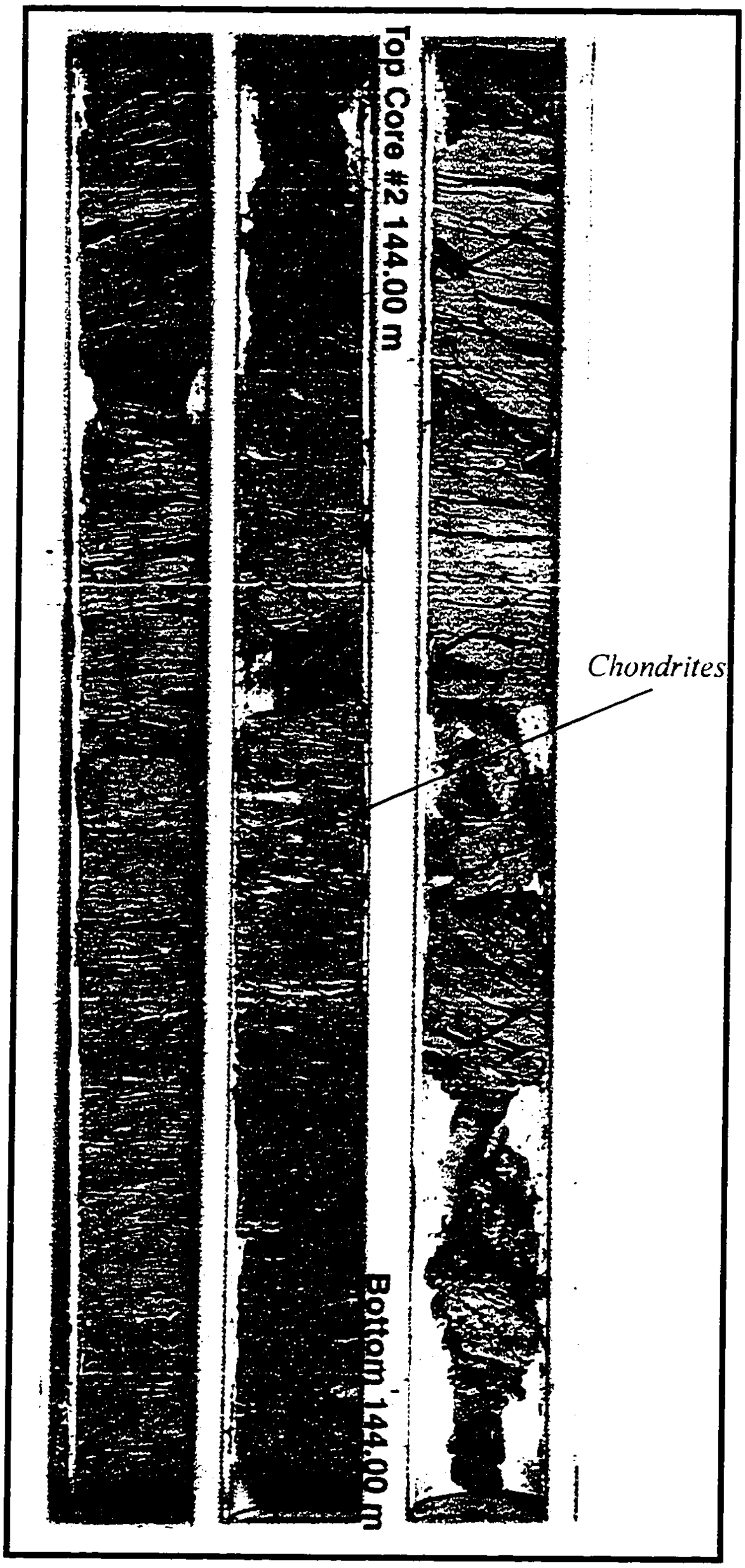

2.30

Facies 7: Inclined heterolithic stratification (IHS)/epsilon cross-stratification (ECS)

F7 is typically gradationally based and consists of inclined interstratified sand and silt/mud layers; the angle of dip is typically 8-12°, although horizontal or high angle (>30°) inclinations are observed. The contact between sand and silt/mud layers is generally sharp and planar, but may appear wavy and irregular where disrupted by intense bioturbation. Individual sand layers consist of well to very well sorted, lower very fine to upper fine ungraded sand. Physical sedimentary structures include small- to medium-scale cross-stratification and planar lamination. Although sand layers are generally unbioturbated, uncommon diminutive *Cylindrichnus* burrows occur. Small (<0.5 cm diameter) coal clasts are present, but are rare.

Although there is little variability in the make-up of the sand layers in F7, sedimentological variations in silt/mud layers are common. Based largely on sand:silt/mud ratios, two subfacies are identified: Epsilon cross-stratified/sand-dominated inclined heterolithic stratification (subfacies 7a) and silt/mud-dominated inclined heterolithic stratification (IHS) (subfacies 7b).

Subfacies 7a: Epsilon cross-stratification/sand-dominated inclined heterolithic stratification

Where mud layers are not present, strata of F7a are described as 'epsilon-cross-stratified', following the terminology of Allen (1963). Both epsilon cross-stratified and sand-dominated inclined-heterolithic stratification deposits range in thickness from 10-30 m and average between 20-25 m. Sand-dominated IHS successions consist of 70 to 90+% sand; individual sand layers are typically heavily bitumen saturated and are ≥30 cm thick. The thickness of silt/mud interlayers vary irregularly upwards from <1 to 30 cm thick, but typically are 5-10 cm thick. Uncommon soft sediment deformation and rare micro-faults are observed. Two distinct lateral and vertical variations in the make-up of silt/mud layers occur: (a) successions of stacked laminae forming units 1-30 cm thick, or; (b) 1-15 cm thick beds (Fig. 2.31). Where silt/mud layers are interlaminated, individual lamina are typically discontinuous, wavy and irregular. Bioturbation is variable, but commonly is dominated by an intense, diminutive, low diversity trace assemblage of *Cylindrichnus*, *Planolites*, and *Ophiomorpha* with uncommon escape traces and *Rosselia* and *Gyrolithes* and very rare *Asterosoma* and *Teichichnus* burrows. Layers densely colonized by a monospecific *Cylindrichnus* assemblage are also common. Locally, silt/mud layers exhibit little to no bioturbation and are dominated only by rare *Planolites* and *Ophiomorpha*. Where the mud/silt layers occur in 1- 15 cm thick beds, bioturbation intensity is low to moderate and consists mainly of *Planolites* and *Ophiomorpha*, although uncommon *Cylindrichnus* and *Gyrolithes* are observed. Dispersed organic debris occurs in some silt beds.

Subfacies 7b: Silt/mud dominated inclined heterolithic stratification

The average thickness of silt/mud-dominated Inclined Heterolithic Stratification is between 15 and 20 m, although thicknesses up to 25 m are observed. Irregularly-spaced sand layers show moderate to heavy bitumen staining and although thicknesses vary from 5-100 cm, beds are usually about 15 cm thick. Although not common, an upward increase in thickness and/or frequency of silt/mud layers is observed in sub-facies 7b (Fig. 2.32). Silt/mud layers are greater than 30 cm thick and occur either as stacked laminae or as thick

Figure 2.31: Facies 7a. Sand-dominated Inclined Heterolithic Stratification (IHS).

Figure 2.31 (a): Muddy heteroliths occur mostly as successions of stacked silt-sand laminae, although several 1-2 cm thick mud beds occur (see arrow). Heterolithic successions are irregularly-spaced and vary in thickness. Note presence of soft sediment deformation structure (see arrow). Photo from well 15-27-91-7W4, Core 13 and Core 14 1 of 2, 169.3 m - 179.6 m depth. Core boxes 75 cm long.

Figure 2.31 (b): Muddy heteroliths occur primarily as 1-2 cm-thick mud beds that are irregularly-spaced and vary in thickness. Mud beds are unbioturbated or burrowed with rare *Planolites* and very rare *Ophiomorpha*. Photo from well 12-34-91-8W4, Core 22 2 of 2 and Core 23, 173.4 m -177.0 m depth. Core boxes are 75 cm long.

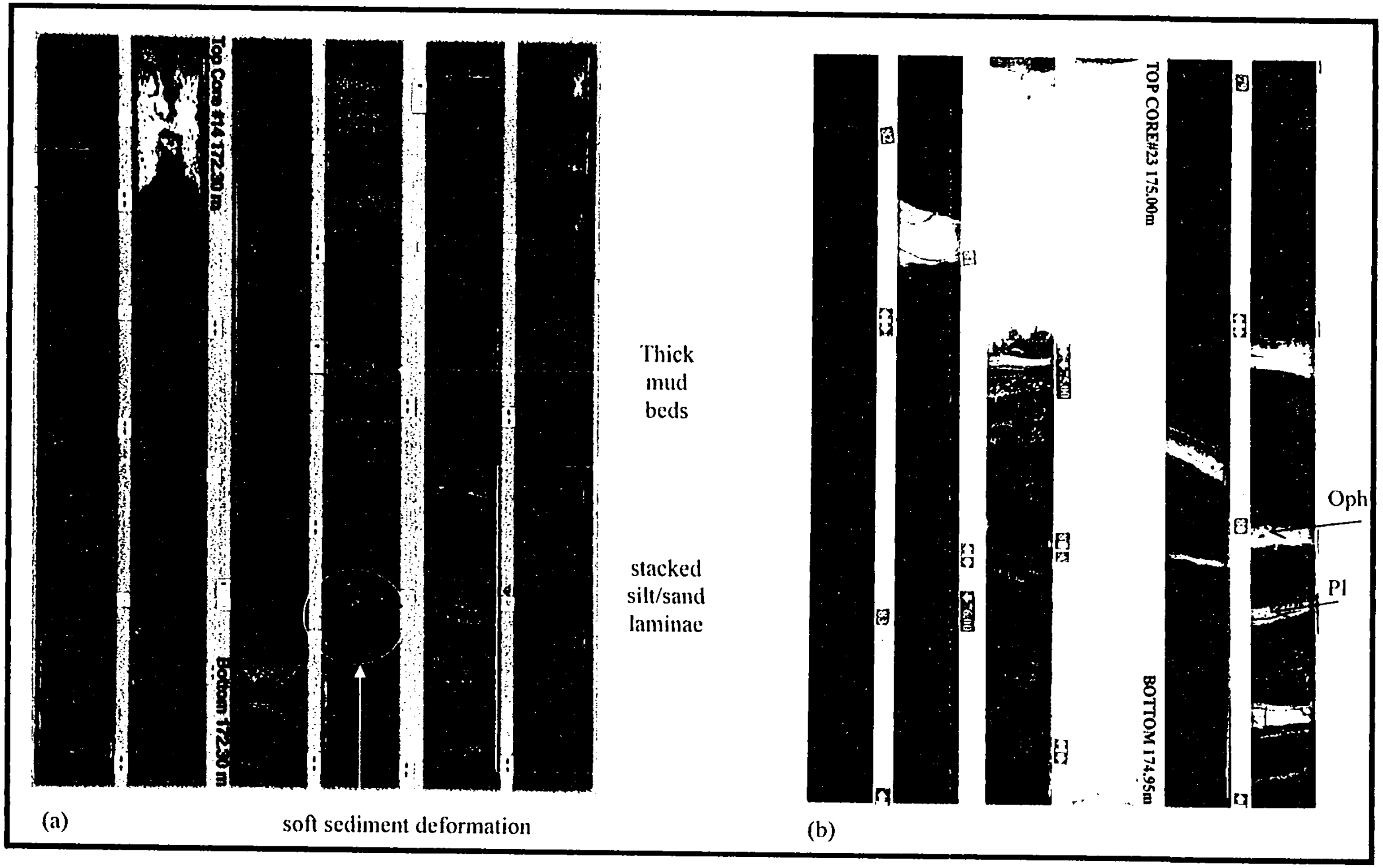
Top Core #14 172.30 m
Bottom 172.30 m
Thick
mud
beds
stacked
silt/sand
laminae
(a)
soft sediment deformation
(b)
TOP CORE#23 175.00m
BOTTOM 174.95m
Oph
Pl

2.31

Figure 2.32: Facies 7b. Mud/silt-dominated Inclined Heterolithic Stratification

Figure 2.32 (a): Silt/mud layers increase in thickness upward. Silt/mud layers vary from laminae and thick beds irregularly up-section, although layers are generally thick. Circled area is location of Fig. 2.24 (c). Photo from well 3-18-91-7W4, Core 5-9, 150.9 m – 163.5 m depth. Core boxes are 75 cm long.

Figure 2.32 (b): Increase in abundance of silt/mud layers up-section. Silt/mud layers occur primarily as stacked laminae. Photo from well 7-14-91-8W4, Core 9 to Core 13, ~154.2 m - ~162.4 m depth. Core boxes 75 cm long.

Figure 2.32 (c): Close-up from figure 2.24 (a) showing abundant *Cylindrichnus* burrows subtending from thick mud layers of Facies 7(b). Photo from well 3-18-91-7W4, Core 9 1 of 2, ~161.4 m – 161.7 m depth. Core boxes is 7.5 cm wide.

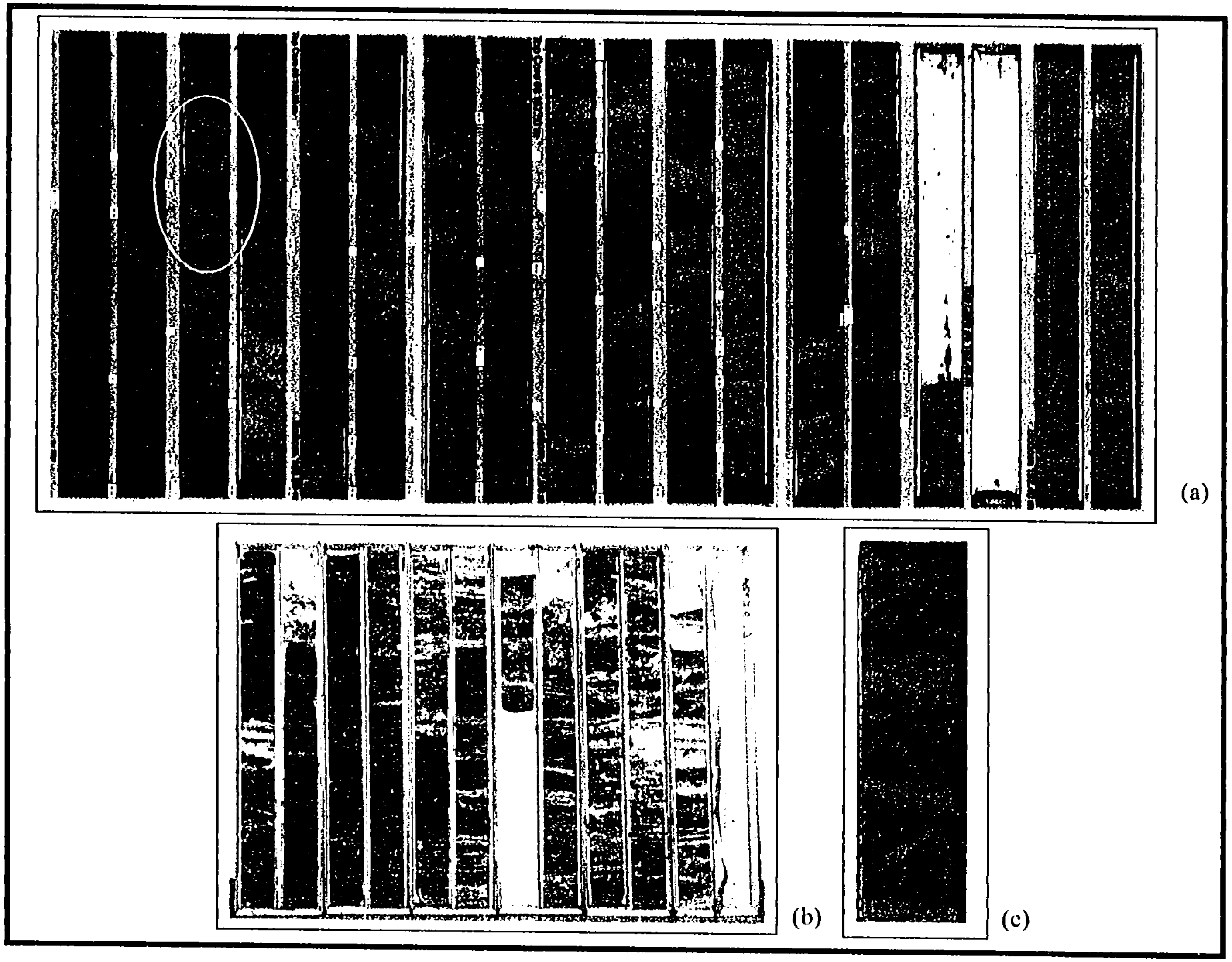
(a)
(b)
(c)
2.32

beds. Although both occur, lateral variations in the make-up of silt/mud occur more commonly than do vertical changes. Stacked silt/mud laminae typically exhibit a low diversity, low to high abundance trace fossil assemblage dominated by *Cylindrichnus*, *Planolites*, and *Thalassinoides*, with common escape traces and *Rosselia* and *Skolithos* burrows. Burrows are generally small (<1cm), although large well developed burrows are observed. Individual laminae are commonly wavy and discontinuous and exhibit cm-scale offsets (micro-faults) and/or soft sediment deformation. Thick silt/mud layers typically exhibit rare bioturbation, although burrowing may be locally intense. *Cylindrichnus* burrows subtending from silt/mud layers are also common (Fig. 2.32(c)).

Interpretation:

The term inclined heterolithic stratification (IHS) was introduced by Thomas *et al.* (1987, p.125) to describe "*modern and ancient large-scale, waterlain, lithologically heterogeneous...siliciclastic sedimentary sequences, whose constituent strata are inclined at an original ("depositional") angle to the horizontal or paleohorizontal. Deposits of such strata typically range in thickness from 1 to 30 m, exhibit internal dips of 1-36°, and, given suitable exposure, may be traceable along their strikes for many tens of meters*". Although the original definition was intended to be non-genetic and indicative of the alteration of sand and mud deposited on a dipping sediment surface, the term IHS has essentially become synonymous with lateral accretion deposits produced by the migration of point-bars (e.g. Allen 1991; Ainsworth and Walker 1994; Wightman and Pemberton 1997; Lavigne 1999;

Gingras *et al.* 2002; Page *et al.* 2003). In fact, to the knowledge of this author, no published accounts of IHS deposits attribute their origin to mechanisms other than lateral accretion.

Sand-dominated IHS deposits (subfacies 7a) require flow conditions with either low concentrations of fine suspended sediment, sufficient erosion of previously deposited silt and mud, or simply rare and/or short-lived low energy conditions for silt and mud deposition (i.e. waning fluvial or tidal flow, flocculation). Conditions such as these can occur on the upstream ends of large point-bars, upstream from the turbidity maximum or maximum tidal limit, or simply within high energy meandering systems. In contrast, silt-dominated IHS deposits (subfacies 7b) require predominantly low energy conditions with high suspended sediment concentration. The abundance of fine suspended sediment is most probably related to clay flocculation superimposed on waning fluvial and/or tidal flow. These conditions can occur on the downstream end of a large point-bar or in low energy, silt- and mud-rich environments such as low gradient meandering systems or in the turbidity maximum zone. As implied above, a single, large point-bar may grade laterally from sand-dominated at the upstream end, to mud-dominated at the downstream end. This rapid facies transition has been observed within modern low-gradient fluvial point-bars of the Athabasca delta (Caverley 1984), the Ursi River, India (Purkait 2002), and tidally-influenced point-bars of the Willapa River, Washington State (Smith 1987).

As described above, both sand- and mud-dominated IHS deposits exhibit internal variations in the makeup of mud and silt layers. These variations can be attributed to the wide spectrum of mechanisms that control fine-grained sediment deposition, including: (1) clay flocculation due to the mixing of fresh and marine water (thick or thin mud beds); (2)

slack-water mud deposition (stacked laminae); (3) daily or seasonal low energy discharge in a fluvial system (thick or thin beds or stacked laminae). Although early descriptions of IHS have acknowledged that many mechanisms can cause mud deposition (cf. Shanley *et. al.* 1992), the muddy heteroliths that typify IHS deposits are generally attributed to tidal processes (e.g. Smith 1987; Allen 1991; Lavigne 1999). Although tides commonly form alternating sand/mud couplets, similar structures have been described from modern *freshwater* lateral accretion deposits (Jackson 1981; Caverley 1984; Page *et al.* 2003). Because of the obvious difficulty in differentiating fluvial from tidally-influenced IHS in both modern and ancient deposits based only on physical sedimentary structures, ichnological assemblages, which can serve as a proxy for paleo-salinity changes during deposition (cf. Land and Hoyt 1966; de Mowbray 1983; Barwis 1978), help make this differentiation possible.

Many bioturbated layers in F7 possess characteristics of brackish-water depositional conditions, including diminutive burrow size, simplistic burrow morphologies, low diversity and a high abundance admixture of forms in both the *Skolithos* and *Cruziana* ichnofacies (Pemberton *et al.* 1982; Wightman *et al.* 1987). Also present, however, are rare to unbioturbated mud layers that may indicate non-marine deposition, or simply reflect other factors that precluded colonization, for example oxygen content, turbidity, substrate and sedimentation rates.

In summary, F7 is interpreted to represent lateral accretion deposits produced by the migration of point-bars. Sand-dominated IHS deposits (sub-facies 7a) indicate deposition within higher energy environments compared to lower energy mud-dominated IHS deposits (subfacies 7b). Changes in burrow size, abundance and diversity can help distinguish between mud and silt layers deposited in freshwater (rare to unbioturbated) or tidal/marine (brackish water assemblage) meandering channels.

Facies 8: Horizontally-stratified sand and mud

Facies 8 is characterized by planar to wavy, regularly-interstratified very fine to lower fine-grained sand and mud (Fig. 2.33). Sand and mud layers are each typically 1-2 cm thick although individual layers of both sand and mud are commonly several decimeters thick (Fig. 2.34). Upward increases in mud or sand are observed. Units of F8 range from <1-23 m thick, but average about 11 m. The base of F8 strata is typically sharp, but may be difficult to discern where it overlies sandy sediment.

Sand beds commonly exhibit small-scale symmetrical or asymmetrical stratification (Fig. 2.35) and are moderate to heavily bitumen stained, although more commonly sand is gas-charged. Synaeresis cracks (Fig. 2.36) and disseminated organic material are both common in mud layers; coal clasts are rare, but observed in both sand and mud layers. Common soft-sediment deformation and rare micro-faults are also observed. Carbonate-cemented zones, less than 5 cm thick, occur at irregular stratigraphic intervals.

Bioturbation in F8 strata is variable and ranges from rare *Planolites* and *Skolithos* to a slightly more diverse and mottled bioturbate texture that includes any or all of *Planolites, Skolithos, Teichichnus, Rosselia, Arenicolites,* and *Cylindrichnus* burrows and escape traces. Where bioturbation is intense, primary physical sedimentary structures, if formerly present,

Figure 2.33: Rhythmic horizontal stratification of Facies 8. Note the increase in sand upwards. Photo from well 6-8-91-7W4, Cores 18 and 19, 152.1 m -156.9 m depth. Core boxes 75 cm long.

Figure 2.34: End-member kinds of Facies 8 strata: Mud-dominated (a) and sand-dominated (b). Photos from well 15-22-91-7W4. Core boxes 75 cm long.

Figure 2.34 (a): Thick unbioturbated mud beds horizontally interstratified with thinner sand beds. Photo from Core 16 2 of 2, ~171.2 m - 172.7 m depth.

Figure 2.34 (b): Thick sand beds horizontally interstratified with thinner silt beds. Also note synaeresis crack (syn) in right core box. Photo from Core 15, 2 of 2, 167.5 m – 169.0 m depth.

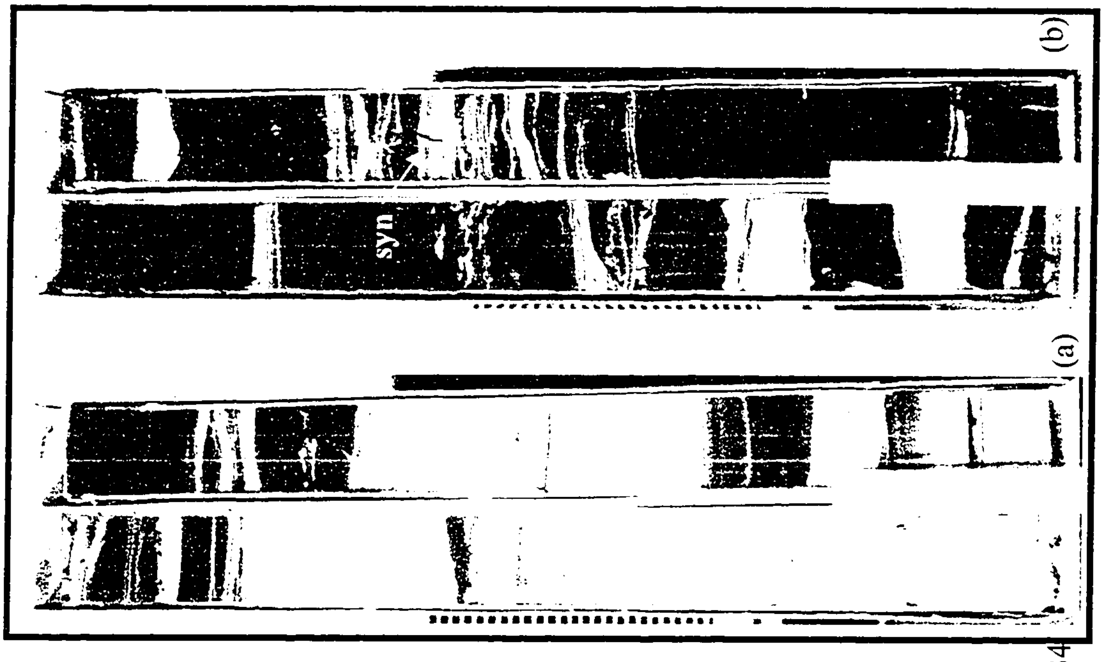
(b)
syn
(a)

2.34

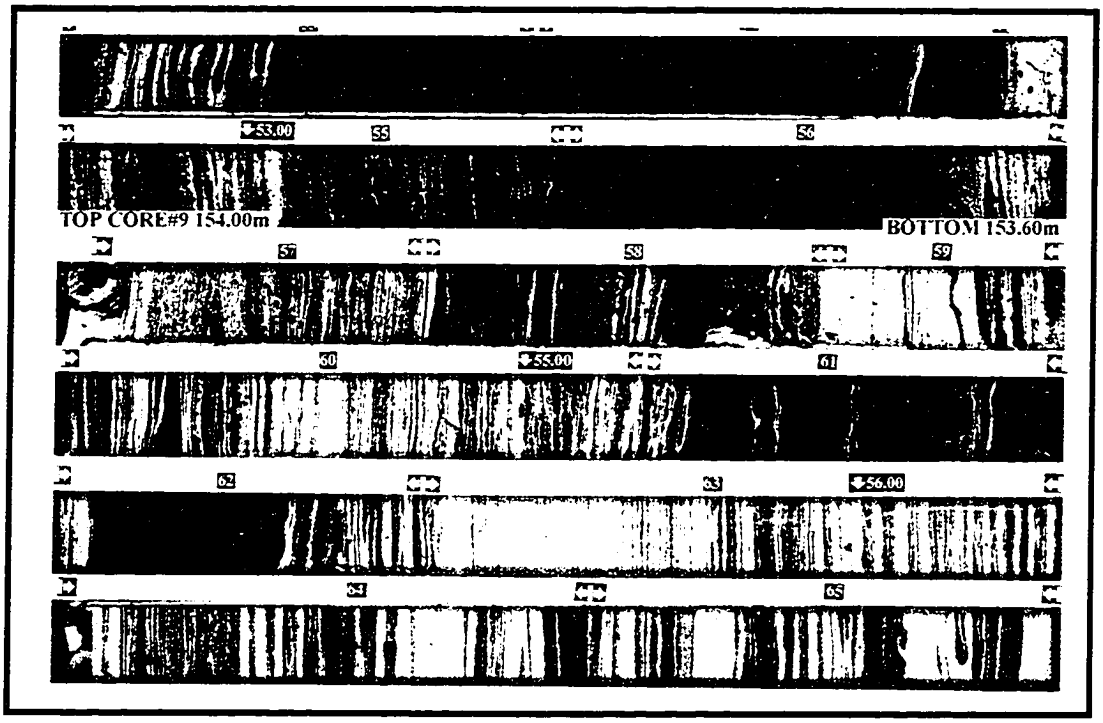
53.00
55
56
TOP CORE#9 154.00m
BOTTOM 153.60m
57
58
59
60
55.00
61
62
63
56.00
64
65

2.33

Figure 2.35: Small-scale cross-stratification in Facies 8.

Figure 2.35 (a): Asymmetrical cross-stratification showing an increase in dip angle along the set. Photo from well 1-23-91-7W4, Core 6 2 of 2, ~189.5 m depth. Core box is 7.5 cm wide.

Figure 2.35 (b): Current ripple cross-stratification cut perpendicular to flow. Photo from well 15-27-91-7W4, Core 9 1 of 2, ~159.2 m depth. Core box 7.5 cm wide.

Figure 2.36: Facies 8. Sand-filled synaeresis cracks (syn) in mud. Also note *Planolites* burrow. Photo from well 12-21-91-7W4, Core 4 1 of 2, ~149.5 m depth. Core box is 7.5 cm wide.

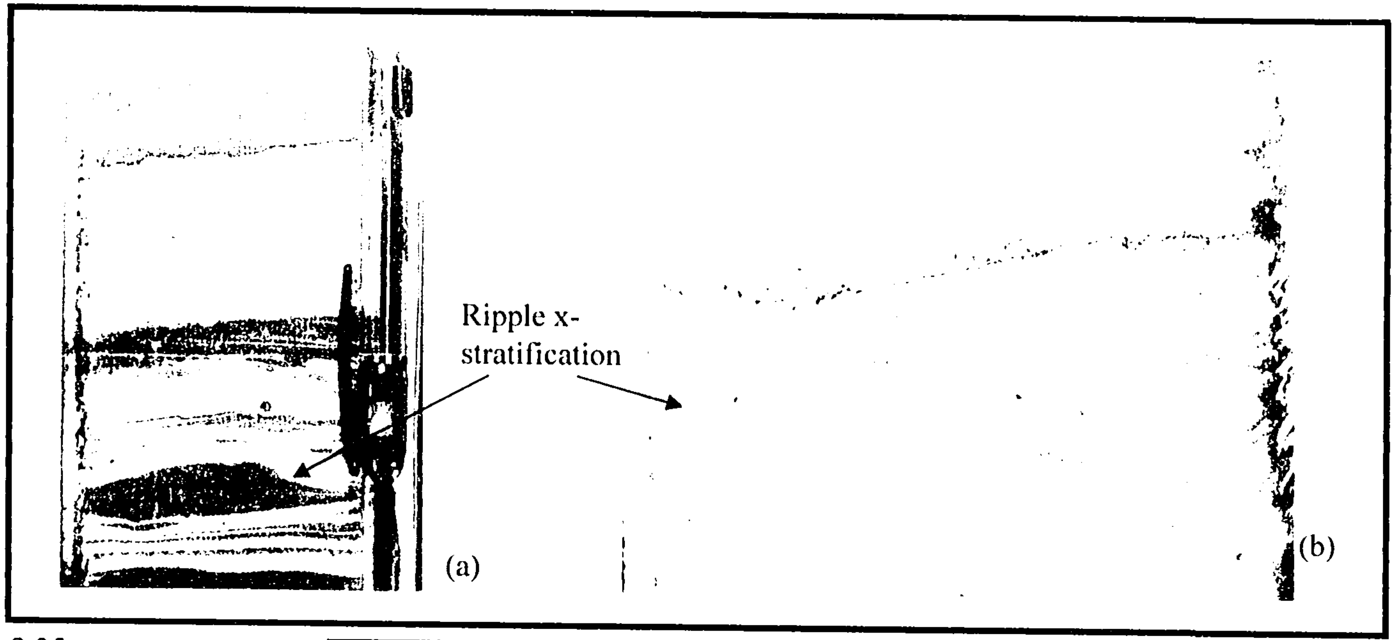

2.35

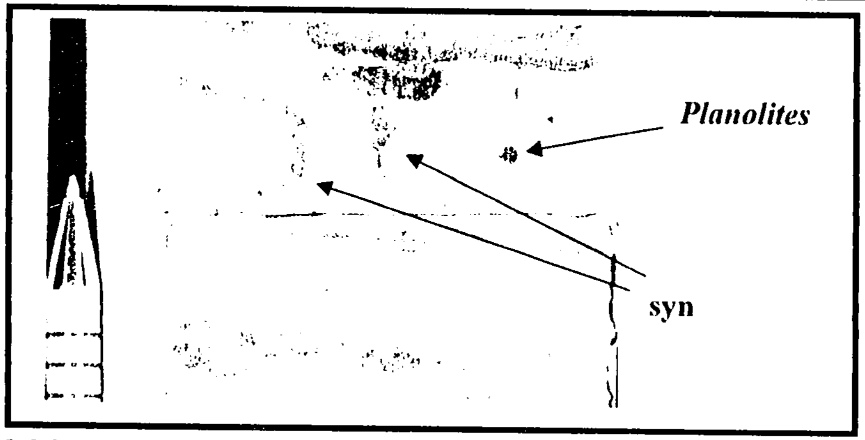

2.36

are destroyed (Fig. 2.37). Abrupt vertical changes in bioturbation intensity are common, typically in decimeter-thick intervals, producing sharp bioturbate contacts in core (Fig. 2.38).

Interpretation:

The preponderance of regular-spaced sand/mud couplets in this facies suggests alternating episodes of bedload (high energy) and suspended (low energy) deposition. Similar regularity is common in many modern coastal environments and is generally attributed to tidal cyclicity (de Raaf and Boersma 1971; Rahmani 1988; Dalrymple *et al.* 1991; Nio and Yang 1991). In a typical flood/ebb tidal cycle, active current ripple migration and deposition of sand occurs during the rise (flood) and fall (ebb) of the tide when currents reach appropriate velocity. Mud, on the other hand, is deposited during the intervening slack-water stage at maximum and minimum water depths when current velocity is negligible (Nio and Yang 1991; Dalrymple 1992). Where diurnal or semi-diurnal tidal rhythmicity is preserved, the resultant stratigraphic record is a repetitive intercalation of sand-mud couplets. In most tidal environments either the flood or the ebb current dominates and deposits a thicker sand layer compared to the opposing tidal component (de Boer *et al.* 1989). Evidence of this inequality is apparent in F8 by the presence of disproportionately thick sand beds interstratified throughout. Alternatively, thick sand beds may represent an amalgamation of successive flood/ebb flow deposits where the intervening mud bed has been eroded (Nio and Yang 1991). Thick mud beds, on the other hand, may be deposited via clay flocculation, a common process in the turbidity maximum zone in modern estuaries (Hughes *et al.* 1998). The position of this zone varies, often seasonally, and is affected by factors like fluvial

Figure 2.37: Abrupt contact (black bar) between rare bioturbated strata (lower) and intensely bioturbated strata (upper) of facies 8. Bed at the top of the lower unit is calcite cemented mud. Photo from well 2-22-91-7W4, Core 10, ~150 m – 151 m depth. Core boxes are 75 cm long.

Figure 2.38: Mottled variation of Facies 8. Physical sedimentary structures (if formerly present) have been destroyed by bioturbation. Photo from well 12-34-91-8W4, Core 10 2 of 2, ~145.5 m – 147 m depth. Core boxes are 75 cm long.

2.37

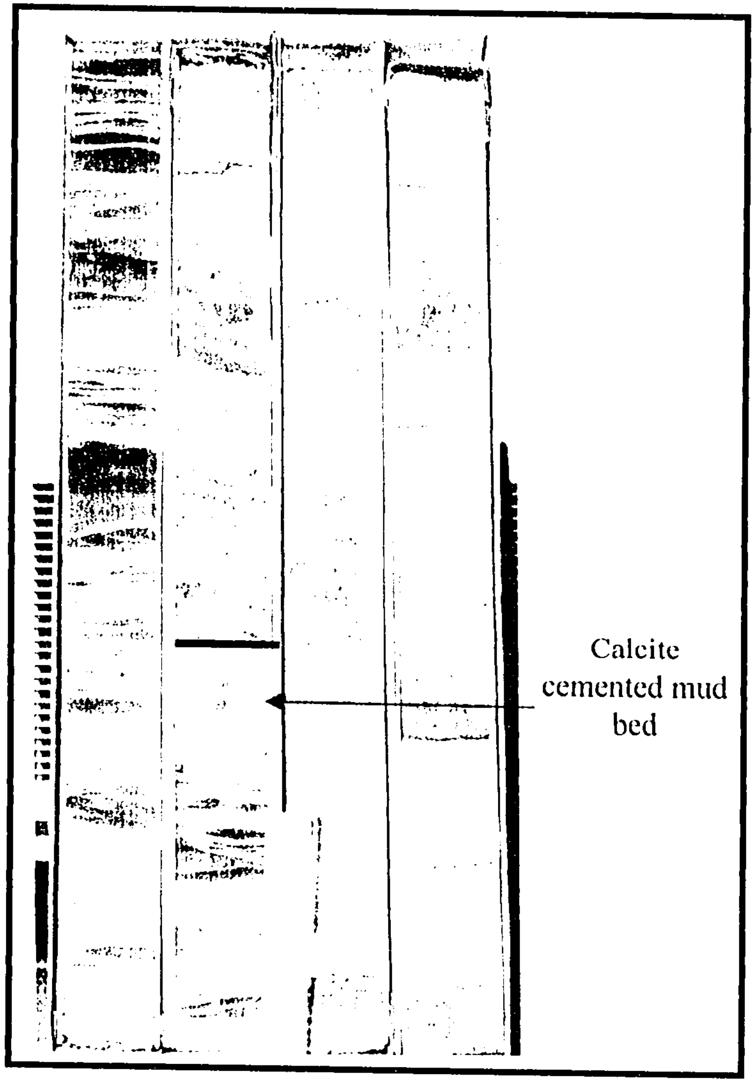

2.38

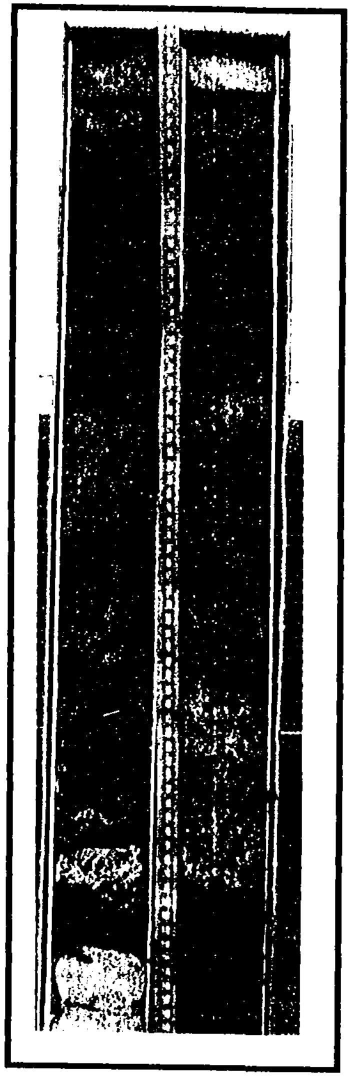

discharge, wave energy, tidal range (Dalrymple *et al.* 1992), and sediment supply (Hughes *et al.* 1998). Shifts in the turbidity maximum may explain variations in sand/mud ratios throughout this succession and why some mud layers are anomolously thick.

Several asymmetrical ripples show a marked increase in foreset angle, from gently dipping at the base to steeply dipping along an individual set (Fig. 2.35). Termed sigmoidal stratification, this feature has previously been described from tidally-influenced settings, resulting from flow acceleration within a tidal flow (Shanley *et al.* 1992; Nio and Yang 1991; Molgat and Arnott 2001). Rare symmetrical cross-stratification suggests that F8 strata were influenced periodically by oscillatory flow conditions associated with wind waves. However, the rare preservation of symmetrical ripples compared to asymmetrical current ripples suggests that unidirectional flow dominanted.

Abundant deformation structures (micro-faulting, synaeresis cracks and soft-sediment deformation) suggests high sedimentation rates. Synaeresis cracks are generally interpreted to be subaqueous shrinkage cracks formed via pore water expulsion and subsequent volume decrease in clay sediments (Leeder 1982). Commonly, they are observed in strata interpreted to have been deposited in marginal-marine environments with fluctuating salinity (e.g. Shanley *et al.* 1992). While none of the above-mentioned physical sedimentary structures are singlely diagnostic of tidally-influenced environments, collectively they are consistent with a tidal interpretation for F8 strata.

Bioturbation has many characteristics of a stressed, or brackish-water assemblage, including low diversity but abundant traces and diminutive forms (Pemberton *et al.* 1982). Because remnants of preserved primary stratification in the mottled parts of this facies are similar to that in unbioturbated parts, the difference in bioturbation is interpreted not to be the result of differences in sedimentation rate or processes, but instead due to changes in other factors like water chemistry. The sharp bioturbate contacts in F8 may reflect temporal changes in salinity conditions at the sea bed because of changes in fluvial discharge, tidal range, or wave energy. For example, in the modern Mahakam River delta (Borneo, Indonesia) differences in bioturbation intensity have been shown to correlate with differences in salinity that vary spatially within the delta complex (Gastaldo *et al.* 1995). Here, intensely bioturbated strata are generally restricted to the open, seaward portion of the delta compared with generally unbioturbated strata in the landward-proximal parts.

Facies Associations and Interpretations

Facies Association 1: Fluvial channel association

Facies Association 1 (FA1) is typically confined to paleo-topographical lows on the sub-Cretaceous unconformity (Figs. 2.6-2.7). On average successions are about 10-12 m thick, but locally range from < 5 m to several 10s of meters thick. The base of FA1 is commonly marked by a soil horizon (F4), which in turn is sharply overlain by massive to high-angle cross-stratified pebbly sand (F2) and locally by well-sorted medium sand deposits (F1a). Although sand successions typically occur as discrete units (e.g. only F2 or F1a), poorly- and well-sorted sand may be abruptly interstratified locally. Coal beds and/or soil horizons (F4) locally mark the base of meter-scale stacked sand successions. The top of FA1 may be marked by a soil (F4) or coal, but more commonly it is marked by a sharp decrease in grain size and better sorting of Facies Association 2.

Interpretation:

The lack of rhythmicity, abundance of coarse-grained sediment, and poorly-developed overbank deposits in strata of Facies Association 1 (FA1) is typical of mixed sand and gravel braided-fluvial systems. Sediment deposition due to a local reduction in flow velocity caused channel bifurcation and subsequent growth and development of pebbly mid-channel bars (McLelland *et al.* 1990). Transverse bar deposits are represented by thick accumulations of high-angle cross-stratified (F1a) sand exhibiting little to no grain size sorting during avalanching on the lee-side of subaqueous dunes.

Facies Association 2: Tidally-influenced channel deposits

Facies Association 2 comprises stacked meter-scale successions of F1 and F7, although locally thin pebbly-sand layers (F2) are interstratified with F1. Lower FA2 channel deposits, consisting of F1 strata, truncate older braided-fluvial channel-fills (FA1), commonly completely eroding this earlier channel system. Paleosols (F4) developed locally between FA1 and FA2. Lower FA2 channels (F1), in turn, are overlain gradationally by stacked successions of inclined heterolithic stratification (F7), with varying sand-mud ratios. In places, lower and upper FA2 channel fills may be separated by strata of FA3 (see below). FA2 ranges in thickness from <5 m up to 60 m thick, with individual stacked successions ranging from <5 to 30 m thick. The base of stacked successions is marked by subtle discontinuities such as mud clast horizons, pebble layers (in F1 strata), changes in thickness and/or frequency of mud layers, or a change in bioturbation type and abundance.

Interpretation:

Facies Association 2 is interpreted to represent deposition within tidally-influenced channel systems. Early high-energy channels that were infilled with strata of F1 and F2 initially developed within and subsequently infilled remnant negative paleotopography along the sub-Cretaceous unconformity (Fig. 2.39). Although estimates of ancient sediment flux are speculative, it has been suggested that the McMurray paleovalley system drained much of west-central Canada (Ranger 1984), and therefore channels in the study area most-probably transported a voluminous sediment flux. High sediment load, a significant fraction of which was coarse-grained bedload material, coupled with periodic discharge fluctuations and unstable channel banks likely caused early (lower) (F1) channel systems to develop a braided pattern. However, the abundance of mud-clasts suggests that interchannel deposits were well developed and that these channels may in fact represent deposition in a low-accommodation meandering system (Arnott *et al.* 2002). Low-accomodation, and also lateral confinement by relief along the unconformity surface, would cause laterally-migrating channels to extensively cannibalize interchannel deposits. Although channel-fills are multiply stacked and no greater than ~5 m thick (based on thickness of upward-fining sequences in core), the overall geometry is sheet-like, with rare pod-like (remnant) interchannel/abandoned channel deposits (FA3) preserved. This, therefore, suggests that the

Figure 2.39: Gross sand map of F1 strata. Note that the thickest accumulation of sand corresponds to paleolows on the sub-Cretaceous unconformity (compare with Fig. 2.5). Contour interval 5 m.

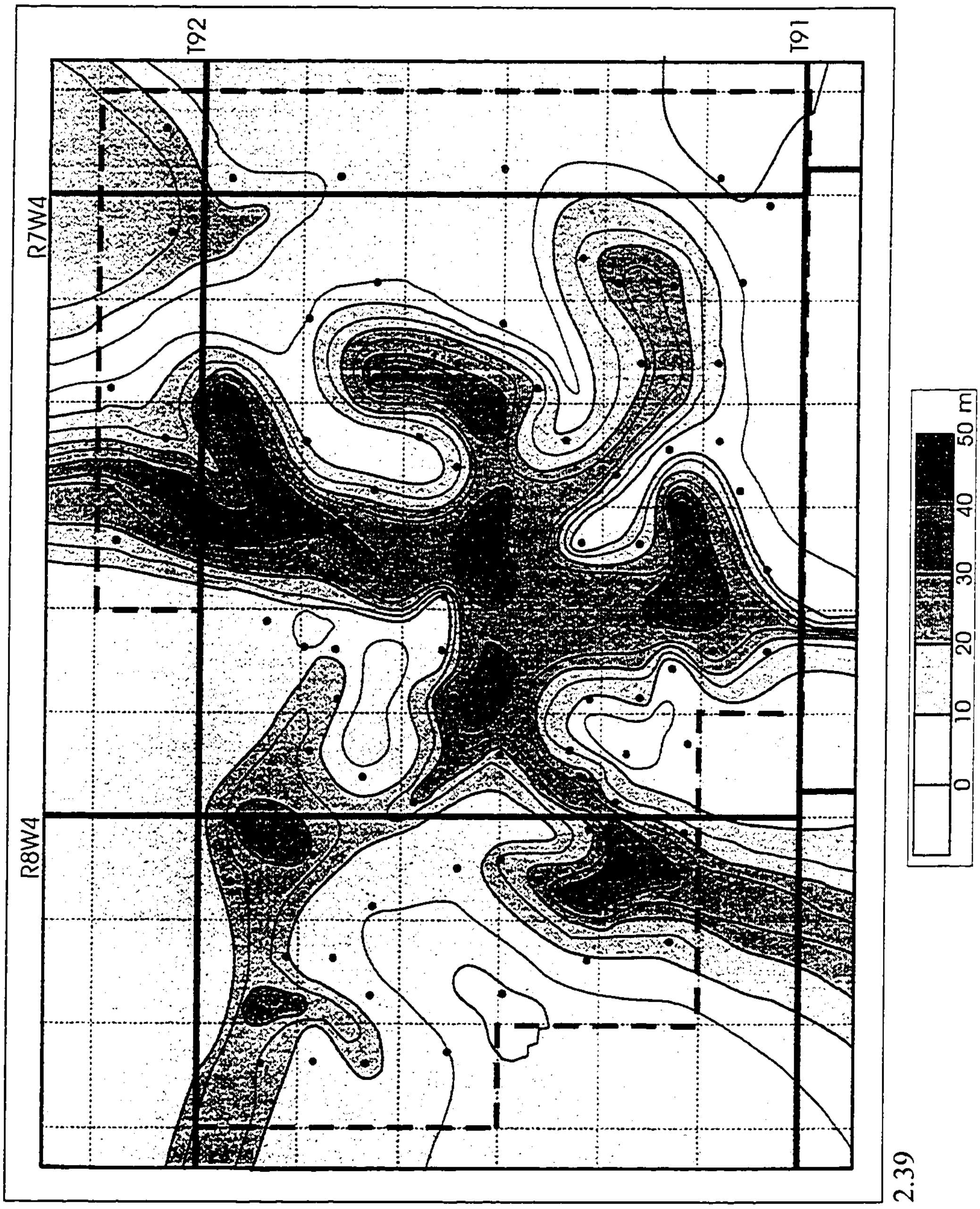

2.39

rate of lateral accretion versus vertical aggradation was high and resulted in a sheet-like deposit dominated by coarse channel strata.

Compared to early FA2 channel-fills, late FA2 channel-fills, which consist mostly of F7 strata, are finer grained (including significant decreases in sand/mud ratios locally), show an increase in diversity and abundance of trace fossils, and exhibit more common tidal sedimentary structures. The gradational vertical transition from lower to upper FA2 strata indicates a landward shift of facies from the upstream reaches of a fluvial-dominated system (F1), to marginal-marine, tidally-influenced channel deposits (F7). In addition, tidal flat deposits (F8) locally separate lower and upper FA2 channel-fill successions, which also supports a landward shift in facies (Figs. 2.6-2.7) (see FA3 below). The commonality of lateral accretion deposits suggests that F7 channel systems developed a sinuous, meandering channel pattern which may have been in response to a significant decrease in coarse-grained sediment load and subdued paleotopography due to burial of the irregular sub-Cretaceous unconformity (Figs. 2.6-2.7). The abrupt upward disappearance of pebbles in F7 strata is likely a function of the abrupt downstream gravel-to-sand transition that occurs in mixed sand-and-gravel fluvial systems (Paola *et al.* 1992; Sambrook and Ferguson 1995). Furthermore, because these late channel systems were no longer confined to paleo-lows along the sub-Cretaceous unconformity, more extensive lateral migration of the channel systems occurred producing multiply-stacked point-bar successions (IHS deposits).

Younger FA2 channels (F7) were indirectly influenced by paleotopography along the deeply-buried unconformity. This is suggested by the tendency of these younger channels to preferentially form over older, buried paleovalleys (Fig. 2.40). This effect has been noted on

Figure 2.40: Gross sand map of F7 strata. Note that the thickest accumulations of sand occur where underlying F1 channel sand is also thickest (Fig. 2.39), suggesting that syn-depositional salt-dissolution of the underlying (Devonian) Prairie Evaporite Formation most-probably controlled channel development (see text for further explanation). Also, because the paleotopography of the sub-Cretaceous unconformity has been buried, IHS deposits were not as confined to the main valley as was the case for lower F1 sand (compare with Fig. 2.39).

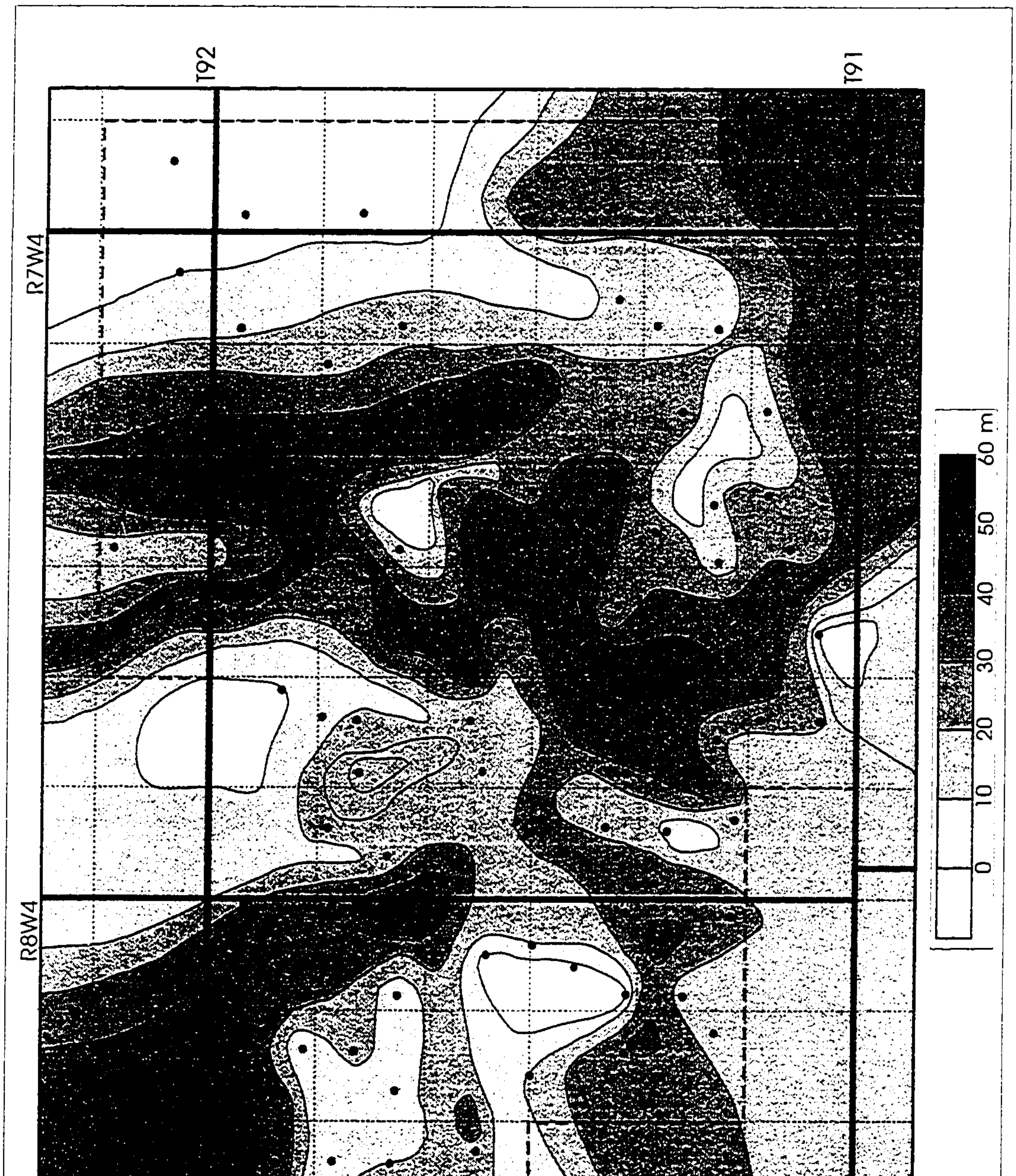

2.40

a regional-scale by Ranger and Pemberton (1997), and appears to persist even to the present where the position of the modern Lower Steepbank River mimics that of the main (Cretaceous) McMurray paleovalley in the Lewis study area (Fig. 2.4). The fact that upper (F7) (and modern) channels overlie lower (F1) FA2 channel systems suggests that syn-depositional salt dissolution occurred throughout McMurray time, and persists even today. Otherwise, younger channels would preferentially deviate towards more easily compacted, and thereby topographically lower, off-channel areas. Continued subsidence due to salt-dissolution ultimately controlled channel position and infilling history in the Lewis study area.

Although the thickest and sandiest accumulations of upper F7 channel fills overlie pre-existing F1 channel systems, IHS deposits are preserved throughout the study area, even in places where the sub-Cretaceous unconformity is topographically high and therefore where lower F1 channel-fills are poorly developed (e.g. 1-23-91-7W4). This suggests that extensive IHS channel migration occurred even outside of the main McMurray paleovalley in the Lewis study area (Fig. 2.40). Outside the main paleovalley, however, IHS successions generally comprise muddier and thinner (<5-10 m thick) stacked channel-fills, contrasting sand-dominated successions preserved within the main paleovalley. This suggests that high-energy flow continued to be focused within the main paleovalley and that IHS deposits outside of this valley system were most probably dominated by lower energy flow with a higher concentration of suspended fine-grained sediment.

Stratigraphically-upward, IHS successions generally become thicker, muddy and more intensely bioturbated. Furthermore, there is an increase in preserved fine-grained tidal flat deposits (FA4) (Figs. 2.6-2.7). Together, these stratigraphic trends suggest that the rate of lateral accretion versus vertical aggradation progressively decreased. This, in turn, is likely due to a combination of factors, including the presence of more cohesive bank material that reduced the rate of lateral migration, and/or base level rise related to rising relative sea level or downstream infilling of the system by autocyclic processes (cf. Smith and Smith 1980). The presence of synaeresis cracks in stratigraphically higher tidal flat deposits is consistent with the former explanation, whereas the latter is supported by the observed increase in bioturbation intensity stratigraphically upwards.

Facies Association 3: Abandoned channel/interchannel deposits

Facies Association 3 sharply to gradationally overlies Facies Association 2, or less commonly Facies Association 1, and locally directly overlies the sub-Cretaceous unconformity (e.g. 15-29-91-7W4). In turn, successions are overlain erosively by Facies Association 2 or sharply or gradationally overlain by Facies Association 4. Successions consist of <1 m up to 20 m thick unbioturbated mudstone that in places is interstratified with burrowed or unburrowed fine sand layers (F5). In places, rare to unbioturbated, planar to wavy interstratified very fine to lower fine sand and mud (F8) locally over- or underlie F5 strata (Figs. 2.6-2.7). These successions, however, are poorly preserved, less than 5 m thick, and occur at several stratigraphic horizons throughout most of the study area. In the easternmost part of the study area, thick (up to 35 m) mottled successions (F8) are preserved. Locally, decimeter- to meter-thick units of mottled clay (F4) are observed and, where present, commonly mark the base of Facies Association 3.

Interpretation:

Facies Association 3 is interpreted to represent vertically-accreting abandoned channel and/or interchannel deposits. In general, the thickest accumulations of FA3 occur above paleotopographic highs on the unconformity (Figs. 2.6-2.7). Here, FA2 successions are poorly developed suggesting spatial variability in vertical versus lateral accretion in the study area.

Mudstone successions (F5) form pod-like structures within the main north-south trending channel belt (see FA2 discussion) in the study area and represent abandoned channel-fills (Fig. 2.8). These deposits are coeval with the development of tidally-influenced channels (FA2). Sand interlayers, commonly bioturbated and bitumen saturated, within an otherwise thick succession of mud are most probably deposited when swamp margins are breached during high energy flood events in laterally adjacent channels. This suggests that mud (F5) successions are generally related to FA2 channels and that sand layers are most probably laterally discontinuous over short distances, possibly several meters. To the west of the main channel belt, and in the northernmost portion of the study area, mudstone successions tend to be thicker and laterally continuous over several kilometers (Fig. 2.8). This area also coincides with a paleotopographical high on the sub-Cretaceous unconformity, suggesting that this area was likely the site of a paleo-lagoon that was only poorly connected to the open ocean. The definitive lack of sand layers in F5 strata within this region suggests that this area was isolated from channel systems, and therefore lacked a direct connection with a marine source of salinity. This implies a general isolation from the open ocean which is also supported by palynomorph data that includes an impoverished dinoflagellate assemblage.

Tidal flats (F8) also form fine-grained interchannel deposits between FA2 channels. However, because of active lateral tidal-channel migration these strata are generally poorly preserved. In the eastern portion of the study area (e.g. 12-30-91-6W4) tidal flat strata are thickly developed and sand-filled channels are uncommon. This suggests that channel migration was generally inhibited in this area, possibly due to a more cohesive bank material and/or because of an absence of salt dissolution in this region to promote channel development.

Facies Association 4: Tidal flat association

Facies Association 4 consists predominantly of planar to wavy, regularly-interstratified very fine to lower-fine sand and mud (F8). In the southwest corner of the study area (section 12, Township 91, Range 8W4), strata comprise high-angle, medium-scale cross-stratified sand (F1a). The thickness of Facies Association 4 varies, ranging from <1 m up to 15 m, with individual stacked sandier- or muddier- upward successions that can be several meters thick. Abrupt changes in bioturbation between successive units are common. Facies Association 4 is overlain sharply or gradationally by F3. Strata are typically underlain sharply or gradationally by F7 strata, but locally by F5.

Interpretation:

Facies Association 4 is interpreted to represent an open estuarine mixed sand and mud tidal flat deposit (F8) that is incised locally by tidal channels and associated deposits (F1 and F8). Gross sand slice maps, measured at 3 m increments beneath the base of the Clearwater Shale, were used to delineate the spatial and temporal distribution of sand versus mud in this facies association (Fig. 2.41). A mixed sand-and-mud tidal flat initially developed throughout most of the study area (Fig. 2.41, 9-12 m increment map). In the southwest corner (sections 12-14, Township 91, Range 8W4), mud-rich tidal flat deposits were incised locally by a northwest-southeast-trending tidal channel that was filled with medium-grained strata of Facies 1 (Fig. 2.41, 6-9 m increment map). An eastward branching tributary channel extended from the main channel and was filled with sharp- or gradational-based sand-dominated successions of Facies 8 (Fig. 2.41, 6-9 m and 3-6 m increment maps). The high-angle (~90°) intersection between the main channel and associated tributaries in Facies Association 4 is consistent with observations in modern tidal channels formed on tidal flats (Meckel 1975; Gastaldo *et al.* 1995; Gingras 1999). Upon subsequent transgression, mixed sand- and mud-tidal flats again developed and covered the entire study area (Fig. 2.41, 0-3 m increment map).

As illustrated in Figure 2.41, the spatial distribution of sand versus mud in this facies association is a function of the relationship between high energy channel and low energy tidal flat deposits. During ebb- or flood-tidal flow, high energy is focused within tributary channels. High-energy sand deposits tend to amalgamate because intervening slack-water mud layers are generally eroded. In places, sand-dominated tributary channel-fills exhibit a

Figure 2.41: Gross sand slice maps through Facies Association 4 measured at 3 m increments from the base of the Clearwater Shale, a flat depositional surface (see map in Appendix 2). Initially mixed sand and mud tidal flats developed (9-12 m) and were subsequently incised by a coarser-grained northwest-southeast trending channel with associated tributary tidal channels. Ensuing transgression and the filling of channels resulted in the re-development of a mixed sand and mud tidal flat across the study area. Contour interval 0.5 m.

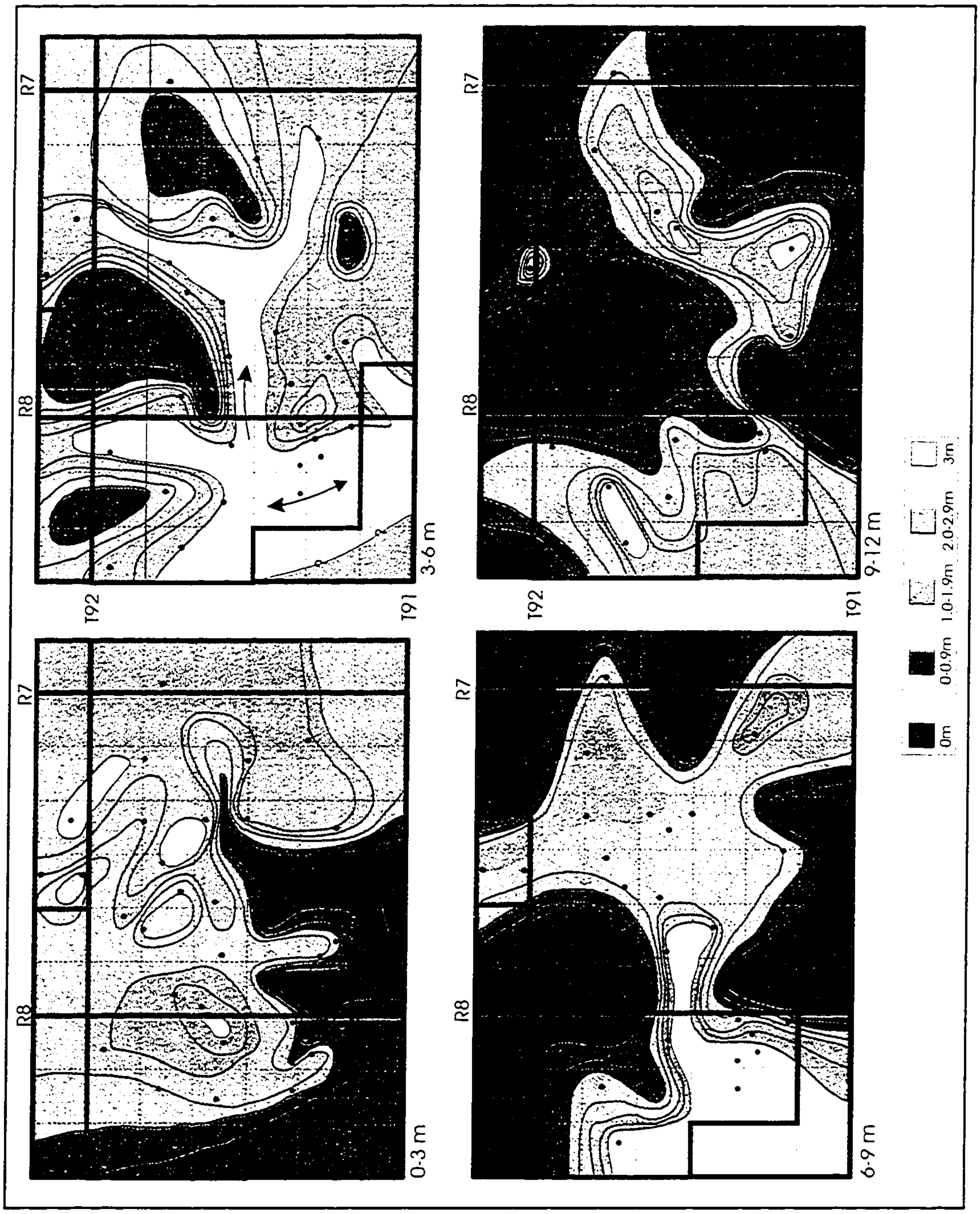

2.41

gradational upward-sandier trend over several decimeters and locally over 1 m (e.g. 9-28-91-7W4). These successions are interpreted to represent channels that shifted laterally and accreted vertically and eventually became superimposed on adjacent muddier intertidal flat strata. Similar upward-coarsening successions have been observed within marine bars of the Holocene Colorado delta (Meckel 1975). In this example, bars shifted laterally as the position of the river mouth changed and because of seaward progradation of coastal deposits. The net result was the accumulation of upward-coarsening successions of sand-dominated bar-crest deposits superimposed on mud-dominated trough strata. Although lateral channel migration most-probably did occur, the absence of point-bar (IHS) deposits in FA4 strata, as well as the spatial and temporal isolation of sand units to east-west and northwest-southeast oriented channels and tributaries suggests that lateral channel migration was at least partially limited. Lateral migration may have been partially inhibited by widespread development of cohesive intertidal flat deposits that caused channels to be preferentially filled by vertical, rather than lateral accretion. Vertical accretion may also have been accentuated by rising relative sea level (see later), which commonly enhances vertical aggradation in marginal-marine settings (cf. Tornqvist 1993). The net result was the development of vertically-accreting, low-sinuosity channels, similar to aggrading anastomosed channels of the Rhine-Muse delta (Tornqvist 1993), or straight channels in the tide-dominated Mahakam River Delta, Borneo (Gastaldo *et al.* 1995).

Facies Association 5: Shoreface to offshore deposits

Facies Association 5 consists of a thin (commonly <1 m) basal unit of glauconitic silty-sand (F3) overlain sharply or gradationally by several meters of *Chondrites* burrowed mudstone (F6). The base of the *Chondrites* burrowed mudstone unit is a relatively flat surface (Appendix 2) with little topographic relief. FA5 sharply or gradationally overlies FA4.

Interpretation:

As discussed earlier strata of F3 are interpreted to represent shoreface deposits overlain by offshore mud deposits (F6) of the Clearwater Formation. This facies association is consistent with the regional transgressive depositional model previously proposed for the Athabasca region (Flach and Mossop 1985; Ranger and Pemberton 1997).

DISCUSSION

Depositional Model of the McMurray Formation

The McMurray Formation in the Lewis study area represents deposition during a long term transgression. Depositionally, there is a preserved continuum from braided-fluvial deposits, tidally-influenced fluvial and tidal channels, upward to open estuarine/tidal flat deposition; the evolution of these deposits is illustrated in Figure 2.42. Lowstand braided-fluvial channels (FA1) of the lower McMurray Formation initially developed and were preserved within paleotopographical lows on the sub-Cretaceous unconformity (Figs. 2.8,

Figure 2.42: Schematic illustration showing the stratigraphic organization of McMurray Formation, which was deposited during a long term rise in relative sea level. (1) Braided-fluvial deposits of the lower McMurray Formation (brown) infilled paleotopographical lows along the sub-Cretaceous unconformity. (2) Rising relative sea level formed tidally-influenced depositional conditions in the study area. This caused lower McMurray strata to be erosionally overlain by transgressive channel-fills and point-bars of the middle McMurray Formation. Coarser-grained channel-fills of the lower-middle McMurray Formation (yellow) were confined by steep walls along the sub-Cretaceous unconformity. Because of limited space lateral channel migration was inhibited and resulted in the deposition of a sheet-like sand deposit with few preserved interchannel deposits (FA3, grey). (3) With the continued deposition and elimination of the irregular topography along the sub-Cretaceous unconformity, upper-middle McMurray channels became unconfined. The rate of vertical versus lateral accretion increased dramatically and upper-middle McMurray channels became progressively more encased in fine-grained overbank sediment. (4) A gradational abandonment of the network of meandering tidal channels resulted in a condition of bedload sediment starvation and preservation of open estuarine tidal flat deposits of the upper McMurray Formation (FA4, red). Tidal channels incised locally into tidal flat mud (yellow). McMurray sedimentation was terminated by a wave-ravinement surface, marking the initiation of Wabasca Member (Clearwater Formation) sedimentation.

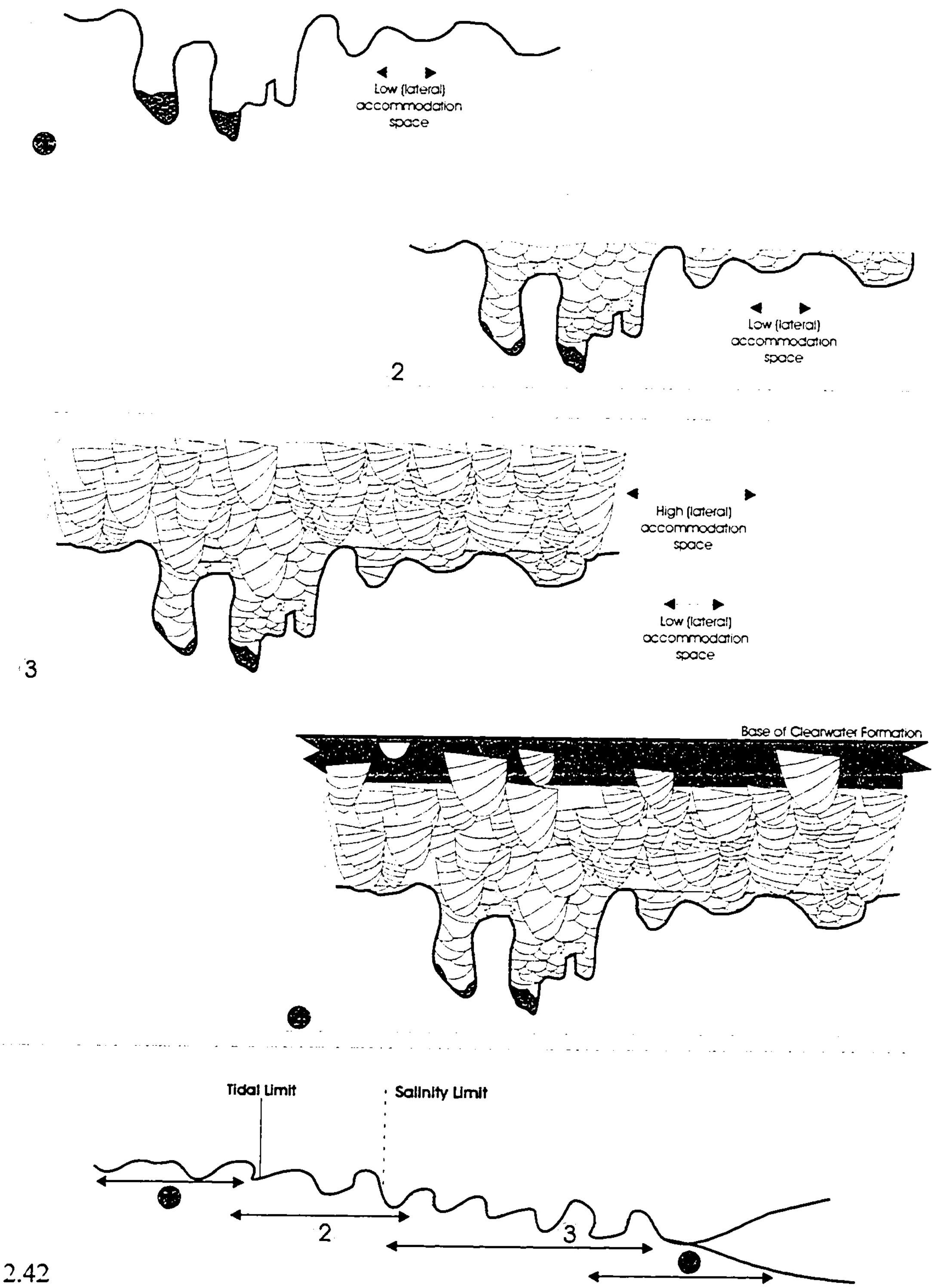

Low (lateral) accommodation space
2
Low (lateral) accommodation space
3
High (lateral) accommodation space
Low (lateral) accommodation space
Base of Clearwater Formation
Tidal Limit
Salinity Limit
2
3

2.42

2.42). The local absence of lower McMurray Formation strata is most probably because of incision by younger FA2 channels. In places, the lower and middle McMurray formations are separated by a paleosol or carbonaceous-rich horizons suggesting floodplain development. In most places, however, the lower McMurray Formation is sharply overlain by tidal channel-fills and point-bar deposits of the middle McMurray Formation (FA2). This contact represents a tidal ravinement surface and can be recognized throughout the Lewis study area and is the result of extensive lateral migration of tidally-influenced channels of the middle McMurray.

Transgressive deposits of the middle McMurray Formation consist of two stratal units: a lower succession of medium to pebbly sand-filled channels and an upper succession of fine sand tidal channel-fills. Although present throughout the McMurray section, abandoned channels and tidal flat deposits are better preserved where associated with the upper succession. Lower-middle McMurray channels developed within a high energy, tidally-influenced braided- to low-accommodation meandering-fluvial system. These channel systems likely developed in a low-gradient coastal plain environment that periodically was influenced by tidal processes. Lower-middle McMurray channels were initially confined by steep valley walls formed along the sub-Cretaceous unconformity (Fig. 2.42). Because of this, space available for lateral channel migration was limited. As a result, much of the coeval interchannel sediment (FA3) was cannibalized by laterally migrating channels and preserved primarily as mud-clasts within channel-fill sand. The net result was the accumulation of a sand-rich, sheet-like deposit with few preserved interchannel deposits, suggesting a high rate of lateral versus vertical accretion (Olsen *et al.* 1995; Arnott *et al.* 2002).

The landward shift in facies from tidally-influenced fluvial channels of the lower-middle McMurray Formation to marginal-marine tidal-channel deposits of the upper-middle McMurray Formation suggests a continuous rise of relative sea level and consequent progressive drowning of the valley system. Lower-middle McMurray channels effectively infilled most of the irregular paleotopography along the sub-Cretaceous unconformity. As surface topography became smoothed and channel systems less confined, upper-middle McMurray channels (IHS) migrated extensively laterally and formed well-developed lateral accretion deposits (Fig. 2.40). Nevertheless, upper-middle McMurray channels were indirectly influenced by the paleotopography along the unconformity surface because the thickest and most sand-rich deposits generally overlie thick underlying lower-middle McMurray channels. This suggests that syn-depositional salt dissolution controlled channel position and later infilling history.

In the Lewis study area, IHS channel-fill successions become thicker and preserve a more complete point-bar sequence stratigraphically upwards. In addition, coeval, off-channel strata and abandoned channel-fills are more commonly preserved upward. Furthermore, there is an abrupt facies shift towards open-estuarine tidal flat and associated tributary channels (FA4) in the upper McMurray Formation. The sharp decrease in the number of preserved point-bar deposits suggests an abandonment of the north-south trending network of laterally-migrating tidal channels. This may have been because of an abrupt increase in the rate of vertical versus lateral accretion which would have effectively prevented the widespread lateral migration of point-bars throughout the study area. Most likely, this would have occurred in response to an increase in the rate of relative sea level rise. Alternatively, other autocyclic processes, for example deltaic lobe abandonment and concomitant decrease in sediment flux, could produce a similar stratigraphy. The latter interpretation may explain the shift in the axis of the main channel several kilometers to the west (Figs. 2.41 3-6 m increment map, 2.42).

Deposition of the McMurray Formation in the study area, and regionally, was terminated by marine sedimentation of the Clearwater Formation. Shoreface sand of the Wabasca Member of the Clearwater Formation is preserved as a thin transgressive lag directly above the wave-ravinement surface that terminated McMurray sedimentation. These deposits, in turn, are overlain by marine shale of the Clearwater Formation.

Although medium sand to pebbles are common in channel-fills of both the lower McMurray (fluvial) and the lower-middle McMurray (tidally-influenced fluvial), sediment supply was dominated by fine sand and mud, which is an important component of IHS, tidal flats and thick mudstone successions that are common throughout the study area. Furthermore, the coastal configuration was most probably a low-gradient, tide-dominated system with high fluvial sediment input and negligible wave energy. The physiography and depositional processes of several modern fine-grained, tide-dominated deltaic systems are analogous to those of the McMurray paleoestuarine in the Lewis study area. The mud-dominated Fly River deltaic system (Papua New Guinea) (Harris *et al.* 1993; Dalrymple 2002), for example, may be analogous to parts of the McMurray Formation, in particular thick accumulations of interchannel mud of FA3. In the Fly River system, high suspended-sediment concentration, coupled with salinity-induced deposition traps mud in channels. During slack water, mud deposition may exceed 2 cm in thickness, and therefore may be analogous to the common thick mud layers present in the McMurray Formation. In deltas, however, the net bedload sediment transport direction is opposite that of estuaries (seaward compared to landward), making these coastal systems poor analogues for the overall stratigraphic framework and geometric stacking patterns observed in the McMurray Formation. Accordingly, the tide-dominated paleo-Yangtze estuary in China, which also evolved during rising relative sea level, may be more analogous to the McMurray depositional system (Hori *et al.* 2001). Although facies and stratigraphic interpretations of the paleo-Yangtze estuary were based on limited core control (Hori *et al.* 2001), the overall stacking patterns are similar to those observed in this study of the McMurray Formation; namely from fluvial through to tidally-influenced rivers and distributaries to intertidal flat deposits. Strata comprise a basal medium trough cross-stratified sand unit that is interpreted to represent meandering-fluvial channel deposition, and therefore is analogous to FA1 of the lower McMurray Formation. Fluvial deposits are then sharply overlain by poorly-sorted, fine to coarse sand interstratified with sand-mud couplets that are interpreted to represent tidally-influenced fluvial channels – a similar interpretation has been proposed for the lower-middle McMurray composed of FA2 strata. Like the McMurray, evidence for continued transgression is indicated by an overlying fine-grained muddy, foraminifera-rich distributary channel deposit. These strata are similar in facies make-up and stratigraphic position to IHS deposits in the McMurray (ichnological assemblages provide a proxy for marine influence). Paleo-Yangtze channels, in turn, are overlain by mud-dominated tidal rhythmite deposits interpreted to represent tidal flat deposits. These strata are similar to Facies Association 4 of the upper McMurray Formation. Unlike other estuarine systems (e.g. Cobequid Bay-Salmon River estuary; Willapa Bay), fluvial sediment flux into the paleo-Yangtze system was high and dominated by fine sediment and therefore presumably similar to the McMurray depositional system. The Gambia River estuary and associated tributaries may also be analogous to the McMurray Formation in the Lewis study area because it is dominated by fine-grained sediment, occurs in a low-gradient coastal setting and exhibits a tidal influence nearly 450 km up-estuary (Guilcher 1985). Further work on this remote and little-known estuarine system may help to better understand the McMurray depositional system in the Lewis study area.

Stratigraphic Nomenclature of the Upper McMurray Formation

Recently, the stratigraphic significance of the contact between the middle and upper members of the McMurray Formation has been debated (Hein *et al.* 2000; Hein and Dolby 2001; Lagenberg *et al.* 2002). In the Lewis study area the contact as viewed in core is marked by a change from inclined mud layers in IHS deposits to horizontal and rhythmically stratified sand/mud couplets in strata of FA4. However, as illustrated schematically in Figure 2.43, this contact is at different stratigraphic levels across the study area, and even between adjacent wells.

A time-correlative contact between the middle- and upper-McMurray Formation would be placed at the base of the lowest preserved FA4 tidal flat deposit in the study area. However, if this contact is genetically significant then micropaleontological changes might

Figure 2.43: Line drawing illustrating the irregular nature of the contact between FA2/3 ("middle" McMurray Formation) and FA4 ("upper" McMurray Formation). The contact between the middle and upper McMurray Formation is interpreted to be at the base of the lowest preserved FA4 deposit in the study area (contact A). However, this contact intersects other, therefore coeval, channel-fill deposits which make up part of the "middle" McMurray. The middle-upper McMurray contact, therefore, is simply a lithological (contact B) contact with no chronostratigraphic significance, and reflects only autocyclic change within the McMurray depositional system.

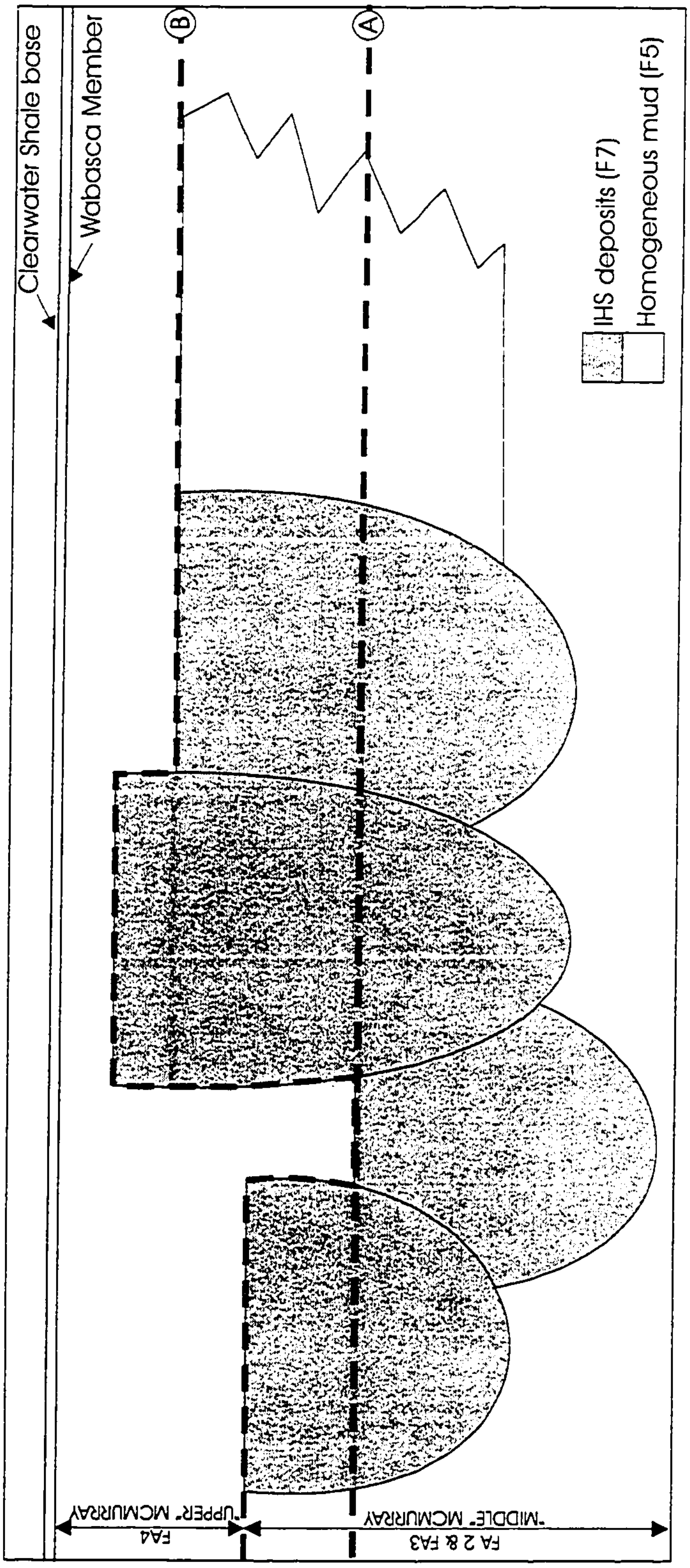
Clearwater Shale base
Wabasca Member
B
A
IHS deposits (F7)
Homogeneous mud (F5)
"UPPER" MCMURRAY
FA4
"MIDDLE" MCMURRAY
FA 2 & FA3

2.43

be expected to occur across it. Although data from this study are limited to only a small number of samples, there are no significant palynological changes to suggest changes in ecological conditions across the contact (Appendix 4). Without detailed micropaleontological control, evidence supporting a truly 'chronostratigraphic' middle-upper McMurray contact is equivocal.

The difficulty in accurately defining a chronostratigraphic contact between the middle and upper McMurray Formation poses the same question proposed by recent workers (Hein *et al.* 2000; Hein and Dolby 2001; Lagenberg *et al.* 2002): is there reason to utilize the tripartite nomenclature for the McMurray Formation within the Lewis study area? Clearly, there is a marked shift in sedimentation from channel-dominated middle- to tidal-flat-dominated upper-McMurray strata. This contact, however, is not stratigraphically significant and only reflects an autocyclic change within the McMurray depositional system. As described earlier (see depositional model discussion), this change in facies is interpreted to represent an abandonment of the north-south trending tidal channel network. This, in turn, starved the study area of coarse-grained bedload sediment and so tidal flat mud deposits were better preserved. These observations suggest that the upper McMurray possesses no chronostratigraphic or sequence stratigraphic significance (North American Commission on Stratigraphic Nomenclature 1983). Nevertheless, this author finds it useful to retain the *descriptive* definition of the tripartite subdivision of the McMurray Formation as originally proposed by Carrigy (1959). The McMurray Formation in the Lewis study area, therefore, comprises fluvial channel-fills of the lower McMurray Formation, tidally-influenced channels and interchannel deposits of the middle McMurray Formation, and tidal flat deposits of the upper McMurray Formation.

Hydrocarbon Distribution

Although most of the sand within the Lewis study area is bitumen saturated, two main reservoir sand units have been identified. These reservoirs consist of strata in Facies 1 (moderately-well sorted cross-stratified sand) (Fig. 2.44) and Facies 7a (epsilon cross-stratified and sand-dominated inclined heterolithic stratification) (Fig. 2.45). Common sand-on-sand contacts in the strata suggest hydraulic continuity between these reservoir units, although mud layers (FA3) may form local isolated compartments.

Lower-middle McMurray channels (F1) were confined to paleotopographical lows on the sub-Cretaceous unconformity surface, which therefore controls reservoir distribution and thickness (Fig. 2.39). Although sand/mud ratios are generally high, strata with little or no bitumen are usually in a structurally low position (see also F1 description). Upper-middle McMurray channels (F7), however, developed after paleotopography was smoothed by F1 channel systems. Nevertheless the thickest sand-rich channel-fills (F7) typically overlie older F1 channel-fills (Fig. 2.40). This suggests that syn-depositional salt dissolution controlled the position and evolution of both lower- and upper-middle McMurray channels (see FA2 discussion). In addition, structural position has no effect on the intensity of bitumen saturation as it does in the older, underlying strata. Instead, bitumen saturation in strata of Facies 7 is more influenced by the ratio of sand-to-mud. In addition, their generally

Figure 2.44: Typical geophysical well log and core example in a thick pay zone in Facies 1 (6-28-91-7W4). Gross sand was determined using an A.P.I. value of 80 measured from the gamma ray log. Reservoir, or net sand, was defined as that with a core-measured porosity of 27%. The resistivity log was used to assess the presence or absence of hydrocarbons and was set at 30 ohm m. Core boxes are 75 cm long.

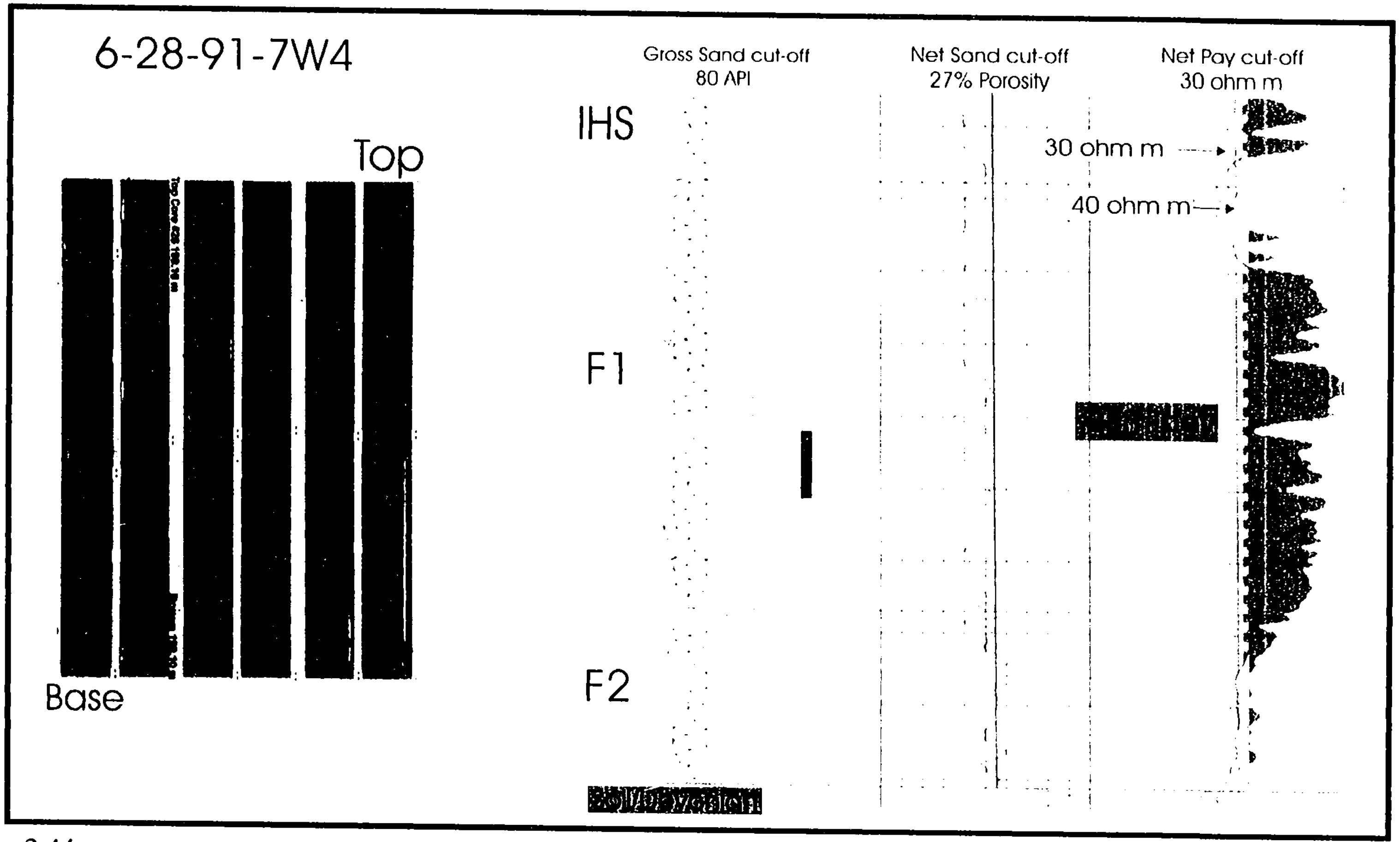

6-28-91-7W4
Top
Base
IHS
F1
F2
Gross Sand cut-off
80 API
Net Sand cut-off
27% Porosity
Net Pay cut-off
30 ohm m
30 ohm m
40 ohm m

2.44

Figure 2.45: Well log response and core examples in a thick pay zone in Facies 7 (12-21-91-7W4). Upper photo illustrates a slightly lower and less "blocky" resistivity trace because of the influence of mud layers. See caption from Fig. 2.42 for details of well-log cut-off values. Core boxes are 75 cm long.

Top

Base

Top

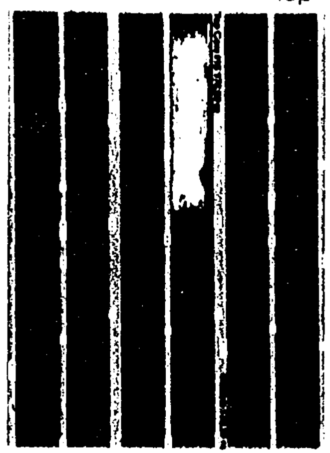

Base

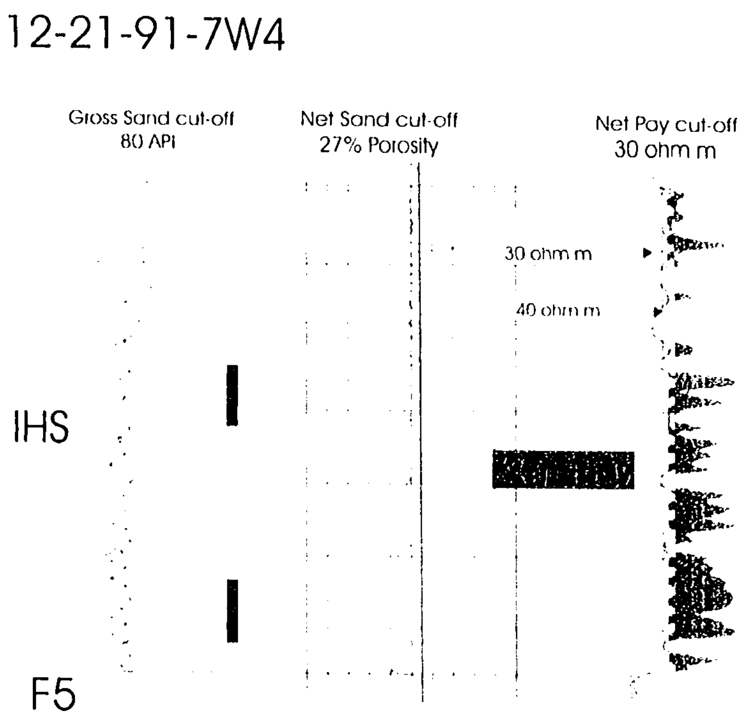

2.45

finer grain size compared to F1 channel-fills commonly yields a slightly lower bitumen saturation.

Although the reservoir generally consists of bitumen-stained sand, mud layers, mud clasts, and finer-grained sand may form local baffles or barriers to steam flow through the reservoir unit (Table 2.3). Where mud clasts are highly-concentrated within sand, bitumen-saturation is typically low. However, because mud clast horizons are interpreted to have originated from channel bank collapse (see F1 discussion), the maximum lateral continuity of these horizons is most-probably of the order of several meters. *In situ* mud layers are more common within IHS deposits (F7) than in underlying F1 channel-fills because of the lower overall energy within F7 channels, resulting in more frequent low energy conditions and/or less common erosion of mud layers. Because many of the IHS deposits consist of incomplete, multiply-stacked point-bar successions, there is a preference for the basal most IHS deposit, and ultimately the most sand-rich part to be preserved. Furthermore, detailed trenching of modern point-bar deposits show that individual mud layers are not continuous across the surface of the point-bar (Caverley 1984), and therefore, may only act as a local baffle, but not a laterally extensive barrier to steam flow. Sand-dominated point-bar deposits may grade laterally into mud-dominated point-bar deposits, which may be a local impediment to steam flow.

Interstratified mud-dominated tidal flat, abandoned channel and interchannel deposits (FA3), which are more common between F7 than underlying F1 channel deposits, may affect steam flow locally. Although estimates on the lateral extent of these deposits are speculative, based on detailed stratigraphic correlations (Appendix 2), the lateral extent of FA3 mud units

Table 2.3: Potential baffles and or barriers to flow within reservoir sand units in the Lewis study area.

Potential Baffles/Barriers to steam flow	Description	Thickness	Occurrence	Interpretaion	Geometry/Lateral Continuity	Comments
Mud Clasts	Variable clast size (mm to m); randomly dispersed or parallel to cross-bedding; +/- bioturbation; +/- sand lamina	Single clasts to horizons several meters in thickness	F1 – rare to abundant; F7 – rare to common	Bank collapse	Laterally discontinuous (max. continuity ~ several meters)	m-scale clasts or highly concentrated horizons appear as thick silt beds on GR log; lean sand where highly concentrated; factor in pay thickness calculations but not a detriment to steam migration
Thick Mudstone (F5)	Unbioturbated mudstone; locally irregularly interstratified with <1-15 cm of burrowed or unburrowed sand	<1 m - 30 m; avg. 12 m	F5	Vertically accreting abandoned channel/interchannel swamp	Pod-like features within the main paleovalley - no larger than the width of a point bar (max. 800 -1200 m)	Local influence on steam flow; factor in emplacement of horizontal well; local sand layers possible indicator of proximity to FA2 channels
Mud Layers F1	Irregularly spaced; silt beds or stacked successions of wavy, lenticular, or pin-stripe laminated sand/silt	Silt beds <5 cm thick; interlaminated layers up to 10-15 cm thick	F1b – rare to locally common	Waning fluvial or tidal flow	Laterally discontinuous, although may thicken/thin locally	High E channel system – poor preservation potential of mud layers; not a significant baffle to steam flow
Mud Layers IHS	Irregularly spaced; silt beds or stacked successions of wavy, lenticular, or pin-stripe laminated sand/silt; commonly bioturbated	<u>Sand-dominated IHS</u>: successions of stacked laminae <1-30 cm thick; silt beds 1-15 cm thick <u>Silt-dominated IHS</u>: >30 cm thick	F7a – rare F7b – common to abundant	(1) Flocculation (thin or thick beds); (2) Slack water deposition (stacked laminae); (3) Seasonal or daily energy fluxes in fluvial system (thick or thin beds or stacked laminae)	Laterally discontinuous layers, although may thicken/thin locally	May be a significant barrier to steam flow if sandy IHS successions (reservoir) grade laterally into mud-dominated IHS (non-reservoir) successions; individual mud layers not significant baffles
Mud Layers F8	Regularly-spaced, double mud drapes, wavy, planar or lenticular bedded; laminae or beds; mottled to rare bioturbation	Individual layers commonly 1-2 cm thick, but max. several meters thickness; sand/mud successions commonly several meter's thick	Rare to common	Tidal cyclicity; thick muds deposited within turbidity maximum zone	Areally continuous; sand/mud ratios vary laterally	Not reservoir sand unit; good top seal to main reservoir sand units (esp. where thick mud layers occur)

within the main north-south trending bitumen-saturated channel-fill is most probably several hundred meters.

Intertidal flat deposits (F8) overlie the reservoir sand unit and are widespread throughout the study area. Because most of these deposits are generally mud-dominated, this succession forms an effective regional seal on top of IHS reservoir sand units.

CHAPTER 3:

ORIGIN AND SIGNIFICANCE OF SEDIMENTOLOGICAL VARIATIONS WITHIN TIDALLY-INFLUENCED POINT-BAR DEPOSITS: EXAMPLE FROM THE LOWER CRETACEOUS McMURRAY FORMATION

INTRODUCTION

Because ancient marginal marine deposits contain economically significant hydrocarbon reserves, sedimentary geologists have focused considerable attention on better understanding both modern and ancient tidally-influenced depositional systems (Allen 1991; Ainsworth 1994; Dalyrymple 1992, 1994; Lavigne 1999; Gingras *et al.* 1999). To date, much of this research has centered on large-scale lateral facies changes and environmental variations related to a combination of auto- and allocyclic processes (cf. Dalrymple *et al.* 1992). As a consequence, work on sedimentological variations within specific depositional elements in tidally-influenced systems, in particular point-bars, have been largely overlooked. Although several noteworthy studies have highlighted sedimentological and ichnological variability within modern and ancient tidally-influenced point-bar deposits (Barwis 1978; de Mowbray 1983; Lavigne 1999; Smith 1987; Turner and Eriksson 1999; Gingras *et al.* 1999; Gingras *et al.* 2002; Purkait 2002; Page *et al.* 2003), the physical and chemical mechanisms responsible for creating this variability remain poorly understood. Understanding the syn- and/or post-depositional processes that control sedimentological variations within and between point-bar deposits would significantly advance our understanding of the tidally-influenced point-bar facies model which would translate directly into improved subsurface exploration and exploitation techniques.

Tidally-influenced point-bar deposits in the Lower Cretaceous McMurray Formation (Athabasca Oil Sands Deposit, Alberta, Canada) contain substantial volumes of exploitable bitumen (Mossop and Flach 1983; Wightman *et al.* 1995). In general, these deposits consist of inclined heterolithic stratification (IHS) (Thomas *et al.* 1987) with sand-mud ratios that commonly vary over lateral distances of only several hundred meters. Production of viscous heavy oil is facilitated through expensive reservoir stimulation methods such as steam-assisted gravity drainage (SAG-D) (Fig. 3.1). In this technique paired horizontal well bores, commonly less than 1000 m long, are used to extract bitumen from the reservoir. Because of their short length, and also high capital cost, a detailed understanding of reservoir architecture, especially net (pay)-to-gross sand ratios and the thickness and lateral continuity of mud layers over a short lateral distances is needed to most effectively arrange the horizontal well bores thereby optimizing heavy oil recovery.

The purpose of this paper is to examine the physical and chemical controls on tidally-influenced point-bar development in order to better understand variability in McMurray Formation IHS deposits. These findings, in turn, will assist in estimating paleochannel and point-bar dimensions, which ultimately will provide a better estimate of the reservoir size. Additionally, distinguishing between single and amalgamated point-bar deposits will assist in stratigraphic correlation and assessment of the lateral variability within these deposits.

Figure 3.1: Schematic illustration of steam assisted gravity drainage (SAG-D) techniques used in subsurface production of viscous heavy oil. Paired horizontal wells are placed in the reservoir. Steam is injected from the upper well bore, resulting in lateral and vertical growth of a steam chamber that heats the reservoir, reduces oil viscosity, and allows it to flow. Via gravity, oil drains into the lower well bore where it is then produced to the surface. Diagram from Cody *et al.* (2001)

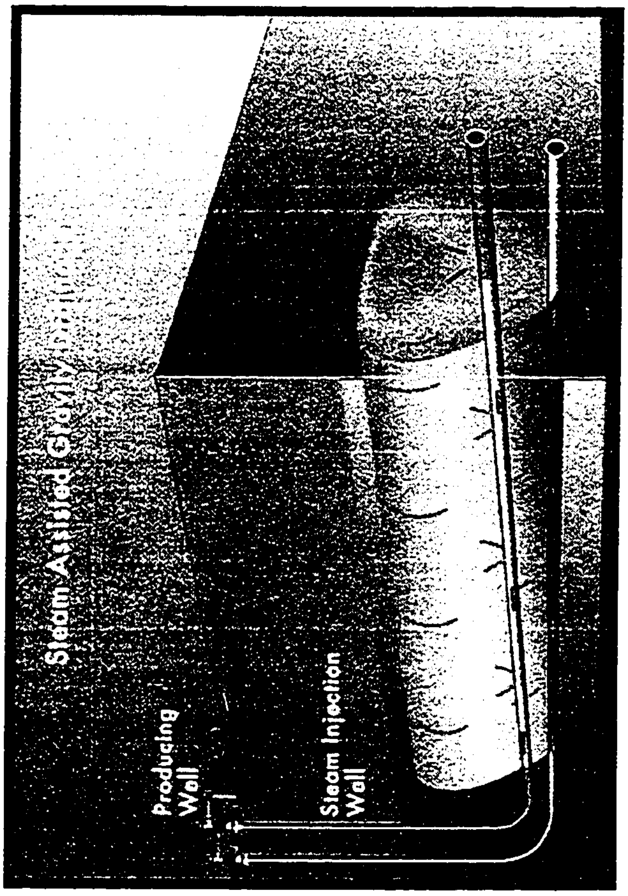
Steam Assisted Gravity
Producing Well
Steam Injection Well

3.1

THE POINT-BAR FACIES MODEL: PHYSICAL SEDIMENTOLOGICAL PROCESSES

Since Fisk's (1944, 1947 in Miall 1978) pioneering work on the Mississippi delta, a large volume of literature discussing fluvial depositional systems has been developed (see Miall 1978, 1987 for comprehensive reviews). Allen (1970) produced the first framework for the point-bar facies model by combining several older concepts in fluvial sedimentology: upward-fining cyclothems (Allen 1963); lateral accretion deposits (Wright 1959), later termed epsilon cross stratification (ECS) by Allen (1963); and the high-angle relationship between unidirectional cross-stratification and the strike of ECS (Allen 1965). Despite the many publications on fluvial depositional systems since the 1970's, few modifications have been made to Allens (1970) original framework for fluvial point-bar model. In part this is because the upward-fining point-bar facies model was based on established hydrodynamic principles that explained the upward shift from coarser bedload-dominated channel bottom and lower point-bar deposits, to finer suspended-sediment dominated upper point-bar and floodplain deposits.

In a meandering channel, the axis of maximum flow velocity is alternately deflected from one bank to the opposite bank in a streamwise direction (Fig. 3.2). The path of maximum flow velocity shifts laterally across the width of the channel, resulting in an imbalance of forces and the development of a secondary helical flow oriented at a high angle to the main flow. Secondary flow is directed from high pressure on the outer bend, or cut-bank, toward low pressure on the inner bank of the meander; the inner, convex bank coincides with the laterally accreting point-bar surface (Fig. 3.3). Sediment deposition and

Figure 3.2: Physical processes of lateral accretion in a meandering channel. Flow deflection from outer bend to next outer bend of a meander (a) results in secondary helical flow across the width of a channel (b) resulting in point bar deposition by lateral accretion (c). Diagrams (a) modified from Boggs 1995 (b) and modified from Thomas *et al.* 1987.

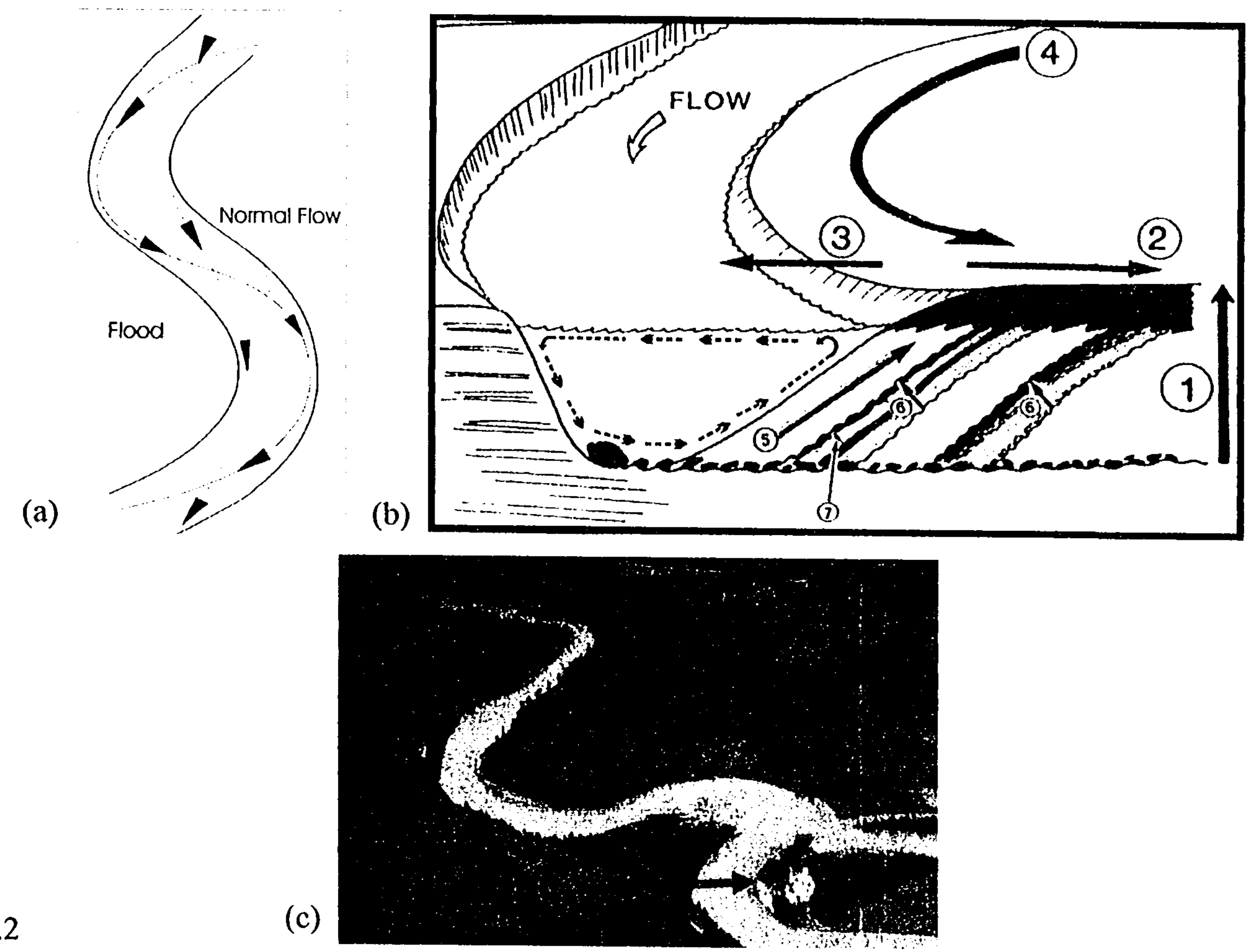

3.2

Figure 3.3: Schematic diagram illustrating the formation of point-bar deposits by lateral accretion. Secondary helical flow develops because of the imbalance of forces created as the path of maximum (main-channel) flow velocity shifts laterally across the width of the channel. Secondary flow is deflected from high pressure on the outer bend, or cut-bank, toward low pressure on the inner bank of the meander, resulting in sediment deposition and the formation of point-bars by lateral accretion. Note the general increase in dip from the toe towards the top of the point bar. Gravitational forces are higher for larger particles than smaller particles (inset); the net result is that coarser particles are deposited near the toe of the point bar and smaller particles are transported towards the top. Main diagram modified from Thomas *et al.* 1987; inset modified from Whiting 1996.

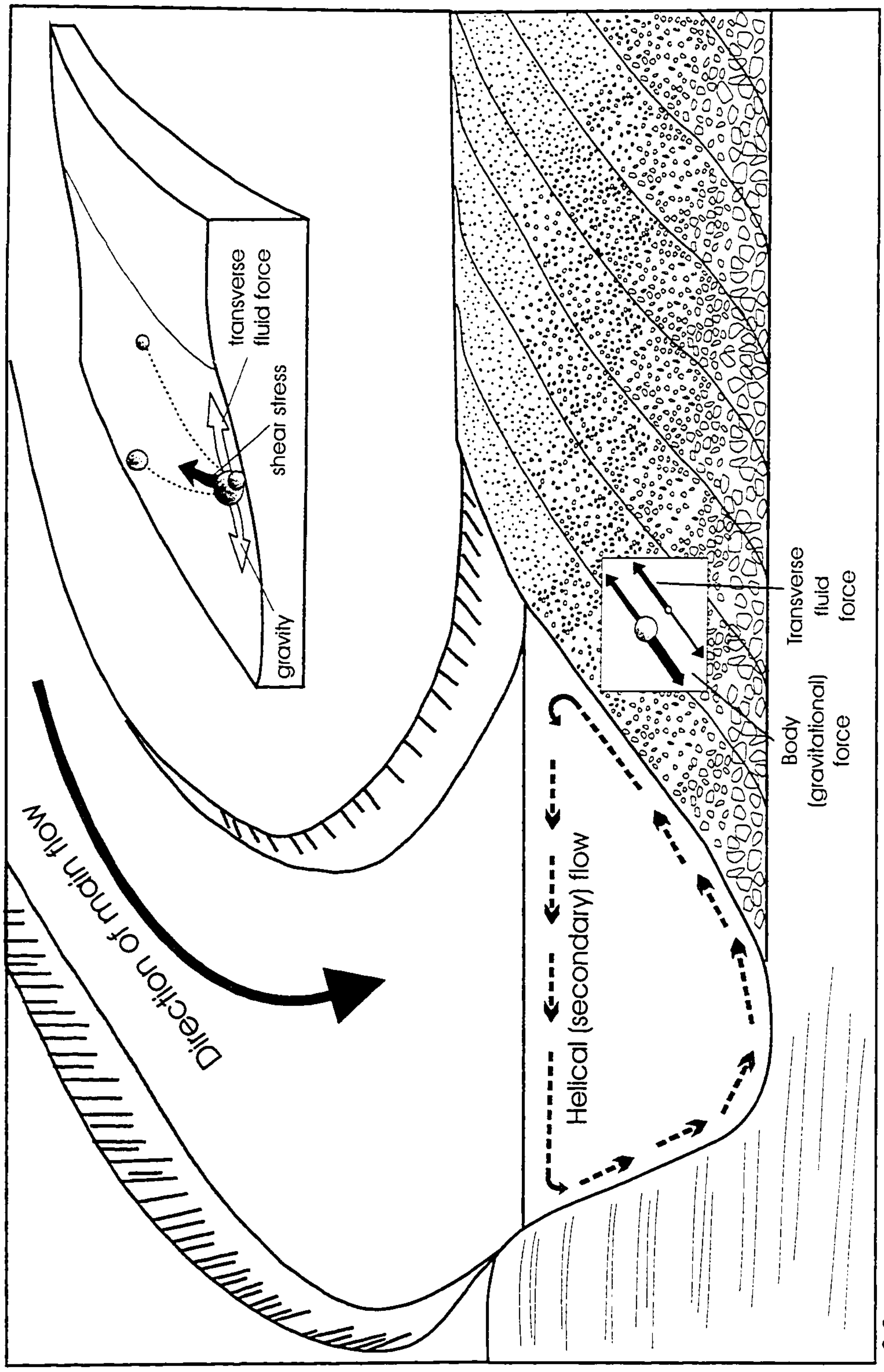

Direction of main flow
transverse fluid force
shear stress
gravity
Helical (secondary) flow
Transverse fluid force
Body (gravitational) force

3.3

particle trajectories on the transverse lateral accretion surface are dependent on the fluid and body forces acting on the grain. Since gravitational force depends on particle mass, this force is greater for larger particles (assuming comparable density). Smaller grains, on the other hand, have a greater surface area per unit mass and therefore the transverse fluid force created by secondary (helical) flow is more influential on the sediment particle trajectory. The net result is a diversion of particle transport pathway within the meander loop with coarser grains directed obliquely downward toward the channel thalweg and smaller particles obliquely up the point-bar surface up-slope (Fig. 3.3); the net result is the formation of an upward-fining succession. However, because secondary flow is much weaker than the main flow of the channel, the net-trajectory of particle transport is in a general streamwise direction. Consequentially, most of the particles are entrained and transported farther downstream.

The physical sedimentological processes that produce lateral accretion deposits are common to all meandering channels, whether developed in high-energy bedload-dominated gravel-fluvial systems (Jackson 1976) to low-energy suspended-mud-dominated meandering tidal creeks (cf. Barwis 1978; Gingras *et al.* 1999). Sedimentologically, however, the lateral accretion (point-bar) deposits vary significantly between and within meandering systems, from poorly-sorted gravel-dominated successions through to heterolithic intercalations of sand and mud, with a myriad of intermediate types. Furthermore, stratal successions have been shown to vary spatially even within a single (modern) point-bar (cf. Caverley 1984). These sedimentological differences are attributed to the multitude of factors that control sediment transport and deposition in channels, including seasonal energy fluctuations and sediment supply, which in turn are superimposed on larger scale extrinsic variables like climate change (Table 3.1). For example, some gravel-dominated meandering-fluvial systems containing little or no mud show no upward-fining trend (Jackson 1976). Notwithstanding, upward-fining successions are commonly observed in modern fluvial and coastal systems because of waning fluvial and/or tidal flow (Jackson 1981; Calverly 1984; Smith 1987) (Fig. 3.4) and consequentially, the classic upward-fining point-bar facies model continues to be generally well accepted.

Research on meandering fluvial systems over the past several decades has resulted in a confusing assortment of terminology describing "lateral accretion" deposits (see Thomas *et al.* 1987 for a comprehensive review). The most common terms are epsilon cross stratification (ECS) (Allen 1963) and inclined heterolithic stratification (IHS) (Thomas *et al.* 1987), describing homo- and heterolithic deposits, respectively. The term inclined heterolithic stratification (IHS) was introduced by Thomas *et al.* (1987, p.125) to describe "*modern and ancient large-scale, waterlain, lithologically heterogeneous...siliciclastic sedimentary sequences, whose constituent strata are inclined at an original ("depositional") angle to the horizontal or paleohorizontal. Deposits of such strata typically range in thickness from 1 to 30 m, exhibit internal dips of 1-36°, and, given suitable exposure, may be traceable along their strikes for many tens of meters*". Although the original definition was intended to be non-genetic and indicative of alternating sand and mud deposition on a dipping surface, the term IHS has essentially become synonymous with lateral accretion deposits produced by the migration of point-bars, in particular those that are tidally-influenced (Allen 1991; Ainsworth and Walker 1994; Wightman and Pemberton 1997;

Table 3.1: Intrinsic and extrinsic controls on point bar development

TABLE 3.1: LIST OF MAJOR INTRINSIC AND EXTRINSIC CONTROLS ON MEANDERING CHANNELS

INTRINSIC CONTROLS

SLOPE (S)

DISCHARGE (Q)

LOAD (L)

GRAIN SIZE (D')

MEANDER WAVELENGTH ( )

CHANNEL SHAPE (WIDTH (W), DEPTH (D))

VELOCITY (V)

EXTRINSIC CONTROLS

CLIMATE

VEGETATION

REGIONAL GRADIENT

BEDROCK GEOLOGY

GENERAL DOWNSTREAM CHANGES (INTRINSIC CONTROLS)

SLOPE (S) ↓

WIDTH, DEPTH ↑

DISCHARGE (Q) ↑

VELOCITY ↑

GRAIN SIZE (D) ↓

GENERAL RELATIONSHIPS (INTRINSIC CONTROLS)

SLOPE (S) $\propto$ LOAD (L), GRAIN SIZE (D)

SLOPE (S) $\propto 1/Q$

MEANDER WAVELENGTH (λ) $\propto 1/Q$

Figure 3.4: Upward- and downstream-fining point bar facies model.

Figure 3.4 (a): Upward-fining point bar (Allen 1970). Diagram modified from Boggs 1995.

Figure 3.4 (b): Downstream sediment-fining in a fluvial to estuarine transition (Diagram modified from Smith 1987).

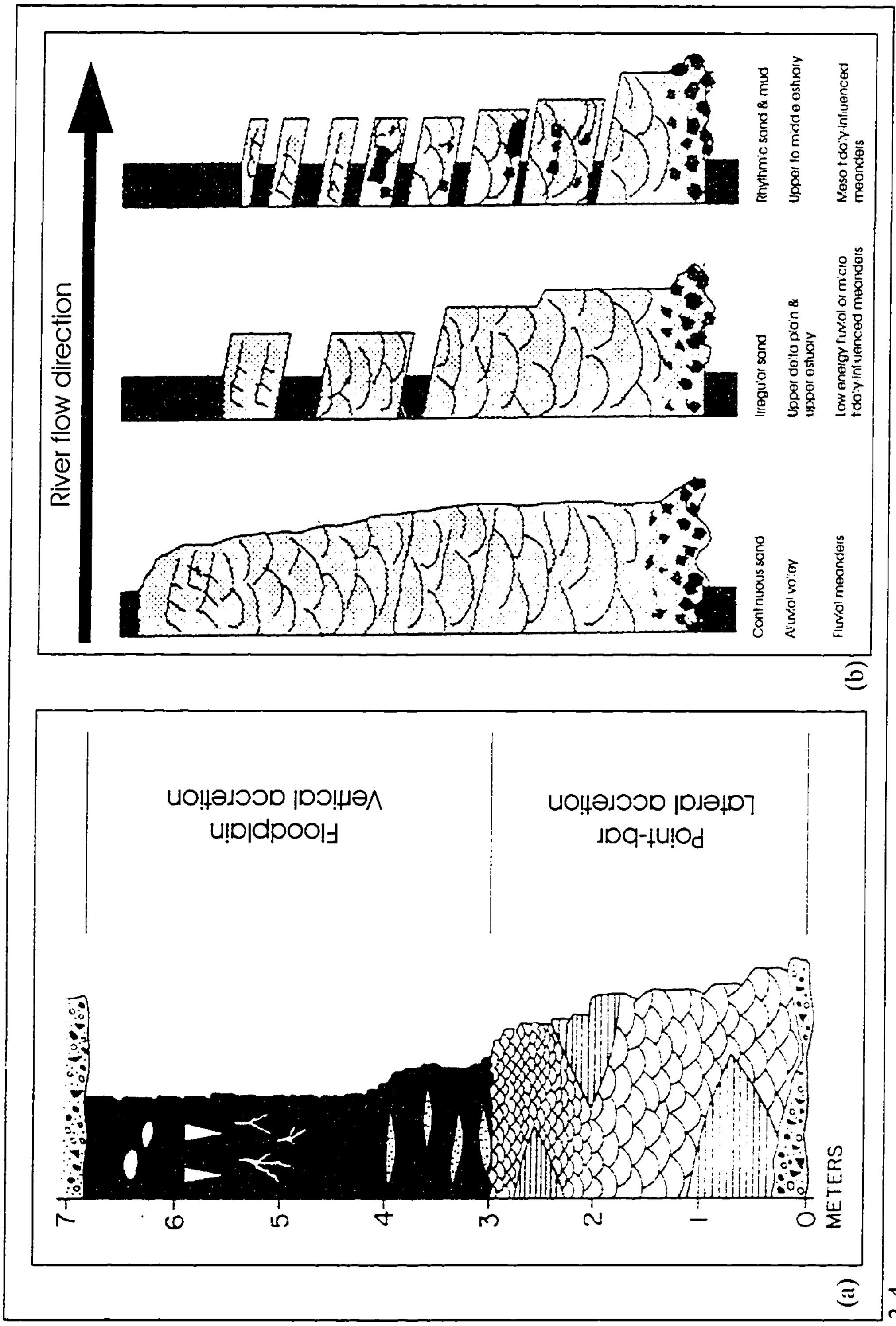

(a)
7
6
5
4
3
2
1
0
METERS
Floodplain
Vertical accretion
Point-bar
Lateral accretion
(b)
River flow direction
Continuous sand
Alluvial valley
Fluvial meanders
Irregular sand
Upper delta plain & upper estuary
Low energy fluvial or micro tidally influenced meanders
Rhythmic sand & mud
Upper to middle estuary
Meso tidally influenced meanders

3.4

Lavigne 1999; Page *et al.* 2003). Although our understanding of the temporal significance of inclined heterolithic stratification (IHS) is limited and in its early developmental stages, recent ichnological studies on Miocene tidally-influenced point-bar deposits have suggested that complex, re-burrowed ichno-fabrics may indicate multiple tidal cycles, suggesting that a single muddy-heterolith may represent one year of deposition (Gingras *et al.* 2002). Notwithstanding, many important physical mechanisms for IHS deposition in tidally-influenced environments are poorly documented but are essential to better understanding the spatial and temporal significance of IHS deposits in the stratigraphic record.

PHYSICAL AND CHEMICAL CONTROLS ON TIDALLY-INFLUENCED POINT-BAR DEPOSITION

Many of the physical sedimentological processes in meandering reaches of tidally-influenced channel systems are similar to those of fluvial channels, including open channel flow dynamics, lateral accretion deposits, lateral migration of point-bars through time, and formation of oxbow lakes. Additionally, physical sedimentary structures, like inclined heterolithic stratification (IHS) and upward-fining successions are similar. However, in tidally-influenced point bars, such as those observed in this study of the McMurray Formation, additional physical and chemical influences also need to be considered, including tides and waves, sediment source, and salinity changes (Table 3.2). Understanding the stratigraphic response to these controls can help to better position point-bar deposits paleogeographically (Fig. 3.5).

Table 3.2: Comparison between tidally-influenced and low-gradient fluvial point-bar deposits.

Depositional Element	Fluvial	Tidally-influenced	Implication for tidally-influenced point-bar facies model
Sediment source	Fluvial	Fluvial +/- marine	Landward fining
Mechanism for mud deposition	Waning fluvial flow	Clay flocculation Waning tidal +/- fluvial flow	More mud deposition; rhythmicity
Biogenic reworking	Absent to rare; *Scoyenia* ichnofacies	Absent to abundant; diminutive & simple marine forms; *Cruziana* & *Skolithos* ichnofacies	More bioturbation
Physical sedimentological processes	Fluvial flow	Fluvial, tidal flow +/- waves	Sediment reworking; rhythmic sedimentation
	Lateral accretion		
Maximum flow velocity	Bankfull stage of fluvial flood	Inflection point during ebb & flood tide	Quantitative models
Minimum flow velocity	Low flow stage (minimum water level)	Maximum and minimum water level (slack water stage)	

3.2

Figure 3.5: Schematic illustration of the interpreted paleogeographical position of various tidally-influenced point-bar deposits of the McMurray Formation within the study area relative to maximum tidal limit, turbidity maximum zone, and salinity limit. Paleogeographic positions based on sand/mud ratios, bioturbation type and abundance, and physical sedimentary structures.

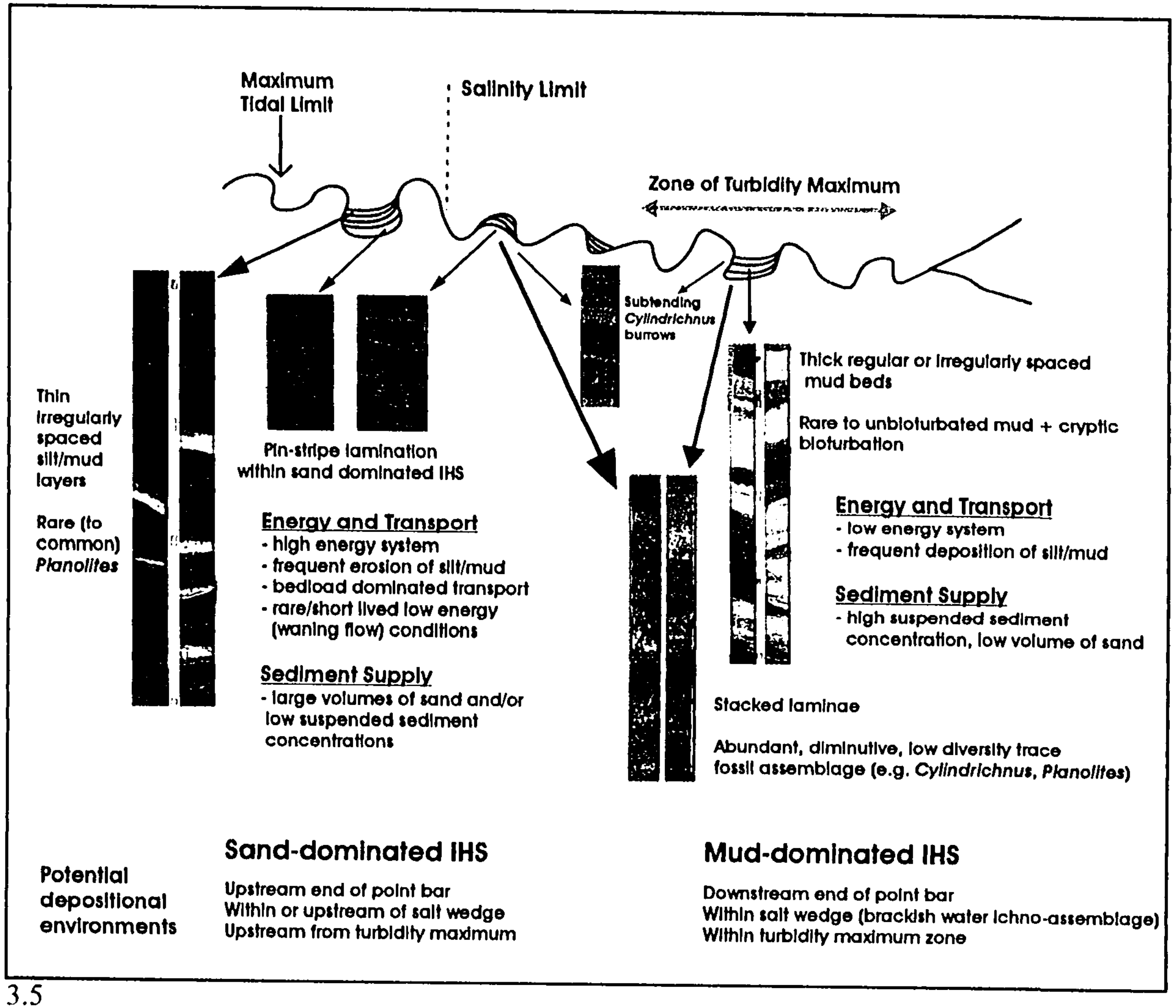

Maximum Tidal Limit
Salinity Limit
Zone of Turbidity Maximum
Subtending *Cylindrichnus* burrows
Thin irregularly spaced silt/mud layers
Rare (to common) *Planolites*
Pin-stripe lamination within sand dominated IHS
Energy and Transport
- high energy system
- frequent erosion of silt/mud
- bedload dominated transport
- rare/short lived low energy (waning flow) conditions
Sediment Supply
- large volumes of sand and/or low suspended sediment concentrations
Thick regular or irregularly spaced mud beds
Rare to unbioturbated mud + cryptic bioturbation
Energy and Transport
- low energy system
- frequent deposition of silt/mud
Sediment Supply
- high suspended sediment concentration, low volume of sand
Stacked laminae
Abundant, diminutive, low diversity trace fossil assemblage (e.g. *Cylindrichnus*, *Planolites*)
Potential depositional environments
Sand-dominated IHS
Upstream end of point bar
Within or upstream of salt wedge
Upstream from turbidity maximum
Mud-dominated IHS
Downstream end of point bar
Within salt wedge (brackish water ichno-assemblage)
Within turbidity maximum zone

3.5

Tides and Waves

Although tide-dominated marginal marine environments may be influenced by several kinds of physical processes including oscillatory flow created by wind-waves, unidirectional currents related to fluvial flow, and combined-flow, each of these processes exerts only a minor influence on sediment transport and deposition in comparison to tidal flow. In a typical flood/ebb tidal cycle, deposition of sand occurs during the rise (flood) and fall (ebb) of the tide. During the intervening slack-water stage, when currents are weak, mud is deposited. Where diurnal or semi-diurnal tidal rhythmicity is preserved the resultant stratigraphic record is a repetitive intercalation of sand and mud layers (Nio and Yang 1991; Dalrymple 1992). Because of the regularity of slack-water mud deposition, tidally-influenced point-bar deposits intuitively should exhibit a greater proportion of mud than fluvial point-bars. However, slack-water mud layers may be eroded by higher energy flood or ebb tidal flow, resulting in the amalgamation of sand layers (Nio and Yang 1991). Furthermore, incoming and outgoing tides also cause rhythmic changes in salinity which affects the distribution of organisms within the environment (see below). The manifestation in the ancient record is a brackish-water ichnological assemblage with an admixture of simple, diminutive marine forms from the *Skolithos* and *Cruziana* ichnofacies.

In this study of the McMurray Formation, IHS deposits do not exhibit wave-formed physical sedimentary structures but show many indicators of tidally-influenced sedimentation. The commonality of pin-stripe and wavy lamination, for example, suggests tidal rhythmicity. Although repetitive intercalations of sand and mud are common, several IHS deposits exhibit thick (several meters) sand units. This is most-likely the result of the amalgamation of successive ebb- or flood-tidal flows and the erosion of intervening mud layers (Nio and Yang 1991). Finally, trace-fossil assemblages within the McMurray Formation suggest brackish-water deposition (see below). Such paleoenvironmental conditions commonly occur where tides transport saline (marine) water landward to mix with fluvial-sourced freshwater.

Sediment Source and Transport Direction

In tidal systems, flood-tides transport sediment landward, or "upstream" from the coeval shoreline. Hydrodynamically, point-bar successions created by flood-tidal flow are similar to those created in meandering-fluvial systems but they generally fine in a landward direction (Barwis 1978; de Mowbray 1983). Although flood-dominated tidal channels are most-probably common, many of these point-bar deposits are likely subject to post-depositional sediment reworking by fluvial or ebb-tidal flow and therefore are only locally preserved in meander reaches located near the coeval shoreline where flood-currents are strongest. As a consequence, flood-tide point-bar deposits are likely uncommon in the stratigraphic record. Nevertheless, based on paleocurrent data, marine-sourced point-bar deposits have been reported in the Upper Cretaceous Horseshoe Canyon Formation of southern Alberta (Ainsworth and Walker 1994).

Sedimentologically flood-tide, or landward-fining, point-bars are likely indistinguishable from seaward-fining (ebb-tide) point-bars unless deposits contain definitive marine indicators such as glauconite or remains of marine macro- or microfossils. Evidence for a seaward source of sand in point-bar deposits of the McMurray Formation in this study is equivocal. Petrographically, all IHS deposits are similar and none of the above-mentioned marine indicators were observed (Appendix 5). Paleocurrent direction could not be determined from unoriented cores. In a more regional paleogeographical context, this study is located about 20 km from the southeastern part of the McMurray estuarine mouth, or bitumount basin (Wightman and Pemberton 1993; Ranger and Pemberton 1997) (Fig 3.6). Tidal creeks of South Carolina exhibit a general upstream (landward) sediment fining trend between successive point-bars, but this was observed less than 2 km inland from the shoreline (Barwis 1978). The Lewis study area may have been situated too far landward from the coeval paleoshoreline to exhibit significant landward sediment fining.

Salinity

The most significant difference between fluvial and tidally-influenced point-bars is the mixing of fresh and marine water in marginal-marine environments. Of particular interest is the zone of the turbidity maximum and ichnological variability.

The turbidity maximum

The turbidity maximum zone is the area in an estuarine system where the turbidity of the water is markedly higher compared to seaward or landward positions (Hughes *et al.* 1998). This zone commonly occurs landward of the salt intrusion and coincides with the area where fluvially-sourced fresh and saline (marine) water mix, and suspended mud rapidly deposits from suspension through the process of flocculation (cf. Allen 1991). Through this process, dispersed clay particles transported in fresh water agglomerate to form larger flocs

Figure 3.6: Lower Cretaceous paleogeography map of the Athabasca Basin. The McMurray Formation is thickest between two Paleozoic salt scarps (main valley) and in an east-west zone termed the bitumount basin (Wightman *et al.* 1991). The bitumount basin is interpreted to represent a paleo-estuarine mouth (Ranger and Pemberton 1997). The study area is located east of the main McMurray paleovalley axis (dashed blue line) and less than 200 km south of the bitumount basin. Because of the small size of the study area relative to the full estuarine system, and because it shifted through time, it is difficult to accurately determine the paleoposition of the turbidity maximum zone. Diagram modified from Wightman *et al.* (1995).

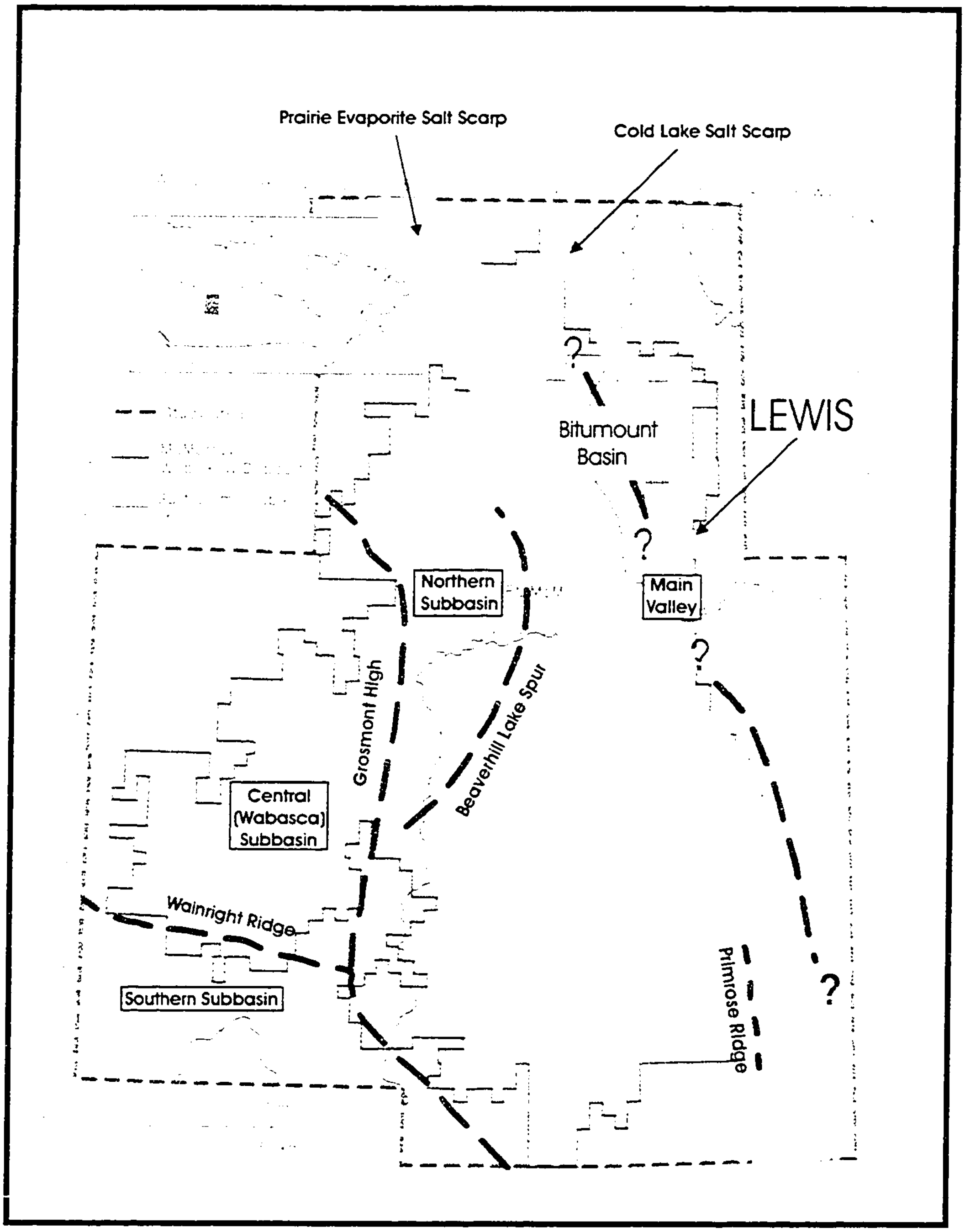

Prairie Evaporite Salt Scarp
Cold Lake Salt Scarp
LEWIS
Bitumount Basin
Northern Subbasin
Main Valley
Grosmont High
Beaverhill Lake Spur
Central (Wabasca) Subbasin
Wainright Ridge
Southern Subbasin
Primrose Ridge

3.6

when they encounter saline water. Because of the increased weight, clay flocs deposit in moderately high energy reaches that are common in the turbidity maximum zone. (Fig. 3.5) (Hughes *et al.* 1998).

Although clay flocculation is an important mechanism for deposition of suspended mud, other mechanisms have been proposed for the deposition of fine-sediment within the turbidity maximum zone (cf. Dyer 1986). Furthermore, the development and maintenance of the turbidity maximum zone is far more complex than the simple mixing of fresh and saline water. Two dominant mechanisms have been proposed for the development and maintenance of the turbidity maximum zone: residual flow associated with gravitational circulation and tidal asymmetry (Dyer 1986; Dyer 1994; Hughes *et al.* 1998). Gravitational circulation is an important process in partially-mixed estuaries (Dyer 1986) and originates because of the differing densities between saline (more dense) and fresh (less dense) water. Because of this density difference, freshwater is transported by a seaward-directed residual surface flow and, likewise, saline water is transported by a landward-directed residual bottom flow. Suspended sediment supplied to the estuary by the river is transported by the seaward-directed surface flow. In the middle part of the estuary this suspended sediment settles into the less energetic bottom flow and is then transported landward towards the head of the salt-water intrusion. Landward of the salt intrusion the surface flow converges with the bottom flow forming a null zone. At this convergence point (null zone), suspended sediment is recirculated back into the seaward-directed surface flow. The concentration of fine sediment is greatest in the null zone and coincides with the position of the turbidity maximum.

A second mechanism proposed for the development of the turbidity maximum zone is the response to the amplification of flood-tide currents. As water flows landward from the funnel-shaped estuarine mouth into the narrower channel, flood-tide currents are distorted and become stronger and shorter in duration than ebb-tide currents. Because this tidal asymmetry is most pronounced towards the head of the estuary, the net sediment transport direction is landward. Where the competence of the seaward-flowing river is equal to that of the landward-flowing flood-tide, a null point develops and fine sediment accumulates to produce a turbidity maximum zone.

Although the mechanisms described above assist in maintaining the position of the turbidity maximum zone, its location also depends on several other factors including tidal range, wave energy and fluvial discharge (Dalrymple *et al.* 1992), and sediment supply (Hughes *et al.* 1998). Each of these parameters varies temporally, and accordingly the position of the turbidity maximum shifts spatially in an estuarine system. For example, Allen (1991) reported a 20 km seaward migration of the turbidity maximum in the Gironde Estuary during periods of high (seasonal) fluvial discharge (Fig. 3.7). More recently, these findings have been applied to ancient successions in the Western Canada Sedimentary Basin where variable sand-mud ratios between closely-spaced (100s of meters) channel-fills have been interpreted as autocyclic shifts in the position of the turbidity maximum zone within an estuarine system (Lavigne 1999).

Mud-dominated IHS deposits observed in the McMurray Formation commonly consist of thick (>10 cm) mud layers (Fig. 3.8). Although many mechanisms can account for mud deposition, the extreme thickness of these layers suggests deposition from very high

Figure 3.7: Schematic illustration of the seaward movement of the turbidity maximum in the Gironde estuary due to seasonal fluvial floods. Diagram from Allen (1991). Location of the turbidity maximum zone relative to the full length of the estuary shown in Fig. 3.5.

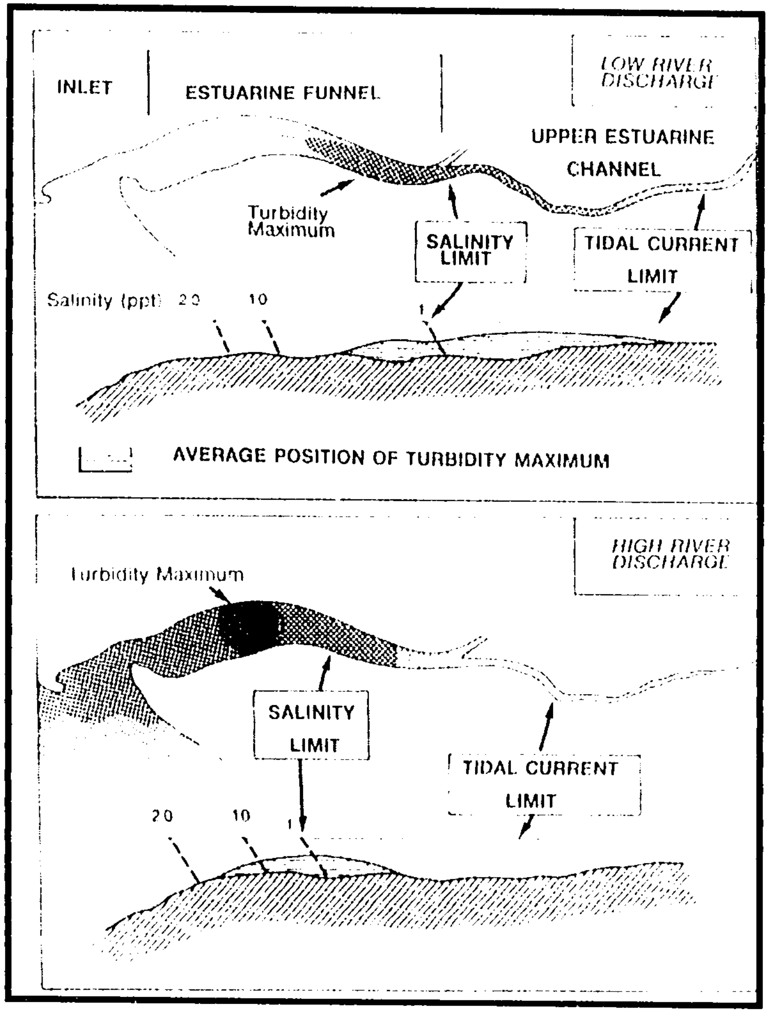
INLET
ESTUARINE FUNNEL
LOW RIVER DISCHARGE
UPPER ESTUARINE CHANNEL
Turbidity Maximum
SALINITY LIMIT
TIDAL CURRENT LIMIT
Salinity (ppt) 20 10 1
AVERAGE POSITION OF TURBIDITY MAXIMUM
HIGH RIVER DISCHARGE
Turbidity Maximum
SALINITY LIMIT
TIDAL CURRENT LIMIT
20 10 1

3.7

Figure 3.8: Muddy heteroliths of mud-dominated IHS deposits. Core boxes are 75 cm long.

Figure 3.8 (a): Thick (>10 cm) mud beds of a mud-dominated IHS deposit. Mud beds are thick because flocculation was superimposed on waning flow conditions. The majority of the mud beds are unbioturbated, which could possibly reflect high sedimentation rates that are common within the turbidity maximum zone. Photo from 10-26-91-8W4.

Figure 3.8 (b): Well-developed *Cylindrichnus* burrows subtending from muddy heteroliths. In contrast to (a), mud beds are thinner (cm-scale) and consistently bioturbated with large, well developed burrows possibly suggesting slower sedimentation rates and depositon outside of the turbidity maximum zone. Photo from 3-18-91-7W4.

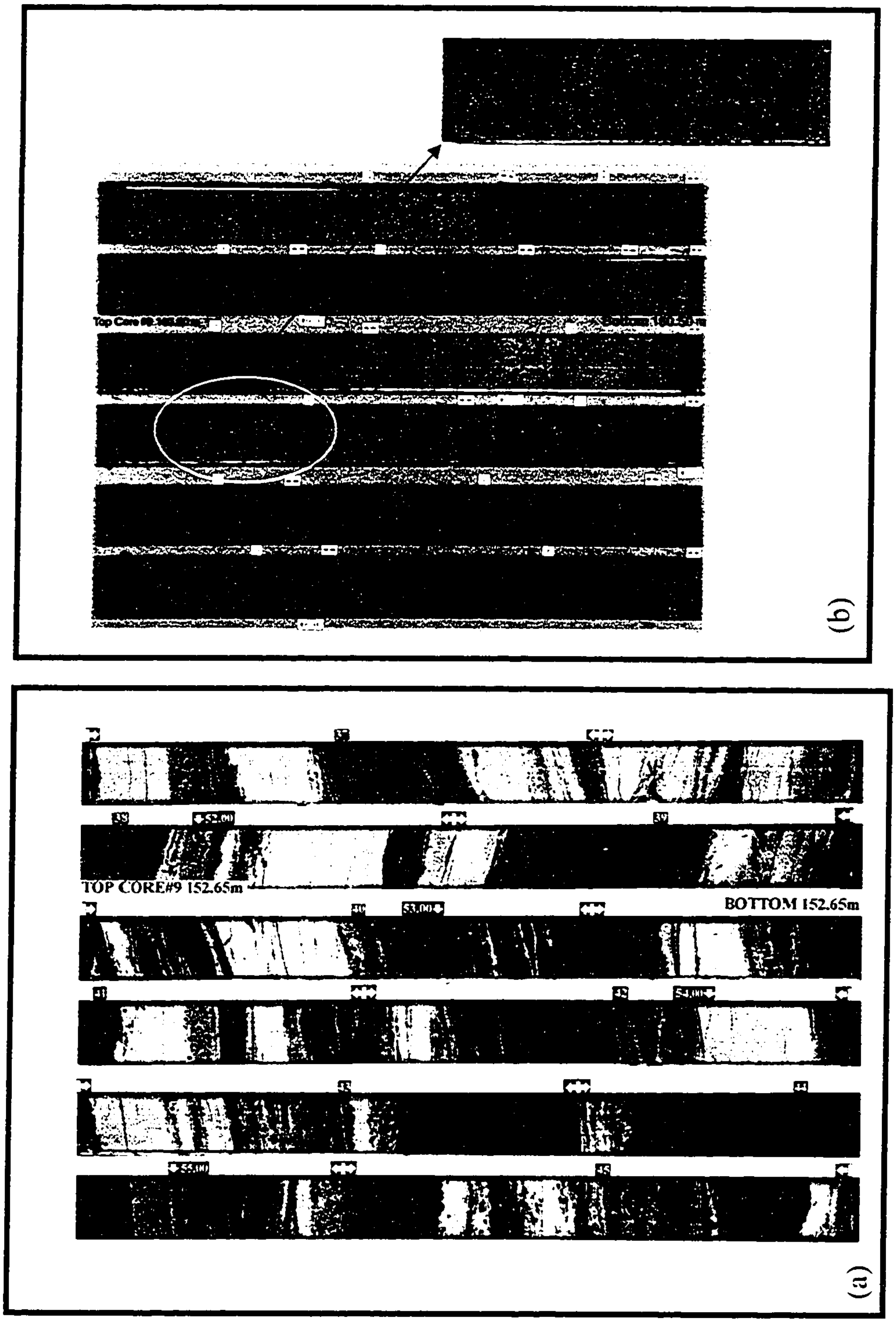

3.8

suspended sediment concentrations that conceivably were related to clay flocculation superimposed on waning fluvial and/or tidal flow. Furthermore, the absence of bioturbation in many layers is likely the result of high-sedimentation rates and the lack of time for tracemakers to colonize the sediment surface; such conditions are observed in the turbidity maximum zone of modern estuaries (Hughes *et al.* 1998; Pejrup 1991). Similar findings have been reported from channels in the Fly River deltaic system (Gulf of Paupa) where slack water mud deposits are >2 cm thick (Dalrymple 2002). Here the turbidity maximum zone is well developed due to a combination of salinity-induced circulation and time-velocity asymmetry.

Because this study represents only a small portion of the much larger McMurray paleo-estuarine system, it is difficult to comment accurately on the paleo-position of the turbidity maximum zone in this system (Fig. 3.5). However, lateral shifting of the turbidity maximum may explain some of the variability in muddy-heteroliths, and also the spatial distribution of interchannel mud deposits in the Lewis study area (see Chapter II). Several mud-dominated IHS deposits in the main paleovalley fill exhibit well-developed *Cylindrichnus* burrows subtending from cm-thick mud layers (Fig. 3.8b). In contrast, northwest of the main paleovalley muddy-IHS deposits consist of thick (>30 cm), unbioturbated, massive mud layers (Fig. 3.8a), and interchannel mud (facies 5) is more areally extensive. Possibly, suspended-mud concentration and sedimentation rates were higher in this area because it occurred in the turbidity maximum zone.

Ichnology

Fluctuations in salinity are common in tidally-influenced estuarine systems because tidally-transported seawater mixes with fluvially-sourced freshwater, producing reduced-salinity, or brackish-water conditions. Several authors have reported modern examples where low salinity and salinity fluctuations have affected the distribution of organisms within marginal-marine environments (cf. Howard and Frey 1973; Gingras *et al.* 1999). More recently, these findings have been applied to ancient successions where the preserved ichnocoenese has been used as a proxy for paleo-salinity (Pemberton *et al.* 1982; Hubbard *et al.* 1999). Trace fossil assemblages in IHS deposits in the McMurray Formation are consistent with brackish-water depositional conditions, including diminutive burrow size, simplistic morphologies, low diversity and an abundant admixture of forms in both the *Skolithos* and *Cruziana* ichnofacies (Pemberton *et al.* 1982; Wightman *et al.* 1987). Because many of the physical sedimentary features of modern low-gradient fluvial and tidally-influenced meandering systems are similar (e.g. sand/mud couplets, lenticular and wavy stratification (Jackson 1981; Caverley 1984)), ichnology is a more reliable tool to differentiate these two depositional systems in the ancient record (cf. Land and Hoyt 1966; de Mowbray 1983; Barwis 1978).

Because of the extreme spatial and temporal variability in salinity concentrations, sedimentation rates, substrate firmness, oxygen concentration, and turbidity within coastal environments, few consistent and predictable ichnological patterns can be ascertained to model brackish-water systems. In general, however, trace fossil assemblages exhibit an overall seaward increase in diversity, abundance and size (Wightman *et al.* 1987; Gingras *et* *al.* 1999) which in turn can help determine the relative paleogeographical position of ancient deposits (Fig. 3.5). This general trend is exemplified in the Palix River (Willapa Bay, Washington state), where taxa inhabiting the mud and silt-dominated lower-estuary are two times more abundant compared to the sandy upper-estuary (Gingras *et al.* 1999). Furthermore, burrow diameters range from 3-15 mm in the lower estuary compared with less than 2 mm in the upper estuary (Gingras *et al.* 1999). These trends have been interpreted to be the result of lower background-salinity and more common salinity fluctuations in the upper (landward-proximal) segment of the estuary. A similar trend is observed in IHS deposits of the Lewis study area, where stratigraphically higher (younger) IHS channel-fill successions are generally muddier and exhibit a more abundant trace fossil assemblage. This may represent a landward shift of facies related to rising relative sea-level.

Recent detailed neoichnological studies on modern tidal point-bars of Willapa Bay, Washington state show a distinct vertical zonation of trace-makers within a single point-bar (Fig. 3.9) (Gingras 1999; Gingras *et al.* 1999). In general, sandy point bars are typically colonized with simple and diminutive burrows created predominantly by maldanid worms, but the upper point-bar (lower intertidal and upper subtidal) is overprinted by larger *Callianassa* (shrimp) burrows. Capping the point-bar succession is a bivalve-dominated intertidal flat. In ancient deposits, therefore, the upper point-bar would consist ideally of larger, more diverse trace fossils, including *Ophiomorpha* and/or *Thalassinoides*, which have been interpreted to have been created by sand-shrimp (Howard and Frey 1975; Frey *et al.* 1978). Trace-makers in mud-dominated point-bars, on the other hand, exhibit a much lower diversity and abundance of smaller (1-3 mm diameter) burrows; burrowing intensity ranges

Figure 3.9: Schematic zonation of tracemakers and trace fossils in the modern sandy subtidal point bars in Willapa Bay, Washington. Shrimp burrows overprint the maldanid-dominated burrow succession in the lower intertidal and subtidal zone. In the ancient record, this zone likely would likely consist of large burrows including *Ophiomorpha* and/or *Thalassinoides*. Diagram from Gingras (1999, fig. 2.14).

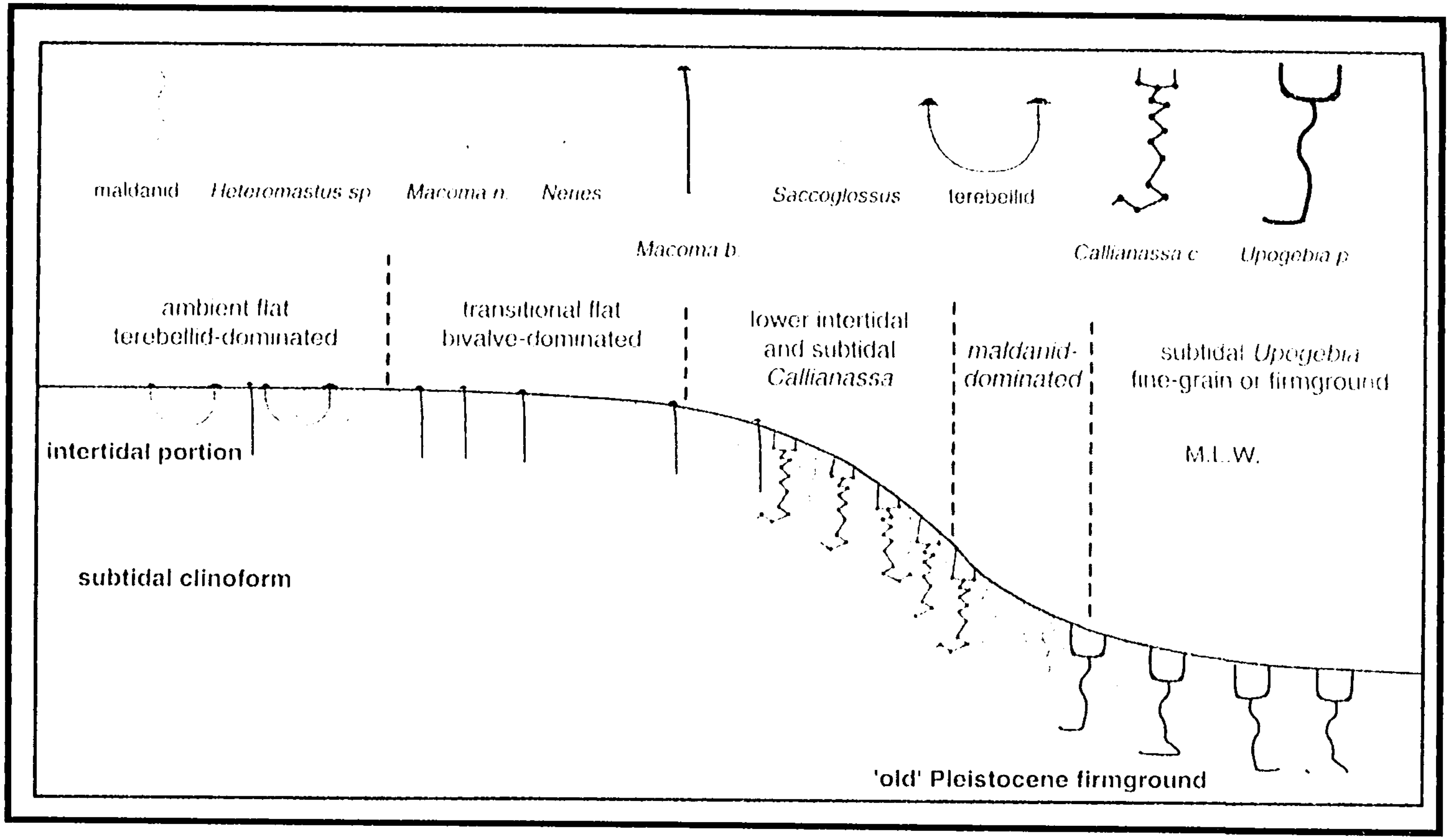

maldanid
Heteromastus sp
Macoma n.
Nereis
Macoma b.
Saccoglossus
terebellid
Callianassa c
Upogebia p
ambient flat
terebellid-dominated
transitional flat
bivalve-dominated
lower intertidal
and subtidal
Callianassa
maldanid-
dominated
subtidal *Upogebia*
fine-grain or firmground
M.L.W.
intertidal portion
subtidal clinoform
'old' Pleistocene firmground

3.9

between unbioturbated to locally moderate. Furthermore, mud-dominated strata exhibit a different neoichnological vertical zonation that, from base to top, consists of deep penetrating (up to 28 cm) *Skolithos*- and *Gyrolithes*-like burrows, siphonate passages at moderate-depths (~1-10 cm), and shallow *Arenicolites*-like burrows. The differing vertical zonation and the lower overall diversity and abundance of trace-makers in muddy- compared with sandy-point-bar deposits have been interpreted to mainly be a function of, (1) the differences in the way organisms colonize sand- versus mud- substrates, and (2) the difficulties in maintaining burrow openings in soupy, muddy substrates. For example, sand-burrowing shrimp such as *Callianassa* continually process sediment and are common in environments with mobile substrates and high rates of sedimentation. In contrast, many mud-burrowing shrimp create *domichnia* burrows and therefore are uncommon in unstable, soupy-mud substrates, which partly explains the reduced diversity in the upper-portion of muddy-point bars. A second reason for lower diversity in muddy-point bar deposits is because burrow openings are difficult to maintain in muddy, soupy-substrates. Burrows that penetrate deeper, more compacted substrates (e.g. *Skolithos*, *Gyrolithes*), on the other hand, are less susceptible to caving. Therefore, the lower portion of deeper burrows have the greatest preservation potential. This, along with the fact that they occur in the lower and more preservable location of the point bar results in an increased preservation potential of deeper-penetrating burrows and therefore the ancient record most probably would show a bias towards these burrow forms (e.g. *Skolithos*, *Gyrolithes*).

The effect of substrate-control on modern ichnological assemblages is similar to observations made in IHS deposits of the McMurray Formation. Here, IHS deposits exhibit an overall increase in bioturbation stratigraphically-upwards, but only where mud layers are thin (Fig. 3.10). In contrast, upper point-bars with thick mudstones exhibit little or no bioturbation, likely because the depositional substrate was too soupy and/or sedimentation rates were too high and precluded bioturbation (Fig. 3.8(a)). It is important to note, however, that the ichnological zonation documented in Willapa Bay point-bars is interpreted to be characteristic only of the middle estuary (M.K. Gingras, personal communication 2003) and therefore the applicability of this model to other parts of an estuary is currently unknown. However, such detailed studies of modern systems are key to understanding the factors that influence deposition and preservation of physical and biogenic structures in marginal marine point-bar deposits. In turn, this knowledge can help to determine what proportion of a point-bar succession is preserved in the ancient record. For example, in a sand-rich point-bar succession, the lack of an upward-increase in abundance and diversity of trace fossils *may* suggest that the upper point-bar has been eroded. Accordingly, this has an important effect on evaluating channel dimensions and related reservoir size (see below) based on point-bar thickness scaling relationships.

VARIABILITY OF INCLINED HETEROLITHIC STRATIFICATION (IHS) DEPOSITS IN THE MCMURRAY FORMATION

Sand- Versus Mud-dominated IHS

In the Lewis study area, IHS deposits of the McMurray Formation are typically gradationally based and consist of irregularly-spaced sand-mud couplets with an average dip

Figure 3.10: Mud-dominated IHS deposit. Note the intensity of bioturbation and also the upward-increase in abundance of mud layers (compare with rare- to unbioturbated muddy-heteroliths in Fig. 3.8(a)). Silt/mud layers occur primarily as stacked laminae. Photo from well 7-14-91-8W4, Core 9 to Core 13, ~154.2 m - ~162.4 m depth. Core boxes 75 cm long.

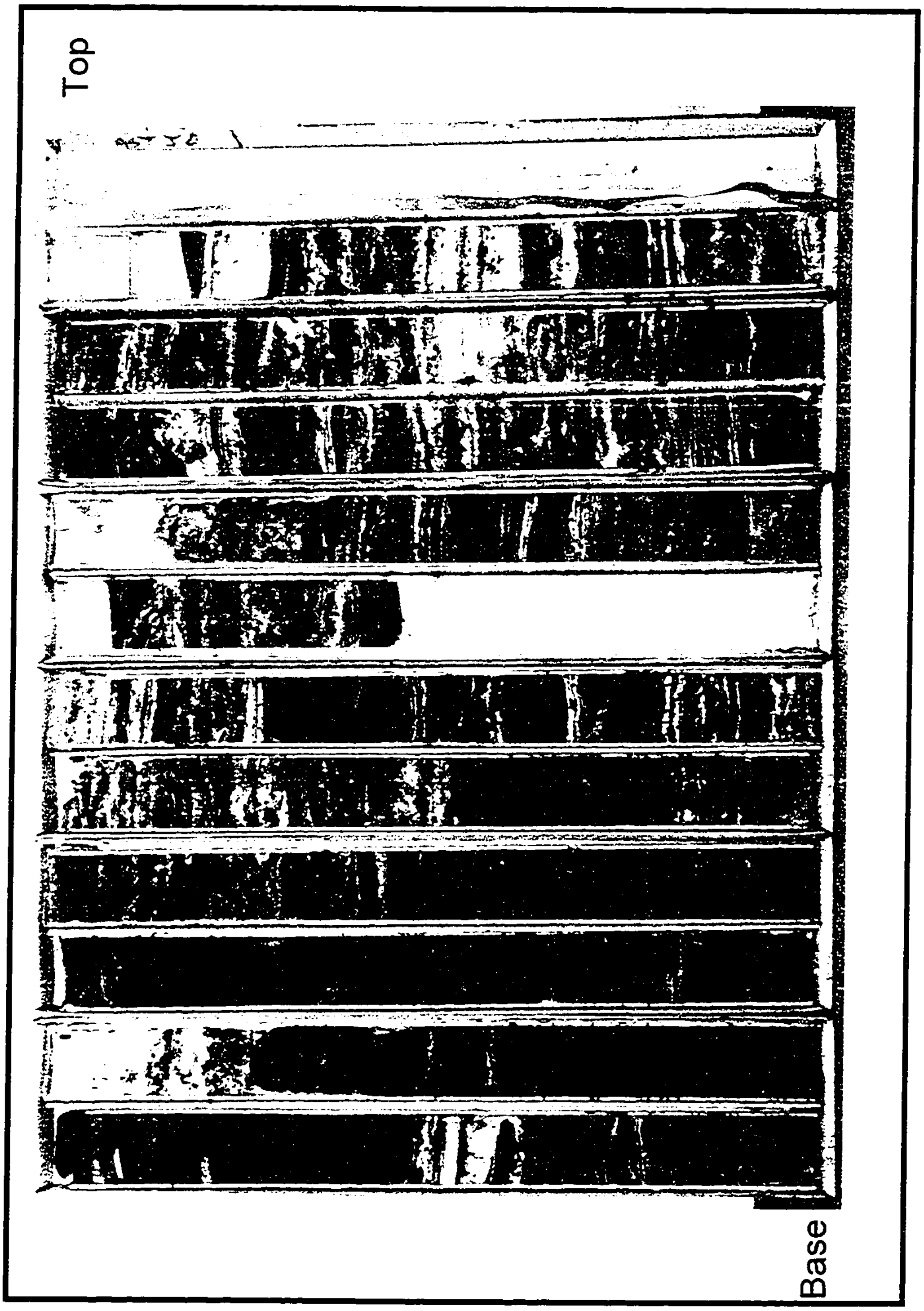

3.10

around 8-12°. Contacts between sand and silt/mud are generally sharp and planar, but are wavy and irregular where intensely bioturbated. Individual sand layers consist of well to very well sorted, lower very fine to upper fine ungraded sand. Physical sedimentary structures include small- to medium-scale cross-stratification and planar lamination. Although sand layers are generally unbioturbated, uncommon diminutive *Cylindrichnus* burrows occur. Small coal clasts, less than 0.5 cm in diameter are present but are rare. In this study, two end-member kinds of point-bar deposits have been identified in the McMurray Formation (with a myriad of intermediate types between them): (1) epsilon cross-stratified, or sand-dominated inclined heterolithic stratification (IHS) (Fig. 3.11) and (2) mud-dominated inclined heterolithic stratification (IHS) (Figs. 3.8 and 3.10).

Sand-dominated successions range in thickness from 10 to 30+ m but average between 20 and 25 m thick. Sand layers comprise ~70 to 90+% of the deposit and individual beds are commonly ≥30 cm thick and typically are bitumen saturated. Irregularly-spaced mud interlayers vary irregularly upward from <1 to 30 cm thick, but are typically 5-10 cm thick. Uncommon soft-sediment deformation and rare microfaults are observed. Two distinct types of mud layers occur: (a) 1-30 cm thick successions of stacked pin-stripe, or more commonly wavy laminae, or; (b) 1-15 cm thick beds. Bioturbation in interlaminaed mud layers varies from none to locally intense. The most common ichnocoenese consists of an abundant, diminutive, low diversity trace assemblage of *Cylindrichnus*, *Planolites*, and *Ophiomorpha* with local escape traces, *Rosselia* and *Gyrolithes* and rare *Asterosoma* and *Teichichnus* burrows. Layers densely colonized by a monospecific *Cylindrichnus* assemblage are also common. Locally, mud layers are dominated only by rare *Planolites* and

Figure 3.11: Sand-dominated Inclined Heterolithic Stratification (IHS).

Figure 3.11 (a): Muddy heteroliths occur mostly as successions of stacked silt-sand laminae, although several 1-2 cm thick mud beds occur (arrow). Heterolithic intervals are irregularly-spaced and vary in thickness. Note soft-sediment deformation structure (arrow). Photo from Well 15-27-91-7W4, Core 13 and Core 14 1 of 2, 169.3 m - 179.6 m depth. Core boxes 75 cm long.

Figure 3.11 (b): Muddy heteroliths occur primarily as 1-2 cm-thick mud beds that are irregularly-spaced and vary in thickness. Mud beds are unbioturbated or burrowed with rare *Planolites* and rare *Ophiomorpha*. Photo from Well 12-34-91-8W4, Core 22 2 of 2 and Core 23, 173.4 m -177.0 m depth. Core boxes are 75 cm long.

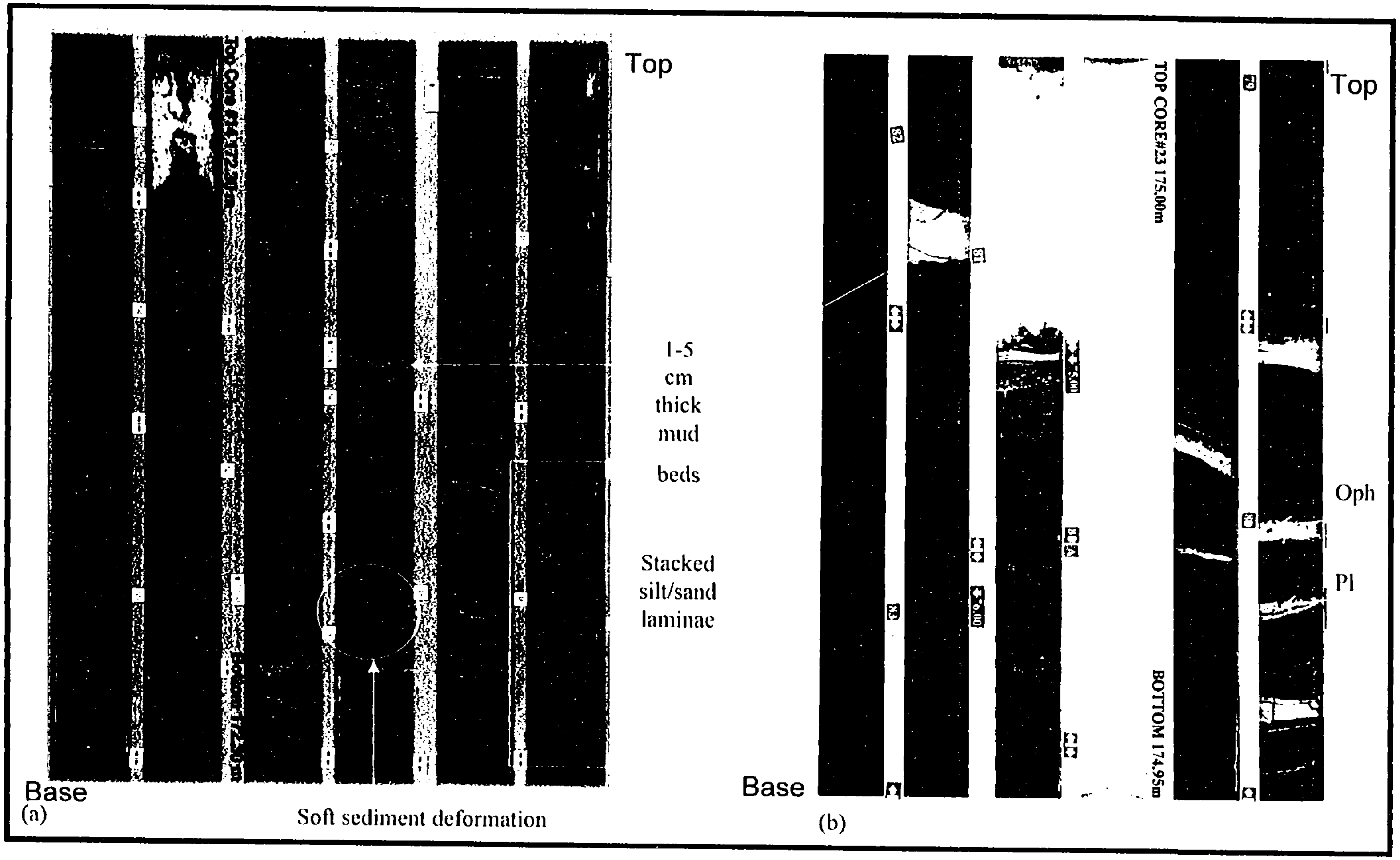
Top
Base
(a)
1-5
cm
thick
mud
beds
Stacked
silt/sand
laminae
Soft sediment deformation
TOP CORE#23 175.00m
BOTTOM 174.95m
Top
Base
(b)
Oph
Pl

3.11

Ophiomorpha. Where the mud/silt layers occur in 1-15 cm thick beds, bioturbation intensity is low to moderate and consists mainly of *Planolites* and *Ophiomorpha*, although uncommon *Cylindrichnus* and *Gyrolithes* are observed. Dispersed organic debris occurs in some silt beds.

Although locally up to 25 m thick, mud-dominated IHS deposits typically vary between 15 and 20 m in thickness. Irregularly-spaced sand layers show moderate to heavy bitumen staining, and although they range between 5-100 cm in thickness, they are usually on the order of 15 cm thick. An upward increase in thickness and/or frequency of mud layers is rarely observed. Muddy layers are >30 cm thick and occur either as stacked sand-mud interlaminated units or as thick beds. Heterolith-type commonly varies laterally more than it does vertically within a single point-bar deposit. Stacked successions of mud laminae typically exhibit a low diversity, low to high abundance trace fossil assemblage dominated by *Cylindrichnus*, *Planolites*, and *Thalassinoides,* with common escape traces and *Rosselia* and *Skolithos* burrows. Burrows are generally small (<1 cm), although large, well developed burrows are locally observed. Individual laminae are commonly wavy and discontinuous and exhibit microfaults and/or soft-sediment deformation. Thick silt/mud layers typically exhibit little to no bioturbation, although locally burrowing may be intense and cryptic. *Cylindrichnus* burrows subtending from silt/mud layers are also common.

Sand-dominated IHS deposits require flow conditions with either low suspended sediment concentrations, extensive erosion of previously deposited silt and mud, or simply rare and/or short-lived low energy conditions for silt and mud deposition (i.e. waning fluvial or tidal flow, flocculation). These conditions can occur at either the upstream end of a large point-bar, upstream from the turbidity maximum or maximum tidal limit, or simply within high-energy meandering systems. In contrast, silt-dominated IHS deposits generally require lower energy conditions with high suspended sediment concentrations and frequent deposition of silt and mud via flocculation and/or waning fluvial or tidal flow. These conditions can occur at either the downstream end of a large point-bar or in low energy, high suspended silt and mud rich environments such as in low-gradient meandering-fluvial systems.

Muddy Heteroliths: Description and Depositional Processes

Although there is little textural variability in the sand layers of McMurray Formation IHS deposits, sedimentological differences in mud layers are common (Figs. 3.8, 3.10, 3.11). Muddy-heteroliths vary between: (1) thin (1-5 cm), light grey to dark grey, unbioturbated to rare *Planolites* and *Ophiomorpha* bioturbated beds (Figs. 3.8b, 3.11); (2) thick (5-50 cm), light grey to dark grey, massive to planar laminated beds exhibiting rare to cryptic bioturbation (Fig. 3.8a); and, (3) stacked (1-30 cm), evenly spaced wavy laminae with rare *Planolites* to an abundant, diminutive, and low diversity trace fossil assemblage (Figs. 3.10, 3.11). These variations can be attributed to the wide spectrum of mechanisms that govern fine sediment deposition on the surface of tidally-influenced point-bars, including (1) flocculation due to the mixing of fresh and marine water (thick or thin mud beds); (2) tidal cycles (stacked laminae); (3) seasonal or daily low energy fluxes in a fluvial system (thick or thin beds or stacked laminae).

In fluvial systems, mud deposition occurs under waning and/or low flow conditions. Trace fossil assemblages within IHS deposits are suggestive of brackish water depositional conditions, commonly formed through the mixing of fresh and marine water. Furthermore, palynomorph assemblages within coeval interchannel deposits are dominated by terrestrial spores and pollen, but also contain rare dinoflagellates and accessory algae and pollen taxa associated with brackish, nearshore, and/or marine conditions (e.g. *Exesipollenites tumulus*) (see Appendix 4 and discussion in Chapter II). Biogenic data, therefore, suggests that the McMurray estuarine system in this study area was most-probably influenced by both fluvial and tidal flow. As such, waning fluvial flow most-likely accounted for the deposition of some muddy heteroliths in IHS deposits. Stacked laminae and thick mud layers, similar to those within the McMurray Formation, have been described in low-energy muddy, meandering-fluvial systems (Jackson 1981; Caverley 1984). However, the repetitive intercalation of sand and mud laminae within IHS deposits of the McMurray Formation is more suggestive of tidal rhythmicity whereby sand is deposited during higher-energy flood- or ebb-tidal flow and mud is deposited during the intervening slack-water stage (Nio and Yang 1991). Similar interpretations of coarse-to-fine couplets have been applied to thick successions of tidal-bundles within lateral-accretion deposits of the Upper Cretaceous Horseshoe Canyon Formation, southern Alberta (Rahmani 1988; Ainsworth and Walker 1994; Eberth 1996). In fact, tidal-rhythmicity is commonly cited as the primary mechanism for deposition of closely-spaced coarse-to-fine couplets common in most IHS deposits (Thomas *et al.* 1987; Smith 1987; Ainsworth and Walker 1994; Gingras *et al.* 2002). In places, however, muddy-heteroliths within McMurray Formation point-bar deposits are substantially thicker – ranging from 1-5 cm up to several decimeters thick. Centimeter-thick mud beds have been observed in modern point-bars of Willapa Bay, Washington state (Clifton and Phillips 1980; Anima *et al.* 1989). Although mud deposition is most probably related to tidal slack-water periodicity, it is also likely enhanced by clay flocculation that resulted in the deposition of anomalously thick mud layers. Mud layers of comparable thickness have been described in the modern Fly River delta where mud beds deposited during a single cycle are >2 cm thick (Dalrymple 2002).

SINGLE VERSUS AMALGAMATED POINT-BAR DEPOSITS

Many of the preserved point-bar deposits of the McMurray Formation comprise multiply-stacked, incomplete IHS successions. Identifying contacts between successive point-bar deposits can be problematic where interchannel/accretionary mud is poorly preserved and because sand-on-sand contacts between successive point-bar deposits are common. However, distinguishing between single and amalgamated point bar deposits is essential in order to accurately calculate paleochannel dimensions, which in turn is used to estimate the size of an individual point-bar, and ultimately reservoir size. Furthermore, the dip-direction of IHS beds may vary between point-bar deposits when they are multiply-stacked. Because steam generally flows up-dip and parallel to stratification, variations in dip between IHS deposits may cause flow deviations within the reservoir. Understanding where these dip variations occur may be important when choosing horizontal well placement for SAG-D production.

In core, numerous sedimentological features suggest the superposition of successive point-bar deposits (Fig. 3.12). These include: >5 cm-thick layers of mud intraclasts at the base of a succession, representing a high-energy channel base; successively-stacked upward-fining successions; abrupt changes in mud-sand ratios and heterolith-type; and abrupt changes in bioturbation type and abundance. Because point bar deposits form on alternating sides of a single meandering channel (Fig. 3.2(c)), IHS deposits with opposite dip-directions should be common in the ancient record. Changes in dip-azimuth, as indicated on the geophysical dipmeter log, can thus be used to specify the boundaries of successively-stacked point-bars. Furthermore, there is a consistent dip-azimuth throughout a single point-bar, and also the slope of the lateral accretion surface exhibits an overall increase in dip from channel base towards the top of the point bar and then a decrease at the top of the point bar (Allen 1963) (Fig. 3.3). Complete point bar successions should exhibit a similar overall change in angle of dip and any deviation from this general trend may represent multiply-stacked point-bar successions rather than a thicker individual point-bar. Sharp decreases in gamma response, suggestive of sand-dominated sediment, may also be indicative of a channel base (Cant 1992). However, if abundant mud-clasts are present, the gamma response will in fact show an abrupt increase.

In core, decimeter-thick intervals of water-wet sand are observed locally. The origin of these intervals is somewhat enigmatic due to the fact that super- and subjacent sand beds, which are sedimentologically and petrographically similar, are bitumen saturated (Fig. 3.13). One possibility is that because middle-McMurray point-bar (and coeval) deposits are sedimentologically heterolithic and stratigraphically complex, subsurface fluid flow is

Figure 3.12: Example of incomplete, multiply-stacked point bar successions based on dipmeter log data and sedimentological characteristics (11-36-91-8W4). Note that the channel base indicated by contact 2 also is marked by a dm-thick, water-wet sand interval similar to that shown in Fig. 3.13 (see text for details).

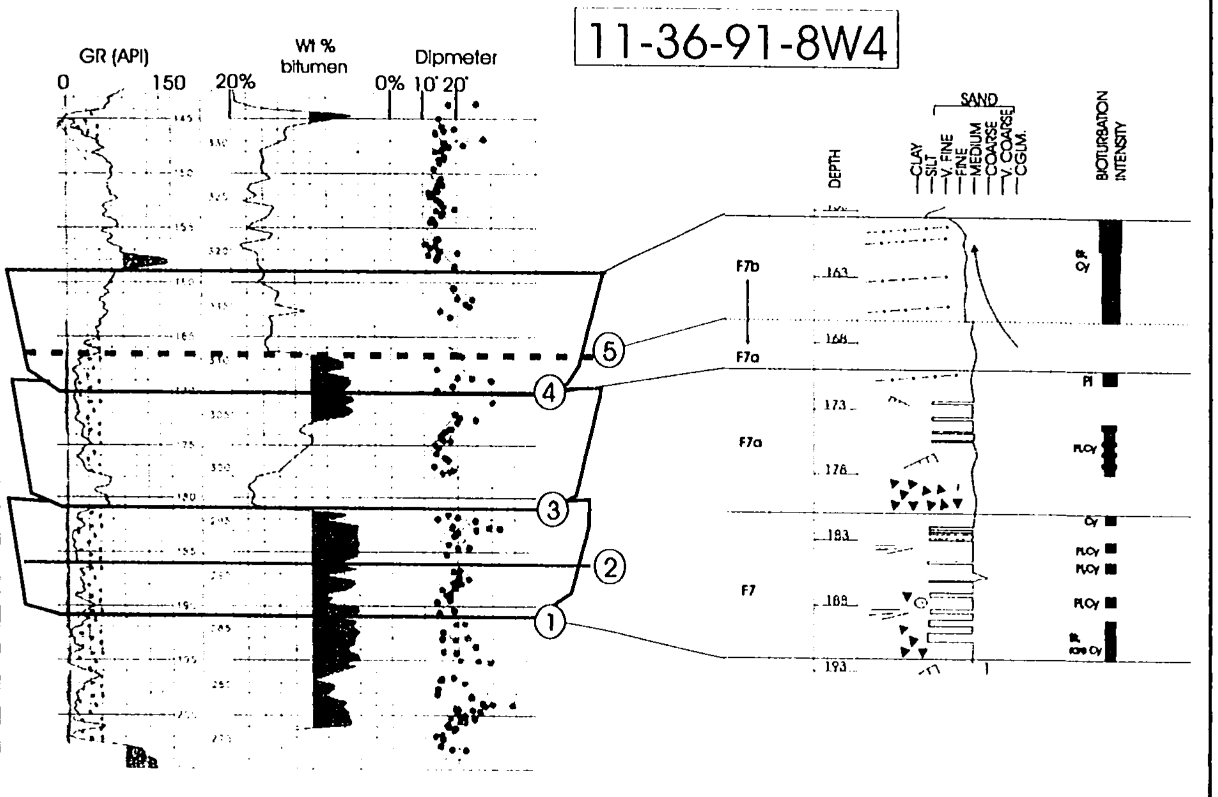

1& 4 - sedimentological changes: mud clasts and abrupt appearance of bioturbation (in 1) and change in dip-direction

2 & 3 - sand-on-sand contact – no sedimentological change (mud clasts above contact 3); change in dip-direction only

5 - sedimentological change (increase in mud & bioturbation); no change in dip-direction suggesting the succession is a single point bar

3.12

Figure 3.13: Core and photomicrographs showing heavy- and lean-bitumen saturated sand within an IHS unit. Although the difference in degree of bitumen saturation is obvious in core, petrographically the sand layers are similar. Scale bar is 0.25 mm long (note the difference in scale between the two photomicrographs). Upper photos show plane-polarized light and lower photographs show cross-polarized light. Photos from Well 5-10-91-7W4.

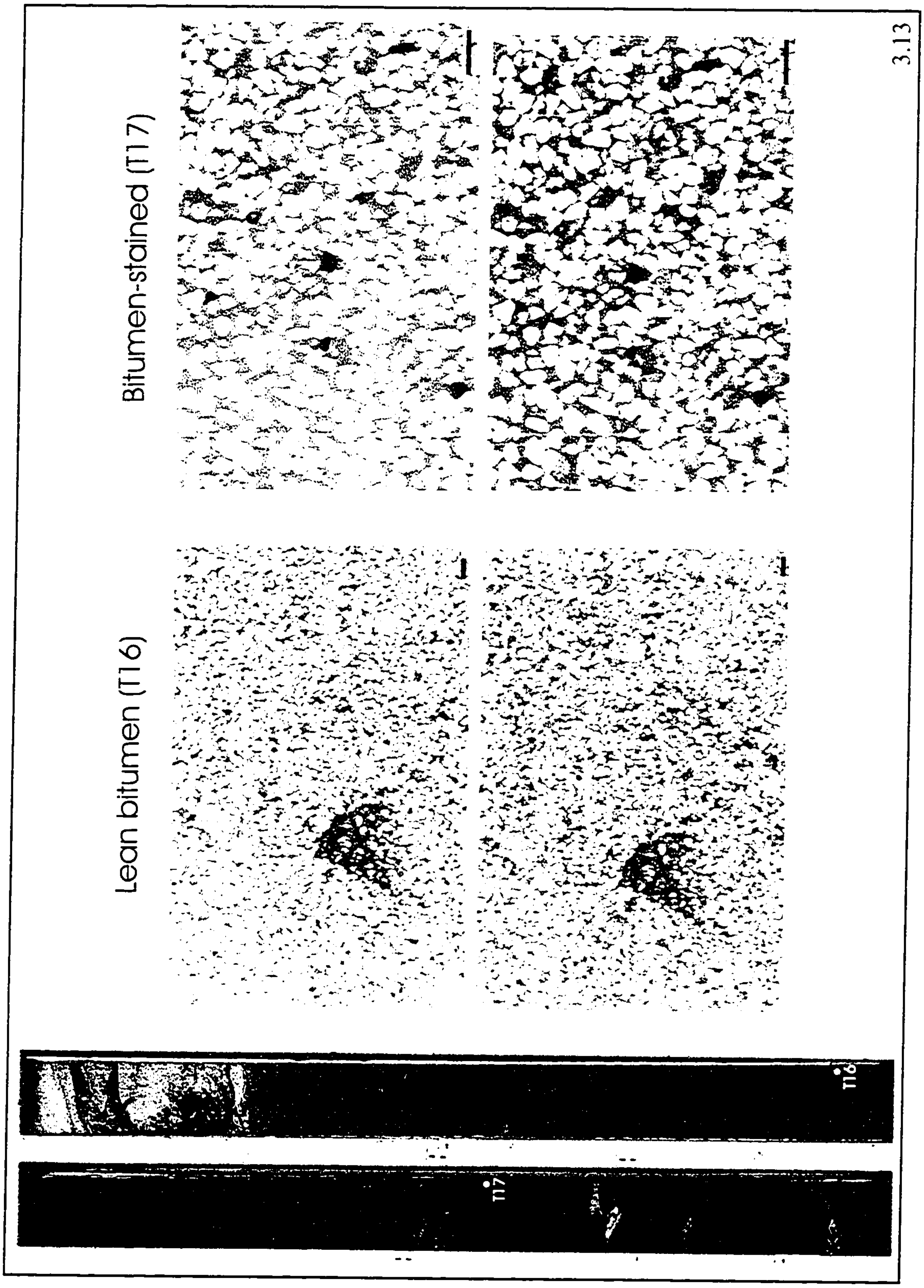
Lean bitumen (T16)
Bitumen-stained (T17)
T16
T17
3.13

commonly interrupted by discontinuities in permeability (M. Robin, personal communication, 2003). As a consequence, the flushing of water by the migration of bitumen was most-likely not uniform, resulting in pockets of water-wet layers interstratified with oil-wet layers. Although there may be several reasons for non-uniform bitumen migration (e.g. presence or absence of interchannel deposits, changes in sand-mud ratios), changes in the dip-direction of lateral accretion surfaces between two vertically-stacked point-bar deposits may be an important cause of hydraulic discontinuity. For example, in places mud layers located several decimeters to meters above this water-wet sand layer dip in the opposite direction to mud layers several decimeters to meters below (Fig. 3.12). Such dip-reversals may indicate the vertical stacking of two successive point-bar deposits. The contact between the two point-bar deposits, however, is difficult to accurately place because there is a commonly a thick (several decimeters up to several meters) homogenous sand unit between the super- and subjacent units with oppositely-dipping muddy heteroliths. Thus, sand-on-sand contacts may exist between the two vertically-stacked point-bar deposits. The decimeter-thick intervals of water-wet sand may indicate a hydraulic discontinuity created by the oppositely-dipping lateral accretion surfaces. Therefore, the contact between two vertically-stacked point-bar deposits may be coincident with the base of the water-wet sand interval.

It should be emphasized that as stand-alone entities, many of these interpreted changes between successive point-bar deposits are not overly-reliable indicators of channel contacts. Rather, it is the combination of several of the above-mentioned features that suggest multiply-stacked point-bar successions.

ESTIMATING PALEOCHANNEL SIZE

Discussion: Methodology and Examples

Estimating paleochannel dimensions may assist in distinguishing between true large-scale incised valley systems and smaller autocylic channels (cf. Lavigne 1999). Furthermore, understanding the areal correlativity of individual point bars should result in more precise subsurface mapping, and ultimately lead to the development of better strategies for subsurface hydrocarbon exploration and exploitation. Previous research on modern fluvial systems in the mid-western United States has produced exhaustive literature relating channel aspect ratios (e.g. width:depth) to variables like meander wavelength, slope, annual stream discharge, and bankfull depth (cf. Leopold and Wolman 1960; Leeder 1973; Ethridge and Schumm 1978). While many sedimentological features of low-gradient fluvial systems are similar to those formed in tidally-influenced channel-fills of the McMurray Formation, hydrodynamic relationships between bankfull depth and flow velocity are inherently different between fluvial and tidally-influenced systems. For example, in fluvial systems maximum flow velocity occurs during bankfull flood conditions. In tidal systems, on the other hand, maximum flow speeds correspond to the intermediate depth inflection point during both the flood and ebb tidal flows, and minimum flow speed coincides with the maximum water depth, when slack-water mud is deposited (Fig. 3.14). Although this hydrodynamic relationship has been previously recognized, (e.g. Barwis 1978) it has not been incorporated into any published quantitative model known to this author.

Figure 3.14: Sinusoidal curves illustrating changes in tidal current velocity in an idealized flood and ebb tidal cycle. High and low water levels correspond to minimum tidal current velocity when slack-water mud is deposited. Current velocity reaches a maximum at the inflection point during each rising (flood) and falling (ebb) tide. In contrast, maximum flow velocity in fluvial systems coincides with high water levels. Diagram from Clifton (1999).

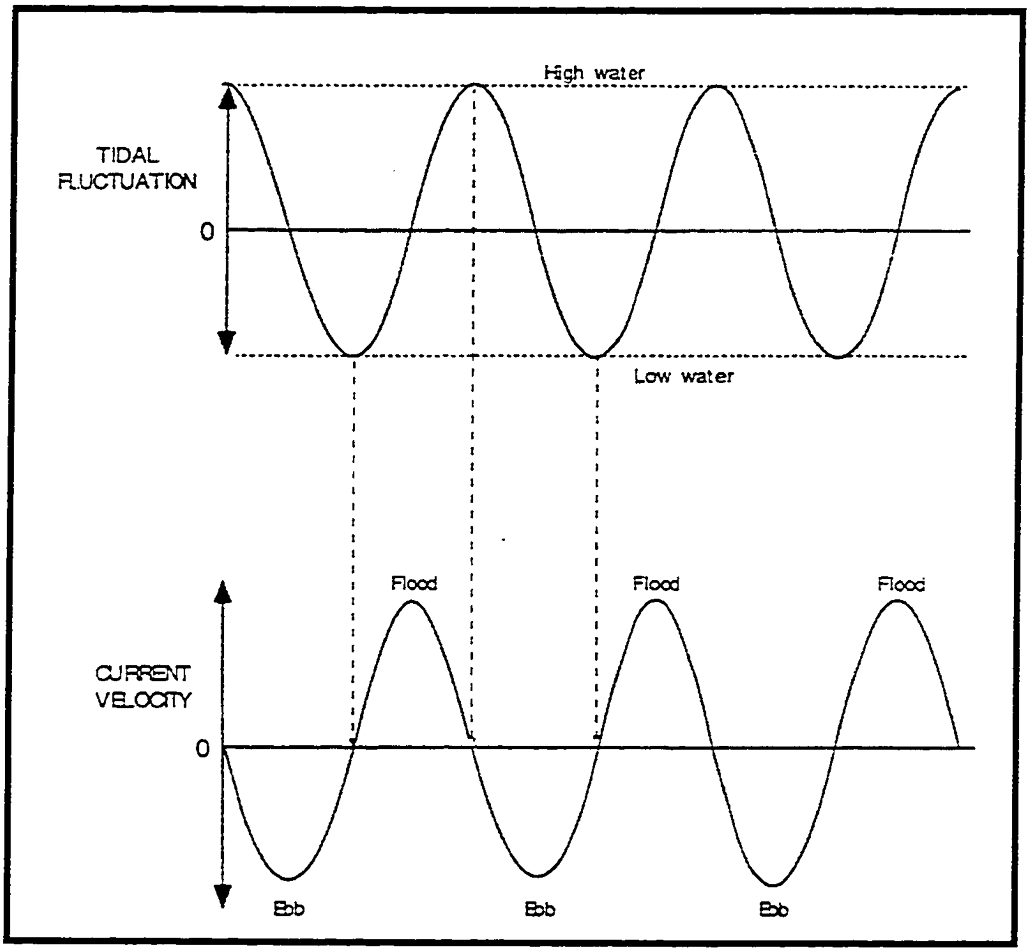
High water
TIDAL
FLUCTUATION
0
Low water
Flood
Flood
Flood
CURRENT
VELOCITY
0
Ebb
Ebb
Ebb

3.14

Despite this hydrodynamic difference between fluvial and tidal systems, small and large natural meandering-fluvial systems from a variety of different climatic regimes which incise into a variety of substrate types, as well as meanders in flumes, all show a consistent relationship between channel width, meander-wavelength, and radius of curvature (Fig. 3.15) (Leopold and Wolman 1960). On average, meandering systems exhibit an 11:1 relationship between meander wavelength and channel width and wavelength is consistently between 10 and 14 times the width of the channel (Fig. 3.16) (Leopold 1994). Radius of curvature is generally one-fifth the wavelength, or approximately 2.3 times the channel width (Leopold 1994). Although tidal meanders have not been incorporated into the datasets on which these relationships have been derived, the remarkable geometric similarity between meandering channels of different scales and from different climatic regimes and substrate conditions suggest that the geometry of meanders is largely governed by mechanical principles and that extrinsic factors (e.g. substrate or climate) play a secondary role (Table 3.1) (Leopold and Wolman 1960). This suggests that despite the hydrodynamic relationships outlined above, geometrical patterns of meandering-tidal channels should be similar to those observed within meandering-fluvial channels because the physical mechanisms of meandering are similar in both types of channels. However, general observations of modern tidal systems suggest that the repetitive hydraulic-pumping action during ebb- and flood-tidal flow may effectively modify channel-shape so they do not conform to fluvial geometric relationships (D.G. Smith, personal communication 2003). One of the observed consequences of this pumping action is an effective seaward-widening of the channel. Until geometrical attributes of modern tidal channels have been related to hydrodynamic conditions, the applicability of fluvially-derived

Figure 3.15: Schematic illustration showing terminology used to describe geometric characteristics of a meandering channels. A = amplitude; λ = meander wavelength. Modified from Leopold and Wolman (1960).

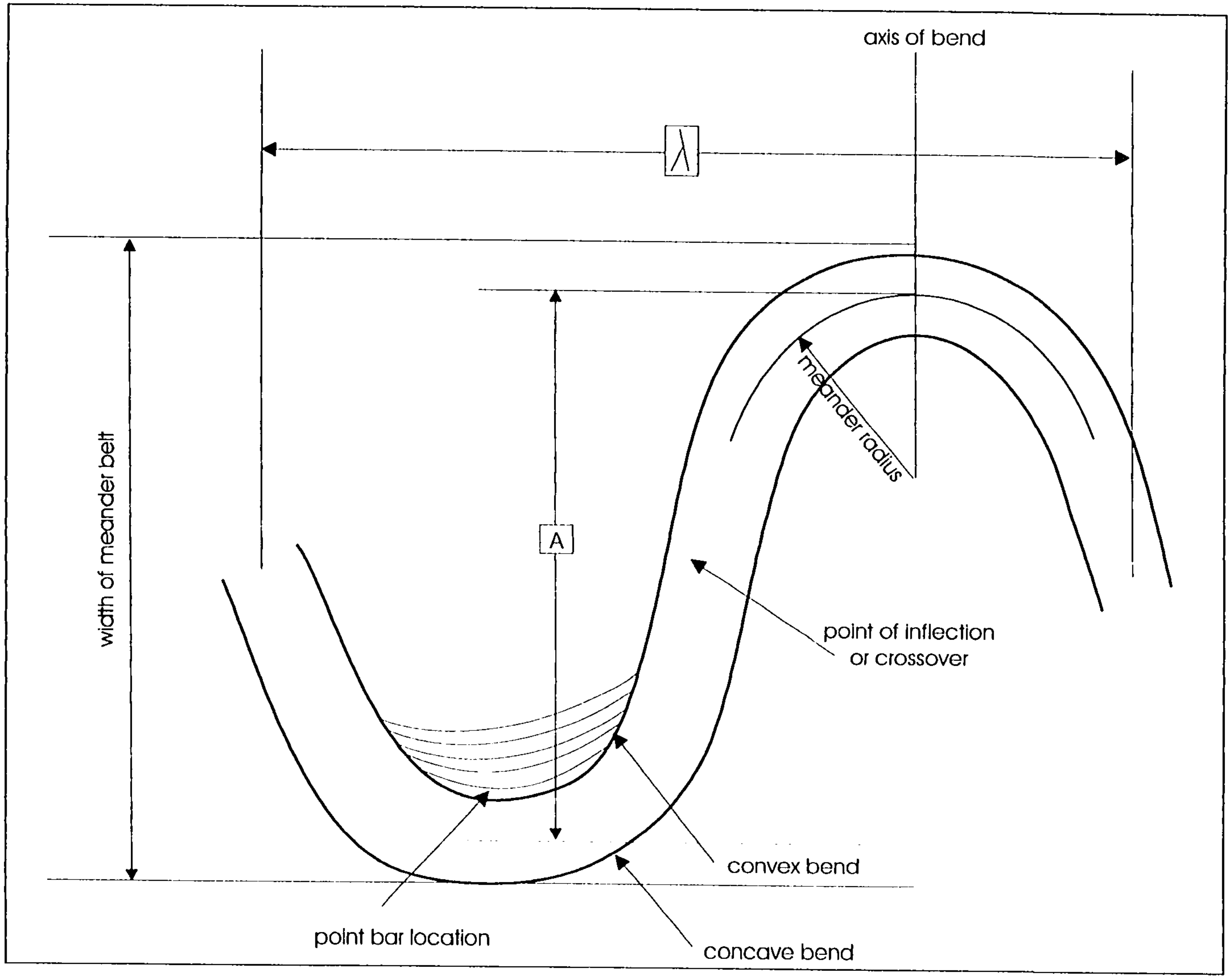

axis of bend
λ
width of meander belt
A
meander radius
point of inflection
or crossover
convex bend
point bar location
concave bend

3.15

Figure 3.16: Graphic representation of the relationship between meander wavelength and channel width (left) and between meander wavelength and radius of curvature (right). Diagram from Leopold 1994.

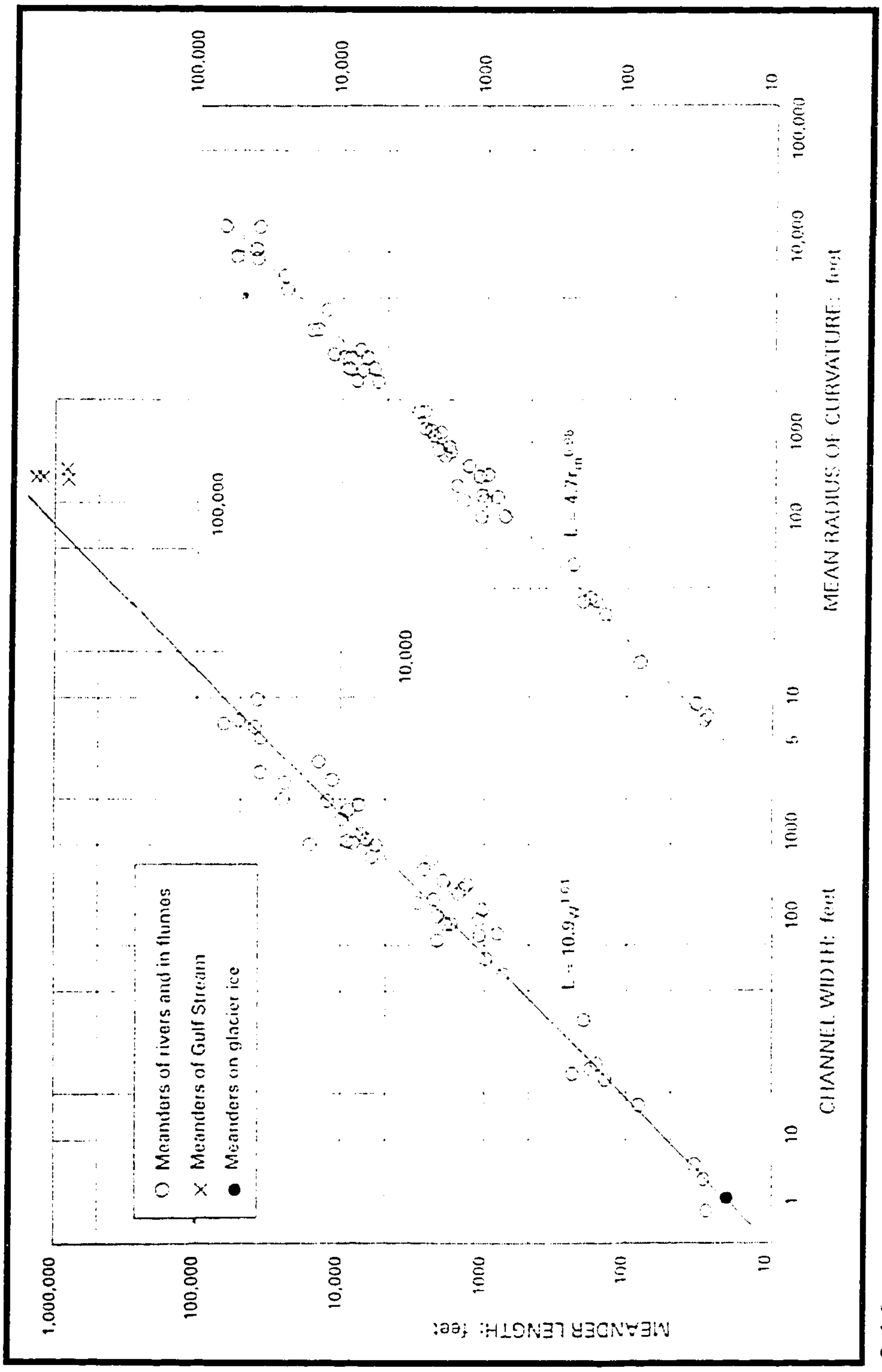

Meanders of rivers and in flumes
Meanders of Gulf Stream
Meanders on glacier ice
MEANDER LENGTH: feet
CHANNEL WIDTH: feet
MEAN RADIUS OF CURVATURE: feet

3.16

equations to model tidal channels remains equivocal. Notwithstanding, equations derived from fluvial systems are used in this study as in previous studies (see below) to estimate the scale of various geomorphic attributes.

Methods used to calculate fluvial paleochannel dimensions have been previously applied to marine-influenced channel deposits of the McMurray Formation that crop out along the Steepbank River (Fig. 3.17) (Mossop and Flach 1983; Flach and Mossop 1985). In these studies, the vertical and lateral thickness of each facies, dip of lateral accretion surfaces, and the thickness of the entire point-bar deposit were measured in order to estimate the width and depth of the paleochannel. These measurements were then used to estimate meander wavelength and sinuosity and thereby better understand the geometry of the sand body (Fig. 3.17). The thickness of the point-bar deposit as measured by Mossop and Flach (1983) was 25 m thick and erosionally overlies fluvial channel deposits of the lower McMurray Formation. They recognized two units within the point-bar succession: a lower 10 m thick trough-cross stratified sand unit gradationally overlain by an upper 15 m thick succession of epsilon cross-stratified (ECS) sand. The point-bar was sharply overlain by horizontally-stratified vertical accretion deposits of the upper McMurray Formation.

The thickness of a complete point-bar deposit is a general approximation of the channel depth at the thalweg, and therefore of the deepest part of the channel. However, as recognized by Mossop and Flach (1983), many of the depth measurements in modern fluvial systems of the mid-western United States were made in the shallower, straight reaches between meander bends (Ethridge and Schumm 1978). The depth in this part of the channel

Figure 3.17: McMurray Formation channel deposit exposed along the Steepbank River studied by Mossop and Flach (1983) and Flach and Mossop (1985). Photograph of the outcrop shows the major sedimentological units of the McMurray Formation (TCS = trough-cross stratified sand; ECS = epsilon-cross stratified sand; VA = vertical accretion deposits). Tabulated calculations for various channel parameters based on middle-McMurray (TCS and ECS) channel deposits. Channel width of 250 m and depth of 25 m used for all calculations. Summary of formulas and original sources from Ethridge and Schumm (1978). Schematic illustration (lower left, not to scale) shows how channel width was obtained.

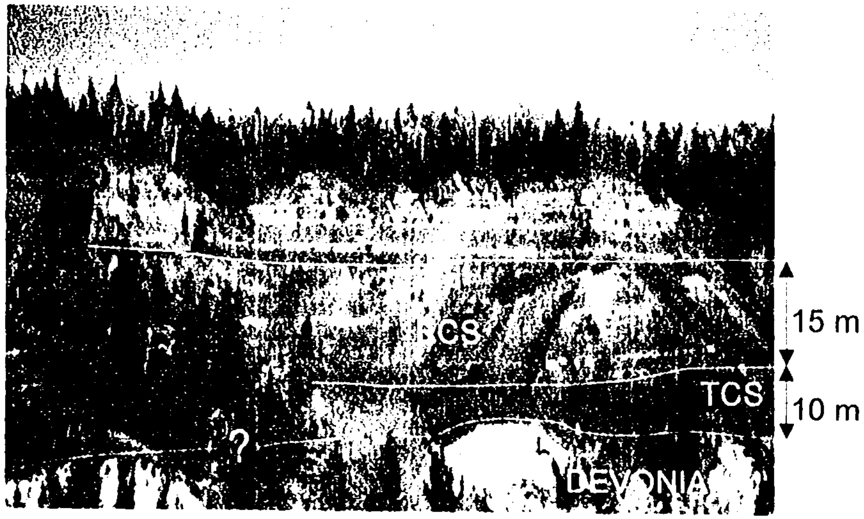

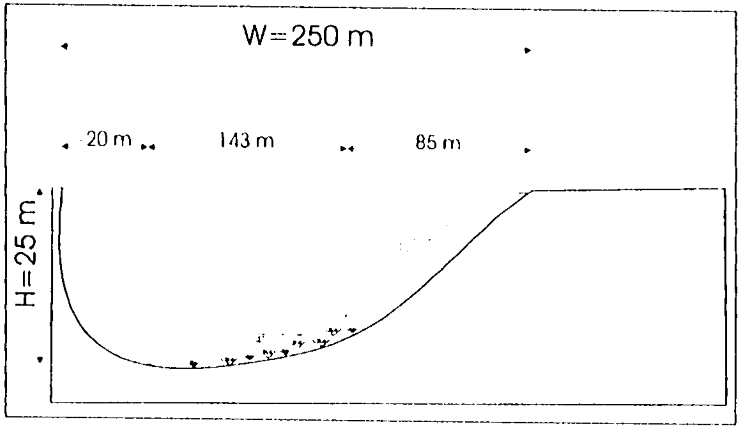

Point bar thickness (h)		TCS 10 m ECS 15 m TOTAL 25 m
Dip of lateral accretion beds		TCS 4° ECS 10°
Channel depth at meander bend (h)		25 m
Channel depth at straight reach (d = 0 595h)		15 m
Channel width (w)	(w = h/tanβ)[1]	250 m
	(w = 6 8h$^{1 54}$) 95% confidence limits	200 – 4000 m
Width/depth ratio (F = w/d)		16 7
Sinuosity (P = 3 5F$^{-0 27}$)		1 6
Mean annual discharge (Q_m = W$^{2 43}$/18F$^{1 13}$)		789 $m^3 s^{-1}$
Mean annual flood (Q_{ma} = 16(W$^{1 56}$/F$^{0 66}$)		2486 $m^3 s^{-1}$
Channel slope (s = 30(F$^{0 95}$/W$^{0 98}$))		0 12 m km^{-1}
Meander wavelength (λ)	λ = 18(F$^{0 53}$W$^{0 69}$)	2497 m
	(λ = 10 9w$^{1 01}$)[2]	~3000 m
Meander belt width (15-20X w) [2]		~ 5000 m
Radius of curvature (λ = 4 7r$^{0 98}$)[2]		700 m

All calculations are in feet and converted to metric

[1]best estimate based on slope of lateral accretion beds

[2] from Flach and Mossop 1985

3.17

is estimated to be about three-fifths (0.595) the depth at the thalweg (Ethridge and Schumm 1978), which at the Steebank River outcrop would be about 15 m deep.

In comparison to channel depth, estimating paleochannel width is more indirect. Using the method of Leeder (1973, equation 1 and fig. 3), which relates channel width exponentially to depth, the paleochannel at the Steepbank River outcrop would be on the order of 200 m to 4 km wide (Fig. 3.17) (Mossop and Flach 1983). Having measured the average thickness and dip of the lateral accretion (ECS) beds, Mossop and Flach (1983) further constrained the estimated width by using trigonometry to determine the sum of the horizontal width of the lower trough-cross stratified sand and the upper lateral accretion (ECS) unit (Fig. 3.17). The calculated width was 230 m, but was subsequently rounded to 250 m to compensate for the distance between the lateral accretion deposit and the thalweg (Fig. 3.17). The estimated width and depth values of 250 m and 25 m respectively were then used to calculate a variety of other channel parameters (Fig. 3.17).

Point-bar Deposits in the Lewis Study Area

Two examples of complete point-bar successions in the Lewis study area were used to estimate channel width, depth and other parameters and the results are compared with the Steepbank River point bar deposits as well as other ancient tidally-influenced point-bar deposits (Table 3.3). The selected point-bar deposits are 21 and 31.5 m in thickness and consist of thick, sharp-based IHS strata gradationally overlain by several meters of mud (see discussion of Facies 5, Chapter 2).

Table 3.3: Comparison between channel parameters of middle-McMurray Formation IHS deposits within this study, the Steepbank river outcrop (Mossop and Flach 1983; Flach and Mossop 1985), and Cretaceous Horseshoe Canyon Formation point-bar deposits (Ainsworth and Walker 1994; Eberth 1996; Lavigne 1999).

Parameter	Method/calculation	McMurray Formation (this study)		McMurray Formation (Steepbank River outcrop, near Fort McMurray, AB)	Horseshoe Canyon Formation (Willow Creek, near Drumheller, AB)
		Point Bar A	Point Bar B		
Point-bar thickness (h)	Measured in core/outcrop	21 m	31.5 m	25 m	12 m
Channel depth (d)	2/3 rule (0.595h)	12.6 m	18.7 m	15 m	7.2 m
Dip of Lateral Accretion Beds (º)	Outcrop: beds measured directly; Subsurface: value from dipmeter logs or estimated based on similar vertical thickness of published point-bar deposits	12º	8º	ECS (10 m): 4º IHS (15 m): 10º	[1] 10º; [2] 12º
Channel width (W)	Method A $W = 6.8h^{1.54}$ 95% confidence limits	[3] 165 m – 300 m	[3] 600 m – 1300 m	200 m – 4000 m	
	Method B $W = 1.5h/\tan\beta$	148 m (486 ft)	336 m (1103 ft)	[4] 250 m (820 ft)	102 m (335 ft)
w:d ratio	$F = w/d$	11.7	10.7	16.7	14.1
Meander Wavelength (λ)	Method A $\lambda = 10.9w^{1.01}$	1718 m (5635 ft)	3930 m (12895 ft)	[5] 2914 m (9561 ft)	1178 m (3866 ft)
	Method B 11:1 ratio between channel width and λ	1628 m (5341 ft)	3696 m (12126 ft)	2750 m	1122 m
	Method C $\lambda = 18(F^{0.53}W^{0.69})$	1443 m (4734 ft)	2418 m (7934 ft)	2497 m (8192 ft)	1232 m (4042 ft)
Point Bar Length (L_{pb})	1/2λ λMethod A	859 m	1965 m	1457 m	589 m
	1/2λ λMethod B	814 m	1848 m	1375 m	561 m
	1/2λ λMethod C	722 m	1209 m	1249 m	616 m
Sinuosity (P)	$P = 3.5F^{-0.27}$	1.8	1.8	1.6	1.7
Channel slope (S)	$S = 30(F^{0.95}/W^{0.98})$	0.14 m/km (0.72 ft/mi)	0.06 m/km (0.30 ft/mi)	0.12 m/km (0.61 ft/mi)	0.24 m/km (1.24 ft/mi)
Meander belt width (w_{mb})	15-20X channel width	2220 m – 2960 m	5040 m – 6720 m	3750 m - 5000 m	1530 m – 2040 m

[1] from Ainsworth (1994) and Lavigne (1999)

[2] from Rahmani (1988) as summarized in Smith (1987)

[3] rounded to 20 m and 30 m, respectively for clarity of graph

[4] value was 230 m with 20 m added to compensate for thalweg

[5] λ rounded to 3000 m in paper

Strata of point bar A (Fig. 3.18) (10-26-91-8W4) consist of a 2 m thick succession of erosionally-based, planar-tabular cross-stratified upper-medium to lower-coarse sand with rare mud clasts and cm- to dm-thick *in situ* mud beds. This sandy unit is sharply overlain by a 15 cm thick layer of angular mud clasts which mark the base of ~12 m thick succession of intercalated upper fine to very fine bitumen saturated sand and mud (IHS). In places this finer sand is small-scale (ripple-) cross stratified. Mud layers within this succession vary between laminae and dm-thick beds and generally increase in thickness stratigraphically upwards. Mud layers in the basal ~3 m of this IHS unit are intensively bioturbated with large (1/2 cm to 1 cm diameter) *Thalassinoides*, *Planolites* and *Skolithos* burrows, but elsewhere in the succession burrows are smaller (1/4 to 1/2 cm in diameter) and rare, except for the upper 1.5 m where bioturbation shows a sharp increase in bioturbation intensity. Furthermore the lateral accretion beds show a progressive upward increase in dip from 10° to 12°. This sandy-IHS unit is gradationally overlain by a 4 m thick mud-dominated IHS succession. Mud layers within this upper unit are generally unbioturbated and 1-2 dm thick, although rare *Planolites* burrowed laminae are observed. The average dip of the lateral accretion beds in this unit is 13°; this increase in dip from the underlying sandy IHS strata is rather subtle in core but readily evident on dipmeter logs. The mud-dominated IHS succession is then gradationally overlain by a 2 m thick mud succession interstatified locally with very-fine, water-wet sand. In places, this succession is cryptically bioturbated with diminutive (~1/4cm diameter) horizontal *Planolites* burrows.

Point Bar B (Fig. 3.19) (3-18-91-7W4) sharply overlies a thick mudstone/mudclast breccia interval. The basal 4 m consist of well-sorted, bitumen-saturated, fine sand with cm-

Figure 3.18: Upward-fining IHS succession showing sand-dominated IHS at the base and mud-dominated IHS near the top. The consistent dip-direction (indicated by dipmeter log) coupled with accretionary mud (am) at the top suggests a single point bar succession. Average dip of the lateral accretion surface is 12° but there is a general increase in degree of dip from sandy to muddy IHS. Calculations of channel width and point-bar size are summarized in Table 3.3. Core boxes are 75 cm long.

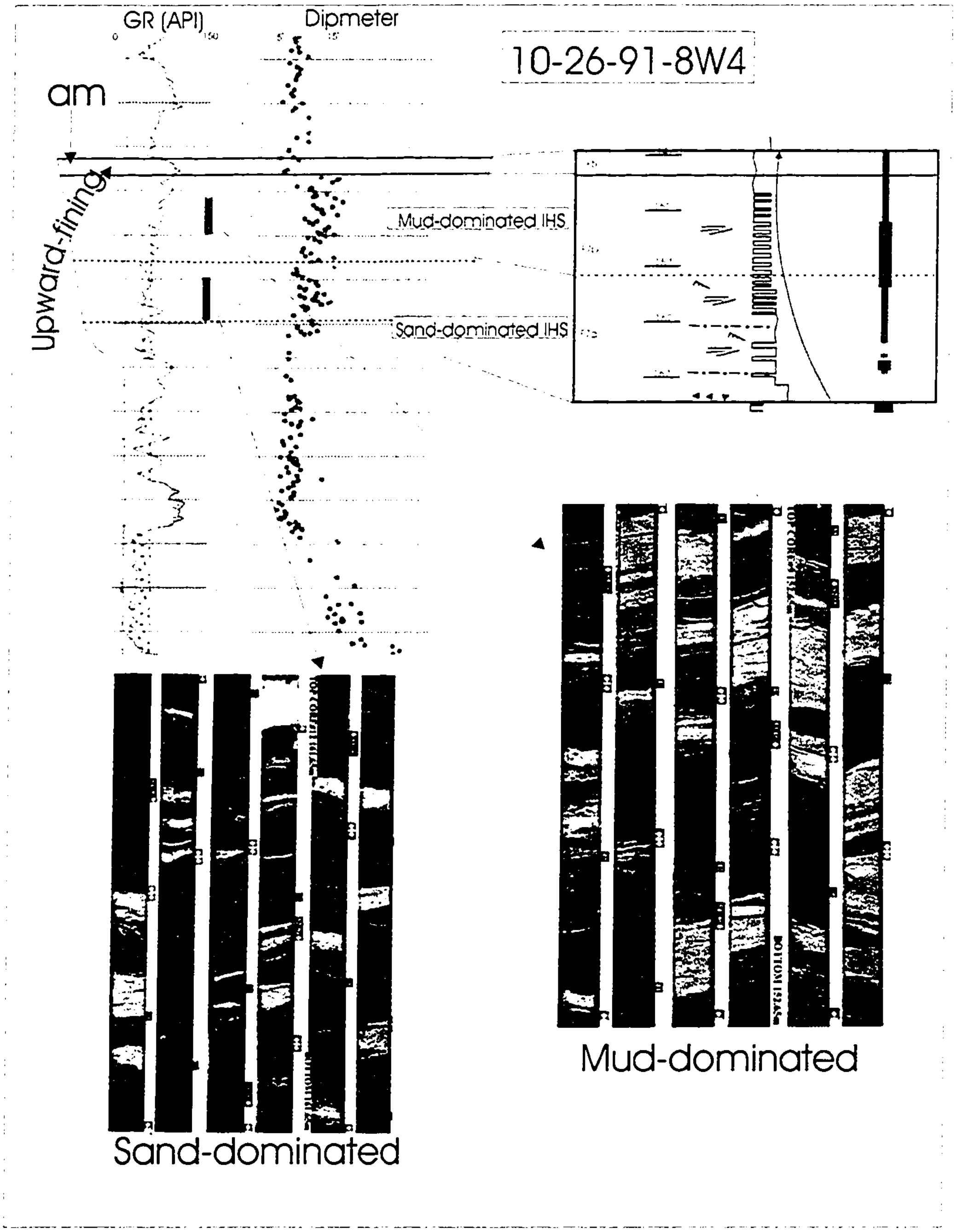
GR (API)
Dipmeter
10-26-91-8W4
am
Upward-fining
Mud-dominated IHS
Sand-dominated IHS
Sand-dominated
Mud-dominated

3.18

Figure 3.19: Core and gamma-ray log of complete point bar succession of the McMurray Formation (3-18-91-7W4). Location of core photograph is indicated by the blue bar. Channel fill is 31.5 m thick, measured from the base of the point bar succession to the base of the accretionary mud (am) deposits (indicated by white bar in core photograph). The point bar base is marked by a 4 m thick succession of fine bitumen-saturated sand with dispersed mud clasts. See Table 3.3 for paleochannel width calculations. Core boxes are 75 cm long.

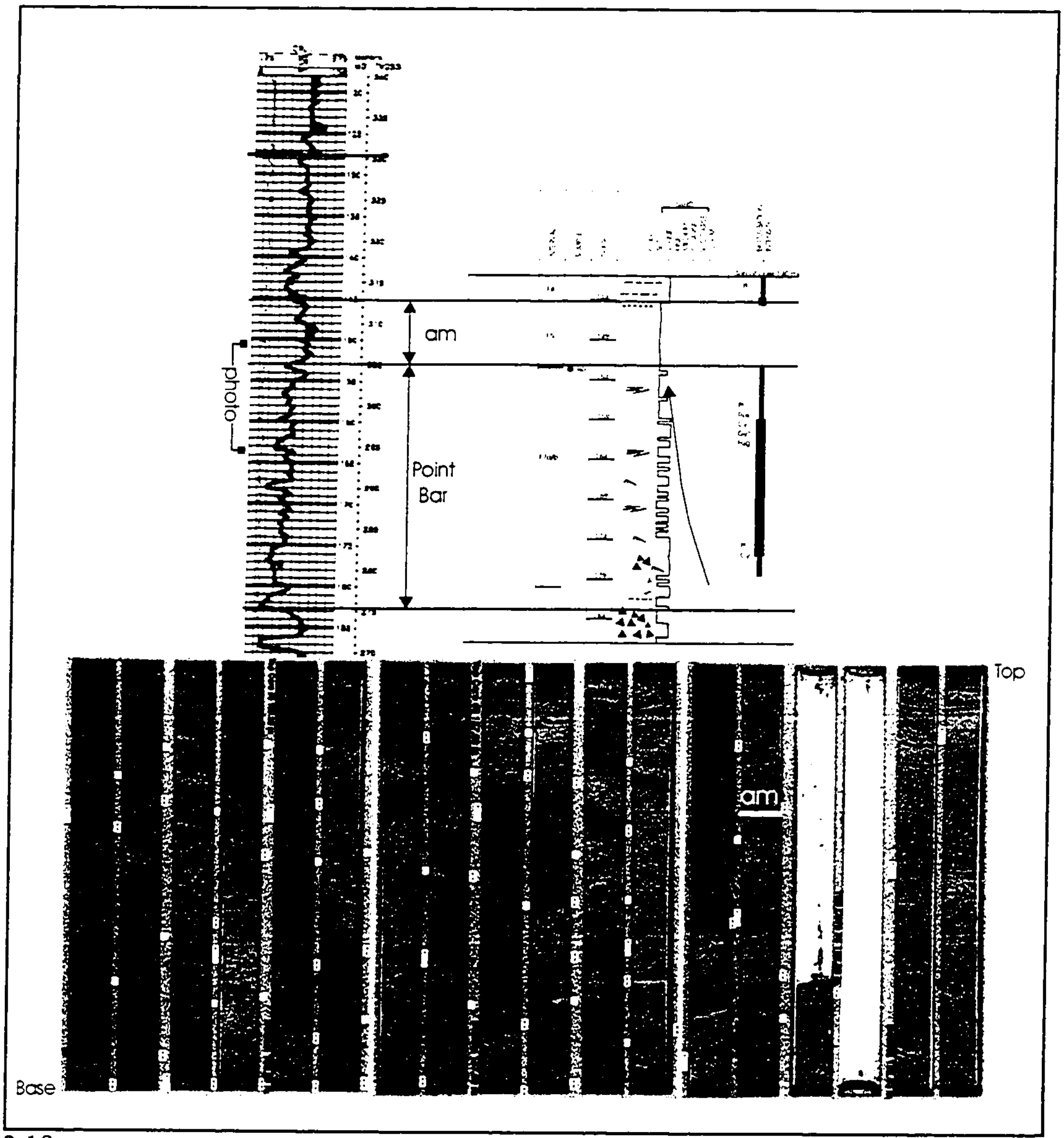

3.19

to dm-wide angular mud clasts and one dm-thick *in situ* pin-stripe laminated sand and mud bed. This basal unit is gradationally overlain by 4.5 m of fine sand with rare bioturbated sand-mud laminated beds. This is overlain by a 23 m thick mud-dominated succession of sand and mud interstratified at low angles. Mud layers vary in thickness between laminae, especially pin-stripe laminated beds, to cm- or dm-thick mud beds. Sand beds average about 1 or 2 dm thick, but in places are up to 1.5 m thick. The mud/sand ratio gradationally increases stratigraphically upwards. IHS strata are gradationally overlain by a 8 m thick muddy-unit with rare very fine sand laminae.

Although they are similar in thickness, the main difference between point-bar deposits in this study and those exposed along the Steepbank River (Mossop and Flach 1983; Flach and Mossop 1985) is the general lack of a basal trough-cross stratified sand unit. Where present in the Lewis area (e.g. point bar A), it is commonly thin (2-3 m) and represents only about 10% of the point bar compared to 40% in the Steepbank example. In the Lewis study area, basal sand units are common, but unlike the Steepbank example, are similar in grain size to IHS deposits. As such, these basal deposits are grouped with IHS deposits as sand-dominated IHS or epsilon cross-stratified sand. Nevertheless, because of the lack of mud beds in these basal sand layers, the dipmeter data measures only the high-angle cross-strata, which is highly variable and does not reflect the dip-angle of the lateral accretion surface. Therefore, because basal sand layers are thin and commonly texturally indistinguishable from the overlying point-bar proper, and there is no reliable mechanism to measure the degree of dip, the channel successions from this study are not subdivided into a lower and upper unit with different dips as the example at the Steepbank River (Mossop and Flach 1983).

In this study, the method of Leeder (1973) ($w = 6.8h^{1.54}$), which uses the thickness of the point-bar deposit (h) to determine channel width (w), was used to estimate channel width for point-bar deposits A and B (Table 3.3). Leeder (1973) showed that this relationship applies only to moderate to high sinuousity channels ($P > 1.7$); based on calculations in Table 3.3, McMurray paleochannels satisfy this criterion. Using the recommended 95% confidence limit, a range of width estimates were derived (Table 3.3) suggesting that an alternative method was needed. Because the basal trough-cross stratified sand unit is either thin or indistinguishable from sandy-IHS deposits, channel width was estimated using a modified version of the trigonometric formula used by Mossop and Flach (1983) (Fig. 3.20). Originally developed by Leeder (1973), this formula was based on the two-thirds rule developed by Allen (1965) whereby the horizontal width of the ECS (in this case equivalent to IHS) represents approximately two-thirds of the paleochannel width at bankfull depth (Fig. 3.20). This method was previously used by Lavigne (1999) to estimate dimensions of paleochannels in the Upper Cretaceous Horseshoe Canyon Formation of southern Alberta.

Because unlithified oil sands deposits are consolidated by viscous heavy oil, a standard practice when coring McMurray Formation strata is to encase the core in plastic tubing. The core is then split into two parts – the thicker slice is made available to enthusiastic sedimentary geologists for study, and the thinner slice is generally used for core analyses. Because the cut surface may be oblique to the true dip of the lateral accretion surface, the dip of the lateral accretion surface measured in core dips may be less than the

Figure 3.20: Method to determine paleochannel dimensions from IHS deposits of McMurray Formation. Geometric relationship between bankfull depth (h), dip of lateral accretion (IHS) beds (β) and channel width (W) (Leeder 1973). The horizontal width of the lateral accretion (IHS) beds is approximately two-thirds the channel width (W). See Table 3.3 for paleochannel width calculations. Diagram modified from Leeder (1973).

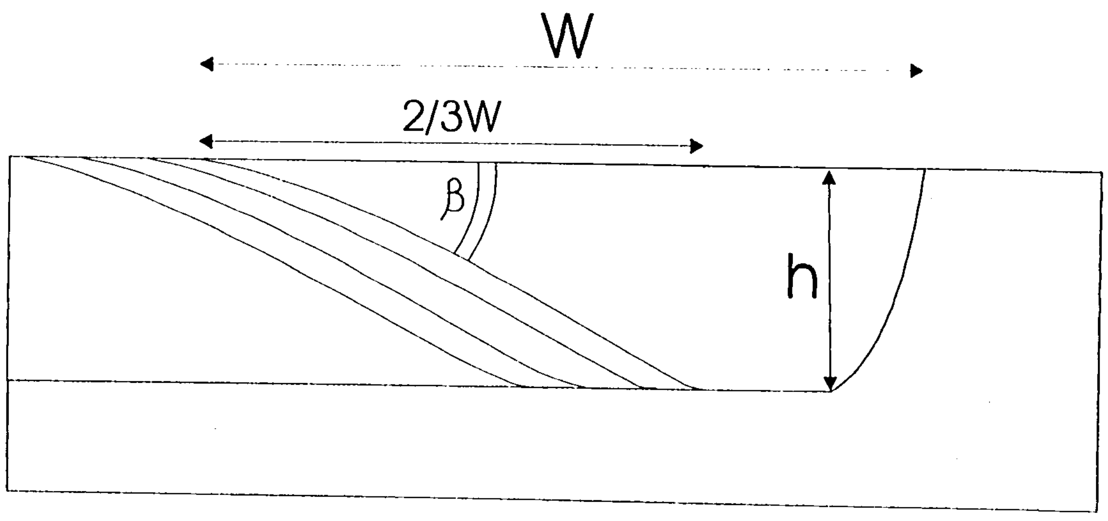

$$\boxed{W = 1.5h/\tan\beta}$$

W = channel width
h = bankfull depth of channel
β = dip of the lateral accretion surface

3.20

true dip. As a result the calculated $\tan\beta$ will be, at worst, less than the true dip. According to published data (Mossop and Flach 1983; Thomas *et al.* 1987; Smith 1987; Ainsworth and Walker 1994; Eberth 1996; Gingras *et al.* 2002), the average range of dip of heterolithic strata forming IHS deposits is commonly 8°-15°. Channel width for point-bar deposits in the Lewis study area were estimated using these values as end-member conditions (Table 3.4). Geophysical dipmeter well logs, which sample 360° of the wellbore, provide a more accurate estimate of the dip of IHS beds and these data suggest a 12° dip for the lateral accretion surface of point-bar A. Although dipmeter log data was not available for point bar B, the average dip of the lateral accretion deposit can still be estimated. According to Allen (1970) and calculations in Table 3.4, the dip of the lateral accretion deposit is inversely related to the thickness of the point bar. Since point-bar B is thicker than both point-bar A and the Steepbank River point-bar example, the lower end-member of 8° was used. Using these values, calculated channel widths are estimated as 148 m and 336 m for point-bar deposits A and B, respectively.

By estimating paleochannel width and depth, the size of other geometrical elements can be calculated (Table 3.3). Of particular importance is the meander wavelength, since this parameter can be used to estimate the length of an individual point-bar. Owing to the fact that two point-bars form in a single meander wavelength (Fig 3.2(c)), the length of a single point-bar can be estimated by dividing the calculated meander wavelength by two. Meander wavelength was computed using a formula derived from Leopold and Wolman (1960) (Table 3.3). This method is preferred to that of Schumm (1972) because it does not rely on the use of variables that are calculated from other formulae, each with some number of inherent

Table 3.4: Calculated channel widths based on a range of dips between 8°-15°, following methods of Leeder (1973) (see Fig. 3.20). Point bar calculations are based on an 11:1 ratio between meander wavelength and channel width. Because there are two point bars per meander wavelength, the average length of the point bar is 5X that of the channel width. The asterisks indicate the most probable channel widths (see text for details).

Well Location	h (m)	Dip (IHS beds)			
		8º	10º	12º	15º
10-26-91-8W4	21 m	224 m	179 m	*148 m	118 m
3-18-91-7W4	31.5 m	*336 m	268 m	222 m	176 m
Point Bar Length (m)	10-26-91-8W4	1232 m	985 m	*814 m	649 m
	3-18-91-7W4	*1848 m	1474 m	1221 m	968 m

3.4

assumptions. In this study, the meander wavelength is estimated to be 1718 m (point bar A) and 3930 m (point bar B), which corresponds to point-bar lengths of 859 m and 1965 m. These estimates, in turn, can help correlate genetically-related point-bar bases, especially where they are only partly preserved. Alternatively, applying the 11:1 principle, the channel width can be multiplied by 5.5 to obtain a rough estimate of point bar size. This yields comparable results of 814 and 1848 m.

It is important to note that the preceding discussion is based on well-established relationships between various fluvial geomorphic elements ad fluid/channel conditions. Currently it is not known if these relationships can be applied directly to tidally-influenced channels, which, therefore, should represent an important objective in future research.

CHAPTER 4:

SUMMARY AND CONCLUSIONS

Lower Cretaceous strata within the Lewis study area consist of sediments from both the McMurray and Clearwater formations. Transgressive deposits of the McMurray Formation constitute the bulk of the sedimentary succession and comprise four facies associations: braided-fluvial deposits (FA1), tidally-influenced braided- to low-accommodation meandering-fluvial and finer-grained tidal channel-fills (FA2), abandoned channels and interchannel deposits (FA3) and, open estuarine tidal flat deposits (FA4). The physical and biogenic sedimentary structures and the lateral and vertical facies relationships between these sedimentary units suggest that the McMurray Formation was deposited within a complex fluvial through to tide-dominated marginal marine system during an overall rise in relative sea level. Deposition of the McMurray Formation was ultimately terminated by marine sedimentation of the Clearwater Formation. Shoreface sand of the Wabasca Member was deposited as a thin transgressive unit directly above the wave-ravinement surface that terminated McMurray sedimentation. In turn, these deposits are overlain by a regional flooding surface and subsequent deposition of offshore marine mud of the Clearwater Formation. The shoreface and offshore strata of the Clearwater Formation constitutes facies association 5.

Lowstand fluvial channels (FA1) of the lower McMurray Formation initially developed and are preserved within paleotopographical lows on the sub-Cretaceous unconformity. These channels are overlain locally by a soil or coal horizon, although in most places lower McMurray strata are sharply overlain by tidally-influenced channel-fills and point-bar deposits of the middle McMurray Formation (FA2) which form the primary reservoir sand unit in the study area. The lower-middle McMurray contact represents a tidal ravinement surface. Middle McMurray Formation strata consist of two stacked stratal units consisting of a lower coarser-grained channel-fills and an upper network of finer-grained tidal channel-fills, and coeval abandoned channels and interchannel deposits (FA3). Lower-middle McMurray channels developed within a high energy, tidally-influenced braided- to low-accommodation meandering-fluvial system. Channels were initially confined by steep valley walls formed along the sub-Cretaceous unconformity. Furthermore, the rate of lateral accretion was likely high in comparison to the rate of vertical aggradation, resulting in the accumulation of a sand-rich sheet-like deposit with few interchannel deposits (FA3) preserved. Lower-middle McMurray channels are gradationally overlain by finer-grained inclined heterolithic stratification (IHS) deposits, or locally by tidal flat deposits (FA3). The contact between lower- and upper-middle McMurray channels represents a landward shift in facies, or a flooding surface that locally is indicated by tidal flat deposits (FA3). Upper-middle McMurray channels were not confined to paleo-lows and deposited thick, areally-extensive lateral accretion deposits (IHS) surrounded by thickly-developed off-channel strata (FA3). These channels were indirectly influenced by the paleotopography of the unconformity surface because the thickest and sandiest deposits directly overlie underlying lower-middle McMurray channel-fills. This suggests that syn-depositional salt dissolution controlled channel position and infilling history.

Middle McMurray strata are sharply overlain by open estuarine, mixed sand-and-mud tidal flat deposits of the upper McMurray Formation. Although the middle-upper McMurray contact is marked by a distinct lithological change, it is not considered chronostratigraphically significant and most-probably represents a simple autocyclical, gradational abandonment of the north-south trending middle McMurray channel system and consequential bedload sediment starvation.

Inclined heterolithic stratification (IHS) deposits of the middle McMurray Formation are common throughout the Lewis study area and form one of the primary reservoir units. IHS deposits are interpreted to represent the lateral migration of point-bar deposits in a tide-dominated marginal marine environment. Although the physical processes of lateral accretion are similar in both fluvial and tidally-influenced meandering systems, several factors influence deposition of tide-dominated point-bars that do not influence fluvial point-bar development: (1) more numerous mechanisms for mud deposition (waning fluvial and tidal flow, flocculation); (2) saline water influx which affects the distribution of organisms and, consequentially, the preserved trace fossil assemblage; and, (3) seaward-sourced sediment.

Two end-member types of IHS (point-bar) deposits occur within the Lewis study area (although many intermediate-types have been observed): epsilon cross-stratified/sand-dominated IHS and mud-dominated IHS. As opposed to mud-dominated point-bar deposits, sand-dominated successions consist of greater than ~70-90% sand; both end-member types of point-bars are composed of well-sorted and ungraded lower- to upper-fine sand exhibiting small- or large-scale cross-stratification. These sand layers are interstratified at low (8-12°)

angles with mud layers to form 10-30 m thick IHS successions. Muddy heteroliths are highly variable, ranging between thin laminae and cm- or dm-thick beds, and exhibit variable degrees of bioturbation from unbioturbated to intense.

The majority of the spatial and temporal variability within point-bar deposits of the Lewis study area can be attributed to the varying mechanisms for mud deposition and the influence of saline water: (1) flocculation due to the mixing of fresh and marine waters (thick or thin mud beds); (2) tidal cycles (stacked laminae); (3) seasonal or daily low energy fluxes in a fluvial system (thick or thin beds or stacked laminae). Saline water influx, as well as reduced salinity controls the variability in ichnological assemblages within point-bar deposits.

Because many point-bar deposits within the Lewis study area are incomplete and multiply-stacked, channel-bases are commonly the only correlatable portions of the point bar. Channel-bases can be identified in IHS deposits using a combination of core data (mud clasts, upward-fining successions, water-wet beds) and geophysical well log characteristics (changes in dip-azimuth, sharp gamma ray log changes). Several point-bar deposits, however, lack many of the above-mentioned discontinuities and have been interpreted as complete sequences. These deposits comprise an upward-fining succession overlain by vertical accretion/coastal plain deposits of Facies 5. Where a complete point bar succession is preserved, the paleochannel width and the point bar size can be estimated using a simple geometric formula that includes the channel height, or thickness of the point bar deposit and the dip of the lateral accretion beds (Leeder 1973). Estimating this value can be useful for correlation of individual point-bar deposits, as well as estimating the size of the individual reservoir. Using this mechanism, point bars of the McMurray Formation are estimated to be between 900 m and 2000 m wide. However, it is important to note that this method is based on observations and measurements in non-marine fluvial systems, and its applicability to tidally-influenced channel systems requires adequate testing.

LIST OF REFERENCES:

Ainsworth, B.R. 1994. Marginal marine sedimentology and high resolution sequence analysis; Bearpaw-Horseshoe Canyon transition, Drumheller, Alberta. Bulletin of Canadian Petroleum Geology, v. 42, p. 26-54.

Ainsworth, R.B. and Walker, R.G. 1994. Control of estuarine valley-fill deposition by fluctuations of relative sea level, Cretaceous Bearpaw-Horseshoe Canyon transition, Drumheller, Alberta, Canada. *In*: Incised-valley Systems: Origin and Sedimentary Sequences. Dalrymple, R.W., Boyd, R., and Zaitlin, B.A. (eds.). Society for Sedimentary Geology (SEPM), Special Publication 51, p. 159-174.

Alberta Energy and Utilities Board (EUB) 2001. Alberta's Reserves 2001 and Supply/Demand Outlook 2002-2011. EUB Statistical Series 2002-98.

Allen, G. P. 1991. Sedimentary processes and facies in the Gironde estuary: a recent model for macrotidal estuarine systems. *In*: Clastic Tidal Sedimentology. D.G. Smith, G.E. Reinson, B.A. Zaitlin, and R.A. Rahmani (eds.). Canadian Society of Petroleum Geologists, Memoir 16, p. 29-40.

Allen, J.R.L. 1963. The classification of cross-stratified units, with notes on their origin. Sedimentology, v. 2, p. 93-114.

Allen, J.R.L. 1965. Fining upward cycles in alluvial successions. Geological Journal, v. 4, p. 229-246.

Allen, J.R.L. 1970. Studies in fluviatile sedimentation: a comparison of fining-upward cyclothems with special reference to coarse-member composition and interpretation. Journal of Sedimentary Petrology, v. 40, p. 298-323.

Anima, R.J., Clifton, H.E., and Phillips, R.L. 1989. Comparison of modern and Pleistocene estuarine facies in Willapa Bay, Washington. *In*: Modern and Ancient Examples of Clastic Tidal Deposits – A Core and Peel Workshop. Reinson, G.E. (ed.). Canadian Society of Petroleum Geology (CSPG), p. 1-19.

Arnott, R.W.C., Zaitlin, B.A., and Potocki, D.J. 2002. Stratigraphic response to sedimentation in a net-accomodation-limited setting, Lower Cretaceous Basal Quartz, south-central Alberta. Bulletin of Canadian Petroleum Geology, v. 50, p. 92-104.

Barwis, J.H. 1978. Sedimentology of some South Carolina tidal-creek point-bars, and a comparison with their fluvial counterparts. *In*: Fluvial Sedimentology. Miall, A.D. (ed.). Canadian Society of Petroleum Geologists, Memoir 5, p. 129-160.

Baum, G.R. and Vail, P.R. 1988. Sequence stratigraphic concepts applied to Paleogene outcrops, Gulf and Atlantic basins. *In*: Sea Level Changes – An Integrated Approach. Society of Economic Paleontologists and Mineralogists (SEPM), Special Publication 42, p. 309-328.

Bechtel, D.J., Yuill, C., Ranger, M.J. and Pemberton, S.G. 1994. Ichnology of IHS of the McMurray Formation, northeastern Alberta. *In*: Mannville Core Conference. S.G. Pemberton, D.P. James, and D.M. Wightman (comp.). Canadian Society of Petroleum Geologists (CSPG), Exploration Update, p. 351-368.

Bell, R. 1884. Report on part of the basin of the Athabasca River, Northwest Territory. Geological Survey of Canada, Report of Progress 1882-83-84, p. 5-35.

Blakney, B. and Gingras, M.K. 2002. Using outcrops of the McMurray Formation to create a reservoir model (ab.). Canadian Society of Petroleum Geologists (CSPG) annual meeting, Calgary, Alberta, Program and Abstracts CD.

Boggs, S. 1995. Principles of Sedimentology and Stratigraphy. McConnin, R.A. (ed.). 774p.

Burden, E.T. 1984. Terrestrial palynomorph biostratigraphy of the lower part of the Mannville Group (Lower Cretaceous), Alberta and Montana. *In*: Mesozoic of Middle North America. Stott, D.F. and Glass, D.J. (eds.). Canadian Society of Petroleum Geologists, Memoir 9, p. 249-269.

Cant, D.J. 1992. Subsurface facies analysis. *In*: Facies Models, Response to Sea Level Change. R.G. Walker and N.P. James (eds.). Geological Association of Canada, p. 27-46.

Cant, D.J. 1998. Sequence stratigraphy, subsidence rates, and alluvial facies, Mannville Group, Alberta foreland basin. *In*: Relative Role of Eustasy, Climate and Tectonism in Continental Rocks. Shanley, K.W. and McCabe, P.J. (eds.). Society for Sedimentary Geology (SEPM), Special Publication 59, p. 49-63.

Cant, D.J. and Abrahmson, B. 1996. Regional distribution and internal stratigraphy of the Lower Mannville. Bulletin of Canadian Petroleum Geology, v. 44, p. 508-529.

Cant, D.J. and Stockmal, G.S. 1989. The Alberta Foreland Basin: relationship between stratigraphy and Cordilleran terrane-accretion events. Canadian Journal of Earth Sciences, v. 26, p. 1964-1975.

Carozzi, A.V. 1993. Sedimentary Petrography. Bonnell, J. (ed.). 263p.

Carrigy, M.A. 1959. Geology of the McMurray Formation, Part III: General Geology of the McMurray Area. Alberta Research Council, Memoir 1, 130 p.

Carrigy, M.A. 1963a. Criteria for differentiating the McMurray and Clearwater formations in the Athabasca oil sands. Alberta Research Council, Bulletin 014, 32p.

Carrigy, M.A. 1963b. The K.A. Clark volume: A collection of papers on the Athabasca oil sands presented to K.A. Clark on the 75th anniversary of his birthday. Alberta Research Council, Information Series 45, 241p.

Carrigy, M.A. 1966. Lithology of the Athabasca oil sands. Alberta Research Council, Bulletin 18, 48p.

Carrigy, M.A. 1971. Deltaic sedimentation in Athabasca tar sands. American Association of Petroleum Geologist Bulletin, v. 55, p. 1155-1169.

Carrigy, M.A. 1973. Mesozoic geology of the Fort McMurray area. *In*: Guide to Athabasca Oil Sands Area. Carrigy, M.A. and Kramers, J.W. (eds.). Alberta Research Council, Information Series 65, p. 77-101.

Carrigy, M.A. and Kramers, J.W. 1973. Guide to Athabasca Oil Sands Area. Carrigy, M.A. and Kramers, J.W. (eds.). Alberta Research Council, Information Series 65, 213p.

Caverley, A. 1984. Sedimentology and geomorphology of the modern epsilon cross-stratified point-bar deposits in the Athabasca upper delta plain. Unpublished M.Sc. Thesis, University of Calgary, 116p.

Christopher, J.E. 1974. The Upper Jurassic Vanguard and Lower Cretaceous Mannville groups. Saskatchewan Geological Survey, Department of Mineral Resources, Report No. 151, 349p.

Clifton, H.E. 1999. Tidal Sedimentation and Facies (supplementary notes to field guide). 42p.

Clifton, H.E. and Phillips, R.L. 1980. Lateral trends and vertical sequences in estuarine sediments, Willapa Bay, Washington. *In*: Quaternary Depositional Environments of the Pacific Coast: Papers Pacific Coast Paleogeography Symposium 4, p. 55-71.

Cody, J., Youn, S., Riddy, A. and Gittins, S. 2001. Implications of reservoir compartments on the design and execution of the Christina Lake thermal recovery project (ab.). Canadian Society of Petroleum Geologists (CSPG) annual meeting, Calgary, Alberta, Program and Abstracts CD.

Dalrymple, R.W. 1992. Tidal depositional systems. *In:* Facies Models, Response to Sea Level Change. R.G. Walker and N.P. James (eds.). Geological Association of Canada, p. 195-218.

Dalyrymple, R.W. 1994. High-resolution sequence stratigraphy of a complete, incised valley succession, Cobequid Bay-Salmon River estuary, Bay of Fundy, Canada. Sedimentology, v. 41, p. 1069-1091.

Dalrymple, R.W. 2002. The transport and deposition of mud in the tide-dominated Fly River deltaic system, Gulf of Paupa (ab.). Advances in Earth Sciences Research Conference (AESRC), University of Ottawa and the Ottawa-Carleton Geoscience Centre, Ottawa, Ontario, Program with Abstracts.

Dalrymple, R.W., Makino, Y., and Zaitlin, B.A., 1991. Temporal and spatial patterns of rhythmite deposition on mud flats in the macrotidal Cobequid Bay-Salmon River estuary, Bay of Fundy, Canada. *In:* Clastic Tidal Sedimentology. D.G. Smith, G.E. Reinson, B.A. Zaitlin, and R.A. Rahmani (eds.). Canadian Society of Petroleum Geologists, Memoir 16, p. 137-160.

Dalrymple, R.W., Zaitlin, B.A. and Boyd, R. 1992. Estuarine facies models: conceptual basic and stratigraphic implications. Journal of Sedimentary Petrology, v. 62, p. 1130-1146.

de Boer, P.L., Oost, A.P., and Visser, M.J. 1989. The Dinural Inequality of the Tide as a Parameter for Recognizing Tidal Influences. Journal of Sedimentary Petrology, v. 59, p. 912-921.

de Mowbray, T. 1983. The genesis of lateral accretion deposits in recent intertidal mudflat channels, Solway Firth, Scotland. Sedimentology, v. 30, p. 425-435.

De Raaf, J.F.M. and Boersma, J.R. 1971. Tidal Deposits and Their Sedimentary Structures. Geologie En Mijnbouw, v.. 50, p. 479-504.

Drees N.C. M. 1994. Devonian Elk Point Group of the Western Canada Sedimentary Basin. *In*: Geological Atlas of the Western Canada Sedimentary Basin. G.D. Mossop and I. Shetson (comps.). Canadian Society of Petroleum Geologists and Alberta Research Council.

Droser, M.L. and Bottjer, D.J. 1986. A semiqualitative classification of ichnofabric. Journal of Sedimentary Petrology, v. 56, p. 558-569.

Dyer, K.R. 1986. Coastal and Estuarine Sediment Dynamics. 342p.

Dyer, K.R. 1994. Estuarine transport and deposition. *In*: Sediment Transport and Depositional Processes. Pye, K. (ed.). p. 193-218.

Eberth, D.A. 1996. Origin and significance of mud-filled incised valleys (Upper Cretaceous) in southern Alberta, Canada. Sedimentology, v. 43, p. 459-477.

Edmunds, R.H., 1980. Salt Removal and oil entrapment (ab.). *In*: Facts and principles of world petroleum occurrence. A.D. Miall (ed.). Canadian Society of Petroleum Geologists (CSPG), Memoir 6, p. 988.

Ells, S.C. 1926. Bituminous sands of northern Alberta: Occurrence and economic possibilities: Report on investigations to the end of 1944. Canada Mines Branch Report 632.

Ethridge, F.G. and Schumm, S.A. 1978. Reconstructing paleochannel morphologic and flow characteristics: methodology, limitations and assessment. *In*: Fluvial Sedimentology. Miall, A.D. (ed.). Canadian Society of Petroleum Geologists, Memoir 5, p. 703-722.

Fisk, H.N. 1944. Geological investigation of the alluvial valley of the lower Misssissippi River. Mississippi River Commission, 78p.

Fisk, H.N. 1947. Fine-grained alluvial deposits and their effect on Mississippi River activity. Mississippi River Commission, 82p.

Flach, P. 1984. Oil Sands Geology – Athabasca deposit North. Alberta Research Council, Bulletin 46, 31p.

Flach, P.D., and Mossop, G.D. 1985. Depositional Environments of Lower Cretaceous McMurray Formation, Athabasca Oil Sands, Alberta. American Association of Petroleum Geologists Bulletin, v. 69, p. 1195-1207.

Frey, R.W., Howard, J.D., and Pryor, W.A. 1978. *Ophiomorpha*: its morphological, taxonomic, and environmental significance. Palaeogeography, Palaeoclimatology, Palaeoecology, v. 23, p. 199-220.

Gastaldo, R.A., Allen, G.P., and Huc, A.-Y. 1995. The tidal character of fluvial sediments of the modern Mahakam River Delta, Kalimantan, Indonesia. *In*: Tidal signatures in modern and ancient sediments. Flemming, B.W. and Bartholomae, A. (eds.). International Association of Sedimentologists (IAS), Special Publication 24, p. 171-181.

Gingras, M.K. 1999. Applications and approaches in ichnology, neoichnology, and sedimentology. Unpublished Ph.D. thesis, University of Alberta, Edmonton, Alberta, 245p.

Gingras, M.K., Pemberton, S.G., Saunders, T., and Clifton, E.H. 1999. The ichnology of modern Pleistocene brackish-water deposits at Willapa Bay, Washington: variability in estuarine settings. Palaios, v. 14, p. 352-372.

Gingras, M.K., Rasanen, M., and Ranzi, A. 2002. The significance of bioturbated inclined heterolithic stratification in the southern part of the Miocene Solimoes Formation, Rio Acre, Amazonia Brazil. Palaios, v. 17, p. 591-601.

Guilcher, A. 1985. Senegal and Gambia. *In*: The World's Coastline. Bird, E.C.F. and Schwartz, M.L. (eds.). p. 555-560.

Harris, P.T., Baker, E.K., Cole, A.R., and Short, S.A. 1993. A preliminary study of sedimentation in the tidally dominated Fly River Delta, Gulf of Papua. Continental Shelf Research, v. 13, p. 441-472.

Hayes, B.J.R., Christopher, J.E., Rosenthal, L., Los, G. and Mckercher, B. 1994. Cretaceous Mannville Group of the Western Canada Sedimentary Basin. *In*: Geological Atlas of the Western Canada Sedimentary Basin. G.D. Mossop and I. Shetson (comps.). Canadian Society of Petroleum Geologists and Alberta Research Council, p. 317-334.

Hein, F.J. 2000. Historical overview of the Fort McMurray area and oil sands industry in northeast Alberta (with expanded bibliographies on oil sands, surficial geology, hydrogeology, minerals and bedrock in northeast Alberta). Alberta Energy and Utilities Board (EUB)/Alberta Geological Survey, Earth Sciences Report 2000-05, 32p.

Hein, F.J., Cotterill, D.K., and Berhane, H. 2000. An atlas of lithofacies of the McMurray Formation, Athabasca oil sands deposit, northeastern Alberta: surface and subsurface. Alberta Energy and Utilities Board (EUB)/Alberta Geological Survey, Earth Sciences Report 2000-07, on CD ROM, 216p.

Hein, F.J. and Dolby, G. 2001. Regional lithostratigraphy biostratigraphy and facies models, Athabasca oil sands deposit, northeast Alberta (ab.). Canadian Society of Petroleum Geologists (CSPG) annual meeting, Calgary, Alberta, Program and Abstracts CD.

Hori, K., Saito, Y., Zhao, Q., Cheng, X, Wang, P., Sato, Y., and Li, C. 2001. Sedimentary facies of the tide-dominated paleo-Changjiang (Yangtze) estuary during the last transgression. Marine Geology, v. 177, pp. 331-351.

Howard, J.D. and Frey, R.W. 1973. Characteristic physical and biogenic sedimentary structures in Georgia estuaries. American Association of Petroleum Geologists Bulletin, v. 57, p. 1169-1184.

Howard, J.D. and Frey, R.W. 1975. Estuaries of the Georgia coast, U.S.A.: Sedimentology and Biology. II. Regional animal-sediment characteristics of Georgia estuaries. Senckenbergiana maritime, v. 7, p. 33-103.

Hubbard, S.M., Pemberton, S.G., Howard, E.A. 1999. Regional geology and sedimentology of the basal Cretaceous Peace River Oil Sands deposit, north-central Alberta. Bulletin of Canadian Petroleum Geology, v. 47, p. 270-297.

Hughes, M.G., Harris, P.T., and Hubble, T.C.T. 1998. Dynamics of the turbidity maximum zone in a micro-tidal estuary: Hawkesbury River, Australia. Sedimentology, v. 45, p. 397-410.

Jackson, P.C. 1984. Paleogeography of the Lower Cretaceous Mannville Group of western Canada. *In*: Elmworth – Case Study of a Deep Basin Gas Field. J.A. Masters (ed.). American Association of Petroleum Geologists, Memoir 38, p. 49-77.

Jackson, R.G. 1976. Depositional model of point bars in the Lower Wabash river. Journal of Sedimentary Petrology, v. 46, p. 579-594.

Jackson, R.G. 1981. Sedimentology of muddy fine-grained channel deposits in meandering streams of the American middle west. Journal of Sedimentary Petrology, v. 51, p. 1169-1192.

James, D.P. 1977. The sedimentology of the McMurray Formation, east Athabasca. Unpublished M.Sc. thesis, University of Calgary, Calgary, Alberta, 198p.

Jeletzky, J.A. 1971. Marine Cretaceous biotic provinces and paleogeography of western and arctic Canada. Geological Survey of Canada, Paper 70-22, 92p.

Keith, D.A.W., MacGillivray, J.R., Wightman, D.M., Bell, D.D., Berezniuk, T. and Berhane, H. 1990. Resource characterization of the McMurray/Wabiskaw deposit in the Athabasca south region of north-eastern Alberta. Alberta Oil Sands Technology and Research Authority (AOSTRA), Technical Publication Series No. 7, 63p.

Lagenberg, C.W., Hein, F.J., Lawton, D. and Cunningham, J. 2002. Seismic modeling of fluvial-estuarine deposits in the Athabasca oil sands using ray-tracing techniques, Steepbank River area, northeastern Alberta. Bulletin of Canadian Petroleum Geology, v. 50, p. 178-204.

Land, L.S. and Hoyt, J.H. 1966. Sedimentology in a meandering estuary. Sedimentology, v. 6, p. 191-207.

Lavigne, J.M. 1999. Aspects of marginal marine sedimentology, stratigraphy and ichnology of the Upper Cretaceous Horseshoe Canyon Formation, Drumheller, Alberta. Unpublished M.Sc. Thesis, University of Alberta, Edmonton, Alberta, 146p.

Leckie, D.A. and Smith, D.G. 1992. Regional setting, evolution, and depositional cycles of the western Canada foreland basin. *In*: Foreland Basins and Fold Belts. Macqueen, R.W. and Leckie, D.A. (eds.). American Association of Petroleum Geologists, Memoir 55, p. 9-46.

Leeder, M.R. 1973. Fluviatile fining-upward cycles and magnitude of palaeochannels. Geological Magazine, v. 110, p. 265-276.

Leeder, M.R. 1982. Sedimentology. Allen and Unwin (pub.). 344p.

Leopold, L.B. 1994. A View of the River. 298p.

Leopold, L.B. and Wolman, MG. 1960. River meanders. Bulletin of the Geological Society of America, v. 71, p. 769-794.

Loutit, T.S., Hardenbol, J., Vail, P.R., and Baum, G.R. 1988. Condensed sections: the key to age determination and correlations of continental margin sequences. *In*: Sea Level Changes – An Integrated Approach. Society of Economic Paleontologists and Mineralogists (SEPM), Special Publication 42, p. 183-213.

MacGillivray, J.R., Strobl, R.S., Keith, D.A.W., Wightman, D.M., Wynne, D.A., Berezniuk, T. and Berhane, H. 1992. Resource characterization of the McMurray/Wabiskaw deposit in the Athabasca south region of north-eastern Alberta. Alberta Oil Sands Technology and Research Authority (AOSTRA), Technical Publication Series No. 8, 68p.

Masters, J.A. 1984. Lower Cretaceous oil and gas in western Canada. *In*: Elmworth: Case Study of a Deep Basin Gas Field. Masters, J.A. (ed.). American Association of Petroleum Geologists, Memoir 38, p. 1-33.

Mattison, B.W., King, B., Parry, D., Knight, J., and Slevinsky, B. 2001. Petro-Canada's Mackay River *In-Situ* oil sands project: current scope and status (ab.). Canadian Society of Petroleum Geologists (CSPG) annual convention, Calgary, Alberta, Program and Abstracts CD.

Mattison, B.W. and Pemberton, S.G. 1988. The McMurray Formation in the Athabasca oil sands area: An ichnological and paleontological perspective. *In*: 4th UNITAR/UNDP Conference on Heavy Crude and Tar Sands, Edmonton, Alberta, Paper No. 87, 18p.

McConnell, R.G. 1891. Tar sands on Athabasca River. Geological Survey of Canada, Annual Report 5, p. 144-147.

McConnell, R.G. 1893. Report on a portion of the district of Athabasca, comprising the country between Peace River and Athabasca River north of Lesser Slave Lake. Geological Survey of Canada, Annual Report 1890-1915, p. 5-7.

McLearn, F.H. 1917. Athabasca river section, Alberta. Geological Survey of Canada, Summary Report 1916, p. 145-151

McLearn, F.H. 1945. Revision of the Lower Cretaceous of the western interior of Canada. Geological Survey of Canada, Paper 44-17.

McPhee, D.A. 1994. Sequence stratigraphy of the Lower Cretaceous Mannville Group of east-central Alberta. Unpublished M.Sc. thesis, University of Alberta, Edmonton, Alberta, 66p.

McPhee, D.A. and Wightman, D.W. 1991. Timing of the dissolution of Middle Devonian Elk Point Group evaporates – Townships 47 to 103 and Ranges 15W3 to 20W4M (ab.). Bulletin of Canadian Petroleum Geology, v. 39, p. 218.

Meckel, L.D. 1975. Holocene sand bodies in the Colorado Delta area, Northern Gulf of California. *In*: Deltas. Broussard, M.L. (ed.). p. 239-264.

Miall, A.D. 1978. Fluvial sedimentology: an historical review. *In*: Fluvial Sedimentology. Miall, A.D. (ed.). Canadian Society of Petroleum Geologists (CSPG), Memoir 5, p. 1-47.

Miall, A.D. 1987. Recent developments in the study of fluvial facies models. *In*: Recent Developments in Fluvial Sedimentology. Ethridge, F.G., Flores, R.M., and Harvey, M.D. (eds.). Society of Economic Palaeontologists and Mineralogists (SEPM), Special Publication 39, p. 1-9.

Minkin, D.F. 1974. The Cold Lake oil sands: geology and a reserve estimate. *In*: Oil Sands, Fuel of the Future. Hills, L.V. (ed.). Canadian Society of Petroleum Geologists (CSPG), Memoir 3, p. 84-89.

Molgat, M. 2000. Sedimentology, stratigraphy, and shallow burial alteration of the Upper Jurassic Swift Formation, southeastern Alberta. Unpublished M.Sc. thesis, University of Ottawa, Ottawa, Ontario, 277p.

Molgat, M. and Arnott, R.W.C. 2001. Combined tide and wave influence on sedimentation patterns in the Upper Jurassic Swift Formation, south-eastern Alberta. Sedimentology, v. 48; p. 1353-1369.

Monger, J.W.H., and Price, R.A. 1979. The geodynamic evolution of the Canadian Cordillera – progress and problems. Canadian Journal of Earth Sciences, v. 16, p. 770-791.

Mossop, G.D. 1980a. Geology of the oil sands. Science, v. 207, p. 145-152.

Mossop, G.D. 1980b. Facies control on bitumen saturation in the Athabasca oil sands. *In*: Facts and Principles of World Petroleum Occurrence. A.D. Miall (ed.). Canadian Society of Petroleum Geologists (CSPG), Memoir 6, p. 609-632.

Mossop, G.D. and Flach, P.D. 1983. Deep channel sedimentation in the Lower Cretaceous McMurray Formation, Athabasca oil sands, Alberta. Sedimentology, v. 30, p. 493-509.

Nadon, G.C. 1994. The genesis and recognition of anastomosed fluvial deposits: data from the St. Mary River Formation, southwestern Alberta, Canada. Journal of Sedimentary Research, v. B64, no. 4, p. 451-463.

Nelson, H.W. and Glaister, R.P. 1978. Subsurface environmental facies and reservoir relationships of the McMurray oil sands, northeastern Alberta. Bulletin of Canadian Petroleum Geology, v. 26, p. 177-207.

Nio, S-D. and Yang, C-S. 1991. Diagnostic attributes of clastic tidal deposits: a review. *In:* Clastic Tidal Sedimentology. D.G. Smith, G.E. Reinson, B.A. Zaitlin, and R.A. Rahmani (eds.). Canadian Society of Petroleum Geologists, Memoir 16. p. 3-28.

North American Commission on Stratigraphic Nomenclature 1983. North American Stratigraphic Code. American Association of Petroleum Geologists Bulletin, v. 67, p. 841-875.

Olsen, T., Steel, R., Hogseth, K., Skar, T., and Roe, S.L. 1995. Sequential architecture in a fluvial succession: sequence stratigraphy in the Upper Cretaceous Mesaverde Group, Price Canyon, Utah. Journal of Sedimentary Research, v. B65, 2, p. 265-280.

Page, K.J., Nanson, G.C., Frazier, P.S. 2003. Floodplain formation and sediment stratigraphy resulting from oblique accretion on the Murrumbidgee River, Australia. Journal of Sedimentary Research, v. 73, p. 5-14.

Paola, C., Parker, G., Seal, R., Sinha, S.K., Southard, J.B., and Wilcock, P.R. 1992. Downstream fining by selective deposition in a laboratory flume. Science, v. 258, p. 1757-1760.

Pejrup, M. 1991. The influence of flocculation on cohesive sediment transport in a microtidal estuary. *In*: Clastic Tidal Sedimentology, D.G. Smith, G.E. Reinson, B.A. Zaitlin, and R.A. Rahmani (eds.). Canadian Society of Petroleum Geologists, Memoir 16, p. 283-290.

Pemberton, S.G., Flach, P.D. and Mossop, G.D. 1982. Trace fossils from the Athabasca oil sands, Alberta, Canada. Science, v. 217, p. 825-827.

Price, R.A. 1973. Large-scale gravitational flow of supracrustal rocks, southern Canadian Rocky Mountains. *In*: Gravity and tectonics. K.A. De Jong and R.A. Scholten (eds.). p. 491-502.

Purkait, B. 2002. Patterns of grain-size distribution in some point bars of the Usri river, India. Journal of Sedimentary Research, v. 72, p. 367-375.

Rahmani, R.A. 1988. Estuarine tidal channel and nearshore sedimentation of a late Cretaceous epicontinental sea, Drumheller, Alberta, Canada. *In:* Tide-influenced Sedimentary Environments and Facies. P.L. de Boer, A. Van Gelder and S.D. Nio (eds.), p. 433-471.

Ranger, M.J. 1984. The paleotopography of the pre-Cretaceous erosional surface in the western Canada basin (abs). *In*: The Mesozoic of middle North America. D.E. Stott and D.J. Glass (eds.). Canadian Society of Petroleum Geologists (CSPG), Memoir 9, p. 570.

Ranger, M.J. and Pemberton, S.G. 1997. Elements of a stratigraphic framework for the McMurray Formation in south Athabasca area, Alberta. *In*: Petroleum Geology of the Cretaceous Mannville Group, Western Canada. Pemberton, S.G. and James, D.P. (eds.). Canadian Society of Petroleum Geologists Memoir 18, p. 263-289.

Retallack, G.J. 1988. Field recognition of paleosols. *In*: Paleosols and Weathering Through Geologic Time: Principles and Applications. Reinhardt, J. and Sigleo, W.R. (eds.). Geological Society of America, Special Paper 216, p. 1-20.

Rudkin, R.A. 1964. Lower Cretaceous. *In*: Geologic History of Western Canada. R.G. McCrossan and R.P. Glaister (eds.). Alberta Society of Petroleum Geologists, p. 156-168.

Rust, B.R. and Jones, B.G. 1986. The Hawkesbury Sandstone south of Sydney, Australia: Triassic analogue for the deposit of a large, braided river. Journal of Sedimentary Petrology, v. 57, p. 222-233.

Sambrook, G.H. and Ferguson, R.I. 1995. The gravel-sand transition along river channels. Journal of Sedimentary Research, v. A65, p. 423-430.

Schumm, S.A. 1972. Fluvial paleochannels. *In*: Recognition of Ancient Sedimentary Environments. Rigby, J.K. and Hamblin, W.K. (eds.), Society of Economic Paleontologists and Mineralogists (SEPM), Special Publication 16, p. 98-107.

Shanley, K.W., McCabe, P.J. and Hettinger, R.D. 1992. Tidal influence in Cretaceous fluvial strata from Utah, USA: a key to sequence stratigraphic interpretation. Sedimentology, v. 39, p. 905-930.

Singh, C. 1964. Microflora of the Lower Cretaceous Mannville Group, east-central Alberta. Research Council of Alberta, Bulletin 15, 239p.

Smith, D.G. 1987. Meandering river point bar lithofacies models: modern and ancient examples compared. *In*: Recent Developments in Fluvial Sedimentology. Ethridge, F.G., Flores, R.M., and Harvey, M.D. (eds.). Society of Economic Paleontologists and Mineralogists (SEPM), Special Publication 39, p. 83-91.

Smith, D.G. 1988. Tidal bundles and mud couplets in the McMurray Formation, northeastern Alberta, Canada. Bulletin of Canadian Petroleum Geology, v. 36, p. 216-219.

Smith, D.G. 1994. Paleogeographic evolution of the western Canada foreland basin. *In*: Geological Atlas of the Western Canada Sedimentary Basin. G.D. Mossop and I. Shetson (comps.). Canadian Society of Petroleum Geologists and Alberta Research Council, p. 277-296.

Smith, D.G. and Smith, N.D. 1980. Sedimentation in anastomosed river systems: examples from alluvial valleys near Banff, Alberta. Journal of Sedimentary Petrology, v. 50, p. 157-164.

Spaargaren, D.H. 1995. A functional model for describing the responses to salinity stress in aquatic animals. Comparative Biochemistry and Physiology, v. 11, p. 501-506.

Stelck, C.R. 1975. Basement controls of Cretaceous sand sequences in Western Canada. *In*: The Cretaceous System of the Western Interior of North America. W.G.E. Caldwell (ed.). Geological Association of Canada Special Paper 13, p. 427-440.

Stelck, C.R. and Kramers, J.W. 1980. *Frebodiceras* from the Grand Rapids Formation of north-central Alberta. Bulletin of Canadian Petroleum Geology, v. 28, p. 509-521.

Stewart, G.A. 1963. Geological controls on the distribution of Athabasca oil sand reserves. *In*: Athabasca Oil Sands: The K.A. Clark volume: A collection of papers on the Athabasca oil sands presented to K.A. Clark on the 75th anniversary of his birthday. M.A. Carrigy (ed.). Alberta Research Council, Information Series 45, p. 15-26.

Stewart, G.A. and MacCallum, G.T. 1978. Athabasca oil sands guide book. *In:* Facts and Principles of World Petroleum Oil Occurrence. Candian Society of Petroleum Geologists international conference, 33p.

Stockmal, G.S., Cant, D.J. and Bell, J.S. 1992. Relationship of the stratigraphy of the western Canada foreland basin to cordilleran tectonics: insights from geodynamic models. *In*: Foreland Basins and Fold Belts. R.W. Macqueen and D.A. Leckie (eds.). American Association of Petroleum Geologists, Memoir 55, p. 107-124.

Stott, D.F. 1984. Cretaceous sequences of the foothills of the Canadian Rocky Mountains. *In*: The Mesozoic of Middle North America. D.F. Stott and D.J. Glass (eds.). Canadian Society of Petroleum Geologists, Memoir 9, p. 85-107.

Strobl, R.S., Cotterill, D.K., Berhane, H., Wynne, D.A., Wightman, D.M., Anderson, M.N., Berezniuk, T., and McGillivray, J.R. 1993. Resource characterization of the McMurray/Wabiskaw deposit in the Athabasca West region of northeastern Alberta. Alberta Oil Sands Technology and Research Authority (AOSTRA), Technical Publication Series No. 9, 78p.

Sweet, A.R. 2002. Applied research report on 15 samples of Early Cretaceous age from the McMurray Formation of northeastern Alberta (NTS74D/14). Paleontological Report, Geological Survey of Canada (Calgary), Paleontological Subdivision, 8p.

Thomas, R.G., Smith, D.G., Wood, J.M., Visser, J., Calverley-Range, E.A., and Koster, E.H. 1987. Inclined heterolithic stratification – terminology, description, interpretation and significance. Sedimentary Geology, v. 53, p. 123-179.

Tornqvist, T.E. 1993. Holocene alternation of meandering and anastomosing fluvial systems in the Rhine-Meuse Delta (central Netherlands) controlled by sea-level rise and subsoil erodibility. Journal of Sedimentary Petrology, v. 63, p. 683-693.

Turner, B.R. and Eriksson, K.A. 1999. Meander bend reconstruction from an Upper Mississippian muddy point bar at Possum Hollow, West Virginia, USA. International Association of Sedimentology (IAS), Special Publication 28, p. 363-379.

Whiting, P. 1996. Sediment sorting over bed topography. *In:* Advances in Fluvial Dynamics and Stratigraphy. Carling, P.A. and Dawson, M.R. (eds.), p. 203-228.

Wightman, D, M., Attalla, M.N., Wynne, D.A., Strobl, R.S., Berhane, H., Cotterill, D.K., and Berezniuk, T. 1995. Resource characterization of the McMurray/Wabiskaw deposit in the Athabasca oil sands area: a synthesis. Alberta Oil Sands Technology and Research Authority (AOSTRA), Technical Publication Series No. 10, 220p.

Wightman, D.M., MacGillivray, J.R., McPhee, D., Berhane, H., and Berezniuk, T. 1991. McMurray Formation and Wabiskaw Member (Clearwater Formation): regional perspectives derived from the north Primrose area, Alberta, Canada. *In*: 5th UNITAR International Conference, Heavy Crude and Tar Sands – Hydrocarbons for the 21st Century, v. 1: Geology, Characterization and Mining, p. 285-320.

Wightman, D.M., and Pemberton, S.G. 1993. The McMurray Formation: an overview of the surface mineable area. Oil Sands: Our Petroleum Future conference, Edmonton, Alberta. Alberta Oil Sands Technology and Research Authority (AOSTRA), p. 3-32.

Wightman, D.M. and Pemberton, S.G. 1997. The Lower Cretaceous (Aptian) McMurray Formation: An overview of the Fort McMurray area, northeastern Alberta. *In*: Petroleum Geology of the Cretaceous Mannville Group, Western Canada. Pemberton, S.G. and James, D.P. (eds.). Canadian Society of Petroleum Geologists, Memoir 18, p. 312-344.

Wightman, D.M., Pemberton, S.G., and Singh, C. 1987. Depositional modeling of the Upper Mannville (Lower Cretaceous), east central Alberta: implications for the recognition of brackish water deposits. *In*: Reservoir Sedimentology. R.W. Tillman and K.J. Weber (eds.). p. 189-220.

Williams, G.D. 1963. The Mannville Group (Lower Cretaceous) of central Alberta. Bulletin of Canadian Petroleum Geology, v. 2, p. 350-368.

Wright, M.D. 1959. The formation of cross bedding by a meandering or braided stream. Journal of Sedimentary Petrology, v. 29, p. 610-615.

Yuill, C., Bechtel, D. and Pemberton, S.G. 1994. Sedimentology and ichnology of the McMurray Formation at the OSLO and Steepbank areas. *In*: Mannville Core Conference. S.G. Pemberton, D.P. James, and D.M. Wightman (comp.). Canadian Society of Petroleum Geologists, Exploration Update, p. 195-209.

Appendix 1
Stratigraphic Columns

List of cores logged for this study

LSD	SEC	TWP	RNG	Cored Interval (m)	# m's
12	**30**	**91**	**6W4**	**166.5-226.5**	**60**
6	8	91	7W4	133.0-185.9	52.9
12	8	91	7W4	131.8-196.0	64.2
5	10	91	7W4	140.7-246.3	105.6
7	10	91	7W4	141.4-226.7	85.3
13	12	91	7W4	145.6-214.0	68.4
10	17	91	7W4	153.7-224.9	71.2
3	18	91	7W4	141.0-232.2	91.2
13	19	91	7W4	141.7-221.2	79.5
5	20	91	7W4	155.8-222.0	66.2
12	**21**	**91**	**7W4**	**144.5-238.6**	**94.1**
2	**22**	**91**	**7W4**	**132.5-222.9**	**90.4**
6	22	91	7W4	142.0-244.7	102.7
15	22	91	7W4	137.6-237.7	100.1
1	**23**	**91**	**7W4**	**173.0-237.5**	**64.5**
16	26	91	7W4	165.9-232.0	66.1
15	27	91	7W4	139.3-244.7	105.4
6	28	91	7W4	139.6-224.4	84.8
9	**28**	**91**	**7W4**	**138.9-235.2**	**96.3**
15	**29**	**91**	**7W4**	**143.7-199.7**	**56**
6	30	91	7W4	144.0-202.0	58
8	32	91	7W4	145.0-193.0	48
1	**12**	**91**	**8W4**	**125.7-206.4**	**80.7**
12	12	91	8W4	127.6-206.4	78.8
15	12	91	8W4	130.0-223.7	93.7
1	13	91	8W4	134.2-204.7	70.5
4	13	91	8W4	131.7-226.1	94.4
2	14	91	8W4	130.0-204.7	74.7
11	23	91	8W4	131.3-189.9	58.6
6	24	91	8W4	137.0-189.8	52.6
10	**26**	**91**	**8W4**	**132.0-206.7**	**74.7**
7	27	91	8W4	136.2-189.7	53.7
12	34	91	8W4	129.3-198.2	68.9
11	36	91	8W4	143.4-211.0	67.6
7	3	92	7W4	154.2-217.7	63.5
2	4	92	7W4	150.7-247.4	96.7
15	4	92	7W4	148.7-232.7	84
				TOTAL	**2824 m**

Core logs included in Appendix 1

LEGEND FOR CORE LOGS

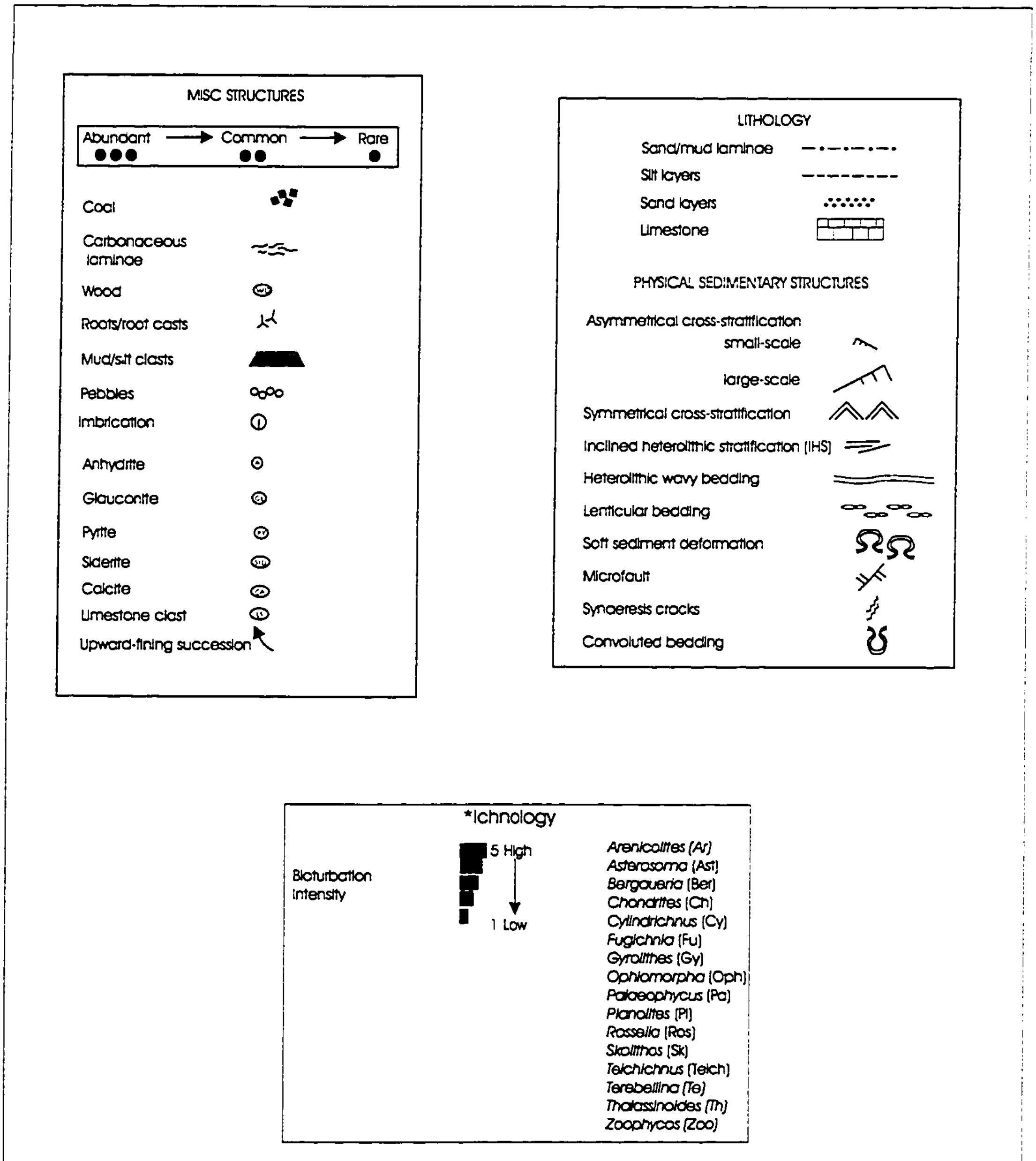

*Bioturbation intensity follows classification of Droser and Bottjer (1986)

Well Name: PC Lewis
Location: 12-30-91-6W4
KB: 483.5m
Cored Interval: 166.5-226.5 m
Logged by: Erin Crerar, University of Ottawa

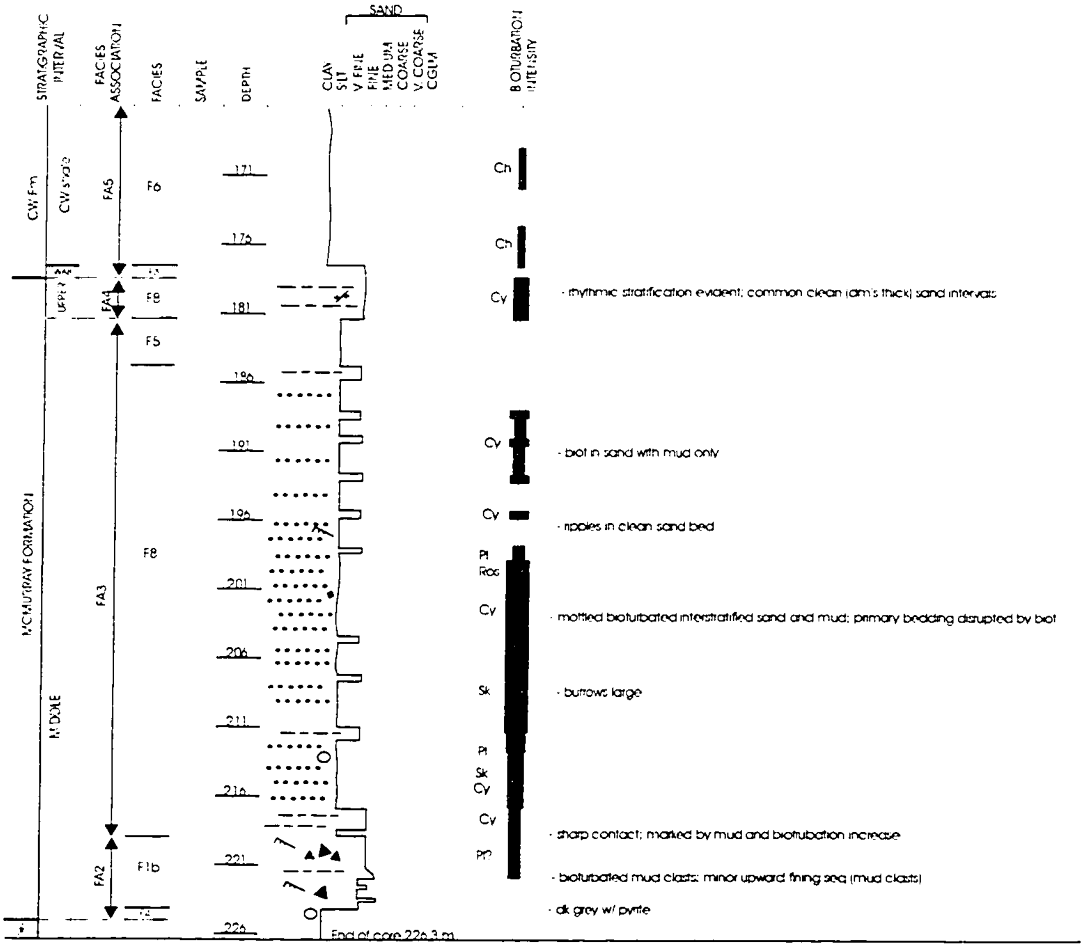

Well Name: PC Lewis
Location: 12-21-91-7W4
KB: 468.3m
Cored Interval: 144.5-238.6m
Logged by: Erin Crerar, University of Ottawa

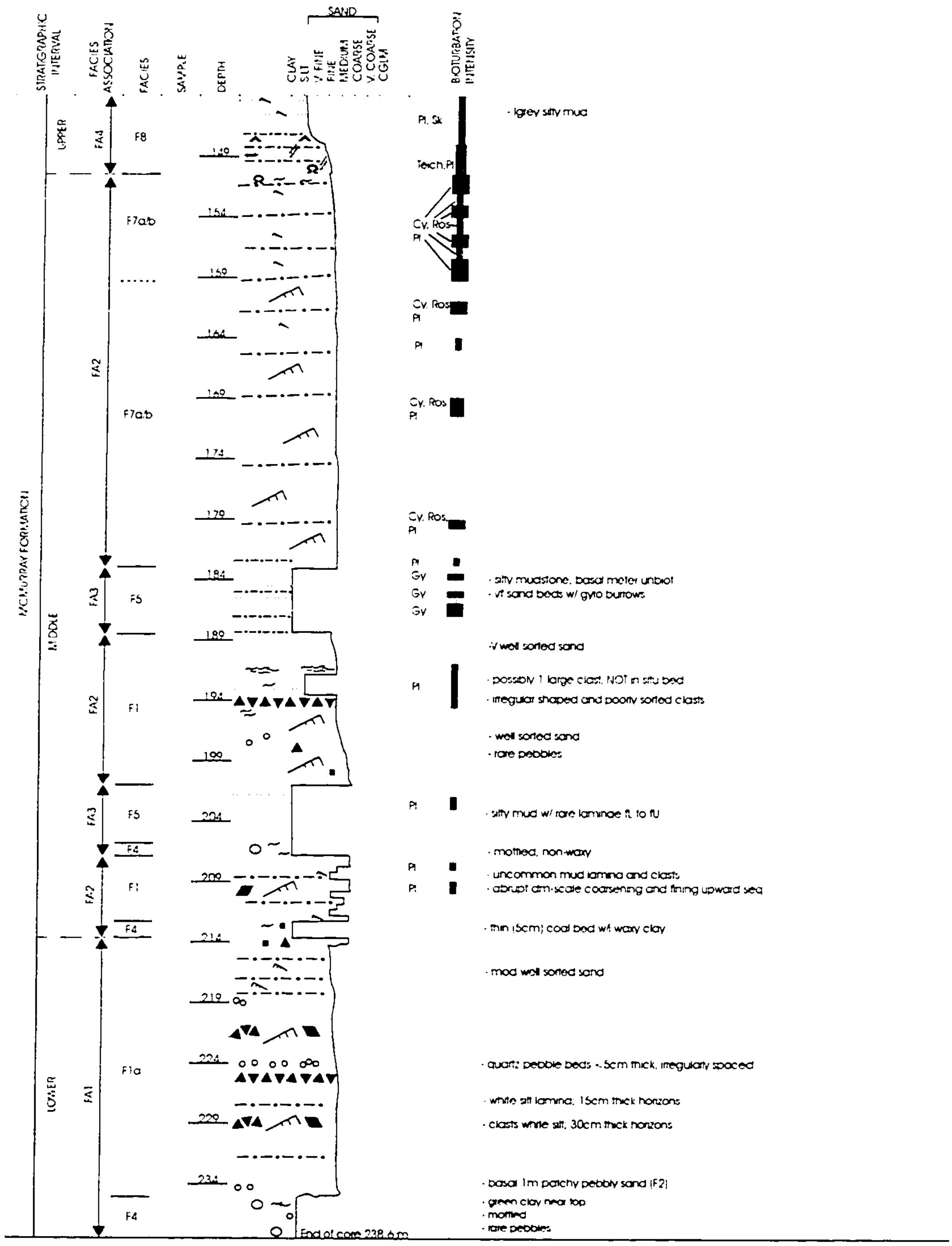

Well Name: PC Lewis
Location: 02-22-91-7W4
KB: 469.6m
Cored Interval: 135.07-222.9m
Logged by: Erin Crerar, University of Ottawa

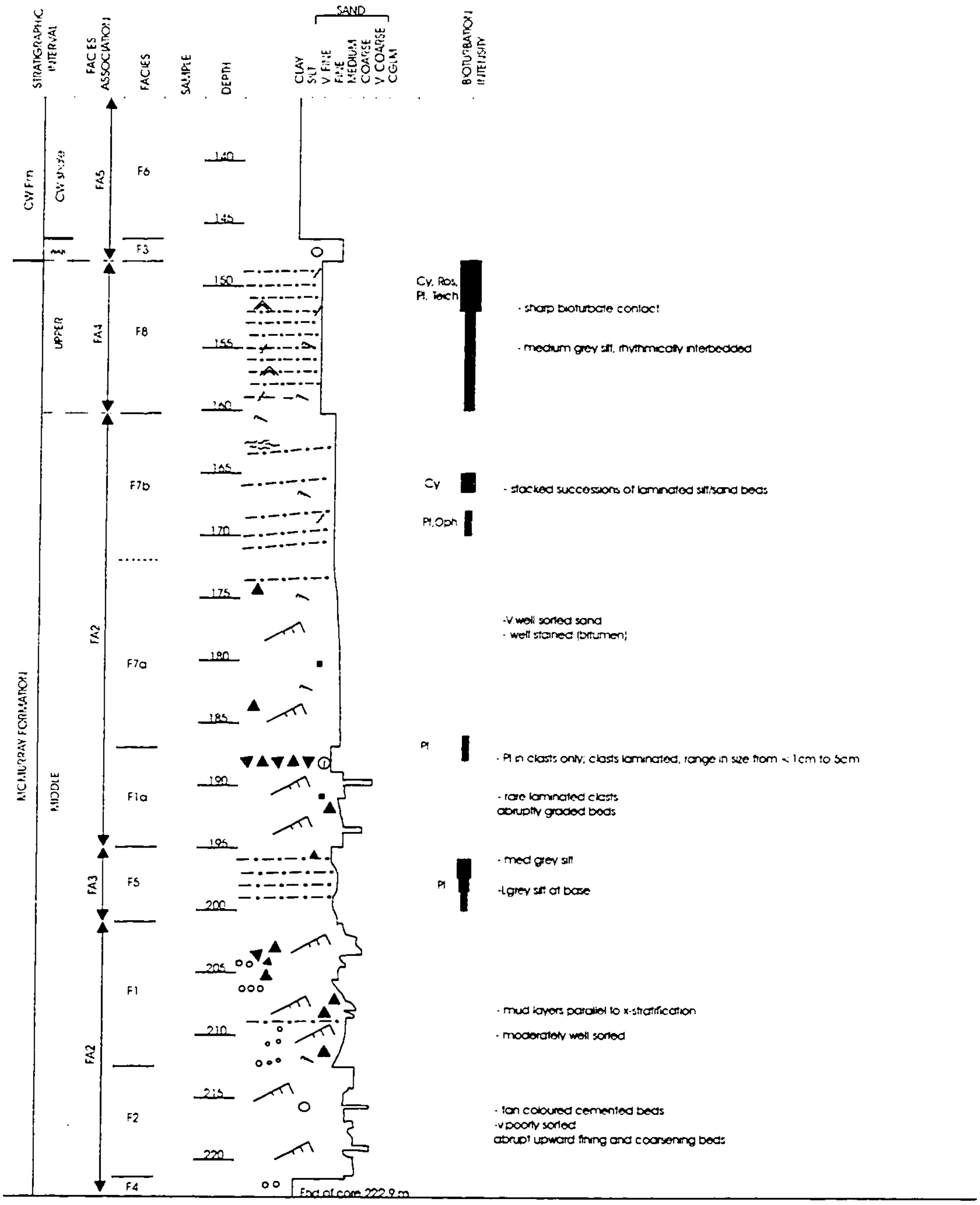

Well Name: PC Lewis
Location: 01-23-91-7W4
KB: 473.0m
Cored interval: 173.0-237.5m
Logged by: Erin Crerar, University of Ottawa

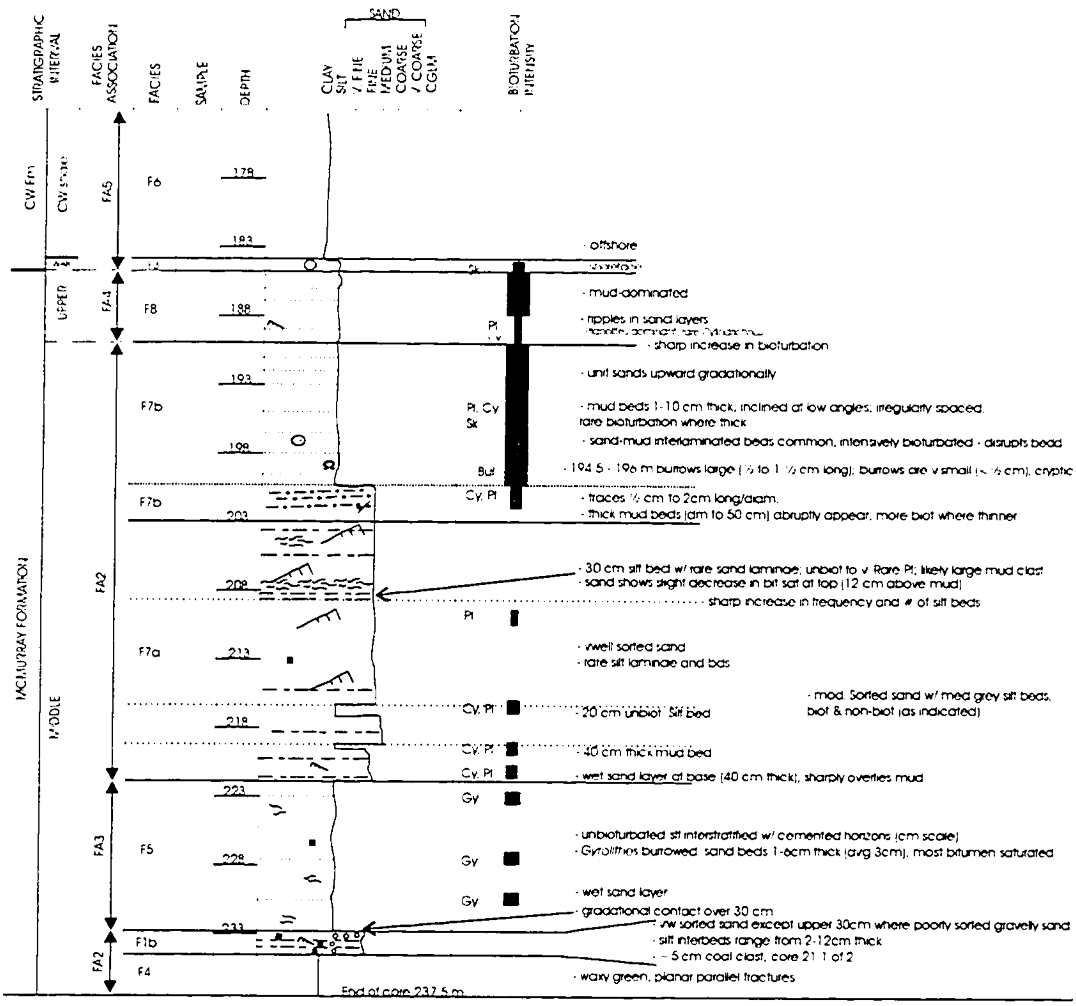

Well Name: PC Lewis
Location: 15-29-91-7W4
KB: 471.6m
Cored Interval: 143.5-199.7m
Logged by: Erin Crerar, University of Ottawa

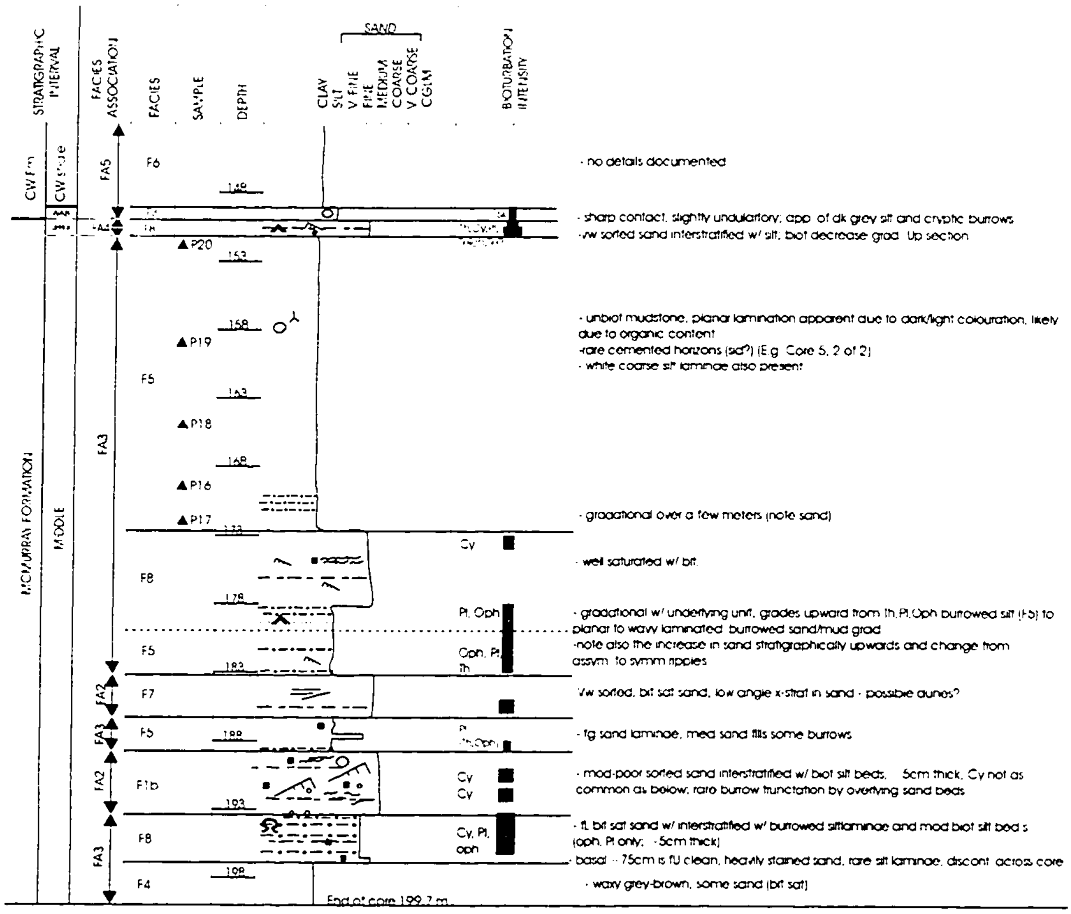

Well Name: PCI Lewis
Location: 09-28-91-7W4
KB: 470.9m
Cored Interval: 138.9-235.2m
Logged by: Erin Crerar, University of Ottawa

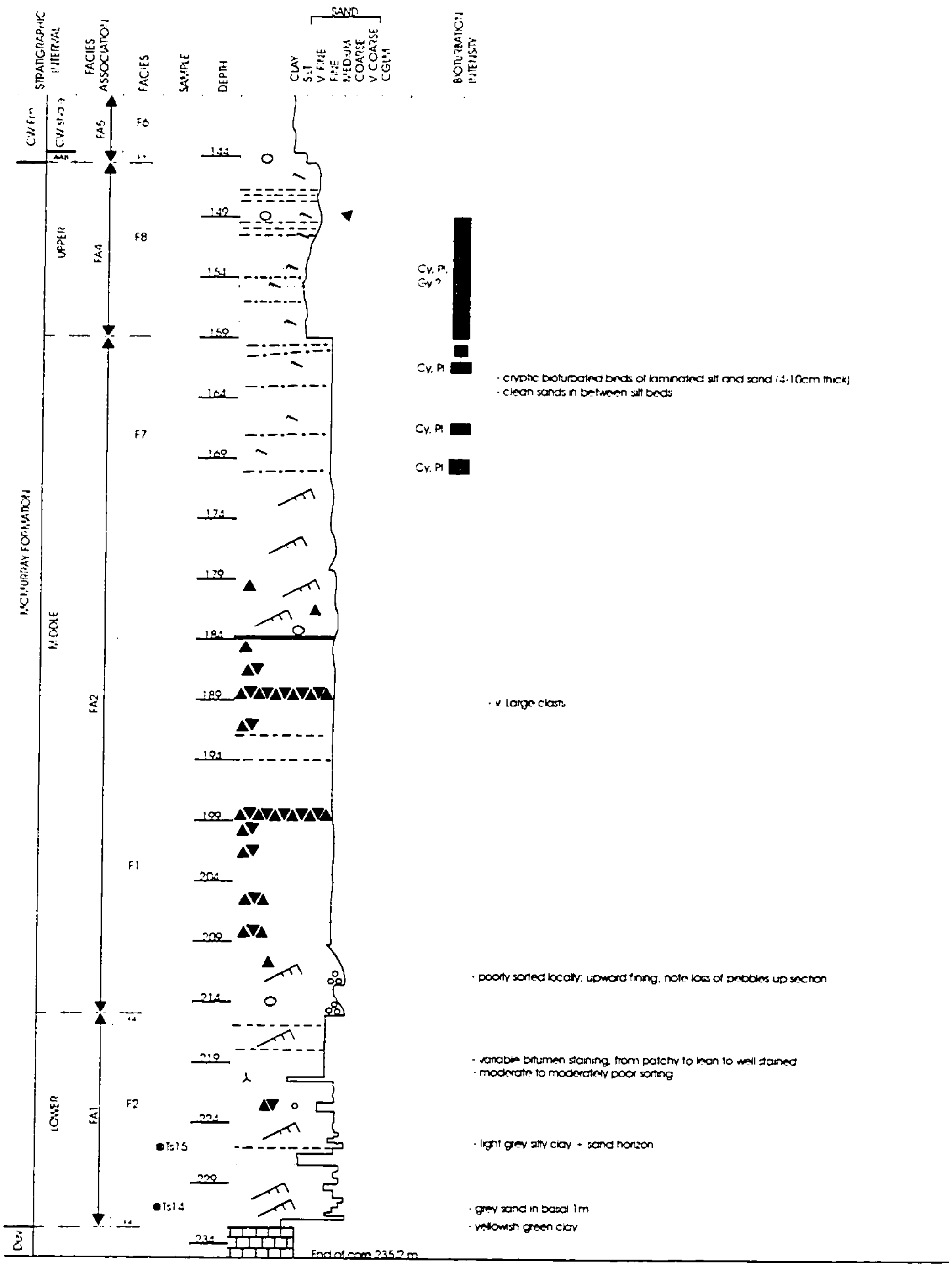

Well Name: Roland et al Lewis
Location: 01-12-91-8W4
KB: 451.8m
Cored Interval: 125.7-206.4m
Logged by: Erin Crerar, University of Ottawa

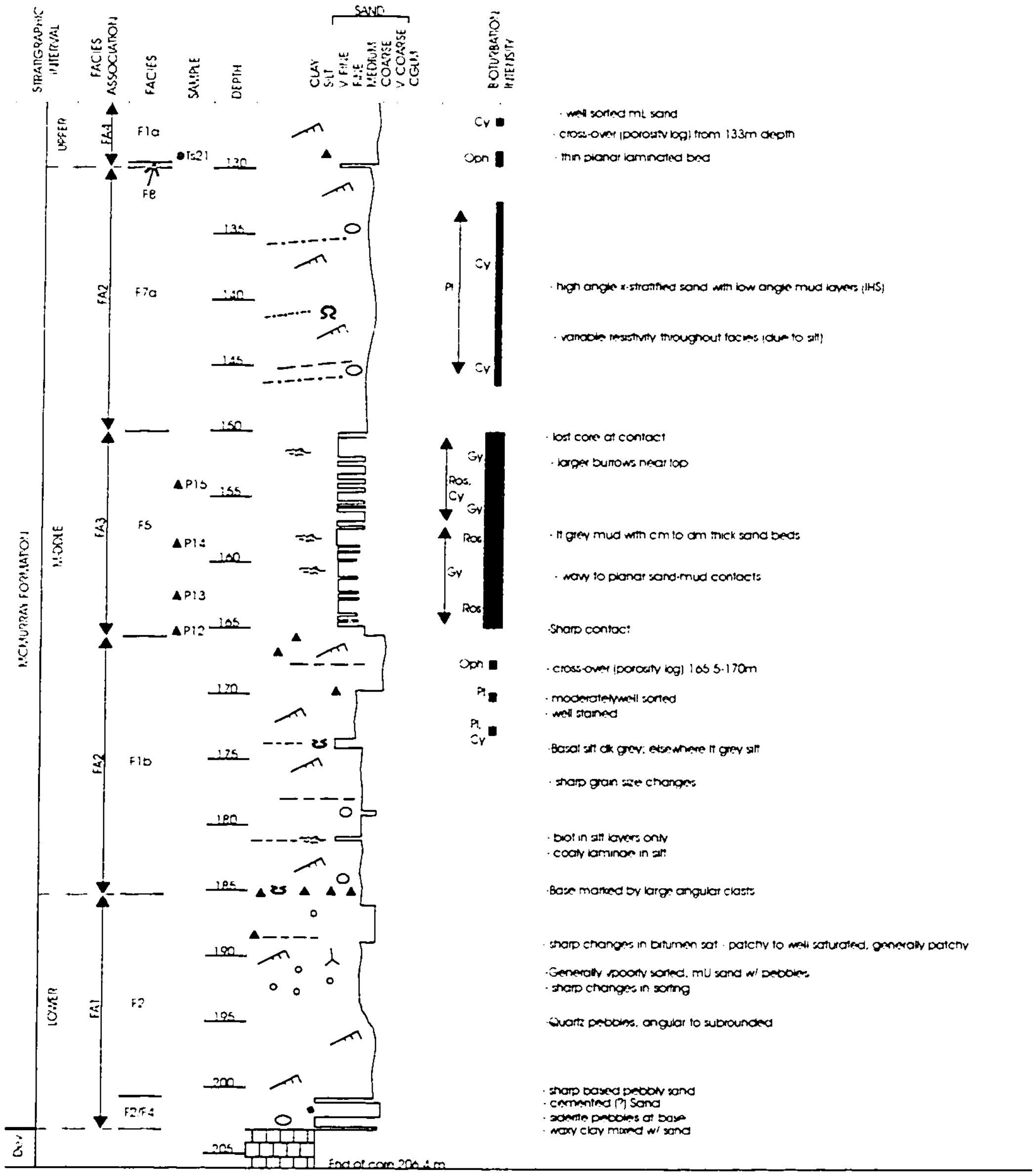

Well Name: Roland et al Lewis
Location: 10-26-91-8W4
KB: 457.6m
Cored Interval: 132.0-205.4m
Logged by: Erin Crerar, University of Ottawa

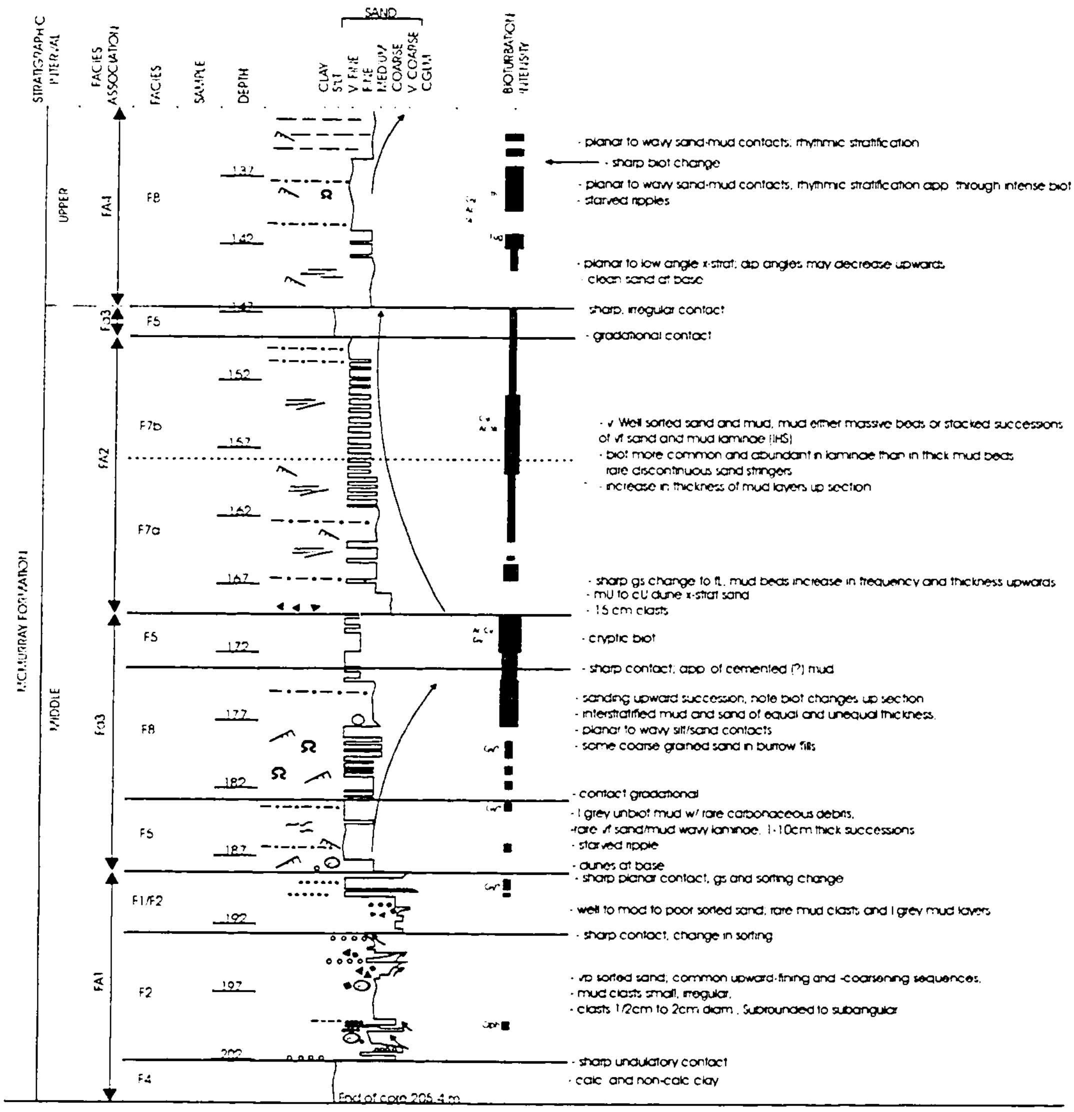

Appendix 2
Stratigraphic Cross-sections

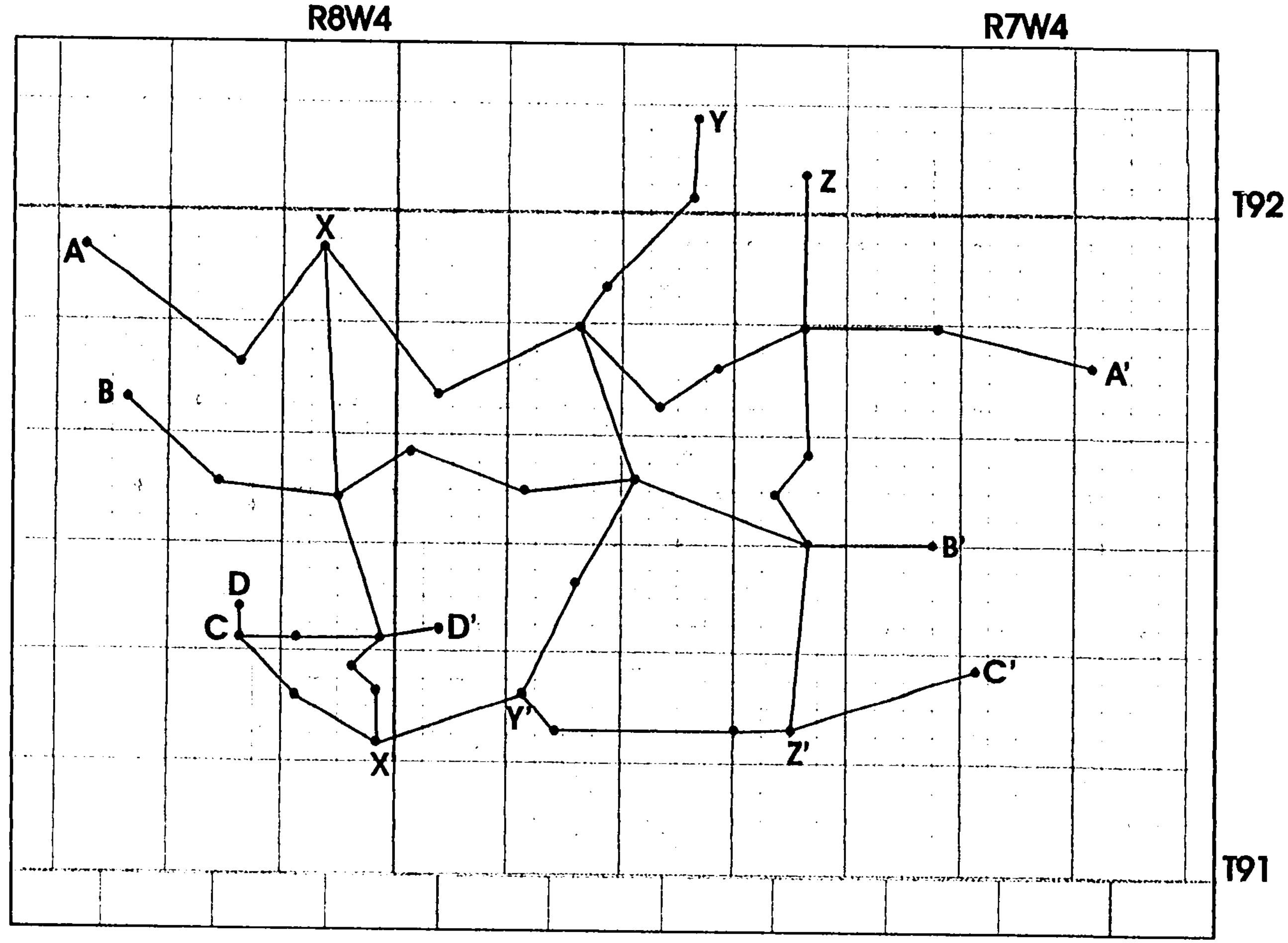

Map illustrating location of cross sections in Appendix 2

Legend for cross-sections

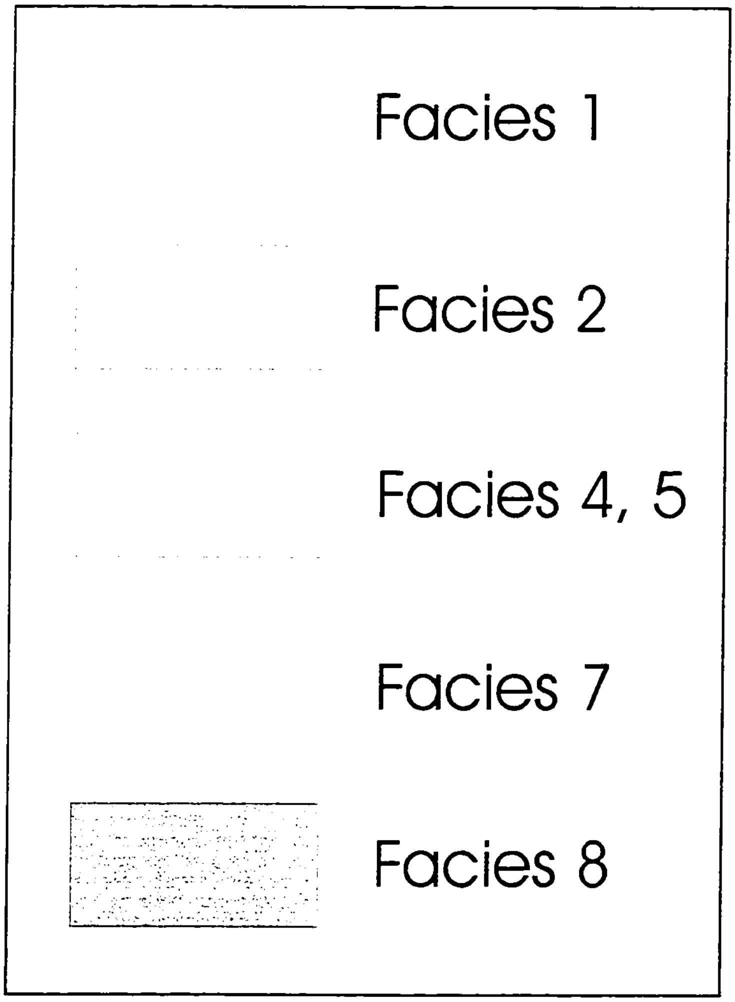

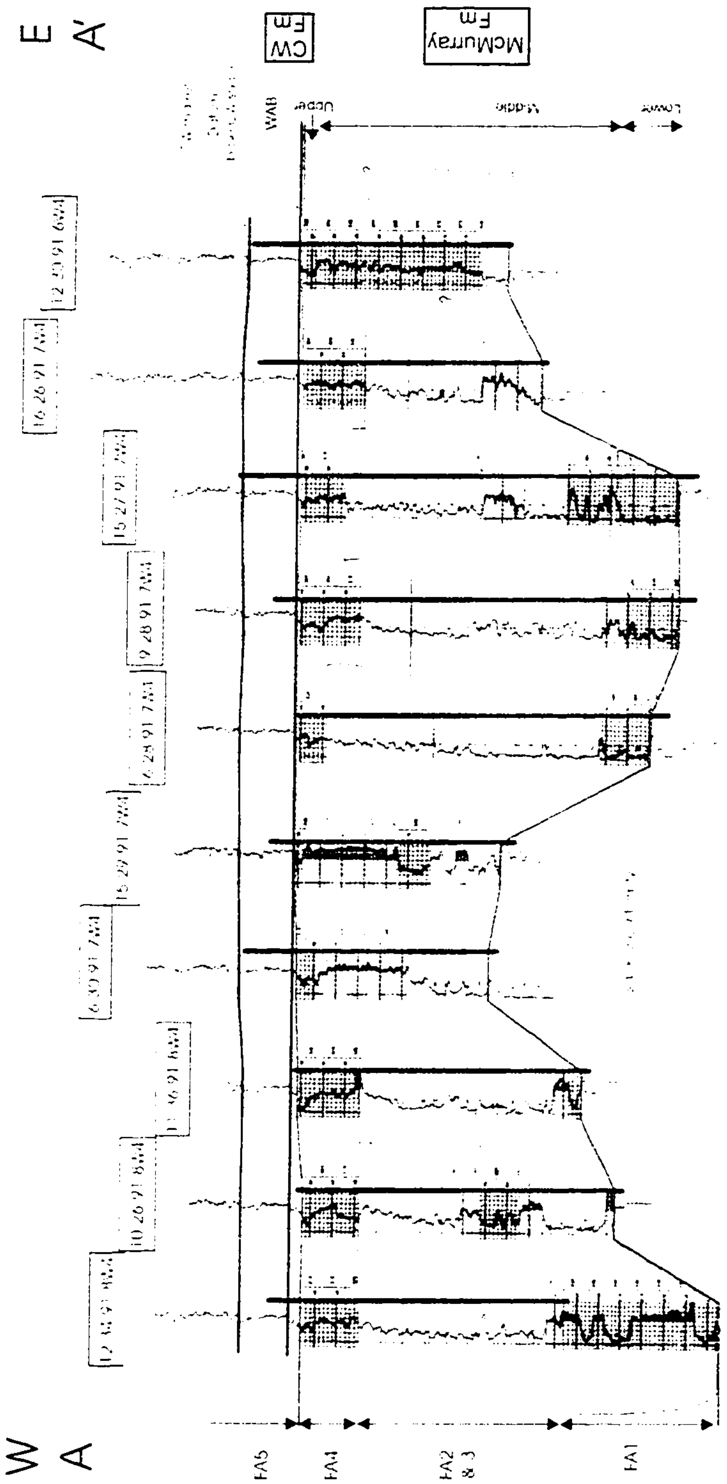
W
A
E
A'
CW Fm
McMurray Fm
WAB
Upper
Middle
Lower
FA5
FA4
FA2 & 3
FA1

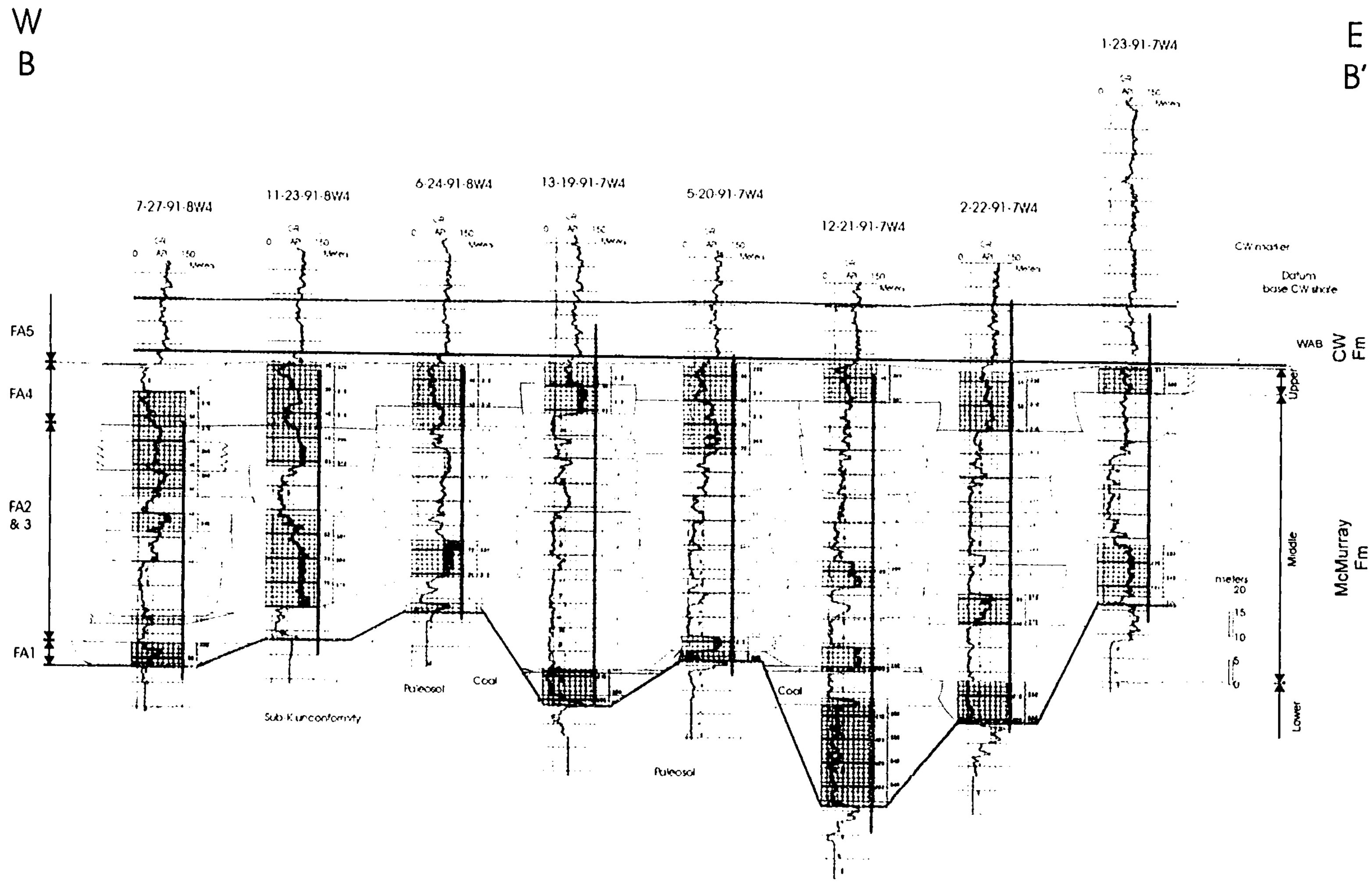
W
B
E
B'
7-27-91-8W4
11-23-91-8W4
6-24-91-8W4
13-19-91-7W4
5-20-91-7W4
12-21-91-7W4
2-22-91-7W4
1-23-91-7W4
CW marker
Datum
base CW shale
WAB
CW
Fm
McMurray
Fm
Upper
Middle
Lower
FA5
FA4
FA2
& 3
FA1
meters
20
15
10
5
0
Paleosol
Coal
Sub-K unconformity

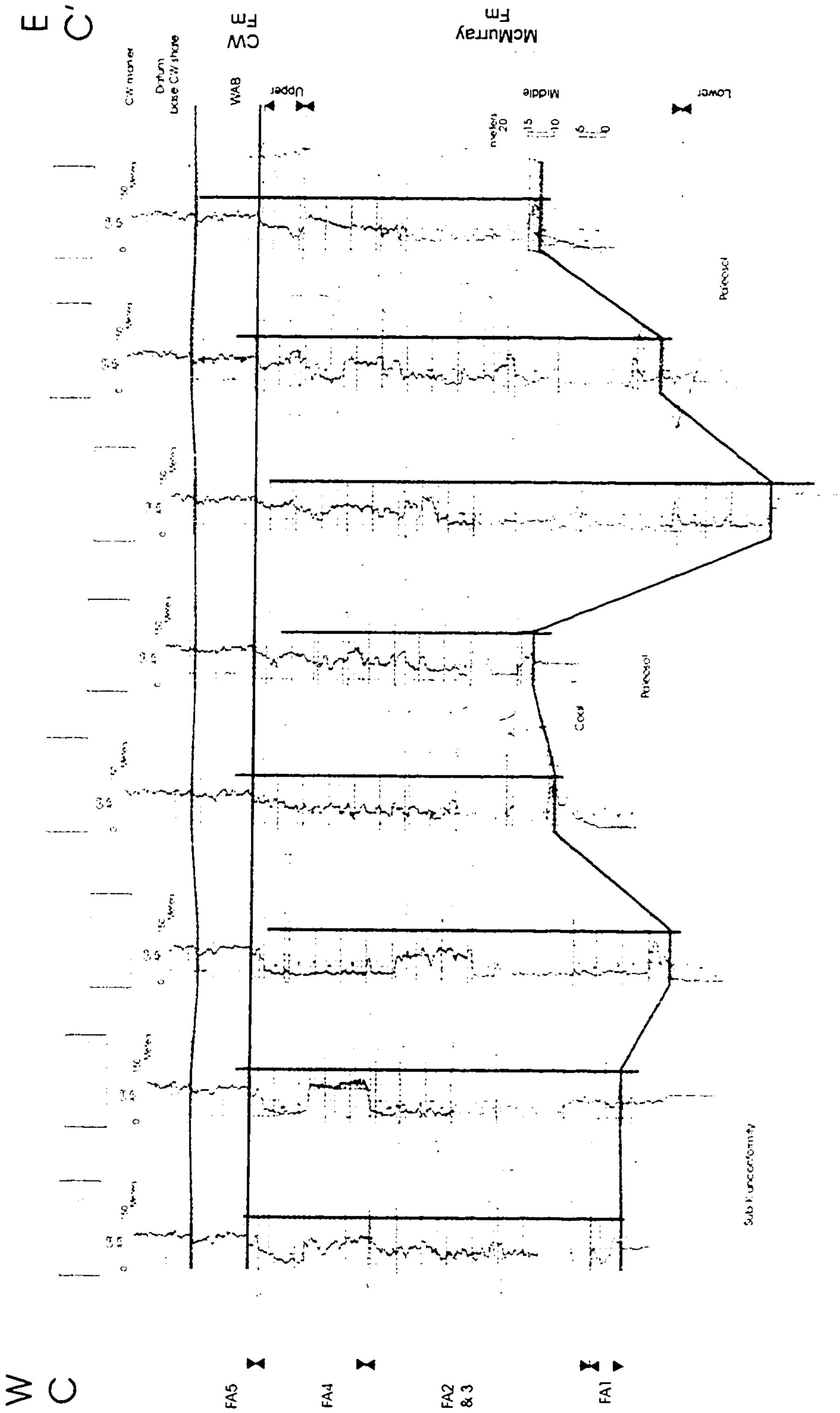
W
C
E
C'
CW Fm
McMurray Fm
WAB
Upper
Middle
Lower
Paleosol
Coal
FA5
FA4
FA2 & 3
FA1

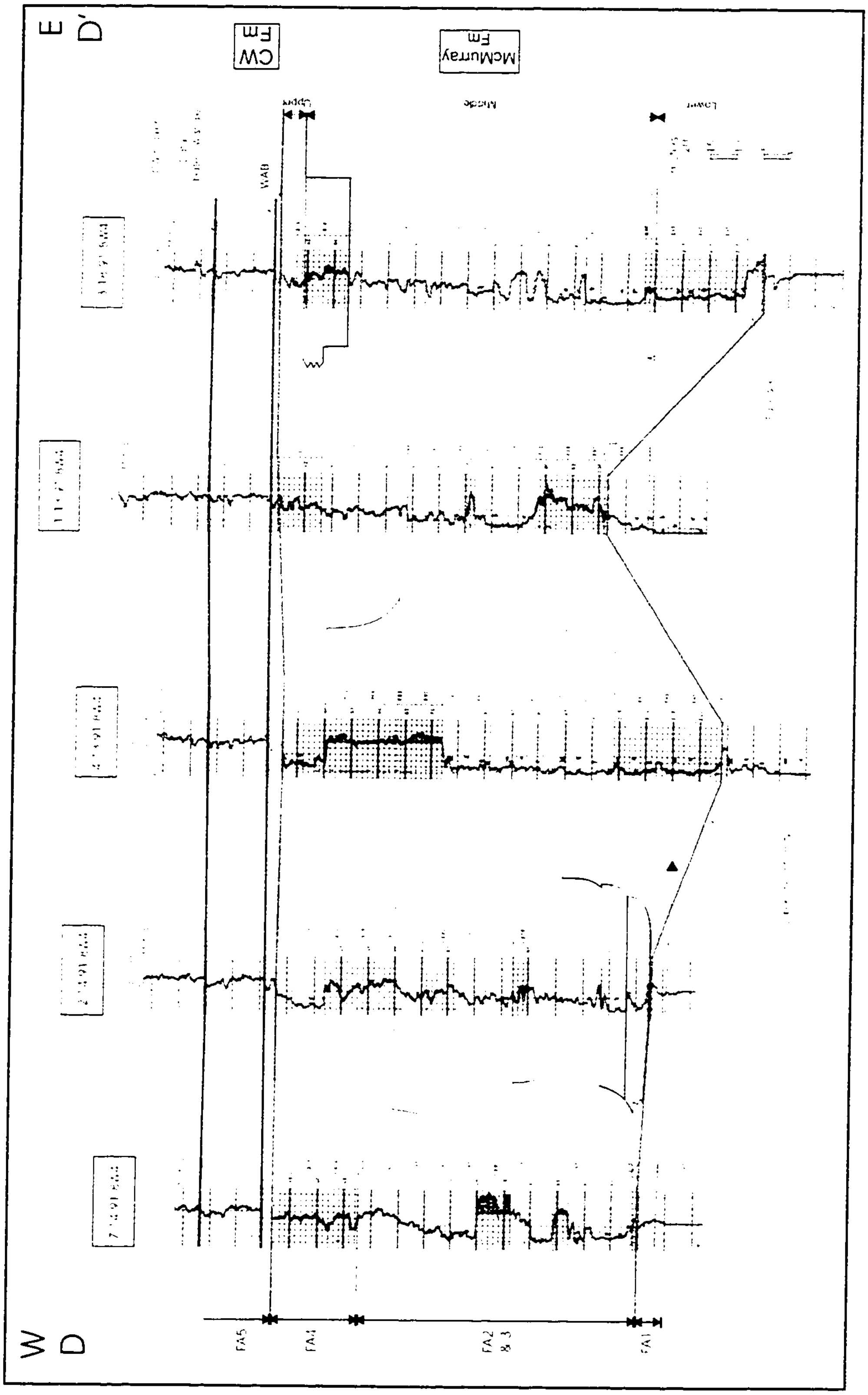
W
D
E
D'
CW
Fm
McMurray
Fm
WAB
Upper
Middle
Lower
FA5
FA4
FA2
& 3
FA1

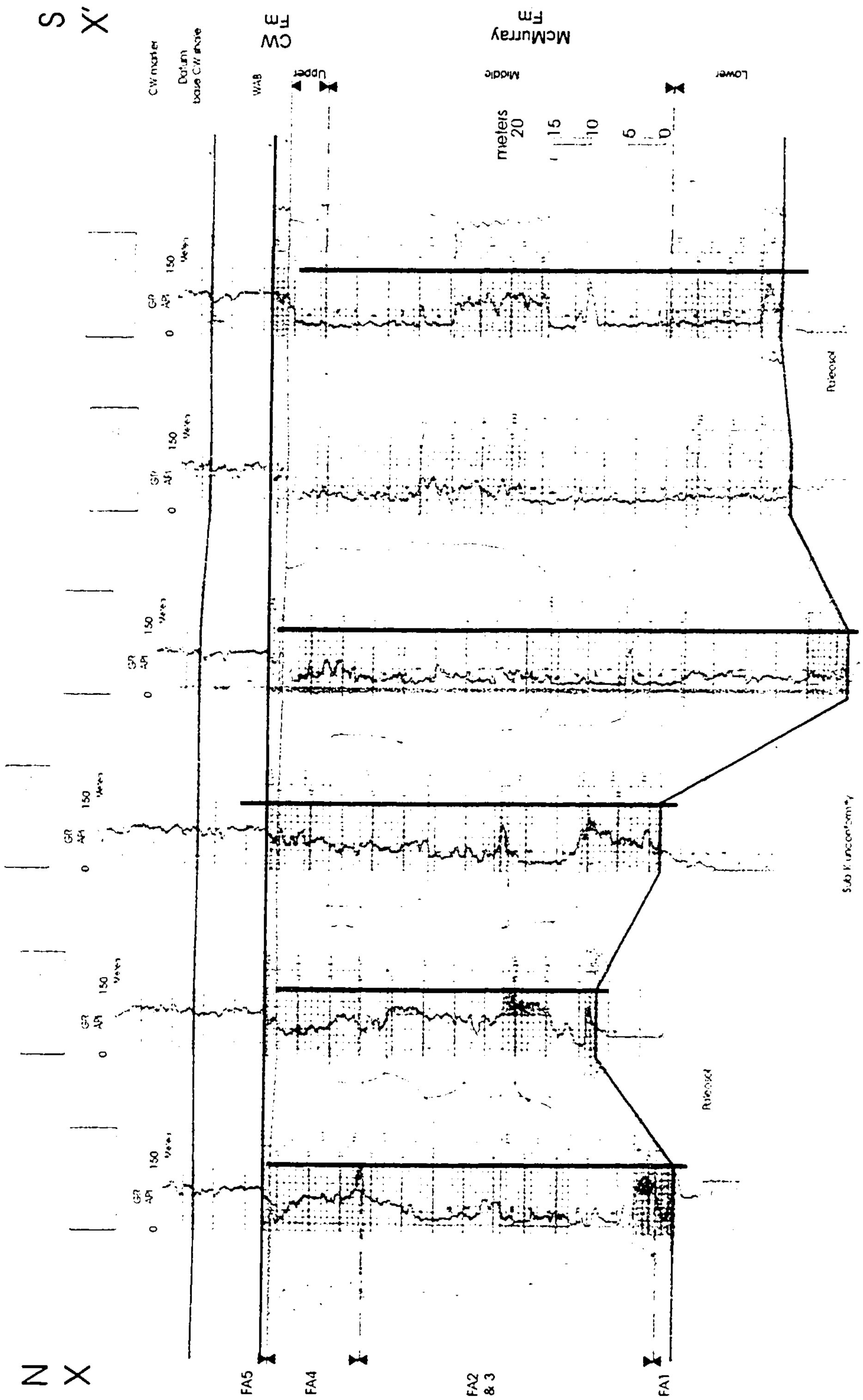
S
X'
N
X
CW
Fm
McMurray
Fm
Upper
Middle
Lower
meters
20
15
10
5
0
FA5
FA4
FA2
& 3
FA1

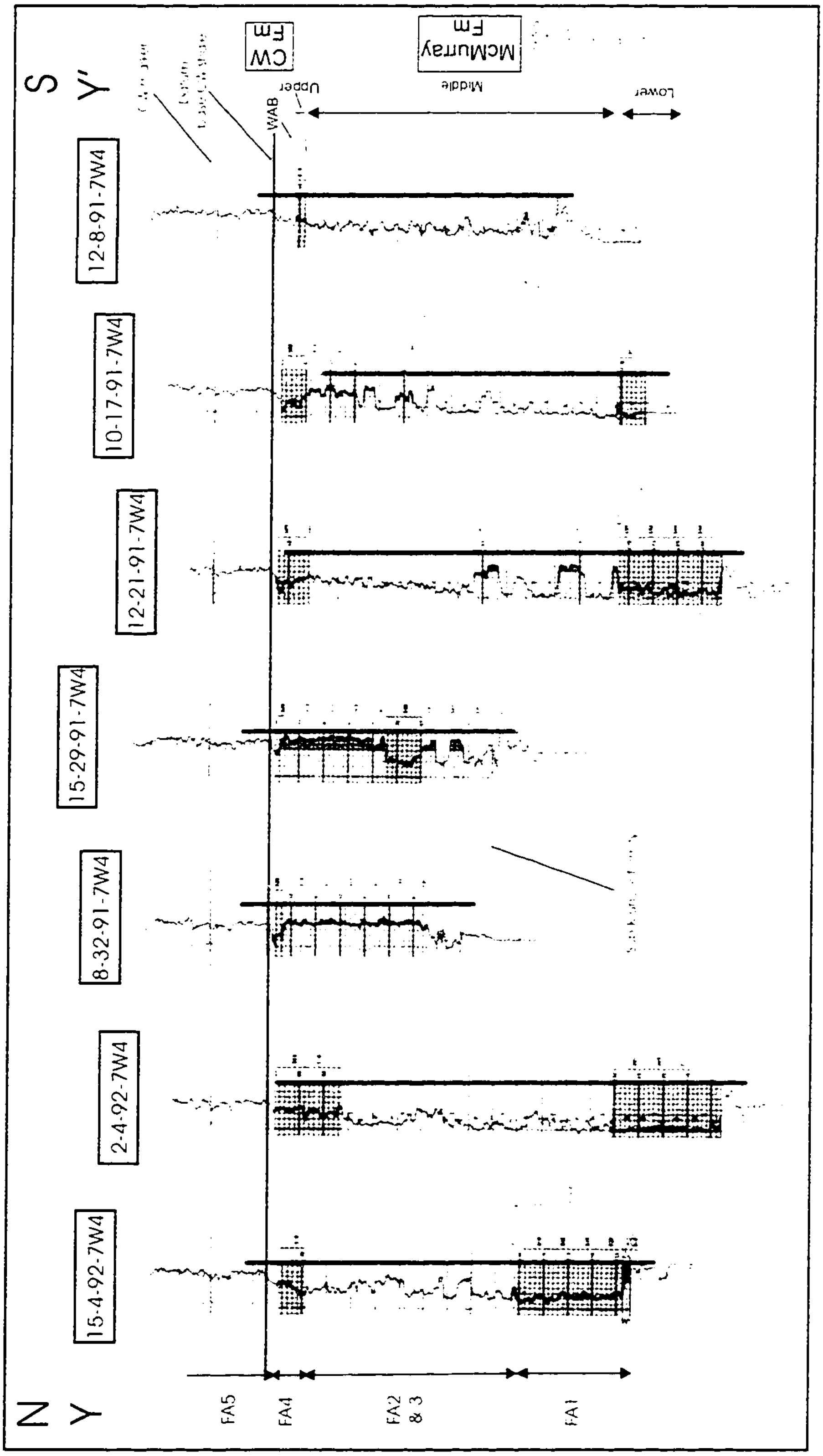
S
Y'
CW Fm
McMurray Fm
WAB
Upper
Middle
Lower
12-8-91-7W4
10-17-91-7W4
12-21-91-7W4
15-29-91-7W4
8-32-91-7W4
2-4-92-7W4
15-4-92-7W4
N
Y
FA5
FA4
FA2 & 3
FA1

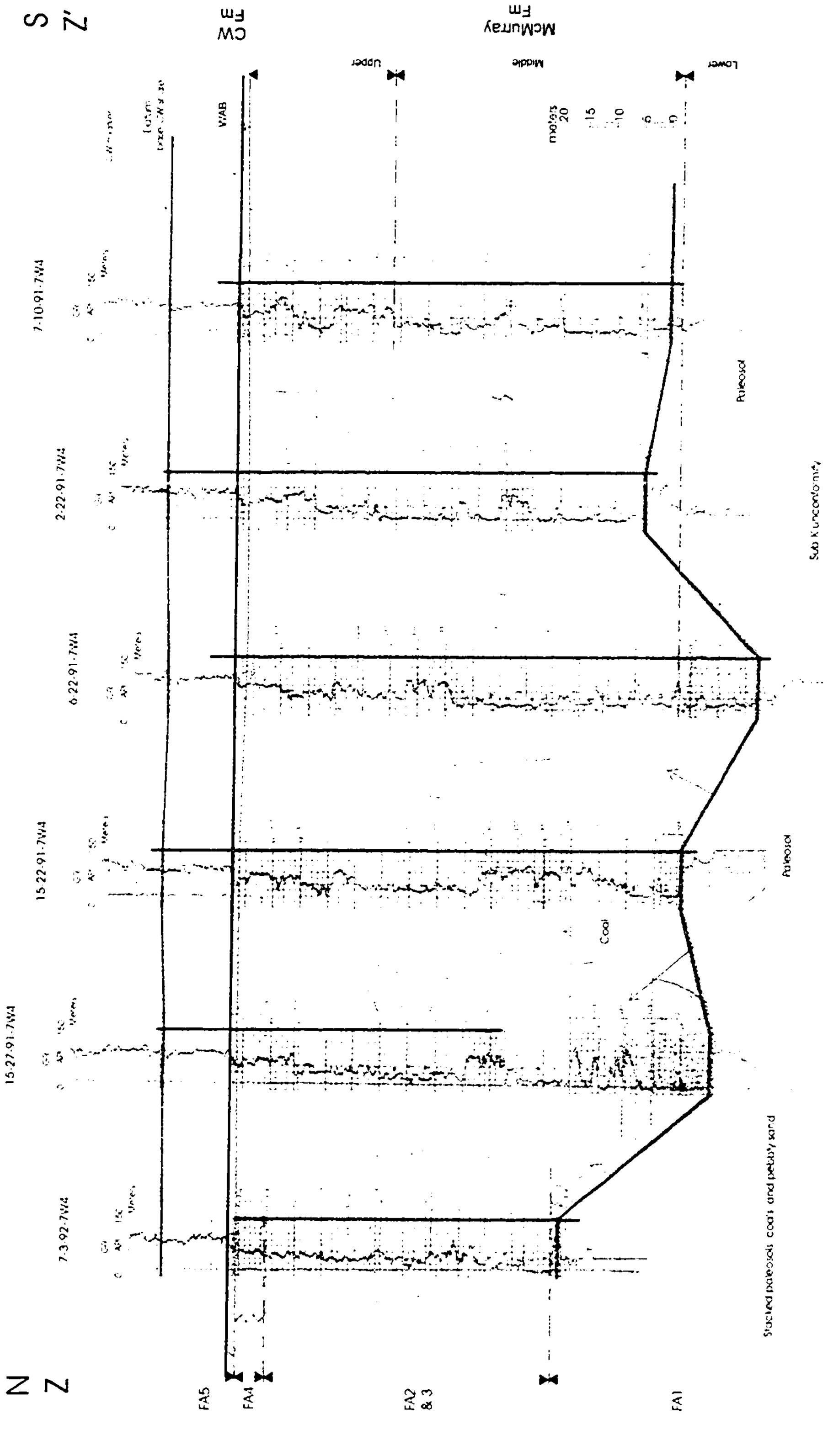

N
Z
S
Z'
CW Fm
McMurray Fm
Upper
Middle
Lower
WAB
FA5
FA4
FA2 & 3
FA1
7-3-92-7W4
15-27-91-7W4
15-22-91-7W4
6-22-91-7W4
2-22-91-7W4
7-10-91-7W4
meters
20
15
10
5
0
Paleosol
Coal
Stacked paleosols coals and pebbly sand

Appendix 3
Geological Maps

Log descriptions and methodology to determine gross sand and net pay cut-off values:

Gross Sand:

The *gamma-ray log* measures the natural radioactivity of the strata within a well-bore, which is related mainly to the content of radiogenic isotopes (potassium, uranium, and thorium). Because these elements are common constituents of clay minerals, the gamma-ray log generally mimics the proportion of shale (high API) and non-shale (low API; typically sand/conglomerate) in the rock column. As such, the gamma-ray log is commonly used to determine *gross sand*, which is a measurement of the vertical thickness of 'sand' (as opposed to 'shale') within a stratigraphic interval as defined by gamma-ray cut-off values. A gross sand cut-off value of 80 API was determined by calibrating the gamma ray log signature to core (Fig. A3-1). First, a high API spike in the gamma ray log present in the Clearwater Shale was selected to represent the shale base line. This horizon was selected because it occurs at a consistent stratigraphic level throughout the study area and because of a consistent API value in each of the well logs. A sand line was then determined by comparing the gamma ray log signatures with core data in order to determine the lowest possible API value that still represents shale, which was determined to be 80 API. Gross sand, therefore, represents all other strata with API value <80.

Net Pay:

The *density log* is used to estimate the porosity of the rock. The density tool measures the electron density of the rock, which is related to the density of the solid material and the amount and density of the pore fluids. When used in combination with other logs, this log can be useful to distinguish between 'tight' and porous sand in clastic reservoirs. The *resistivity log* measures the resistance of fluids to the flow of an electric current. This is log is used to evaluate the type of fluid within a formation and can indicate the presence of water (low resistivity) or oil (high resistivity).

Net-pay represents the vertical thickness of hydrocarbons within a stratigraphic succession. A net pay cut-off value of 30 ohm-m was determined from the resistivity log (deep induction). Note that net-pay values must also comply with the above-mentioned gross sand cut-off and also the *net sand* cut-off which is determined from a core-measured porosity of 27% (see Figs. 2.42, 2.43).

Dipmeter Logs:

Dipmeter logs are used to determine the orientation and magnitude of dipping surfaces (e.g. IHS, dunes). This log is commonly used in combination with the resistivity log and is constructed by mounting several electrodes on separate arms at different elevations. The orientation of these electrodes is continuously recorded, and so when a dipping bed is encountered, each electrode responds to the lithological change at different elevations.This data is then used to calculate the direction and magnitude of the dip of the beds.

(Reference: see Cant 1992)

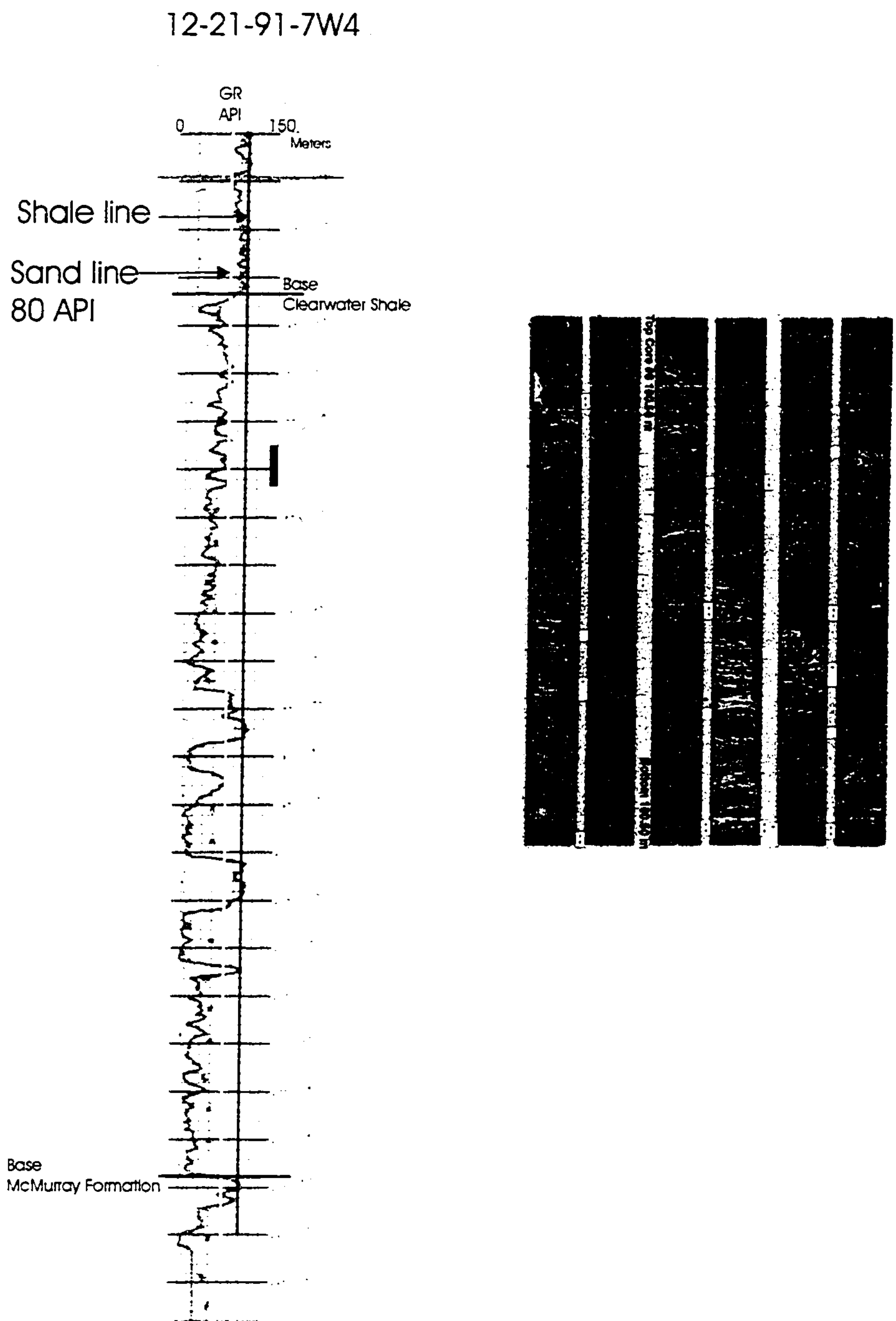

Figure A3-1: Gamma ray and core photograph illustrating gross sand cut-off values. Core boxes are 75 cm long.

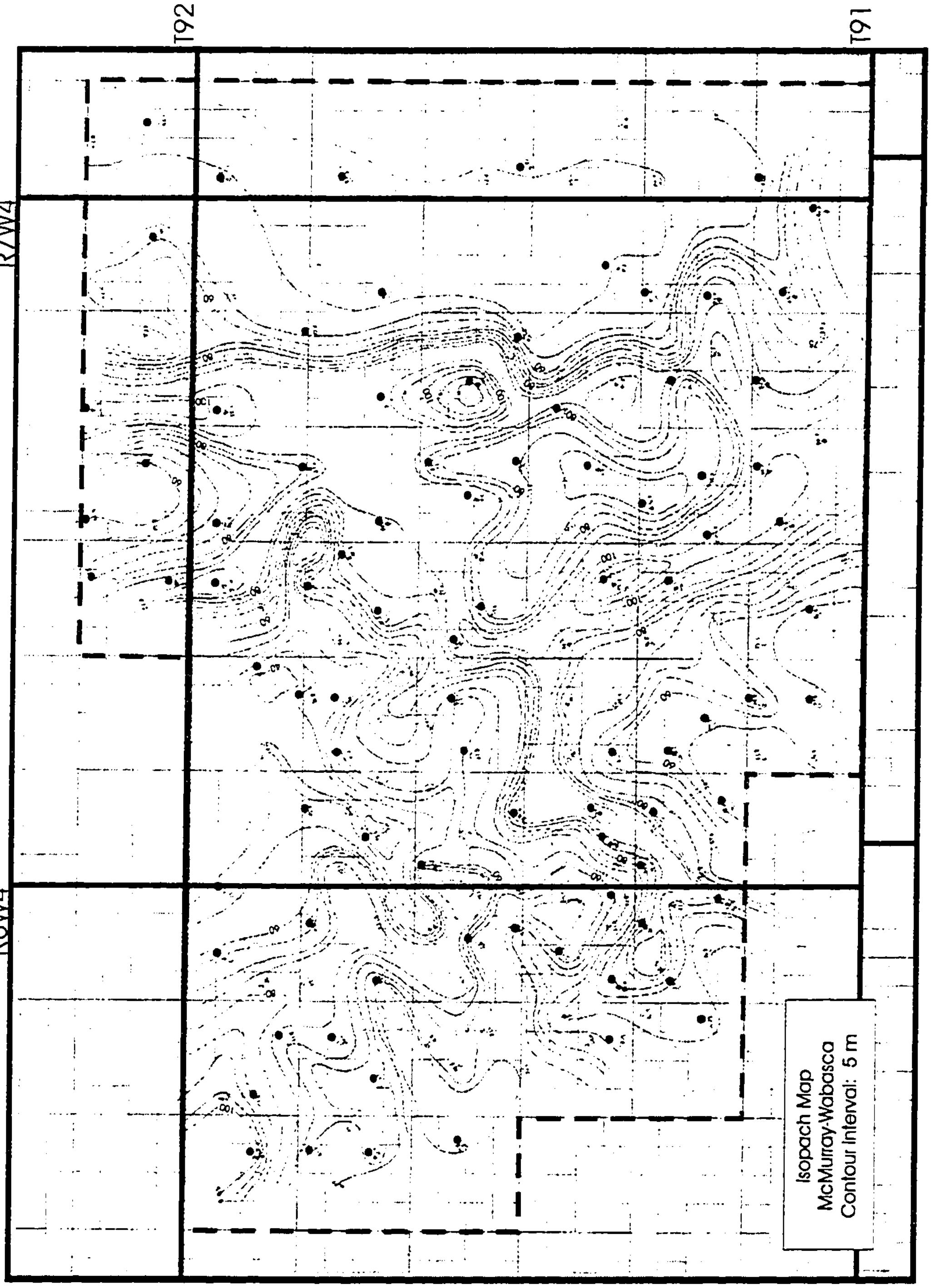
T92
T91
R7W4
R8W4
Isopach Map
McMurray-Wabasca
Contour Interval: 5 m

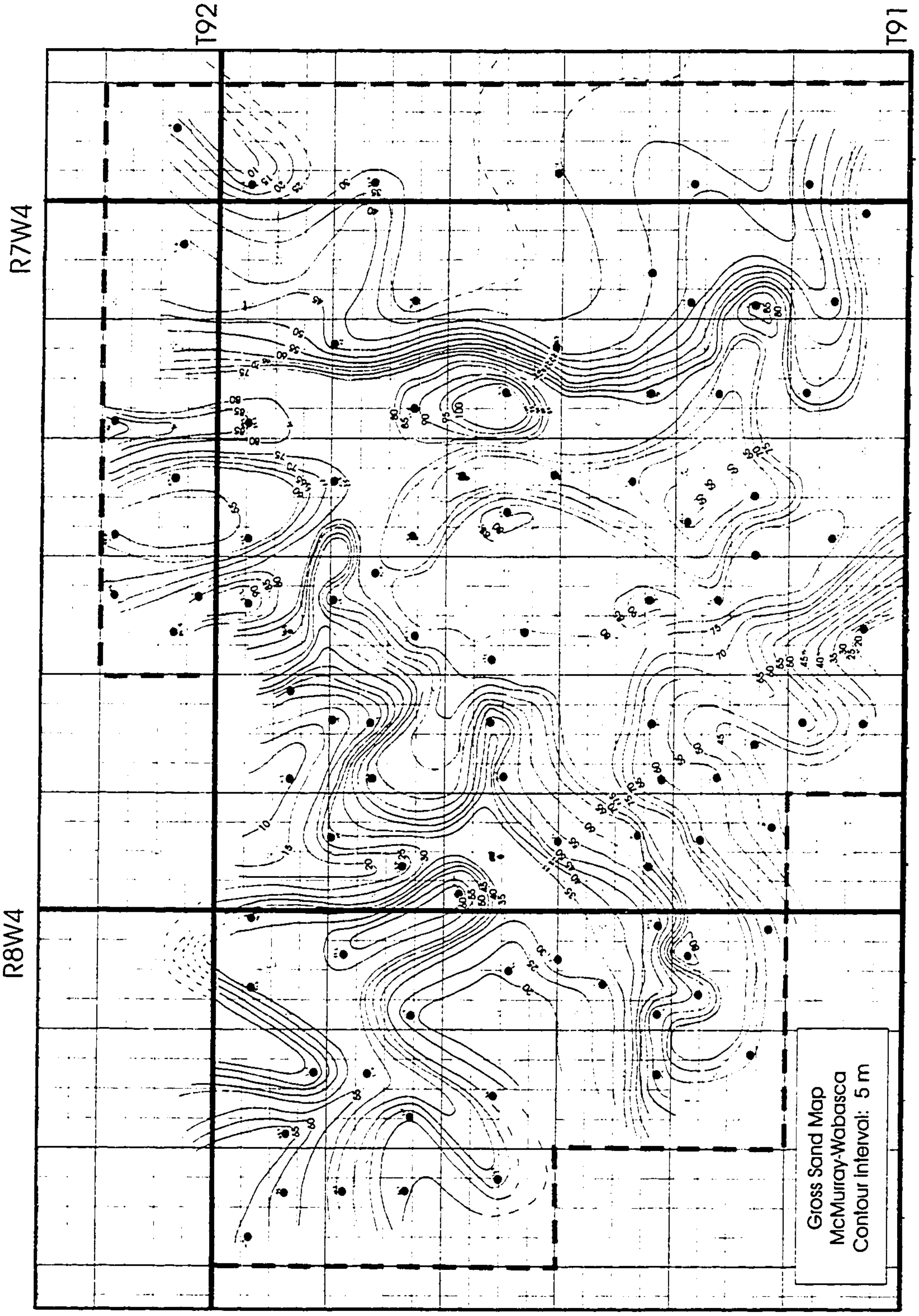
T92
T91
R7W4
R8W4
Gross Sand Map
McMurray-Wabasca
Contour Interval: 5 m

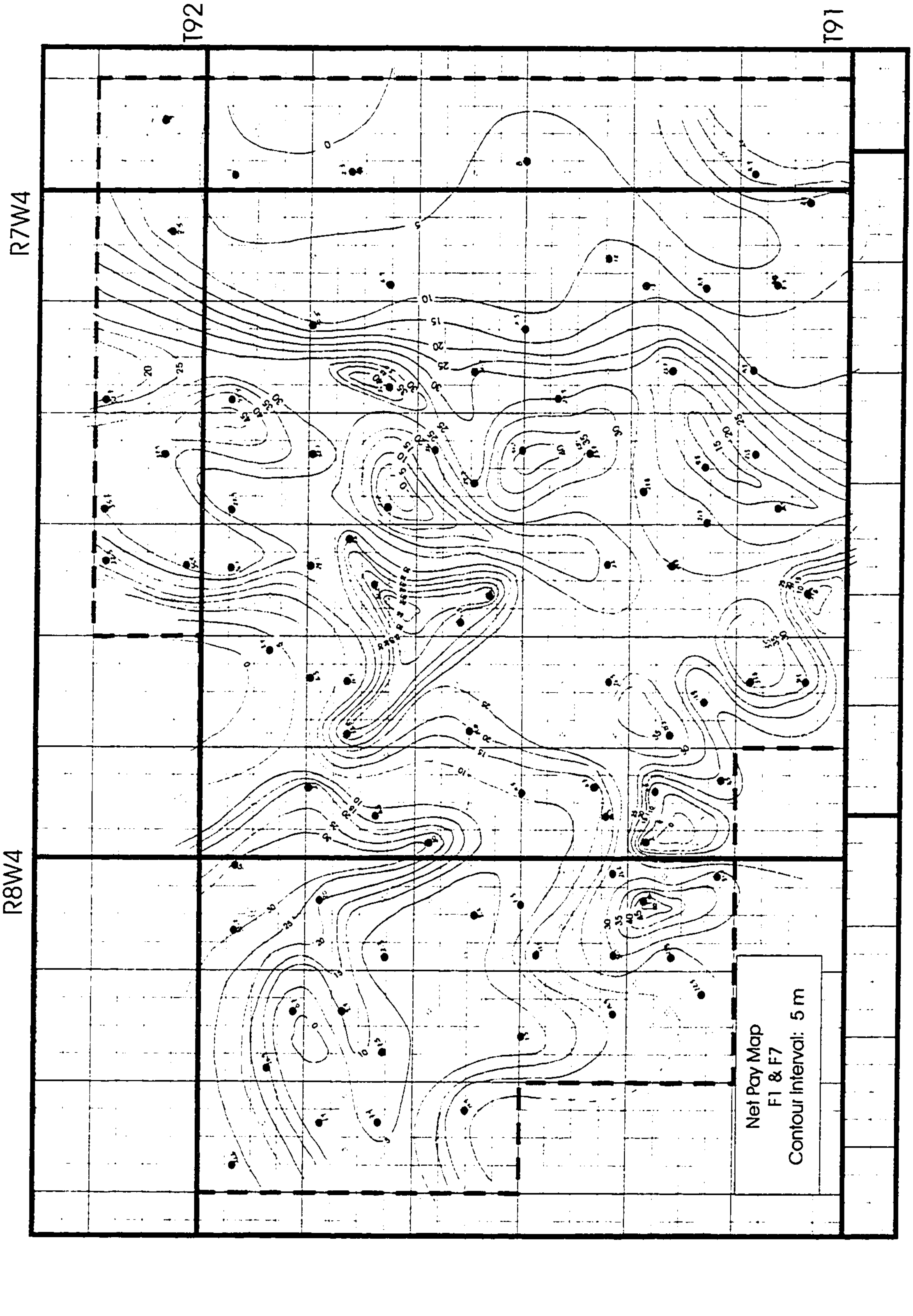
R7W4
R8W4
T92
T91
Net Pay Map
F1 & F7
Contour Interval: 5 m

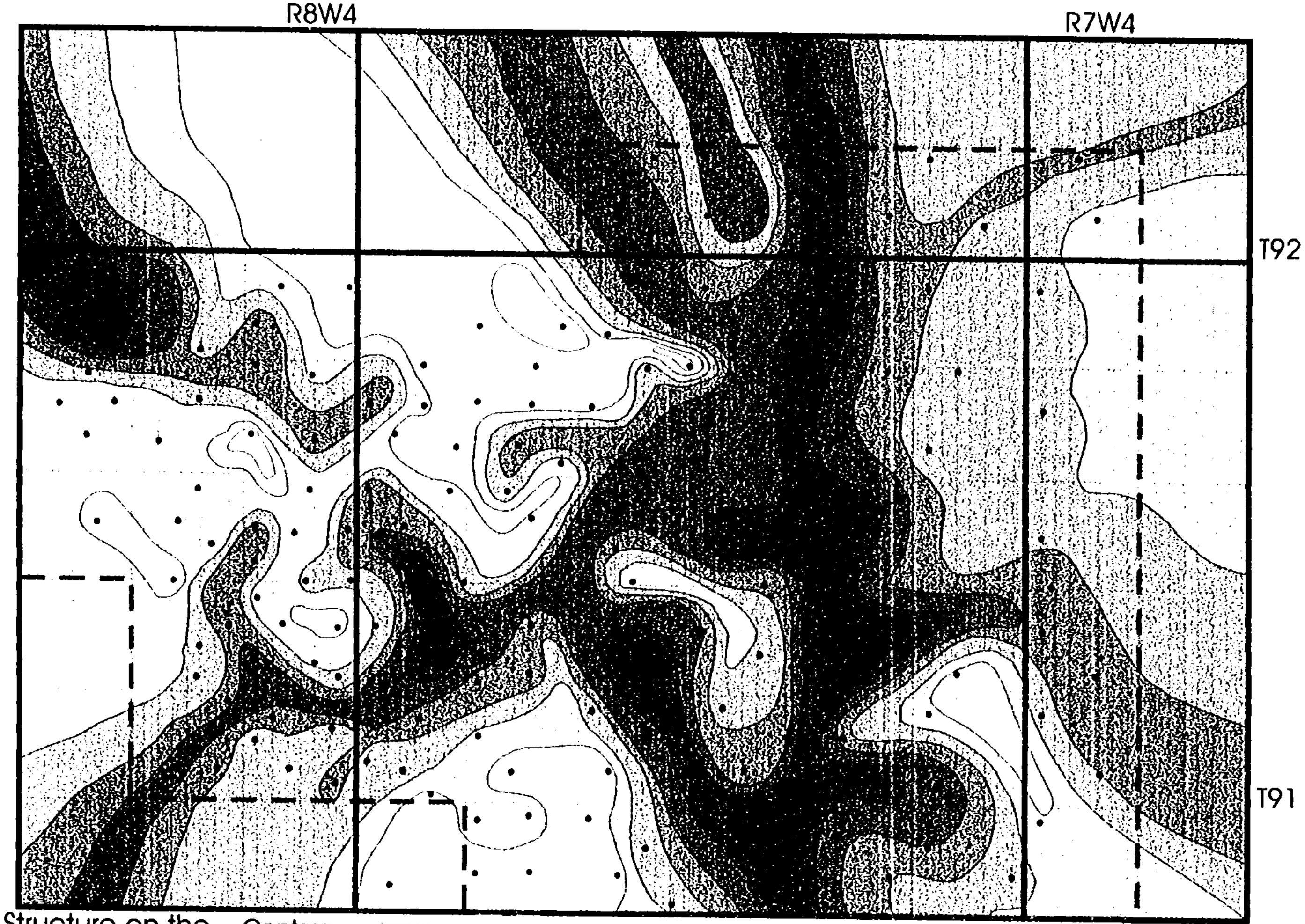

Structure on the sub-Cretaceous unconformity

Contour interval: 5 m

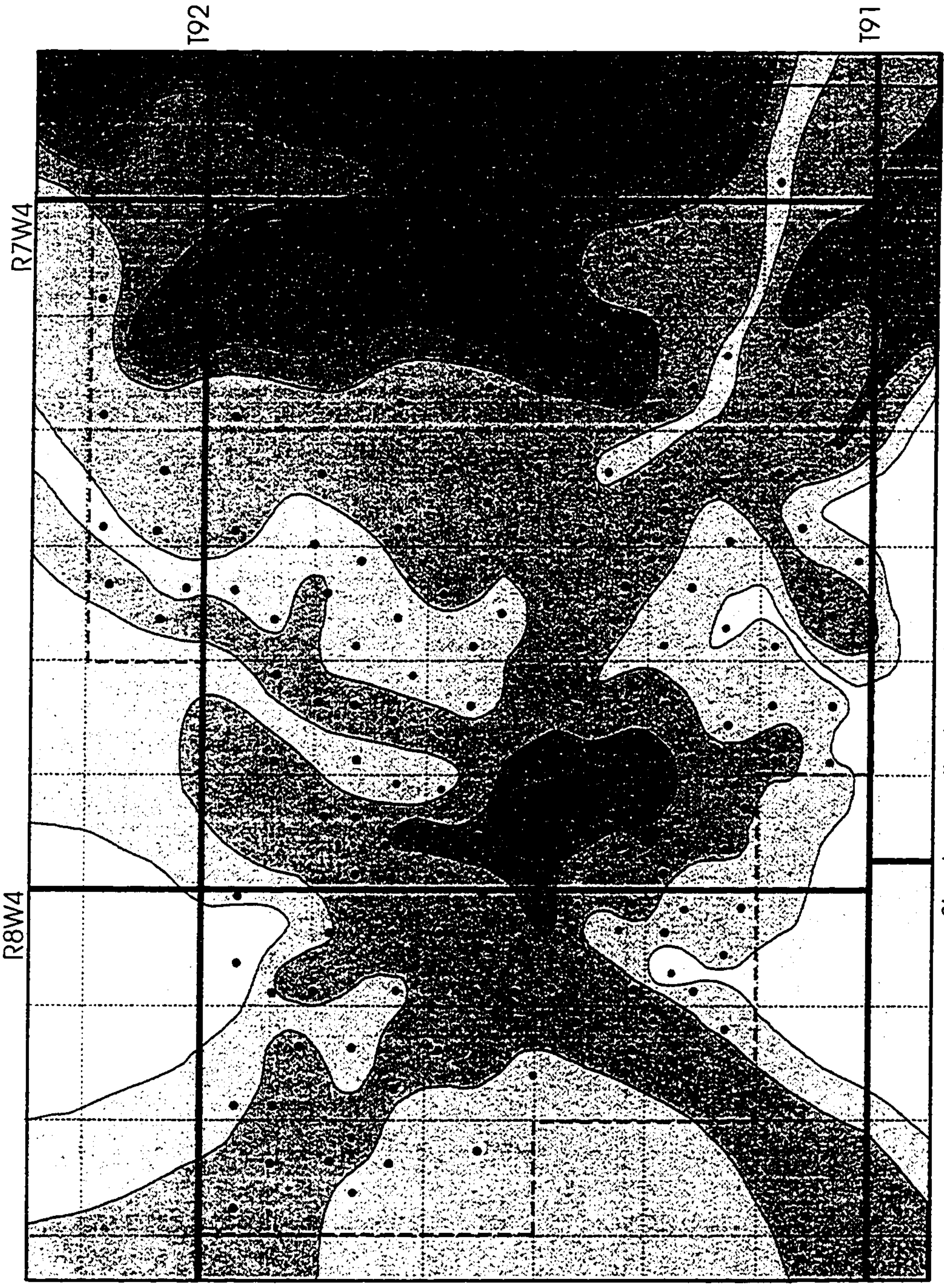

Structure on the base of the Clearwater Shale

Appendix 4
Palynological Report

PALEONTOLOGICAL REPORT
RAPPORT DE PALÉONTOLOGIE

02-ARS-2002

Applied research report on 15 samples of Early Cretaceous age from the McMurray Formation of northeastern Alberta (NTS74D/14) as requested by Erin Crerar and Bill Arnott (University of Ottawa, Department of Earth Science, 140 Louis Pasteur, Ottawa, Ontario, K1N 6N5).

A.R. SWEET

Natural Resources Canada
Ressources naturelle Canada

Applied research report on 15 samples of Early Cretaceous age from the McMurray Formation of northeastern Alberta (NTS74D/14) as requested by Erin Crerar and Bill Arnott (University of Ottawa, Department of Earth Science, 140 Louis Pasteur, Ottawa, Ontario, K1N 6N5).

The relevant parts of any manuscript prepared for publication that paraphrase or quote from this report should be referred to the Paleontology Subdivision, Calgary for possible revision.

The primary purpose of this report is to determine the depositional environment of the sampled rock units.

Although presented as being precise, UTM locality coordinates are approximate as they were obtained from the conversion of the legal description provided for the coreholes.

Table 1 provides relative abundances based on primary counts of between 200 and 300 specimens and qualitative occurrence records. The qualitative R (rare, 1 to 2 specimens), S (scarce, 3 to 5 specimens), C (common, 6 to 9 specimens), and A (abundant, more than 10 specimens) (plus a number in the case of dinoflagellates and some other algal spores) indicates qualitatively the number of specimens seen outside of the area of the primary count. It is estimated that the slides scanned to arrive at the qualitative estimate of relative abundance contained at least between 20 and 40 thousand specimens .

Appendix 1 provides a list of taxa from Table 1 and authorship for the formal taxa.

A. Roland et al. 11-23-91-8-W4 ; Zone 12V, UTM 489335 m E, 6307145 m N.
Sample P4625-1; P09; core 9, 150 m; C-412935.
Sample P4625-2; P10; core 8, 147 m; C-412936.
Sample P4625-3; P11; core 7, 146 m; C-412937.

Comment on dinoflagellates: The few dinoflagellates seen in these samples are broken and or folded and include at least three different taxa.

B. Roland et al. 1-12-91-8-W4 ; Zone 12V, UTM 491767 m E, 6303096 m N.
Sample P4626-1; P12; core 19, 166 m; C-412938.
Sample P4626-2; P13; core 17, 162.9 m; C-412939.
Sample P4626-3; P14; core 16, 158.1 m; C-412940.
Sample P4626-4; P15; core 14, 154 m; C-412941.

Comment on dinoflagellates: The few dinoflagellates seen in these samples are broken and or folded and include up to five different taxa.

C. Roland et al. 15-29-91-7-W4 ; Zone 12V, UTM 494641 m E, 6309166 m N.
Sample P4627-1; P16; core 13, 169.5; C-412942.
Sample P4627-2; P17; core 19, 172 m; C-412943.

Sample P4627-3; P18; core 11, 165 m; C-412944.
Sample P4627-4; P19; core 08, 159 m; C-412945.
Sample P4627-5; P20; core 05, 151.75 m; C-412946.
Comment on dinoflagellates: The dinoflagellates in the 5 samples from this core hole are common to abundant. Most specimens can be assigned to either *Canningia* or *Pseudoceratium peliferum* (in a ratio of about 6 *Canningia* to each *Pseudoceratium*) with one specimen of *Oligoshaeridium*? sp. observed and a few unidentifiable specimens. There are no complete specimens.

D. PC Lewis 5-20-91-7-W4 ; Zone 12V, UTM 493831 m E, 6306733 m N.
Sample P4628-1; P21; core 9, 174.9 m; C-412947.
Sample P4628-2; P22; core 6, 171.6 m; C-412948.
Sample P4628-3; P23; core 5, 166.1 m; C-412949.
Comment on dinoflagellates: One specimen of *Canningia* was seen in the sample from 174.9 m, the other two reported specimens were not identifiable. The few dinoflagellates seen in these samples were broken and or folded.

GENERAL COMMENTS

Preservation and Recovery

The preservation and recovery from all of samples was good to excellent. The residues were dominated by palynomorphs with accessory amounts of terrestrial plant, woody and cuticular debris.

Age

The age of the samples falls within the range of Barremian to lower Albian based on the occurrence of monocolpate angiosperm pollen, the absence of more advanced tricolpate angiosperm pollen and the listed fern spores. The occurrences (albeit rare) of the monocolpate angiosperm and *Triporoletes simplex* (herein included under *Zilvisporis* spp.) ally the assemblages of this report to the *Retimonocolpites crassatus- Retimonolcolpites peroreticulatus* (CP) Assemblage -zone described from the middle and upper McMurray Formation by Burden and Hills (1984), to whom the reader is referred for more detailed age discussions.

Environment of deposition

First the more general observations. The recovered assemblages are overwhelmingly dominated by terrestrial, wind-distributed gymnosperm pollen. This indicates the area of sediment accumulation was either forested or adjacent to a forested area. The ferns are mostly under story plants, and abundant ferns are usually associated with swamp and swamp margin habitats during the Mesozoic/Tertiary. In these samples, their relative abundance is comparatively low, although their diversity is relatively high. This suggests a separation, albeit limited, between the site of deposition and the ferns favored habitats.

What farther refinement can be given to this generally terrestrially dominated environment of deposition? The following account provides as detailed rationalization of the environmental significance of the recovered palynomorphs in as much detail as seems reasonable.

The operating assumptions behind the following interpretations are that the plants reported in Table 1 can be ranked in a general way according to their preferred habitats. The following list is ordered starting with the taxa with no direct association with shore environments or marine conditions through to those with a preference for marine waters.

Miospores produced by parent plants favoring terrestrial habitats independent from marine influences are considered to include:

T/C/T and bisaccate pollen, spores of the ferns and fern allies (with the possible exception of *Gleicheniidites* as the Gleicheniaceae are associated with the open habitats and often sterile soils like what might be found in back shore areas) and angiosperm pollen.

Algae associated with fresh water:

Ovoidites parvus, Schizosporis reticulatus and *Sigmopollis psilatus.*

Pollen which has been found in association with back shore and shore environments:

Classopollis (less consistent association) and *Exesipollenites*: *Exesipollenites tumulus* is recorded relatively persistently in the Ellerslie Member of the McMurray Formation (Singh 1963, Tables2 and 3) and in the overlying Wabiskaw Member of the Clearwater Formation where it occurs in association with dinoflagellates. Dr. E. Burden (pers. comm. February 26, 2002) also found *Exesipollenites tumulus* to be relatively abundant immediately prior and in association with the occurrence of dinoflagellates in the upper McMurray Formation.

Algae whose occurrences are generally associated with near shore possibly brackish to marine conditions (personal experience and literature based examples):

Januasporites spiniferus and to a greater extent *Lecaniella foveata.*

Algae (dinoflagellates) generally reported from fully marine settings.

Canningia, *Pseudoceratium* and others.

The interpretations given below assume that the salinity of the depositional environment was tied to marine versus mon-marine influences (not from salt solution of Paleozoics etc.).

a) The samples from **Roland et al. 15-29-91-7-W4** yielded the best evidence for raised salinity as they contained common to abundant dinoflagellates, most being assignable to only two taxa. As these taxa occur in similar numbers and ratios of abundance over an interval of 17.75 m one is led to conclude they lived at the site of deposition rather than being transported into the site by storm surges or tides. The fact that the diversity of the dinoflagellate assemblage is very low, a stressed. relative to the requirements of dinoflagellates i.e likely lower than normal marine salinity, environment is indicated. This is certainly compatible with the presence of *Pseudoceratium*, which is allied to a group of dinoflagellates with fresh water species in the Recent, and the associated comparatively high numbers of *Classopollis*, *Exesipollenites* and *Gleicheniidites*. For this core hole a lagoon or some such setting is indicated (requires general isolation from marine waters -otherwise a greater diversity of dinoflagellates would be anticipated - yet a level of salinity approaching sea water).

b) The samples from **Roland et al. 11-23-91-8-W4** and **Roland et al. 1-12-91-8-W4** have similar environmental signatures. Only a very low numbers of dinoflagellates are recorded from the samples from these core holes, all being distorted and or broken and appear to represent a number of species. However, the presence of *Januasporites* (somewhat more abundant in 11-23 than 1-12) and the relative abundances of the accessory taxa *Classopollis*, *Exesipollenites* and *Gleicheniidites* suggests a similar general setting, one in close proximity to shore line conditions, for the deposition of the sampled mudstones to that of 15-29. The fundamental difference is in

the character of the dinoflagellate assemblage and this may mean that the depositional setting of 11-23 and 1-12 was not amenable to supporting living dinoflagellates (i.e. fresh water conditions, no direct connection to marine waters) and that the few specimens observed were introduced into the site of deposition through ???? (wind, birds, little green men etc.).
c) Of the four core holes, the samples from **PC Lewis 5-20-91-7-W4** yielded the fewest dinoflagellates and lowest relative abundance of *Exesipollenites*, no specimens of *Januasporites* were recorded but one specimen of *Lecaniella* was found. The single dinoflagellate specimen seen in the sample from 174.9 was one of *Canningia* whose preservation was very similar to those from the 15-29 core hole raising the possibility of it being a laboratory produced contaminant. The relative abundances of *Classopollis* and *Gleicheniidites* are on the low side relative to that in the other core holes and that of T/C/T pollen was relatively high. Hence, an argument could be made for this core hole being farthest removed from a marine influence during the deposition of its sediments. Note however this is a matter of degree rather than absolutes in that the listed differences are not great enough to imply a strong disjunction between the environments of deposition, especially between core holes PC Lewis and Roland et al. 11-23 and 1-12.

In summary: The sampled mudstones were probably deposited in dominantly continental or near shore settings based on the over whelming dominance of terrestrially derived organic matter. The presence of what is probably an in situ dinoflagellate assemblage in Roland et al. 15-29 ties the depositional environment for the sampled horizons in this core hole closely with a marine influence. The overall similarity of the pollen and spore assemblages in the other three coreholes with those of Roland et al. 15-29 provides the sense of a relatively close proximity of all core holes to marine conditions with the arguments being ones of degree rather that absolutes. Of these, samples from the the PC Lewis core hole provided the weakest indication of a marine influence.

The generally good state of preservation of the miospores indicates relatively rapid burial, and limited biological recycling.

REFERENCES

Alvin. K.L. 1982. Cheirolepidiaceae: biology, structure and paleoecology. Review of Palaebotany and Palynology. v. 37, p. 71-98.

Batten. D.J. 1974. Wealden paleoecology from the distribution of palnt fossils. Proceedings of the Geologists' Association, v. 85, p. 433-458.

Burden. E.T. 1984. Terrestrial palynomorph biostratigraphy of the lower part of theMannville Group (Lower Cretaceous), Alberta and Montana. *In:* The Mesozoic of Middle North America, eds. D.F. Stott and D.J. Glass. Canadian Society of Petroleum Geologists, Memoir 9, p. 249-269.

Harris. T.M and Moody-Stuart, J.C. 1974. *Williamsoniella lignieri*; its pollen and the compression of spherical pollen gains. Palaeontology. v. 17, p. 125-148.

Muller. J. 1966. Miospores of the Pedawan and Plateau Sandstone Formations (Cretaceous-

Eocene) in Sarawak, Malaysia. Micropaleontolgy, v. 14, p. 1-37.

Singh, C, 1964. Microflora of the Lower Cretaceous Mannville Group, east-central Alberta. Research Council of Alberta, Bulletin 15, 238 pp.

Sladen, C.P. and Batten, D.J. 1984. Source-area environments of Late Jurassic and Early Cretaceous sediments in southeast England. Proceedings of the Geologists Association 95, Part 2; p. 149-165.

Srivastava, S.K.(1976. The fossil pollen genus *Classopollis*. Lethaia, v. 9, p. 437-457.

APPENDIX 1. COMPOSITE LIST OF TAXA

<u>Marine and nomarine algae</u>
dinoflagellates (including *Canningia*)
Januasporites spiniferus Singh 1964
Lecaniella foveata Singh 1971
Exesipollenites tumulus Balme 1957
Ovoidites parvus (Cookson & Dettmann) Nakoman 1966
Schizosporis reticulatus Cookson & Dettmann 1959
Sigmopollis psilatus Piel 1971
<u>Gymnosperm pollen</u>
bisaccate pollen
Callialasporites dampieri (Balme) Dev 1961
Cerebropollenites mesozoicus (Couper) Nilsson 1958
Classopollis classoides Pflug emend. Pocock & Jansonius 1961
Eucommiidites minor Groot & Penny 1960
Scadopityspollenites sp.
T/C/T - Taxodiaceae/Cupressaceae/Taxaceae pollen
Vitreisporites pallidus (Reissinger) Nilsson 1958
<u>Selected lycopod, fern and bryophyte spores</u> (lists includes about 75% of taxa present)
Aequitriradites spinulosus (Cookson & Dettmann) Cookson & Dettmann 1961
Cicatricosisporites spp.
Concavissimisporites punctatus (Delcourt & Sprumont) Brenner 1963
Cooksonites variabilis Pocock 1962
Coronatispora valdensis (Couper) Dettmann 1963
Costatoperforosporites foveolatus Deak 1962
Cyathidites/Deltoidospora spp.
Foraminisporis asymmetricus (Cookson & Dettmann) Dettmann 1963
F. wonthaggiensis (Cookson & Dettmann) Dettmann 1963
Gleicheniidites senonicus Ross 1949 ex Delcourt & Sprumont 1955
Impardeispora trioreticulosa s.l. Cookson & Dettmann 1958
Impardeispora apiverrucata s.l. Couper 1958
Klukisporites granulatus (Pocock) Burden & Hills 1989
K. pseudoreticulatus Couper 1958
K. areolatus Singh 1971

Laevigatosporites sp.
Lycopodiumsporites spp.
Microreticulatisporites uniformis Singh 1964
Osmundacidites sp.
Perinopollenites elatoides Couper 1958
Plicatella spp.
Pilosisporites trichopapillosus (Thiergart) Delcourt & Sprumont 1955
Sestrosporites pseudoalveolatus (Couper) Dettmann 1963
Stereisporites antiquasporites (Wilson & Webster) Dettmann 1963
Tigrisporites spp. (*T. reticulatus* Singh 1971 and *T. scurrandus* Norris 1967)
Zilvisporis spp.
<u>Monoclopate angiosperm pollen</u>
Clavatipollenites hughesii Couper 1958
Liliacidites spp.

A.R. Sweet

Paleontology Subdivision
Institute of Sedimentary and Petroleum Geology
Calgary, Alberta.

TABLE 1

C-number	Depth	Preparation Number	dinoflagellates	*Januasporites spiniferus*	*Lecaniella foveata*	*Ovoidites parvus*	*Schizosporis reticulatus*	*Sigmopollis psilatus*	bisaccate pollen	*Callialasporites dampieri*	*Cerebropollenites mesozoicus*	*Classopollis classoides*	*Eucommiidites* sp.	*Exesipollenites tumulus*	*Scadopityspollenites* sp.	T/C/T	*Vitreisporites pallidus*	*Aequitriradites spinulosus*	*Cicatricosisporites* spp.	*Concavissimisporites punctatus*	*Cooksonites variabilis*	*Coronatispora valdensis*	*Costatoperforosporites foveolatus*	*Cyathidites/Deltoidospora* spp.	*Foraminisporis asymmetricus*	*F. wonthaggiensis*	*Gleicheniidites senonicus*	*Impardecispora trioreticulosa*	*Impardecispora apiverrucata*	*Klukisporites granulatus*	*K. pseudoreticulatus*	*K. areolatus*	*Laevigatosporites* sp.	*Lycopodiumsporites* spp.	*Microreticulatisporites uniformis*	*Osmundacidites* sp.	*Perinopollenites elatoides*	*Plicatella* spp.	*Pilosisporites trichopapillosus*	*Sestrosporites pseudoalveolatus*	*Stereisporites antiquasporites*	*Tigrisporites reticulatus*	*Zlivisporis* spp.	*Clavatipollenites hughesii*	*Liliacidites* spp.	Total count
			Marine-Algae-Nonmarine							Gymnosperm pollen							Selected lycopod, fern and bryophyte spores																											angiosperms		
COUNTS AND QUALITATIVE ABUNDANCES																																														
Roland et al. 11-23-91-8-W4; Zone 12V, UTM 489335 m E, 6307145 m N.																																														
412935	150m	4625-1	R(2)	R(1)			R		37		2	6		4.0	1	167		R	2				R	3			7	1	R	C	R	R		S		2	1	R	R		1		S	R		234
412936	147m	4625-2	S(3)	S(3)		R			49		5	19		7.0	1	119		R	4		R			2	2		7			R	R					2	1	R			2	R	R			220
412937	146m	4625-3	R(2)	S(3)			R		42		1	9		17.0		151		1	2		R			1	R		7		R				2	2		1		R	R				R	R		236
Roland et al. 1-12-91-8-W4; Zone 12V, UTM 491767 m E, 6303096 m N.																																														
412938	166m	4626-1	R(1)	R(1)			R	R	16		1	3		10.0	1	159	R		R		R		R	7			16	R	R	R		R		2							2	S	S	2		219
412939	162.9m	4626-2	S(3)			R	R		33		R	3		4.0	1	180	1	R	1	R	R		R	3	R	R	11	R	R			R	1	1			R	R	R		1		C		R	240
412940	158.1m	4626-3	S(4)	R(1)					24	R	C	6		1.0	R	160	1	S	R	S				4	R	R	11	R	R	R				1		1	R	R	R		1	S				210
412941	154m	4626-4	S?(3)	S(3)				1	16	R	C	5		1.0	R	174	1	R	S	R				4	R	R	11		R	S			4				C	R			2	R	S			219
Roland et al. 15-29-91-7-W4; Zone 12V, UTM 494641 m E, 6309166 m N.																																														
412942	169.5m	4627-1	A(12)		R	R		1	43			2		5.0	R	179	R		C	S	R		R	1	R	R	17	R	S	R			1	S		R		R	R			R				249
412943	172m	4627-2	C(7)	R(1)		R		R	15	R	1	6		2.0		192	1	R	S	R	R			3	R	R	7		R	R		R	5	S		4	R				1	R	R			237
412944	165m	4627-3	A(11)	R(1)					16		C	4		A	1	184		R	A	1	R	R	1	1	R	R	11	S	R	C		R		4		1	R				3	S	R	R		227
412945	159m	4627-4	A(11)	R(1)	R				30		2	3		4.0	3	161		R	R	R	S			1	R	R	19	S		R		R	1	R	R	1	R	R	R		1	R	R			226
412946	151.75m	4627-5	C(7)	R(1)		R			32			8	1	2.0	1	170		1	R	R	C			1	R	R	10	R	R	R		R	1		1	2	R	R		R	1	R	R			231
PC Lewis 5-20-91-7-W4; Zone 12V, UTM 493831 m E, 6306733 m N.																																														
412947	174.9m	4628-1	R(1)				R		23	R	1	1		1.0	R	173	R	R	1		R	R				R	6	R	R	R			S	R	R	1			R	R	R	1	R			208
412948	171.6m	4628-2					R		19	R	1	2		S	R	179		R	C	R	S			1	R		5	R	R	R				R	R	1		R	R		2		R			210
412949	166.1m	4628-3	R(2)		R				15		2	5	R	1.0		180		S	A	S	R			4	R	R	4	R	S	R			3	R	R	1	R		R		2	R	R	S	1	218
PERCENTAGES AND QUALITATIVE ABUNDANCES																																														
Roland et al. 11-23-91-8-W4; Zone 12V, UTM 489335 m E, 6307145 m N.																																														
412935	412935	4625-1	R(2)	R(1)			R		15.8		0.9	2.6		1.7	0.4	71.4		R	0.9				R	1.3			3.0	0.4	R	C	R	R		S		0.9	0.4	R	R		0.4		S	R		
412936	147m	4625-2	S(3)	S(3)		R			22.3		2.3	8.6		3.2	0.5	54.1		R	1.8		R			0.9	0.9		3.2			R	R					0.9	0.5	R			0.9	R	R			
412937	146m	4625-3	R(2)	S(3)			R		17.8		0.4	3.8		7.2		64.0		0.4	0.8		R			0.4	R		3.0		R				0.8	0.8		0.4		R	R				R	R		
Roland et al. 1-12-91-8-W4; Zone 12V, UTM 491767 m E, 6303096 m N.																																														
412938	166m	4626-1	R(1)	R(1)			R	R	7.3		0.5	1.4		4.6	0.5	72.6	R		R		R		R	3.2			7.3	R	R	R		R		0.9							0.9	S	S	0.9		
412939	162.9m	4626-2	S(3)			R	R		13.8		R	1.3		1.7	0.4	75.0	0.4	R	0.4	R	R		R	1.3	R	R	4.6	R	R			R	0.4	0.4			R		R		0.4		C		R	
412940	158.1m	4626-3	S(4)	R(1)					11.4	R	C	2.9		0.5	R	76.2	0.5	S	R	S				1.9	R	R	5.2	R		R				0.5		0.5	R		R		0.5	S				
412941	154m	4626-4	S?(3)	S(3)				1	7.3	R	C	2.3		0.5	R	79.5	0.5	R	S	R				1.8	R	R	5.0		R	S			1.8				C	R			0.9	R	S			
Roland et al. 15-29-91-7-W4; Zone 12V, UTM 494641 m E, 6309166 m N.																																														
412942	169.5m	4627-1	A(12)		R	R		1	17.3			0.8		2.0	R	71.9	R		C	S	R		R	0.4	R	R	6.8	R	R	R			0.4			R			R			R				
412943	172m	4627-2	C(7)	R(1)		R		R	6.3	R	0.4	2.5		0.8		81.0	0.4	R	S	R	R			1.3	R	R	3.0		R	R		R	2.1			1.7	R				0.4	R	R			
412944	165m	4627-3	A(11)	R(1)					7.0		C	1.8		R	0.4	81.1		R	A	0.4	R	R	0.4	0.4	R	R	4.8	S	R	C		R				0.4	R				1.3	S	R	R		
412945	159m	4627-4	A(11)	R(1)	R				13.3		0.9	1.3		1.8	1.3	71.2		R	R	R	S			0.4	R	R	8.4	S		R		R	0.4		R	0.4	R	R	R		0.4	S	R			
412946	151.75m	4627-5	C(7)	R(1)		R			13.9			3.5	0.4	0.9	0.4	73.6		0.4	R	R	C			0.4	R	R	4.3	R	R	R		R	0.4		0.4	0.9	R			R	0.4	R	R			
PC Lewis 5-20-91-7-W4; Zone 12V, UTM 493831 m E, 6306733 m N.																																														
412947	174.9m	4628-1	R(1)				R		11.1	R	0.5	0.5		0.5	R	83.2	R	R	0.5		R	R					2.9	R	R	R			S	R	R	0.5			R	R	R	0.5	R			
412948	171.6m	4628-2					R		9.0	R	0.5	1.0		S	R	85.2		R	C	R	S			0.5	R		2.4	R	R	R				R	R	0.5		R	R		1.0		R			
412949	166.1m	4628-3	R(2)		R				6.9		0.9	2.3	R	0.5		82.6		S	A	S	R			1.8	R	R	1.8	R	R	R			1.4	R	R	0.5	R		R		0.9	R	R	S	0.5	

Appendix 5
Petrology

Table A5-1: Summary of petrographical analysis

Sample	Location	Depth (m)	Facies	Grain size	% of Framework Grains (approx.): Quartz: monocrystalline	Quartz: polycrystalline + chert	Feldspar: plagioclase	Feldspar: K-feldspar	Lithic Fragments	Micas: Biotite	Micas: Muscovite	opaques (pyrite)	zircon	matrix/cement: carbonate (calcite)	matrix/cement: clay	Comments
TS-1	12-12-91-8W4	199.65	F1b	fU	90	5	1	2	tr			2	tr			subrounded to angular
TS-2	12-12-91-8W4	201.80	F2	gravel	90	5	2	tr		tr		2				subrounded; moderately to poorly sorted
TS-3	4-13-91-8W4	204.60	F2	vf + fU	90	4					1	5		Y		oil staining in vf sand; pyrite crystals in carbonate cement; mod-well sorted; subrounded to angular
TS-4	4-13-91-8W4	219.25	F2	fU - vc	85	7	1		2		3	2	tr			plag. vC; quartz fU to vC; vpoorly sorted; subangular to rounded
TS-5	3-18-91-7W4	152.50	F5	silt										Y		
TS-6	3-18-91-7W4	201.35	F1a	fU	87	5	tr		3		1	1				poorly sorted; subrounded to angular
TS-7	3-18-91-7W4	219.50	F2	vcL - gravel	88	5	2	tr	4		1					vpoorly sorted; subrounded to angular; lithic frags incl. mud clasts; intergranular bitumen but unsat. in core
TS-8	5-10-91-7W4	152.60	F8	clay - vf	96	tr	tr				3			Y		microcrystalline calcite cement throughout; vw sorted, angular to subangular
TS-9	13-19-91-7W4	158.25	F8	clay								5			Y	
TS-10	13-19-91-7W4	194.30	F7a	clay								1			Y	
TS-11	6-22-91-7W4	222.60	F1b	fU	95	2	tr				1	1				unsaturated sand, but sub- and superjacent strata bitumen saturated; well sorted; subangular to subrounded
TS-12	6-22-91-7W4	199.70	F7a	fU	94	tr	tr					5				poor quality section; bitumen saturated
TS-13	6-22-91-7W4	190.00	F7a	fU	94	3					1	2				low bitumen saturation; moderately-well sorted; subrounded
TS-14	9-28-91-7W4	231.10	F2	fL - cL	88	8	3				tr	1				poorly sorted; subrounded to subangular; feldspars disaggregated
TS-15	9-28-91-7W4	226.00	F2	fU - cL	82	10	3		1	1	1	2				poorly sorted; finer grained beds exhibit low bitumen saturation
TS-16	5-10-91-7W4	173.56	F7a	fU	95	2	tr					2	tr			2 samples each: cleaned + oil in place
TS-17	5-10-91-7W4	173.90	F7a	fU	95	2	tr					2	tr			2 samples each: cleaned + oil in place
TS-18	5-10-91-7W4	180.63	F7a	fU	95	2	tr					2	tr			moderately well sorted; subrounded to subangluar; 2 samples each: cleaned + oil in place
TS-19	5-10-91-7W4	206.10	F2	cL	90	5						5		Y		2 samples each: cleaned + oil in place
TS-20	5-10-91-7W4	207.20	F1a	cL	92	5	1					2				2 samples each: cleaned + oil in place
TS-21	1-12-91-8W4	129.25	F1a	mL	92	2	4				tr	1	tr			moderately well sorted; subrounded to subangluar

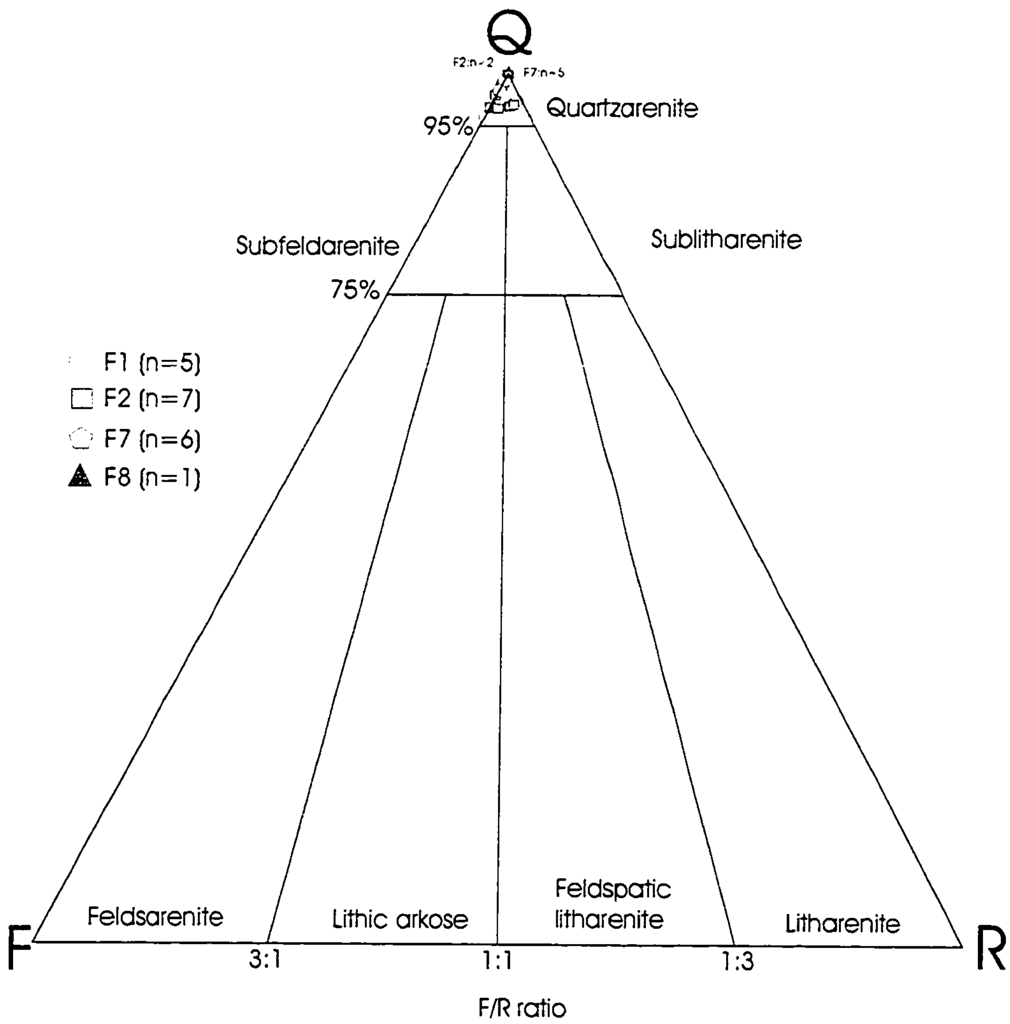

Figure A5-1: QFR ternary diagram. The Q pole comprises chert, mono- and polycrystalline quartz (see Table A5-1 for relative percentages of each), the F pole includes both potassium feldspar and plagioclase, and the R pole comprises rock and mudstone fragments